SOME ASPECTS OF THE ROLE OF THE CENTRAL NERVOUS SYSTEM IN CONTROLLING THE REPRODUCTIVE CYCLE OF THE FEMALE AMPHIPOD "GAMMARUS SETOSUS DEMENTIEVA"

CENTRE FOR NEWFOUNDLAND STUDIES

TOTAL OF 10 PAGES ONLY
MAY BE XEROXED

(Without Author's Permission)

BRIAN ROGER MACPHERSON

385782

CENTRE FOR NFLD. STUDIES
OCT 6 1975
MEMORIAL UNIVERSITY
OF NEWFOUNDLAND

Some aspects of the role of the central nervous system in controlling the reproductive cycle of the female amphipod *Gammarus setosus* Dementieva

by

Brian Roger MacPherson B.Sc.

A thesis submitted in partial fulfillment
of the requirements for the degree of
Master of Science.

Department of Biology
Memorial University of Newfoundland

St. John's Newfoundland

May 1974

ABSTRACT:

The various neuropiles and cellular glomeruli of the brain, subpesophageal ganglion and ventral ganglion chain were identified in *Gammarus setosus* Dementieva. Two types of neurosecretory cells, A and B, were present in the brain glomeruli, two in the glomeruli of the suboesophageal ganglion, A and A', and four in the glomeruli of the ventral ganglia, A, A', B and C, all based on perikaryon size. There were two types of neurosecretory granules in the cells of the brain glomeruli, type I were small, dense spheres 98-160 nm in diameter found only in the A cells, while the larger type II vesicles ranged from 195-815 nm, resembled mitochondria and were found in both A and B cells. The type I granules were Golgi-formed but the origin of the type II vesicles is uncertain, the possibilities being transformation of Golgi-formed multivesicular bodies (MVB), or mitochondrial fission and alteration of conformation. Accessory cephalic structures present in the anterior head region were the sinus gland, paired statocysts and a dorsal, medial, unpaired frontal organ. Production and release of neurosecretory material (NSM), was observed in the frontal organ neurons and they were divided into two types, I and II, based on the size of their secretory granules. Those of type I ranged from 1000-4500 nm in diameter, similar in morphology to the type II vesicles of the brain but larger, while the type II vesicles of the frontal organ neurons were 300-900 nm and Golgi-formed. The frontal organ appears to be a neurohemal organ with the NSM liberated through rupture of the cell membrane. The sinus gland contained variable amounts of NSM but release was not observed and no X organ was found. Morphological alteration of the follicular epithelium was noted before vitellogenesis begins and the hepatopancreas was indicated as a probable source of the vitellogenic materials. Decrease in photoperiod stimulates vitellogenesis in late summer and long photoperiods (14 hours light) prolong the ovarian cycle, while shorter ones (12 and 8 hours light) accelerate it respectively. Complete darkness resulted in successive

cycles after resorption of the oocytes. The type I frontal organ neurons appear to release an ovary-inhibiting hormone while the role of the type II neurons is unknown. The secretions of the neurosecretory cells of the brain and ganglia also have an uncertain effect upon reproduction with evidence to support either a stimulatory or inhibitory effect dependent upon the type of release exhibited.

ACKNOWLEDGEMENTS:

I would like to express my sincere appreciation to Dr. V.J. Steele under whose supervision and encouragement this study was carried out. Thanks are also due the other members of my supervisory committee - Dr. A.K. Bal for his instruction and interpretation of the electron micrographs and Dr. D.H. Steele for his critical analysis of the manuscript. My appreciation is also extended to Dr. V.C. Barber for his assistance with the scanning electron microscope and to Mr. E.T. Fitzerald and his staff of technicians who endeavoured to provide all materials required. Special thanks are extended to Mr. Roy Ficken for his instruction and assistance with all aspects of the photography used in the following pages. I wish to extend my personal appreciation to Cynthia Long for her assistance with orientation to the animal and its habits as well as the graphic illustrations found within the text.

Financial aid was provided in the form of a Memorial University Fellowship (1971-72), National Research Council Bursary (1972-73) and support from a National Research Council Grant awarded Dr. V.J. Steele (1973-74).

TABLE OF CONTENTS

Introduction 1

  Biology of *G. setosus* 5

Materials and methods 7

Results 11

  Structure of the central nervous system 11

    The brain 15

    Nerves of the brain 16

    Neuropile localization in the brain 17

      Protocerebrum 17

      Deutocerebrum 19

      Tritocerebrum 20

    Ganglionic cell layers of the brain 20

    The suboesophageal ganglion 21

    The ventral ganglia 22

  Neurosecretory cells of the central nervous system 24

  Ultrastructure of brain neurosecretory cells 26

  Ultrastructure of ganglionic neurosecretory cells 29

  Accessory cephalic structures 30

    The sinus gland 30

    The frontal organ 32

    The statocysts 33

  Cells of the frontal organ 35

  The ovary 39

    Morphology 39

    Glands 41

  Oogonial development 42

    Phase I: formation of oogonia 42

    Phase II: oogonial growth 43

    Phase III: vitellogenesis 43

  The ovarian cycle 46

  Effect of photoperiod on the ovarian cycle 48

Field 48
Experimental 48
Neurosecretion and reproduction 53
Neurosecretory cells of the brain 53
Neurosecretory cells of the protocerebrum 53
Neurosecretory cells of the deutocerebrum 54
Neurosecretory cells of the tritocerebrum 55
Neurosecretory cells of the suboesophageal mass ... 55
Neurosecretory cells of the ventral thoracic ganglia ... 55
Neurosecretory cells of the abdominal ganglia 56
Seasonal activity of neurosecretory cells in the central nervous system 57
Vitellogenesis and neurosecretion 59
Discussion 62
The central nervous system 62
Accessory cephalic structures 65
The neurosecretory system 70
Neurosecretory cells 70
Neurohemal organs 73
Non-neural endocrine organs 74
Neurosecretory cell ultrastructure 76
NSM production 79
Migration and release of NSM 83
The ovary and vitellogenesis 85
The hepatopancreas 88
Effect of photoperiod on reproduction 90
Neurosecretory effect on reproduction 94
Photoperiod effect on neurosecretion 100
Correlation of neurosecretory activity with physiological processes ... 101
Summary and conclusions 104
Figures 107
Tables 157
Literature cited 166

INTRODUCTION:

The purpose of this study was to present the morphology of the central nervous system and neurosecretory system of *G. setosus* as well as defining the seasonal activity of the neurosecretory cells regulating reproduction and the effect of photoperiod on the reproductive cycle.

The history of knowledge of neurosecretion begins with the description by Speidel (1919) of neurosecretion-containing neurons in the caudal region of the elasmobranch spinal cord. Workers such as Bellonci (1881, 1882), Nansen (1886), Metalnikoff (1900), Reupsch (1912), Bretschnieder (1914) and Dahlgren (1914) had all preceeded Speidel in describing similar cells in the nervous system of the animals investigated but they attached no importance to these cells, some not even recognizing their glandular activity. Speidel (1919) was the first to attach glandular significance to the cells described by Dahlgren (1914) in the spinal cord of the skate, rejecting his hypothesis that they were giant motor neurons but rather glandular in nature with internal secretions.

About ten years after Speidel's discovery, Ernst Scharrer (1928), reported evidence of secretory activity in hypothalamic neurons of the minnow. During the 1930's, Scharrer described similar neurons as a constant occurrence in the hypothalamus of other vertebrate groups.

Perkins (1928) and Koller (1928) were the first workers to initiate studies on neurosecretion in crustaceans. Following this neurosecretion was described in crustaceans by Hanstrom (1935, 1937a, 1937b), in insects by Weyer (1935) and in several other invertebrate groups by Berta Scharrer (1935, 1936, 1937). The phenomenon of neurosecretion has been found in every metazoan animal so far examined possessing a central nervous system with some degree of cephalization. These cells congregate to form organs or are scattered throughout the nervous system of the animal. When Hanström (1931) described the eyestalk hormone in the sinus gland of brachyurans, it motivated others to establish neurosecretory pathways in many crustacean species (Brown, 1944; Hanström, 1947, 1948, 1953, 1957; Passano, 1951; Bliss & Welsh, 1952; B. Scharrer, 1959 and E. Scharrer, 1959). The significance of these systems in the physiology of the decapod crustacean has been investigated by several authors (Scharrer, 1955; Welsh, 1955 and Carlisle & Knowles, 1959).

Panouse (1943, 1944) was the first to observe hormonal influence on the reproductive activity of crustaceans. The presence of an ovary-inhibiting hormone was confirmed by Brown & Jones (1947, 1949), Démeusy & Veillet (1952) and Carlisle (1953) in a number of crustacean species. Otsu (1960) discovered the presence of an ovary-stimulating principle secreted by the neurosecretory cells of the thoracic ganglia of *Potamon dehaani*. Gomez (1965) showed that in another species, *Paratelphusa hydrodromous*, the gonad-stimulating substance was present in the neurosecretory cells of the brain and thoracic ganglia of both sexes.

The first indications of cyclic changes in neurosecretory cells was described by Pyle (1943) studying the sinus gland of higher malacostracans. Perryman (1969) correlated morphologic changes in the neurosecretory cells identified by Bliss *et al.* (1954) in the brain of *Procambarus simulans* to its reproductive cycle. Other authors such as Lowe (1961), Bhargava (1972) and Perryman (1969) have mentioned the correlation of changes in the neurosecretory pathway with the moult cycle of insects and crustaceans.

There is little information on the neurosecretory system in Amphipoda. The neurosecretory cells themselves have not been extensively studied. The only well documented endocrinological phenomenon that has been examined in the amphipods is the discovery and function of the androgen gland by Charniaux-Cotton (1956) in *Orchestia gammarella*. This structure is completely independent of the gonads and is classified as a non-neural endocrine organ. Another non-neural endocrine organ present in malacostracans is the paired Y organ, first described by Gabe (1953a). The ovary hormone release sites responsible for female characteristics have not as yet been pinpointed.

Other neural endocrine features of the neurosecretory system in amphipods have only been initially investigated. The neurosecretory cells have been little more than identified and described in the sinus glands of *Gammarus pulex, Gammarus fluviatilis* (Gräber, 1933) and *Gammarus locusta* (Stahl, 1938) and in the cephalic statocyst which Dahl (1963) equates to the X organ of higher malacostracans. Závadský and Prag (1914) investigated the statocyst and frontal organ of *G. pulex* while Thore (1932) also elaborated on these structures in *G. locusta* and *G. pulex*. Gräber (1933) described the morphology of the brain of *G. fluviatilis* in great detail while Thore (1932) described that of *G. pulex* and *G. locusta* but in far less detail. Baid and Dabbagh (1972) were the first workers to describe the protocephalic neurosecretory system of a gammarid, *Rivulogammarus syriacus*, and classify the types of neurosecretory cells present. Shyamasundari (1973) has initially described only two types of neurosecretory cells found in the brain and ganglia of two talitrid amphipods, *Talorchestia martensii* and *Orchestia platensis*.

Because the amphipods are more primitive members of the malacostracans, it is interesting to compare the morphology of the neurosecretory systems of these species with those of higher malacostracans, particularly the decapods. The neurosecretory systems of many crustaceans have been thoroughly examined by authors such as Bliss & Welsh (1952), Knowles (1953), Bliss *et al.* (1954), Potter (1954, 1958), Miyawaki (1956), Hentschel (1963, 1965), Fingerman *et al.* (1964), Nagabhushanam (1962), Fingerman & Oguro (1967), Lake (1969b, 1971), Kulakovskii (1970) and Smith & Nayla (1972).

BIOLOGY OF *G. SETOSUS*

Gammarus setosus Dementieva is a littoral amphipod that inhabits sheltered to moderately exposed beaches where it is found under rocks, algae or other cover when the tide is low. It has a circumpolar distribution in Arctic regions and is found as far north as land extends. In the northwest Atlantic region it occurs as far south as the Bay of Fundy in New Brunswick (Steele & Steele, 1970).

South of Labrador, *G. setosus* is rarely found on exposed beaches but north of this it may reside in upper tide pools on the shore. The species is euryhaline as it may live in low salinity areas such as in outflow regions of brooks, rivers and beach seeps. South of Labrador, only areas with cool waters throughout the summer support populations of *G. setosus*. North of Newfoundland it is the most abundant species of *Gammarus*, but on Newfoundland beaches it is generally less common with isolated populations inhabiting selected rocky beaches (Steele & Steele, 1970).

The population of *G. setosus* at Witless Bay, Newfoundland reaches 50% sexual maturity at about 13.7 mm in length. Animals kept in the laboratory at 3°C attain sexual maturity after the 13th moult - about 12 mm in the female and 14 mm in the male. Mature females usually produce only one brood in the fall of each year. Animals kept in the laboratory at 12°C and exposed to shorter photoperiods can be induced into a second brood per year (Steele & Steele, 1970).

Fecundity increases with the size of the female and their size at maturity. Continued growth and a relatively long lifespan help to compensate for the production of a single brood per year. These animals have a high survival rate in the laboratory and are less cannibalistic than other species of *Gammarus*. After 120 days into an experiment there is at least a 50% survival rate.

In the field the oogonia of the female enlarge in August. Approximately two or three weeks prior to ovulation the male couples with a selected female (precopula) and releases her only after copulation and fertilization of the eggs in the brood pouch has occurred in late September to October. The rate of development of the embryos is dependent upon the incubation temperature but the first young are released as early as December. The later maturing animals do not have their broods until later in the fall and release their young as late as May. Therefore, the release of the young takes place over a period of five to six months, although the majority of the population release their young in January and February (Steele & Steele, 1970).

After each brood the females enter an obligatory resting stage (Steele, 1967). Those females that release their young in December are prevented from having a second brood by the low temperatures during the winter and this tends to prolong the reproductive phase. The bulk of the population in February to March is made up of one-year-olds as few animals are larger than 20 mm.

Gammarus are not specialized feeders and consume both living and dead plant or animal food. The released young feed on a form of filamentous algae that is present first in February and persists until August or September, with a peak of development in late June. Therefore, the reproductive cycle of *G. setosus* corresponds with the availability of nutrients and for this reason a single brood per year may be of advantage (Steele, 1967).

MATERIALS AND METHODS:

FIELD COLLECTIONS: The animals used in the study were taken from a population of *G. setosus* at Witless Bay on the Atlantic coast of the Avalon Peninsula of Newfoundland. They were sampled monthly during the year, except for those months in which ice made sampling impossible, and during the breeding season when collections were made more frequently to obtain sufficient numbers for use in light experiments. Collections were made during the neap tide period as the species inhabits the mid-region of the intertidal zone at Witless Bay. The representative samples were obtained by handpicking the animals from the coarse substrate under flat rocks with forceps or dip nets. The average size of the females collected was 14.5 mm, ranging from 11.0 mm to 24.0 mm. The average size of males was 16.8 mm, ranging from 13.5 mm to 26.0 mm in length.

EXPERIMENTAL ANIMALS: After fixing a representative number of females (24) from each sample, the rest were used in the photoperiod experiments. The animals were sorted into groups of 50 females and 35 males and placed into Lewis Stack-n-Nest Tote Pans (fiberglass reinforced polyester) of a 0.14 cubic meter capacity. For use in light, the covers had plexiglass windows installed and for use in the dark, the exterior of the cover and pan was painted black to eliminate any possible light transmission. Each pan was supplied with air.

Culture pans were kept in environmental chambers with photoperiods of 8, 12 and 14 hours light. The temperature was kept at 10°C ±1°C and the salinity adjusted to 30°/00 with demineralized water. Each pan had a maintained volume of one liter of sea water. Marble chips, shells and larger pebbles were added to absorb excreta and duplicate their natural physical environment. There was no attempt to simulate the tides and the animals were constantly submerged. They were fed twice weekly with dried fish food flakes (Tetramin) or fresh mussel, periwinkle or sea urchin meat when available. Other food was obtained from the detritus and algal blooms in those pans exposed to light.

The animals were checked weekly and all experimental data was collected after an acclimation period of 14 days. They were killed at predetermined intervals of time after exposure to each photoperiod, complete darkness or combinations of these. Animals were also kept at the Marine Sciences Research Laboratory (MSRL) at Logy Bay, Newfoundland, where they were held in similar containers supplied with running sea water. These animals were fed and checked less frequently and existed mainly on detritus and algae that passed through the sea water filters. The water temperature varied seasonally in these pans and was usually around 0°C during the winter months when the MSRL facilities were utilized. These animals were collected during the autumn breeding season when they are present in large numbers and were kept at the MSRL for experimental use through the winter months when *G. setosus* are unaccessible on the ice-covered beaches.

GROSS HISTOLOGICAL STUDY: Whole specimens from the field collections or from photoperiod experiments were fixed in aqueous Bouin's fluid. The integument was slit and legs cut off to facilitate infiltration. The specimens were dehydrated in the alcohol series, cleared in xylene and embedded in paraffin (Tissue-prep 56.5°C, Fisher). Serial frontal, cross and sagittal sections of 8 to 10 microns were obtained.

These samples were stained routinely with the following techniques considered selective for the visualization of neurosecretory material (NSM): Bargmann's (1949) modification of Gomori's (1941) chrome hematoxylin-phloxine technique (CHP), Cameron & Steele's (1959) modification of Gabe's (1953b) modification of Gomori's (1950) paraldehyde-fuchsin with Halmi's (1952) counterstain (PF) and Dogra & Tandan's (1964) modification of Humberstone's performic acid-Victoria blue technique (PAVB). Controls were also carried out by omitting the oxidation step in each technique.

Other newer or experimental techniques were also tested but many involved procedures too long or expensive to lend themselves to routine work. The more useful of these for invertebrate tissue were: Wendelaar Bonga's (1971) modification of Peute & van de Kamer's (1967) alcian blue/alcian yellow technique, Hubschman's (1962) modification of Heidenhain's Azan technique, Ittycheriah & Marks (1971) performic acid-resorcin-fuchsin technique and Shoumaker & VanDamme's (1971) modification of Maillet's OsO_4-ZnI_2 fixative and alcian blue staining technique.

FINE AND ULTRASTRUCTURAL STUDY: Epoxy resin sections were used for observation of fine and ultrastructural detail. Both light and electron microscope sections were examined. All tissue was fixed in Karnovsky's (1965) gluteraldehyde-paraformaldehyde fixative and postfixed in 1% OsO_4. It was dehydrated in alcohol and propylene oxide then embedded in Epon 812 resin. Sections for light microscopy were cut at 0.5 to 1.5 microns with glass knives on a Sorvall Porter-Blum JB-4 microtome. Sections used in electron microscopy were cut on a Reichert Um 03 ultramicrotome and examined with the Zeiss 9A electron microscope.

The epoxy sections for the electron microscope were stained with uranyl acetate and lead citrate. Those examined under the light microscope had the epoxy resin removed with aged 1-2% sodium hydroxide in absolute methanol (Erlandsen *et al.*, 1973) and were stained with one of the following methods: toluidine blue pH 11.1 (Trump *et al.*, 1961), basic fuchsin (Winklestein & Menefee, 1963), hematoxylin and phloxine stain for osmium-fixed tissues (Munger, 1961), aldehyde-fuchsin technique for epoxy resin sections (Stoeckel *et al.*, 1972) and tribasic stain for epoxy resin sections (Grimley, 1964). Of the above, the toluidine blue and aldehyde-fuchsin techniques were the most useful. The stained sections were mounted with Epon 812 resin and polymerized.

SCANNING ELECTRON MICROSCOPY: Whole specimens were fixed by injection of Karnovsky's fluid (1965). After washing in the phosphate buffer (pH 7.2), the appropriate organs were dissected out and stored in 70% alcohol. Before freeze-drying in a Speedivac - Pearse Tissue Dryer model 1, the material was taken down to 25% alcohol. After freeze-drying for approximately 4 hours the tissue was gold coated in an Edwards Pirani and Penning model 4 vacuum coater and then examined with a Cambridge Stereoscan.

PHOTOGRAPHY: Light microscope photographs were taken on a Zeiss Photomicroscope II with Kodak Panatomic X film (ASA 32). Kodak Kodachrome II film was used for color slides and photographs. Electron micrographs were taken on Kodak 4489 EM film (estar thick base). Whole mounts of the nervous system were photographed on a Nikon stereoscope model SM equipped with a Nikon microflex model AFM camera on Kodak Panatomic X film. Scanning electron micrographs were taken on Tri X film by Kodak.

Filters were used to increase the contrast of the neurosecretory material in the black and white light photomicrographs. With animals stained by paraldehyde-fuchsin a Kodak Wratten gelatin filter #22 (orange) was placed over the light source. Animals stained with chrome hematoxylin-phloxine required a #25 (red) filter. All photographs were printed on Ilford single weight, glossy photographic paper, labeled with Letraset, arranged in plates and photographically copied.

RESULTS:

STRUCTURE OF THE CENTRAL NERVOUS SYSTEM: (terminology adopted from Bullock & Horridge, 1965).

The central nervous system of *G. setosus* is composed of a supraoesophageal ganglion (brain), circumoesophageal commissures leading to a suboesophageal ganglion and a ventral chain of ganglia. Each of these components has two zones, the core and the rind, the nomenclature being based on their position (fig. 6). The core is the inner central mass of fibers which is free of perikarya while the rind is the external layers of neuron perikarya. There are no fibers ending in the cellular rind as the synaptic fields and pathways are in the fiber core (Bullock & Horridge, 1965).

CELL TYPES: The common neuronal type in the nervous system is unipolar with branching processes, axon collaterals (fig. 28). The central nervous system contains most of the motor and internuncial cell bodies while the peripheral system contains all the sensory neurons (Bullock & Horridge, 1965).

Supporting elements of the central nervous system, the neuroglial cells, can be found in a great number of locations and are of such great variety that classification is difficult. The outer capsule of fibrous connective tissue is secreted by the underlying non-nervous perilemmal (glia?) cells. The outer membrane of the perilemma is distinct from the capsule and the perilemmal cells have distinct tinctorial properties.

The larger cell bodies have a sheath of glial processes wrapped around them arising from adjacent neuron satellite cells. Glial cells also form an axonal sheath, the neurilemma (fig. 24), by spiralling loosely around the axon with several cells forming the overlapping sheath. Smaller axons are completely enveloped by a single glial cell. The nuclei of these cells are seen occasionally within the fiber core (figs. 12, 20). Glial cells of this type are called nerve fiber satellite cells. The ultrastructure of the neuron and glial cell will be described later.

FIBER CORE: The fiber core of the nervous system is differentiated into tracts and neuropile (figs. 20, 22). These tracts are the equivalent of vertebrate white matter and are axons en route with few terminations or synapses. The neuropile is a dense plexus of fibers tightly matted together with a large number of axon terminations and synapses (figs. 12, 13). They consist mainly of ~~the~~ axons of motor neurons and the cytoplasmic-rich neurons concerned with association. The neuropile is the principle region for integrative nervous events and is differentiated to various degrees (figs. 7,8) with the loose, coarse-textured areas being of lesser importance. An increase in differentiation of texture and separation of tracts from neuropile indicates a region of greater importance (Bullock & Horridge, 1965).

ULTRASTRUCTURE OF THE FIBER CORE: In a cross section through the fiber core of the nervous system mitochondria, neurotubules, neurofilaments, free ribosomes (fig. 16), dense-cored and electron lucent vesicles (fig. 18) as well as other tubular structures can be identified within the boundaries of the axons. A single supporting glial cell ensheaths from one to any number of axons of varying diameter. Mesaxons can be seen throughout the fiber core. These supporting elements are distinguished from the axons in cross section by their more vacant, paler cytoplasm. They contain an occasional mitochondrion, sparsely scattered ribosomes, dark staining glycogen granules and gliotubules. The remaining space is filled with a flocculent material (fig. 18).

The neuropile of the brain and ganglia of *G. setosus* consists of unmyelinated axons, axon terminals, synapses and supporting glial cells. The elements are closely packed separated only by spaces 12 to 19 nm wide. The axons are delimited by a single unit membrane although the appearance of a double membrane is imparted by the closeness of the apposing membranes. There is great variation in axon diameter ranging anywhere from .035 to 2.5 microns in the sections examined (fig. 17, 18).

In the synaptic regions, the mitochondria appear circular in cross section and exhibit a spiral internal configuration (fig. 18). Along the axons the mitochondria are found in various configurations but their long axes parallel those of the axons (fig. 16). The degree of internal organization is also variable with some being more distinct than others. The spherical mitochondria show the typical double membrane features and their crests exhibit various degrees of swelling. In cross section the crests appear to be directed inwards; in sagittal or frontal sections they tend to be parallel with the long axis of the elongated organelle. The mitochondria in the sections examined ranged from .135 to .75 microns in diameter and .45 to 3.40 microns in length (figs. 16-18).

The neurotubules are prominant structures in the axon cross section extending its length and ranging from 23 to 38 nm in diameter (fig. 16). They appear as small hollow spheres and have no particular arrangement. The neurofilaments are tiny fibrillar structures with a beaded appearance arranged in no special pattern (fig. 16). The bead-like portions of the neurofilaments measure 15 to 30 nm in diameter and are connected by crossbars 5 nm thick. The neurofilaments are characteristic of the axon and are far less common in the perikaryon. Both these structures appear to be proteinaceous in character.

Synaptic endings are marked by a thickening of the cell membrane (fig. 18). The opposing surfaces are equally thickened with the spacing between the membranes in the region of the synapse being little different from that of adjacent areas. An intermediate bond is not readily visible at this magnification suggesting that these synapses are of Type 2. An electron dense substance accumulates in the cytoplasm and is disposed symmetrically on either side of the synaptic cleft. There is also an accumulation of two types of vesicles in this region - dense core and electron lucent (fig. 17, 18). The dense core vesicles range from 50 to 116 nm in diameter and the electron lucent variety are about 50 to 77.5 nm.

Other tubular structures present in the sections examined were primarily of two types. The first appears as a large membrane-bounded structure 77.5 to 158 nm in diameter (fig. 17). The other is a hollow cisterna with a single bounding membrane ranging in diameter from 108 to 120 nm in the sections examined (fig. 16). This last type appears to have small granules on the external surface of the membrane in some cases and may be cross sections of rough endoplasmic reticulum found in the axon (fig. 16).

Different types of neuropiles are present within the fiber core. Glomeruli are knots or small spherical masses of neuropile of tighter weave than that surrounding it (figs. 7, 8). Tracts and fascicles of axons also show marked decussation behind each eye in the optic lobes of *G. setosus* across a plane in the axis of the system.

In the brain, areas of small neurons with very large nuclei extremely rich in chromatin, but relatively poor in cytoplasm, are packed tightly together in the rind into a glomerular (ganglionic) cell layer (figs. 6, 7). These are centers of high integrative functioning. A marked uniformity of cell type or absence of very large or giant neurons, cell masses set off from one another, or abrupt transitions from one cell type to another are all signs of localized specialization (Bullock & Horridge, 1965). The differentiation of the cell rind is based mainly on the size of the neuron perikarya and position or proportion of cytoplasm to chromatin.

THE BRAIN:

The brain of *G. setosus* is anterior to the alimentary canal between the eyes and slightly posterior and lower than the anterior and upper limits of the eyes in the head somite. It is bent upwards into a wholly vertical position (fig. 1). The external form is lobular bearing two large pairs of lobes dorsolaterally and ventrally (fig. 2). It is embedded in a web-like network of adipose connective tissue which is attached to the fibrous connective tissue capsule of the brain and also to the hypodermis (fig. 5). The optic nerves connecting the left and right lateral extremities to the eyes also help keep the brain in its upright position (fig. 8). There are two pairs of nerves to antennae I and II arising from the anterior aspect of the brain as well as tritocerebral connectives linking the brain to the ventral ganglion chain (fig. 1). All these points of attachment and continuities with the rest of the central nervous system as well as the nerve connecting the accessory cephalic structures with the brain help hold it in place.

The brain of the females averaged 0.79 mm at its widest point (between the tips of the optic lobes of the protocerebrum) and 0.53 mm in height from dorsal to ventral tip. It is composed of three divisions; the protocerebrum, the deutocerebrum and the tritocerebrum (figs. 1, 3). The morphological division is partially obscured by the reduction of the deutocerebrum.

The protocerebrum is the most superior (dorsal) part of the brain and also the largest. This is partially due to the size of the optic lobes as they are associated with the animal's relatively well developed eyes. They comprise 3/4 the volume of the dorsolateral lobes of the protocerebrum, tapering towards the optic nerves (figs. 2, 7, 8).

The deutocerebrum is not as large or as well developed as the protocerebrum. It is a bundle lying below the protocerebrum giving rise to the antennary nerves of antenna I as well as the olfactory lobes (figs. 1, 9). The antennary I nerves arise from the anterior aspect of this section and the olfactory lobes lie lateral to these. The posterior side of the deutocerebrum is relatively smooth and curved in a gentle concavity (fig. 1).

The tritocerebrum is a swelling below the deutocerebrum and is the smallest section of the brain. It is the ventral and caudal portion sending branches anteriorly and posteriorly (fig. 1). The antennary II nerves extend anteriorly and the tritocerebral connectives posteriorly merge into the circumoesophageal connectives. It also gives rise to the tegumentary nerve and other minor nervous connections (figs. 2, 10, 11).

NERVES OF THE BRAIN:

The three main pairs of nerves originating from the brain of *G. setosus* are the optic, antennary I and antennary II. Several secondary nerves innervate the accessory cephalic structures and they are the statocyst, sinus gland, frontal organ and tegumentary nerves (figs. 1, 2, 3). Only the tegumentary nerve of this last group will be discussed in this section leaving the rest to be included with the description of the various structures.

The optic nerve of *G. setosus* stemming from the distal hump of the protocerebral optic lobe is short and barely recognizable as a nerve (fig. 8). It is exposed only to a small degree and is generally surrounded by the ganglionic cell layer in that region (the optic lobe glomeruli). The nerve is sturdy and enters the eye at its mid-posterior region.

The antennary I nerve is a large structure originating in the superior anterior portion of the deutocerebrum (fig. 9). It contains both sensory and motor bundles that unite to form a uniformly thick cord. Before it enters the brain it divides internally sending part of the cord to the olfactory lobe and the remaining portion into the antennary I neuropile in the form of a thick interspersed cord (figs. 1, 9).

The antennary II nerve arises from the superior anterior part of the tritocerebrum just ventral to the point where the antennary I nerves join the deutocerebrum (fig. 1). This nerve is also a stout structure but of smaller diameter than the antennary I nerve. The neuropile into which its fibers enter is developed to a lesser degree in both size and texture (fig. 10). Both these antennary nerves have numerous branching collaterals extending to the peripheral regions of the antenna (fig. 14).

The tegumentary nerve originates in the superior part of the tritocerebrum (fig. 3). It extends dorsally, parallel to the hypodermis and divides into two equal branches just under the eye. One branch extends to the hypodermis just under the eye while the other branch passes by the protocerebral optic lobe to the hypodermis of the head above the eye (fig. 15). They facilitate sensory reception from small groups of sensory cells located in the hypodermis at the locations mentioned.

NEUROPILE LOCALIZATION IN THE BRAIN:

PROTOCEREBRUM: The protocerebrum receives the nerves from the eyes, statocysts and frontal organ. It contains three well developed neuropile masses; the optic ganglia, medulla terminalis and central body.

The optic ganglia are located in each dorsolateral extension of the protocerebrum where they form the path for inward flow of excitation from the eyes (figs. 7, 8). They are composed of three optic neuropiles; the lamina gangliaris, medulla externa and medulla interna respectively from the eye medially. All three appear to be distinct entities with the lamina ganglionaris and medulla externa in close proximity. These two optic neuropiles are large and well developed, corresponding to the degree of development of the compound eye. The medulla interna is poorly developed and further separated from the other two ganglia than they are from each other. Its connection to the medulla externa is not developed as a chiasma. In the remaining medial portion of the protocerebrum, the medulla terminalis is located receiving innervation from the paired statocysts (fig. 8).

The central body is a spindle-shaped mass of neuropile situated in the ventral region of the protocerebrum extending into the dorsal region of the deutocerebrum. In thick section it appears to composed of up to seven small subunits although a fair degree of fusion is evident (fig. 8). In thin section the central body is a single, well developed, laterally elongated neuropile (fig. 12, 13), with short ventrally directed tips at each extremity. It is a meeting point for axons from diverse sections of the brain, such as fibers from the deeper optic glomeruli, antennal II lobes and the cell bodies from the anterior and posterior sides of the protocerebrum. Its structure and location suggest an integrative function.

The protocerebral bridge is a poorly developed median neuropile that consists of two glomeruli connected across the midline by a thin band (fig. 2). It is found in the dorsal region of the protocerebrum. The corpora pedunculata and ocellar centers found in the protocerebrum of higher crustaceans are both absent in *G. setosus*.

DEUTOCEREBRUM: The deutocerebrum of *G. setosus* is of a simpler nature than that of higher crustaceans (Bullock & Horridge, 1965). Although the antennal I neuropiles are complex, a distinct olfactory lobe is also present. A weak antennary commissure connects the deutocerebrum on both sides in this region. There are several neuropile masses present in the deutocerebrum (fig. 9).

The antennal I neuropile is extremely highly developed. It extends for some distance out the antenna I nerve having originated at its distal end as a single neuropile mass and then becomes perforated with a series of holes (figs. 2, 9). The vacuolation starts as two adjacent spaces which extend into two rows in the deutocerebrum with four large vacuoles in the ventral row and four smaller ones in the upper. It is also in this region that the large fibers of the statocyst nerve terminate.

The olfactory lobes lie directly lateral to the antennal I neuropiles, resembling a bunch of grapes clustered around a vine (figs. 2, 9). The olfactory neuropile glomeruli are positioned around the periphery of the lobes and a tract extends into the lobe sending fibers to each of these glomeruli. The olfactorio-globularis tract is extensive crossing over and ending without glomeruli in the medulla terminalis as the central glomeruli are reduced. It passes from the olfactory lobe to the medulla terminalis and may be chiasmatic. There are two bundles of single antennal I nerves, one extending to the antennal glomeruli of the olfactory lobe and the other to the tiny spherical glomeruli situated in the trailing edge of the neuropile.

The parolfactory lobes also found in the deutocerebrum lie immediately central to the olfactory lobes (fig. 9). They are small, of no distinct shape and almost indistinguishable from the ordinary fiber core. Also found here are the accessory olfactory lobes between the olfactory lobes and the lateral antennal I neuropile, referred to as "Nebenlappen" or accessory lobes by Gräber (1933). They are well developed and connected by a commissure crossing the deutocerebrum (fig. 9).

TRITOCEREBRUM: The tritocerebrum consists of tracts of fibers from the circumoesophageal connectives surmounted on the dorsal aspect by the large antennal II lobes. It receives sensory and motor tracts from the antennary II nerves as well as the tegumentary nerve from the hypodermis of the head region. The tritocerebrum is not divided into obvious regions and the tegumentary neuropile lies at the root of the nerve in the lateral region of this section. The antennal II neuropiles lie laterally at the base of their corresponding nerves (figs. 1, 2). The two halves of the ventral tritocerebrum are joined by a neuropile bridge (fig. 11) and many transverse fibers just prior to its separation into two parts (fig. 10). From this point the fiber tracts extend into the tritocerebral connectives.

GANGLIONIC CELL LAYERS OF THE BRAIN: (nomenclature adopted from Gräber, 1933).

The glomerular layers forming the cellular rind around the brain are not evenly distributed over its entire surface. They occur in areas of strategic importance for the integrative functioning of the brain. To illustrate the various glomerular groups, the brain is divided into an inferior (front or anterior) and superior (back or posterior) portion.

On the front aspect of the protocerebrum of *G. setosus* the following ganglionic cell layers are present; the anterior inferior lateral glomeruli (ailg, fig. 6), the optic lobe glomeruli (olg, fig. 6), the anterior inferior medial glomeruli (aimg, fig. 7), the anterior inferior medial glomerular bridge (aimgb, fig. 6) and the inferior lateral anterior glomeruli (ilag, fig. 7). On the posterior side of the protocerebrum the anterior superior medial glomeruli (asmg, fig. 7), the anterior superior lateral glomeruli (aslg, fig. 6) [illegible] part of the posterior superior lateral glomeruli (pslg, fig. 7) are found. These glomeruli are shown diagramatically on the surfaces of the brain of *G. setosus* in figures 3 and 4.

The anterior face of the deutocerebrum is covered by the inferior anterior medial glomerulus (iamg, fig. 9), the olfactory lobe glomeruli (oflg, fig. 9) and part of the inferior lateral (ilg) and inferior medial glomeruli (img, fig. 10). On the posterior side of this section the remainder of the posterior superior lateral glomeruli (pslg, fig. 9) is found. Figures 3 and 4 show the glomeruli of this region diagramatically.

The tritocerebrum has the rest of the inferior medial (img) and inferior lateral glomeruli (ilg, fig. 10) as well as 1/2 the inferior posterior glomeruli (ipg, fig. 110m) on its anterior face. The posterior side of the tritocerebrum has only the remaining portion of the inferior posterior glomeruli (ipg, fig. 4) on it. This last glomerulus is found lying along the outside lateral portion of the tritocerebral connectives (fig. 110o). The glomeruli of the tritocerebrum of *G. setosus* are shown diagramatically in figure 3 and 4.

THE SUBOESOPHAGEAL GANGLION:

The circumoesophageal connectives that extend posteriorly from the tritocerebral connectives around the oesophagus to the suboesophageal ganglion are relatively short. The suboesophageal ganglion is a fusion of the first four thoracic ganglia into an elongated mass with an average length of 0.67 mm and a width of 0.27 mm (fig. 19). The number of ganglia fused into this mass is variable in the Amphipoda, but always includes those ganglia corresponding to the mandible and maxillae. Some of the nerves associated with this mass are the extracentral longitudinal, median longitudinal, nerves of the leg region and nerves of the integument (Bullock & Horridge, 1965).

The suboesophageal mass is relatively flat along its dorsal side in sagittal section but has a smooth bilobed appearance in cross section. The neuropile is confined to the ventral portion and the roots of the many nerves that arise from this region (fig. 20). There are many nerves projecting from different positions on the mass, the most anterior of these are thick and extend in a dorsolateral direction from the circumoesophageal connectives just before they join the mass.

From each of the four fused ganglion bodies there are two relatively thick nerves passing to the lateral extremities, one superior to the other. The superior nerve extends slightly dorsolaterally to the integument while the inferior one passes ventrolaterally to the appendages of the region (fig. 19, 20). Each of these bifurcates into two smaller nerves a short distance from the mass. Two other ventral nerves originate almost perpendicularly from the ventral side of the suboesophageal mass.

The ganglionic cell layers on the dorsolateral aspect of the fused portions also line the ventral side of the neuropile masses in these areas. Some neurons also line the neuropile of the nerves extending ventrally from the mass (fig. 20). The major tracts of fibers course directly through the mass and continue down into the connectives and ganglia of the ventral nerve chain. The axons of cell bodies on the periphery pass through the neuropile and out the lateral nerves that innervate the anterior appendages, integument and muscle bundles.

THE VENTRAL GANGLIA:

The number of ganglia in the ventral nerve chain corresponds to the number of body segments. There are eight thoracic and four abdominal ganglia in *G. setosus*. The connectives extending between the ganglia are adjacent but remain separate giving the ganglion chain a ladder-like appearance (fig. 21). The thoracic and abdominal ganglia differ in that the two lobes have fused into a single mass in the abdominal region (fig. 23, 26).

The thoracic ganglia generally appear bilobed when viewed dorsally or ventrally with slightly more of the ganglionic mass in the ventral portion (fig. 24a). They average 0.53 mm in width and 0.33 mm in length while the connectives average 0.13 mm in width. The length of the connectives is variable and great variation in ganglion morphology was observed both within and between individuals.

There is a layer of neuron perikarya on the ventral side of each ganglion as well as four dorsolateral groups, one in each free corner of the ganglion (figs. 22, 25). The neurons vary in size ranging from 7 to 35 microns in diameter and also vary in chemical composition as shown by the diverse array of color after staining with Hubschman's modified Azan technique for crustacean tissue. These cells are mainly unipolar with a rare bipolar example. The axons of these neurons pass through the fiber core of the ganglion and a number of axon collaterals arise before the main portion terminates or passes out of the ganglion often with a decussation (fig. 25).

The dorsolateral neurons send their axons out along the segmental nerve (fig. 21). These nerves are a bundle of axons sheathed in a glial cell wrapping and then tightly bound into a single unit by the fibrous connective tissue capsule secreted by the underlying perilemmal cells and continuous with that of the ganglion body (fig. 24b). The ganglion is a compact structure with extracellular spaces occurring largely in the cell layers (fig. 25). The segmental nerves are compacted and contain both sensory and motor axons, while the two main tracts entering and leaving the ganglion from the connectives consist of dorsal (mainly ascending) and ventral (mainly descending) tracts (Bullock & Horridge, 1965).

The thoracic ganglia have differentiated neuropile regions. There are two large lateral neuropiles into which the tracts of the segmental nerves merge along with the axons from the dorsolateral ganglionic cell layers (fig. 22c). Two parallel cylindrical neuropiles extend in the same direction as the longitudinal tracts of the connectives (fig. 22b) and are joined in the posterior part of the ganglion (fig. 22a). In cross section this portion of the neuropile appears arc-shaped.

The abdominal ganglia have undergone lateral fusion and taper posteriorly (fig. 27). The connectives have also fused to form a single structure and the once lateral segmental nerves now originate from an extreme ventrolateral position. The nerves that in the primitive malacostraca arise from a lateral position on the connectives, originate here from a ventral position (fig. 23). The neuropile in the ganglia has been rearranged with a large spherical mass found in the anterior portion of the ganglion. In the posterior portion there are two thin ovoid masses paralleling each other. The neuron layer is still ventral with some dorsolateral cells present especially in the anterior region (figs. 26, 27). The last abdominal ganglion is the largest and nerves radiate from its posterior region into the telson which is without a ganglion.

NEUROSECRETORY CELLS OF THE CENTRAL NERVOUS SYSTEM:

Two types of neurosecretory cells were distinguished in routine paraffin sections of the brain and designated type A and type B on the basis of perikaryon size. The shape of the perikaryon and morphology of the neurosecretory granules were not found to be useful guidelines in this study. The crowding of neurons into the glomerular layers accounts for the majority of variation in shape and routine paraffin sections do not sufficiently distinguish the condition of the neurosecretory material (NSM) within the perikaryon. The relative intensity of the stain in these sections was used as an indicator of secretory activity. In most cases the secretory material was found to be evenly distributed throughout the perikaryon differing only in density and staining intensity.

Type A neurosecretory cells are small, unipolar neurons 9 to 20 microns in diameter with a large nucleus and very little cytoplasm (figs. 28, 29). The neurosecretory material in these cells appears as a thin ring around the nucleus filling the cytoplasm between it and the cell membrane.

Type B neurosecretory cells are neurons 20 microns or larger in diameter. The cytoplasmic:nuclear volume ratio is much greater. The cells exhibit varying intensities of NSM staining usually distributed evenly throughout the perikaryon (fig. 29). The largest of these B cells are located in the posterodorsal portion of the anterior inferior medial glomerular bridge (aimgb) and are easily recognized by their unusually large size (48-58.5 microns in diameter) and staining intensity (figs. 30, 110a,b).

Thin section shows these B cells have a wispy, vacuolated cytoplasm and little nuclear chromatin during periods of peak synthetic activity (fig. 30). Observations on adjacent type A and B neurosecretory cells reveals an inverse relationship between the amount of chromatin and condition of the cytoplasm (fig. 29). Neurons with a good deal of dense chromatin have fairly homogeneous cytoplasm with few NSM-positive regions. Those with scattered chromatin have a more vacuolated cytoplasm (fig. 30a) while those with even less chromatin have a severely vacuolated cytoplasm and many NSM-positive granules scattered throughout the perikaryon (fig. 30b). Localization and identification of the neurosecretory cells in the glomeruli of the brain, suboesophageal mass and ventral ganglia is dealt with under the heading "Neurosecretion and Reproduction" (pg. 53).

ULTRASTRUCTURE OF BRAIN NEUROSECRETORY CELLS:

The perikarya in a glomerular layer are closely packed with 15-38 nm spaces between them. The vacant areas of thin section (fig. 28) are actually filled with large glial cell processes as well as axons (fig. 31). Each neuron is ensheathed by between 2-20 overlapping layers - processes from the surrounding glial cells. Trophospongia infiltrate the perikarya for distances up to one micron in the material examined. The trophospongia arise from the innermost layer of this glial sheath and the cell membrane is invaginated by this process but the two cells remain separated by their respective plasma membranes (fig. 31).

The individual neurosecretory and non-neurosecretory neurons differ appreciably in shape, cytoplasmic density and configuration of the endoplasmic reticulum (ER) as well as number of other synthetic organelles present. The nucleus is enclosed by a double membrane system 46-270 nm thick (fig. 35). The two membranes of this system are separated by an electron lucent space of 30-230 nm and is perforated irregularly by pores ranging from 90-260 nm in diameter. No fibrous lamella was observed beneath the nuclear membrane nor was any continuity between it and the cisternae of the rough ER in the sections examined.

The nucleoplasm is generally electron lucent with scattered electron dense particles that also form localized masses (chromatin). The chromatin tends to be condensed around the periphery of the nucleus as well as scattered throughout (fig. 31). The nucleolus has no membrane but is universally present being composed of chromatin granules in denser concentration than those of the nucleus.

Electron microscopy revealed production of two types of neurosecretory granules. Type I granules are small, dense spheres with no surrounding halo defining a limiting membrane (fig. 36). These granules range from 98-160 nm in diameter and occur in clusters of varying number scattered throughout the cell (figs. 34, 36). The density of the granule appears to increase with its size suggesting a maturation process. The granules are found to be in close association with active Golgi regions (figs. 35, 36) and areas of lesser density can be seen within the flocculent Golgi cisternae (fig. 36). Type I granules have been found primarily in the A cells of the brain but not in every example.

The majority of B cells and some A cells exhibit production of a second type of neurosecretory granule. The cytoplasm of these neurosecretory cells contains many spherical vesicles 195-815 nm in diameter (fig. 40). These vesicles are double membraned and have a variety of internal configuration and matrix density.

The cytoplasm of these cells contains a number of active Golgi dispersed throughout that are characteristically crescent shaped and large numbers of various sized Golgi vesicles radiate from their distal face (fig. 37). Short, dilated cisterns of rough ER, some so fragmented as to resemble microsomes, are scattered throughout the cell (fig. 38).

The cytoplasm is heterogeneous with definite electron lucent and dense areas due primarily to the distribution of the polyribosomes, Golgi and a variety of vesicles (figs. 39, 40). Distinct mitochondria are scarce and hard to distinguish among the numerous type II vesicles. (fig. 38). Single membraned residual bodies containing accumulations of cellular debris or lamellated fibrillar structures resembling fingerprints are present in the cytoplasm (fig. 40).

The type II neurosecretory vesicles are present throughout the perikaryon, axon hillock, axon and glial cell processes that encapsule the neuron (fig. 39). Migration of these vesicles into the glial processes appears to be through perikaryon release, especially in the region of the trophospongia. Both membranes break down allowing free passage of these vesicles into the trophospongia and along the glial cell process (fig. 39).

Neurons not actively involved in neurosecretory material synthesis have fewer Golgi regions and longer, randomly arranged cisternae of rough ER scattered throughout the cytoplasm (fig. 31). Ribosomes and polyribosomes are still found in the cytoplasm that has an overall homogeneous appearance in these cells (fig. 31).

Synthesis of type II neurosecretory vesicles is poorly understood with evidence present supporting two quite different modes of production. Nishiitsutsuji-Uwo (1960, 1961) working with a lepidopteran suggested mitochondrial fission as a source of the mitochondrion-like neurosecretory vesicles found in the neurosecretory neurons of that animal. The type II neurosecretory vesicles found in the neurons of *G. setosus* bear a striking resemblence to mitochondria (figs. 39, 40). These organelles have the characteristic double limiting membrane of mitochondria (58-60Å thick) and the wide array of their internal crests are of types not uncommon to that organelle. In some instances mitochondrial fission (fig. 40) and budding (fig. 33) have been seen.

The second, more recently described mode of synthesis deals with the formation of multivesicular bodies (MVB) by the Golgi and their subsequent transformation into neurosecretory vesicles. Authors such as B. Scharrer (1971) and Borg *et al.* (1973) have suggested this type of synthesis.

The distal face of the Golgi complex produces large numbers of Golgi vesicles ranging from 38 to 85 nm in diameter. These small vesicles appear to become encapsulated by a single limiting membrane forming a much larger vesicle, an MVB. The area between the internal vesicles becomes electron dense and the accumulation of these ultraparticles results in apparent distension of the smaller vesicles causing them to appear as tubular structures in some sections. A second inner membrane appears and gives the organelle its double membrane appearance (fig. 41). After this point the vesicles become more electron dense and continue to grow in size until they resemble mitocondria.

These type II vesicles extruded from the perikaryon through the cell membrane, or seen along the axons, are smaller but similar to those seen in the type I frontal organ neurons (fig. 64). These vesicles were also seen in the axons leading to these frontal organ neurons (fig. 68). These frontal organ type I vesicles could be the result of continued enlargement of the protocerebral, perhaps elementary, type II neurosecretory vesicles. The vesicles have perhaps undergone some form of maturation before their hormonal components are released.

ULTRASTRUCTURE OF GANGLIONIC NEUROSECRETORY CELLS:

The ultrastructure of the neurosecretory cells in the thoracic ganglia is strikingly similar to that of the protocerebral neurosecretory neurons. The most obvious difference is the common occurrence of elongated mitochondria in the perikaryon and axon of ganglion neurons. These mitochondria are present in various configurations, the majority having transverse or tubular crests (figs. 42, 45).

The cytoplasm contains free ribosomes, polyribosomes, scattered short dilated cisterns of rough ER and Golgi containing a flocculent matrix (fig. 42). Trophospongia are common and the neurons are encapsuled by layers of glial cell processes (fig. 43). There are many types of vesicles being produced by the Golgi regions including small dense core vesicles from 58-143 nm diameter and single membraned vesicles 131-442 nm in diameter containing a flocculent matrix (fig. 42).

Production of MVB's is evident (figs. 43, 44) and the presence of the type II mitochondrion-like neurosecretory vesicles was also noted (fig. 42). The transition from MVB to type II vesicle was more noticeable here as neurons in the early stages of NSM synthesis contained large numbers of MVB's as well as double membraned MVB-like vesicles (fig. 43). Neurons in later stages of synthesis contained this double membraned type of MVB but the internal matrix appeared somewhat denser (fig. 46). By the time the vesicles reached the axon hillock they were well into their maturation phase and bore a striking resemblence to mitochondria (fig. 42).

ACCESSORY CEPHALIC STRUCTURES:

THE SINUS GLAND:

The sinus gland of *G. setosus* is an ovoid mass of tissue at the end of a thick stalk composed of a large number of cell bodies. The overall projection averages 580 microns in length and 175 microns in width. The structure lies slightly lateral and caudal to the medulla externa of the optic lobe arising from the optic lobe glomeruli (figs. 2, 47). The cellular stalk projects from the posterolateral aspect of these glomeruli at the lateral extremity of the protocerebral optic lobes and it appears curved with the concavity directed medially and ventrally. The sinus gland lies in the general plane of the body.

Its globular form is surrounded by a smooth envelope of fibrous connective tissue continuous with that of the optic lobe of the brain mass. This sheath is cyanophilic when stained with a trichrome dye. The gland is packed with cells that have large nuclei and are relatively poor in cytoplasm (fig. 49). PF and CHP-positive material can be seen within the perikarya at various times of the physiological cycle which will be defined later (fig. 48). The fiber mass of the sinus gland has a texture similar to that of the adjacent optic lobe (fig. 49).

The sinus gland has been termed an accessory cephalic structure rather than a simple projection of the nervous system in this study because it deviates from the rind/core arrangement found throughout the nervous system of the amphipod. The regions are more interspersed in this structure (figs. 49, 50). The fiber section appears vacuolated in this section in the proximal portion and more compact in the distal portion of the sinus gland (fig. 49).

In the concavity between the sinus gland and the optic lobe of the protocerebrum there is a nucleated tissue pad formed from the cellular components of the adipose connective tissue that supports the brain (figs. 49, 50). It appears to function as a cushion helping to hold this delicate projection in place. There are many other points of attachment with the adipose connective tissue network along the capsule of the sinus gland and these further facilitate support (fig. 49).

THE FRONTAL ORGAN:

The frontal organ of *G. setosus* is a simple sac-like mass of cells just under the hypodermis in the anterior dorsomedial region of the head cavity (figs. 1, 51, 53). The organ has a wide dorsal dimension extending both laterally and posteriorly. It is defined by a connective tissue membrane that sets it off from the interior region of the head (figs. 53, 54). On each side the hypodermal lining of the head region forms a canal with a sac on the end that grows ventrolaterally to engulf the eye. From its laterally convexed dorsal base it tapers in all directions resembling an inverted cone with a slightly concave surface. The frontal organ is bounded posteriorly by the web-like adipose connective tissue network that supports the brain mass (fig. 59).

Where the ventrally sloping boundaries of the frontal organ come to its vortex, an unpaired, relatively thick cord connects its body to a dorsomedial point on the protocerebrum (fig. 51). The cells of this organ have been previously described by Thore (1932) in *G. pulex* and *G. locusta* as nerve cells with axonal processes. The axons of these neurons pass ventrally from the frontal organ into the layer of ganglionic neurons in the central region of the protocerebrum. This ganglionic layer splits itself into the lateral and medial anterior inferior and anterior superior glomeruli which cover the surface of either side of the fiber core's central depression (figs. 3, 4). This medial frontal organ nerve appears to be double-rooted, originating from both sides of the protocerebrum and the branches are pulled together near the base of the origin of the antennary I nerves. Both parts arise behind and beneath the dorsal ganglionic cell layers of the anterior part of the protocerebrum (fig. 52).

Within the frontal organ extend thin, perpendicular connective tissue strands to which chromatin-rich, cytoplasm-poor and granule-laden neurons are attached (fig. 55). They cling to these strands in rosette clumps resembling grapes on a vine. The spaces between the cells is filled with a flocculent material tinctorially similar to the blood within the dorsally located heart found just posterior to this (fig. 56). Since the dorsal aorta empties into the head region just behind the brain, this could indeed be a blood sinus. The granules seen within the cells are of varying sizes and are CHP, PF and PAVB-positive. They appear to be NSM and the frontal organ of *G. setosus* may be a neurohemal organ (fig. 56).

THE STATOCYSTS:

The statocysts are paired structures in the dorso-anterior portion of the head in *G. setosus* (figs. 1, 54, 59). They are immediately in front of and above the eye and on each side of the posterior portion of the frontal organ. They lie obliquely with the dorsal tips pointed inward toward the medial frontal organ. Dorsally they slope forward to the hypodermis and ventrally to the eye forming an excretory duct. At any point they are roughly egg-shaped in cross section with the widest portion directed inward (fig. 62). In longitudinal section the statocyst is bag-shaped, tapering drastically at the dorsal end while the ventral end is more rounded (fig. 60). The medial part is connected to the brain by a large nerve (figs. 57, 62b). The statocysts are about 350 microns long and 120 microns wide in average sized females.

The external membrane of the statocyst is very thin. In paraffin sections its pattern is irregular (fig. 61), but in thin section it appears smooth (fig. 62). Within the membrane the wider innermost portion of the statocyst is lined by a layer of sensory neurons (Thore, 1932), and lateral to this is an intensely staining structure, the statolith (figs. 60, 61, 62).

Within the statocyst, along the widest portion, an extremely thin membrane parallels the outer one creating a crescent-shaped chamber (fig. 62c). This chamber is of varying length and width depending upon the diameter of the statocyst at that point. It contains the sensory neurons whose axons pass ventrally via the statocyst nerve to the most dorsal tip of the protocerebrum (figs. 57, 58, 62b), where they penetrate the medulla terminalis. In thick section the axons appear to spiral so that each neuron seems to be encapsulated by its own axon - similar to that seen in the spinal ganglia of vertebrates (fig. 61). In thin section the neurons appear to be embedded in a homogeneous matrix and the axons cannot be distinguished. Only in a few instances the neurons appear to be situated in a vacuole (figs. 62b,c).

In the mid region of the statocyst a stalk arises from this neuronal layer connecting it with the statolith (figs. 62b,c). The statolith gives the statocyst its form and overall shape. It is a spindle-shaped structure tapered at both ends and ventrally elongated into a stalk that extends deep into the ventral region of the statocyst (fig. 60). In *G. setosus* the statolith is medium-sized with ample space between it and the statocyst wall. In thick section it has a striped appearance and resembles a muscle bundle (fig. 54).

When viewed in thick cross section, the statolith has an irregular shape with a homogeneous core (fig. 61), but in thin section at least three different regions can be distinguished by textural differences (fig. 62c). The inner core is very dense and bounded irregularly by a lighter region. On the very edge of the statolith large vacuoles bounded by this lighter outer layer are found. Two different homogeneous tissue types compose the statolith. Septa forge their way into the core giving the statolith its striped or lobulated appearance in thick and thin sections respectively.

In the dorsal region of the statocyst, the statolith loses its differentiated appearance and becomes web-like, stretching out and filling the entire area (fig. 62a). The neuronal layer is absent from this portion. In the most ventral parts of the statocyst, the statolith maintains its zoned appearance becoming more organized but with no vacuolation of the outer layer (fig. 62d).

The statolith is a living/tissue in *G. setosus* as nuclei appear on the outer membrane of the vacuolated region. There are anywhere from four to six of these nuclei along the length of the statolith (figs. 62b, c). They are scarce in the extreme dorsal and ventral sections, being more common in the mid region of the statolith. The statocyst of the gammarids function in integrating balance and orientation (R. Barnes, 1963), and the statolith is probably secreted as the external duct is not visibly open nor large enough to facilitate the uptake of sand grains to be incorporated into this structure.

CELLS OF THE FRONTAL ORGAN:

During the morphological study of accessory cephalic structures in the head of *G. setosus*, large, dark, PF-, CHP- and PAVB-positive granules were observed in the perikarya of the frontal organ neurons (fig. 56). In routine thin section these granules were as strongly basophilic as the nuclear chromatin when stained with toluidine blue pH 11.- (fig. 63a). The granules were epoxy PF-positive wheras the chromatin did not stain (fig. 63b). In control epoxy PF sections (omitting the permanganate oxidation) the granules were not stained and could not be distinguished but the chromatin was distinctly stained (fig. 63c).

After examining the frontal organs of females in differerent physiological stages of their annual cycle, it was evident that there are two types of frontal organ neurons and they exhibited two extreme morphological conditions; empty and full. Type I neurons contain from 10-15 extremely large granule-packed vesicles, 1.2-4.5 microns in diameter that almost obliterate the cytoplasm (fig. 64). When the cells vesicular contents are released, large empty vacuoles, equal in size to the released vesicle, are left in the cytoplasm (fig. 65). When viewed under low light intensity, pale "ghost" granules can be distinguished in the empty vacuole (fig. 66b).

In animals where the majority of the frontal organ neurons were in the empty state, a second cell type (type II) was found. These differ from cell type I in the content of large numbers (75-90 per cell) of much smaller (0.20-0.85 microns in diameter) epoxy PF-positive granules (fig. 66).

Both cell types were studied in electron microscopy (fig. 67). They are generally spherical to ovoid and occasionally periform with processes. Each has an axon arising from the perikaryon enveloped by an irregular glial sheath varying from 96-270 nm in thickness (fig. 68). Neurofilaments are common and extend for great distances along the axon (fig. 70). Vesicles can be seen in various locations throughout the axons and perikarya of both types (figs. 67, 68).

Type I neurons show very little cytoplasm when filled with vesicles and that present is amassed around the nucleus. Some nuclear chromatin is condensed around the periphery of the nuclear membrane. There are large nuclear pores 95-270 nm in diameter, spaced irregularly so that the electron lucent nucleoplasm appears confluent with the cell cytoplasm (fig. 76). The double nuclear membrane is discontinuous in the regions of the nuclear pores. The inner component of this double membrane system is more regular than the outer, the space between them ranging from 35-115 nm. The outer membrane is studded with ribosomes and may be continuous with the rough ER system of the cell (fig. 71).

Type I neurosecretory vesicles have a spherical configuration during the early accumulative stages but by the time they are released they have become compacted into ovoids and various other shapes (fig. 73). In the earlier stages, the vesicles resemble mitochondria in orthodox configuration. They appear to have a double membrane and mitochondrial crests (cristae) project short distances into the finely granulated matrix (figs. 70, 71). As the vesicles enlarge there is an increase in the number of smaller granules within the retaining vesicular membrane. The rough ER is closely associated with the vesicles during the maturation phase (fig. 70). In a fully mature state the vesicles become more electron dense and the crests are no longer visible in the granular matrix (figs. 72b, 73). The tiny granules of the matrix range from 6-10 nm in diameter (fig. 72b).

These granule-laden vesicles eventually either push their way to the cell boundary or expand outwards to meet it. The cell membrane has a configuration similar to the typical unit membrane seen in the protocerebral and ganglionic neurons (fig. 72a). When the mature vesicles come into contact with the cell membrane prior to the release of its granular contents, the membrane becomes indistinct, without any particular configuration and the limiting membranes of the vesicle also disappear (fig. 72b). The cytoplasm is pushed back around the nucleus and contains free ribosomes, scattered rough ER and flattened Golgi cisternae. The vesicles eventually push their way through the cell boundary and the finely granulated contents diffuse into the surrounding sinus (fig. 74).

The empty vesicle retains its shape after release of the contents, possibly by an influx of the sinus fluid (fig. 75). None of the ghost granules of light microscopy were seen in the empty vesicle when examined in electron microscopy. Only a small number of unextruded granules remain in the vesicles (fig. 75). The vacuolated vesicles eventually shrink and the cells appear to have many more cellular organelles actively involved in new neurosecretory vesicle formation (fig. 69).

Active Golgi regions with dilated cisternae are seen forming large numbers of Golgi vesicles - or elementary neurosecretory vesicles (figs. 69, 75). These single membraned vesicles are pinched off the dilated, sac-like ends of the distal regions of the Golgi. These vesicles enlarge and become filled with a finely reticulated matrix of tiny granules. This matrix becomes denser as the vesicles enlarge and a double membrane appears.

The mitochondria at this stage are large and faintly delineated with an electron lucent flocculent matrix (fig. 76). The matrix also appears to become denser and they may swell into the orthodox configuration possibly accounting for the mitochondrion-like appearance of the maturing neurosecretory vesicles (fig. 70). Rough ER becomes much more abundant and may be arranged in lamellated stacks in the cytoplasm in close association with the maturing vesicles as well as the nucleus (fig. 69).

Type II neurons contain a large number of the smaller, more dense vesicles with no mitochondrion-like crests (fig. 67b, 78). There are numerous small Golgi from which vesicles with finely granulated contents, but no delineating membrane, seem to have arisen (fig. 78c). The vesicles increase in number, size and density of their granular contents. Those vesicles that become homogeneously dense have a double limiting membrane similar to the type I vesicles (fig. 78). This gradation in vesicular size, density and presence of a limiting membrane suggests that the formation of the membrane is a step in the maturation of the type II frontal organ neuron neurosecretory vesicle.

The cell boundary is similar in morphology to that described in the type I neurons. Actual release of the vesicles was not observed in the material examined. The vesicles however, were not grouped near the cell boundary but dispersed throughout the perikaryon (fig. 67b). This suggests a gradual release of the neurosecretory vesicles from the type II neurons.

The cytoplasm of the type II neuron is coarse and disjunctive containing more organelles than the type I neuron. The mitochondria are smaller and have a pale, flocculent matrix. Rough ER is present in shorter cisterns than in the type I neuron while the free ribosomes are in dense clusters interspersed between the vesicles (fig. 78c). The cyclic neurosecretory vesicle formation and release phenomena of the type I and II frontal organ neurons is outlined under "Neurosecretion and Reproduction" (pg. 53).

THE OVARY:

MORPHOLOGY:

The ovary of *G. setosus* is similar in morphology to that of *Gammarus duebeni* (LeRoux, 1933; Steele, 1964) and *Orchestia gammarell* (Charniaux-Cotton, 1960; Meusy, 1963). These paired organs are dorsolateral to the digestive tract and extend from the second thoracic to the first abdominal somite. Each is cylindrical in shape connected to the other in the midline and attached laterally by adipose connective tissue to the hepatopancreas (hepatic caecae). Additional connective tissue membranes extend to the anterior and posterior regions functioning as suspensory ligaments. The ovarian volume increases between broods and following ovulation the ovaries appear as two parallel narrow bands. An oviduct is attached to the inferior part of each ovary in the fifth thoracic somite and extends posteriorly and obliquely to the inner ventral side of the fifth epidermal plate at the base of the oostegite.

At the point of junction between the ovary and the oviduct and extending about half-way down the oviduct is a large mucous-secreting gland. The oviducts are blocked either by the eggs pending their release or by a mucous plug secreted by this gland between ovulations (fig. 80). Ovulation is preceded by the release of an albuminous substance secreted by the mucus cells in the oviduct. The substance coagulates on contact with water forming a temporary capsule around the eggs. The sac disappears within hours of ovulation and may serve to protect the eggs in their most critical stages just after final maturation and through fertilization.

The mucous secreting columnar epithelial cells seen in this gland exhibit three main phases of activity corresponding closely to those described by LeRoux (1933) in *G. duebeni*. (1) The preparatory stage begins three or four days after ovulation and continues until the onset of the successive ovulation. The cells have a finely reticulated cytoplasm and the nuclei are situated near the base of the cells. (2) The secretory phase is identified by the accumulation of secretory droplets in the cytoplasm of the cells. The cell boundaries become indistinct and the outer surface of the droplets appears finely reticulated. The droplets shrink when treated with an acid fixative and stain strongly with eosin and phloxine but are not differentiated with mucicarmine. (3) The excretory phase is of short duration beginning with the arrival of the first oocyte in the oviduct and terminating with the passage of the last oocyte. When ovulation terminates the cells are empty of secretory material.

GLANDS:

In the sagittal plane of the ovary, triangular wedges of connective tissue extend up and around the oocytes dividing the ovary into compartments. An occasional lipid droplet is embedded in the tissue as well as many types of cells (fig. 82). In some areas the cells are indistinct and only the elongated nuclei can be distinguished (fig. 81) while in others the cells are quite distinct with a nucleus and granule-laden cytoplasm (fig. 82). Some of these granule-filled cells have tail-like processes resembling axons or pseudopodia suggesting a possible neuronal character (fig. 83). The granules stain deeply with toluidine blue and are PF-positive as well (fig. 83). These cells could be the source of the ovarian hormone that controls female sex characteristics in crustaceans but this remains to be investigated.

Some of the other cells in these septa resemble those seen in lobular sac-shaped glands found in close proximity to the hepatopancreas and ovary as well as in other scattered areas of the body cavity. These glands bear a striking resemblance to the mucous Bowman's glands in the olfactory epithelium of vertebrates, even in dimensions (fig. 84). Each consists of approximately 25 cells and is divided into as many as six lobes. The cells will not take up routine mucous stains such as mucicarmine but stain with toluidine blue and are PF-positive (fig. 85). The glands have ducts extending deep into folds and surface concavities of the hepatopancreas. In these areas the cells release their granules and appear vacuolated (fig. 85). The released material is taken into the hepatopancreas by pinocytosis (fig. 86). The droplets are homogeneous dense bodies with no limiting membrane and average 62 nm in diameter. The rest of the cytoplasm of these granule-carrying cells is void of any great accumulation of organelles except for scattered bits of dilated rough ER (fig. 87).

OOGONIAL DEVELOPMENT:

In *G. setosus* oogonial development proceeds as localized egg formation within a well defined gonad. By longitudinal extension of the gomad, cylindrical ovarioles are formed. In many other invertebrate groups the ovaries are solid but those of *G. setosus* have a lumen early in oogenesis which is later obliterated by rapid yolk deposition and oocyte enlargement. Oogenesis can be classified as localized alimentary egg formation (Raven, 1961) and can be divided into three phases.

PHASE I: FORMATION OF OOGONIA.

The ovarian wall is lined internally by an epithelial layer and covered externally by a thin tunica propria. The oogonia are produced from the epithelial cells and are surrounded by connective tissue and a few small follicle cells (fig. 88, 89). The primary oogonia are formed within the ovarian epithelium layer at the inner portion of the ovary and they give rise to successive groups of secondary oogonia. There are one or more rows of oogonia maturing simultaneously, the number depending upon the size of the female (fig. 89).

This initial phase begins with the formation of the oogonia but growth is very weak and almost imperceptible. A sequence of pre-meiotic phenomena occurs (Raven, 1961) within the nucleus at the end of which the oogonium is pushed out into the lumen of the ovary by the proliferation of new primary oogonia in the inner region of the ovary. The undeveloped oogonia are small (0.05-0.10 mm), roughly spherical with a central nucleus and contain no form of yolk granules (fig. 88).

PHASE II: OOGONIAL GROWTH.

The second phase is one of relatively slow growth extending over most of the year. The developing oogonia have little cytoplasm and LeRoux (1933) reported the appearance of mitotic figures within the nucleus of oogonia in *G. duebeni*. The oogonia darken as they enlarge and become oblong and roughly rectangular in shape with a central nucleus. The growing oogonia are accompanied by follicle cells that lie around their periphery and play an important role in nutrition (fig. 89).

During oogonial development, the follicle cell undergoes a series of morphological changes. The nucleus is large and contains a great deal of RNA indicating some degree of activity. The cytoplasm is strongly basophilic nearest the ooplasm when stained with PF. Dilated Golgi and rough ER as well as numerous mitochondria accumulate in this region. Extrusion of the follicle cell through the zona radiata of the oocyte was observed in the form of cytoplasmic connections extending from the follicle cells with disintegrated cell membranes (figs. 92, 93).

During the first two phases of oogonial development the morphology of the follicle cell changes only slightly. The membrane of each cell is well defined and only a slight enlargement of the oogonia causes a minimal degree of stretching of the follicle cell (fig. 90). At this point ~~the main~~ role of the follicle cell is to protect the oogonia (Raven, 1961).

PHASE III: VITELLOGENESIS.

The oogonia finally enters the phase of rapid enlargement and within a period of weeks (8-10) reach their full-term size. During this phase the bulk of the yolk is deposited and it is termed the period of vitellogenesis. The mature oocytes are compressed by crowding within the ovary and the nucleus becomes ventrally displaced lying adjacent to the vitelline membrane (fig. 101n) while the cytoplasm is packed with proteinaceous yolk granules, lipid globules and interspersing polysaccharide material. The number of follicle cells seems to increase in this phase and they become widely spaced along the periphery of the oocyte at irregular intervals (fig. 90).

The follicle cell begins to alter its morphology to accept the additional role of nutrition as the oocyte enters vitellogenesis. The cell membrane becomes indistinct and begins to disappear and the cells coalesce into a continuous band of multinucleate cytoplasm about one micron thick which completely surrounds the oocyte (fig. 91). The cytoplasm becomes filled with granules of various shapes, sizes and densities, numerous mitochondria, dilated Golgi and rough ER. The cell membrane on the external surface of the follicle cell and on the side adjacent to the ooplasm is entirely lacking so that free passage of materials into the oocyte becomes possible (figs. 92, 93).

As deposition of the yolk nears completion, the follicle cell becomes fusiform with its thin extremities stretching out to form a syncytium with the next one and the nucleus forms the thicker "belly" of each cell. The cell membrane has reformed and becomes distinct (fig. 90). At the end of vitellogenesis the cytoplasm is practically obliterated as a result of resorption by the oocyte as well as stretching of the outer layer of cells effected by the gross enlargement of the oocyte. At this point a follicle cell seen in thin section appears as a nucleus surrounded by a minimal amount of cytoplasm embedded in an indentation of the peripheral area of the oocyte's yolk mass (fig. 90).

The oocyte of *G. setosus* is isolecithal and three main yolk components can be distinguished in varying amounts: carbohydrate, lipid and protein. The *Gammarus* oocyte is rich in polysaccharides present in the form of granules scattered throughout the ooplasm. The polysaccharide granules arise in the peripheral zone of the ooplasm and then extend centripetally, dispersing throughout the oocyte as ooplasmic vacuolation begins (fig. 99c).

The lipid component of the yolk is deposited after the carbohydrate portion but usually before the protein yolk - somewhere in the last half of vitellogenesis. Lipid globule formation was not observed but transfer of lipid droplets from the hepatopancreas to the ovary is shown in figure 96. The close proximity of the two organs, as well as the presence and apparent cyclic nature of lipid storage in the hepatopancreas helps to substantiate this theory of synthesis (fig. 94).

The hepatopancreas is rich in lipid globules, polysaccharides (PAS-positive reaction) and granular PF-positive protein material (figs. 95, 98). Electron micrographs reveal a dense lamellar arrangement of rough ER in the secretory columnar cells of the hepatopancreas as well as numerous mitochondria of varying lengths that help to account for the protein synthetic activity (fig. 79). The lipid globules become evenly distributed throughout the oocyte, interspersing with the already present polysaccharide yolk granules (fig. 94).

The protein yolk components are incorporated into the maturing oocyte during the last phase of vitellogenesis. These small granules accumulate near the cell membrane and then spread through the ooplasm filling the spaces between the lipid and carbohydrate yolk granules (fig. 97a). The protein granules are much smaller in size, infilitrating the ooplasm and gradually filling the spaces with a solid protein mass (fig. 97b). The protein granules stain with PF and the intensity of the staining becomes stronger as vitellogenesis nears completion. The percentage composition of the mature oocyte yolk is approximately 2:2:1 in order of occurrence.

THE OVARIAN CYCLE:

The stages of ovarian maturation in *G. setosus* were defined by examination of paraffin sections of females collected during various months of the year at Witless Bay, Newfoundland. The oogonia and oocytes were measured in sagittal and frontal sections although in stages of late maturation heavy yolk deposition made sectioning difficult. Sections greater than 15 microns are necessary in these cases but are of little use in cellular detail. Not all the oocytes in the ovary are at the same stage at the same time. The stage of maturation was determined by the stage of the majority of oocytes in an ovary.

Oogonial and oocyte maturation stages were determined for *G. setosus* by Steele & Steele (1970). The measurements for oogonia in stage 1 (S_1), were modified in the appearance of the oogonia and oocytes in histological sections is added to the previous information and shown in table 1.

Approximately two to three weeks before ovulation the male will couple with a selected female (precopula). The female undergoes the pre-reproductive moult assisted by the male and immediately following this ovulation occurs. The oocytes are expelled into the brood pouch for fertilization. This occurs sometime between late September to December at Witless Bay and in the laboratory usually at night or early morning.

Following ovulation it is not clear whether the secondary oogonia remaining in the ovary begin maturation and the rate appears slow due to low ambient temperatures or are hormonally inhibited until release of the hatched young. A small but steady increase in size is experienced by the oogonia. They appear cuboidal to rectangular with a well-defined nucleus, nucleolus and dense, solid ooplasm surrounded by a thin oogonial epithelium (fig. 101a-d). The oogonia remain in stage 1 until late spring. In May as the temperature rises oogonial growth proceeds at a quicker pace (fig. 101e) and by late May the increase is steady (fig. 101f).

From late June to July, the oogonia reach 0.20 mm and yolk deposition begins (fig. 101g-i). Stages in vitellogenesis are pictorially represented in figure 99. The oogonia are now referred to as oocytes. Yolk deposition is preceeded by the appearance of small vacuoles in the peripheral region of the homogeneous ooplasm. Within the nucleus there appears to be some degree of activity marked by the appearance of phloxine-positive granules (fig. 99b). Yolk is first deposited around the periphery of the oocyte, this activity initiating stage 2 (figs. 99c, 101i). From here the stages of the oocytes are determined mainly by size and the position of the nucleus.

Throughout July and August the oocyte continues to enlarge through to stage 3 and the ooplasmic vacuolation increases (fig. 99d). It now has a web-like appearance resembling adipose connective tissue with small yolk granules on the tissue webs and larger granules concentrated inside the vacuoles (fig. 99e).

The most rapid period of oocyte growth is in August when the yolk deposition is very heavy (fig. 101j,k). The oocytes pass rapidly through stages 3 and 4. At the end of August the oocytes are between 0.35 and 0.48 mm and contain a dense concentration of yolk granules. Stage 4 is recognized by its size and yolk concentration as well as a slightly eccentric position for the nucleus (figs. 101k,l).

When the females enter precopula the oocytes are in stage 5. recognized by a size of 0.50 mm or more and the nucleus abutting on the ventral periphery of the oocytes to facilitate oncoming fertilization (fig. 101n). The next generation of oogonia can be seen squeezed against the inside wall of the ovary (fig. 99b).

Following ovulation which occurs sometime between late fall and early winter, the secondary oogonia left in the ovaries exhibit a minimal degree of enlargement due mainly to the effect of the low incumbent temperature and possibly hormonal control. After the release of the brood from early winter on, the female enters a period of reduced physiological activity - the resting stage. Inhibition of active oogonial growth continues and may again be under the influence of temperature or hormones or both. The annual gonad maturation cycle of G. *setosus* at Witless Bay, Newfoundland is shown in figure 102.

EFFECT OF PHOTOPERIOD ON THE OVARIAN CYCLE:

FIELD:

The correlation between average hours of light per day per month and increase in oogonial and oocyte size in females at Witless Bay is shown graphically in figure 103 (and tables 2 & 3). It appears that the period of rapid oocyte enlargement (vitellogenesis) occurs during the months of decreasing photoperiod suggesting that a decrease in day length stimulates ovarian maturation.

EXPERIMENTAL:

Photoperiod has been shown to have a definite effect on the ovarian cycle of *G. setosus*. Subjecting groups of females to one of the four photoperiods; 8, 12, 14 hours light, complete darkness or a combination of these, resulted in deviations from and variations of the normal ovarian cycle as shown in figures 104-108.

The experiments were based on placing females, usually without males, into a photoperiod for various lengths of time at different physiological stages of their annual cycle. Males were generally excluded so females would not ovulate and carry embryos but rather enter the successive ovarian cycle following oocyte resorption. Experiments in which males were included showed that their survival rate was extremely poor in comparison with that of the female. Sampling of the animals was conducted after an acclimation period of at least two weeks.

Ovulation rarely occurred after the completion of ovarian maturation and resorption was the most common method of disposal of full-term oocytes from the ovary. Yolk resorption is first evidenced by vacuolation of the dense yolk granules within the stage 5 oocytes (fig. 100a). This is followed by resorption of the remaining ooplasm resulting in a collapse of the oocyte epithelium which has become shrunken and irregularly shaped. A total disintegration follows and the ovary appears full of scattered yolk granules, bits of oocyte epithelium, nuclei and other cytoplasmic material (fig. 100b). The young, healthy stage 1 oogonia can be seen lining the inside wall of the ovary amongst the deteriorating mass of ovarian material. The oogonia begin their normal maturation and enlargement cycle once the majority of the debris has been resorbed (fig. 100c). The first two stages of oogonial development proceed at a much faster or slower rate than observed in females at Witless Bay, depending upon the photoperiod. Once this resorption cycle has begun it cannot be stopped and will go on to completion before a new oocyte cycle can begin.

In the graphs illustrating the experimental results (fig. 104-108), the ordinate represents mean oogonial size of oocytes from stage 1 through resorption of stage 5 oocytes (0.10-0.50 mm), back to stage 1 of the successive cycle. This allows a direct comparison to be made between two or more groups in the form of a single line. In cases where the animals of a particular sample were between cycles, *ie.* some with resorbing stage 5 oocytes while others have enlarging stage 1 oogonia, a sample range was used to plot the results (figs. 106-108). By using the difference between the two means a more accurate position in the cycle was obtained. In all cases the mean oogonial size was used to plot the results and the values were derived from measurements of the oogonia found in paraffin sections of each female.

The first set of experiments was to determine the influence of the four light conditions on females in resting stage. The animals were sampled at two intervals after acclimation to the photoperiod: 31 and 79 days. Figure 104 (and table 5) show that a decrease in photoperiod caused an increase in the oogonial growth rate and that the difference between animals kept in the four photoperiods becomes greater the longer they are exposed. The females kept in constant darkness had the greatest ovarian growth rate while those exposed to 8, 12 and 14 hours light had a substantial decrease respectively in that order.

In the second experiment, the two extreme photoperiods, complete darkness and 14 hours light were used. The females were intially subjected to the experimental photoperiod in their final stages of ovarian maturation (S_{4-5}) and sampled at greater intervals - 121, 150 and 165 days. The results of this experiment are shown graphically in figure 105 (and tabel 6). Those animals kept in constant darkness had completed the successive ovarian cycle by 150 days and had just entered their third after 165 days. The animals kept in 14 hours light matured considerably slower and after 165 days were only in mid maturation (S_3) of the first successive cycle.

In the third experiment females in mid maturation stages (S_{3-4}) of ovarian development were exposed to one of the four photoperiods for 165 days. Figure 106 (and table 7), show the influence of photoperiod on the rate of ovarian maturation. The animals kept in constant darkness were almost a full cycle ahead of those exposed to 14 hours light. The animals in 12 and 8 hours light had an increase in ovarian growth as the photoperiod decreased.

The second set of experiments demonstrated the effect of photoperiod changeovers. The females were subjected to a given photoperiod and after a period of time a portion of the animals were sampled and the remainder placed into a different one. After a further time lapse the animals were sampled. In the first experiment a group of females was placed in complete darkness for 117 days, the survivors sampled and the remaining divided up into one of the other three photoperiods: 8, 12 or 14 hours light. After 14 days the animals were sacrificed and the change in ovarian growth is shown in figure 107 (and table 8). After 117 days the animals had progressed from the initial stages of late maturation (S_{4-5}) to the same stage in the successive cycle with a mean oocyte size of 0.52 mm. After plotting the sample range for the mean oogonial size of the females in each photoperiod, the graph showed a decrease in maturation in each case corresponding with an increase in photoperiod length.

In the second experiment the animals were first exposed to a 14 hour photoperiod for 117 days and then transferred to one of the remaining photoperiods. The results are shown graphically in figure 108 (and table 9). After 117 days the females had progressed from the initial stages of late maturation (S_{4-5}) to a stage of mid maturation (S_{3-4}) in the successive cycle with a mean oogonial size of 0.35 mm. After exposure to the second photoperiod, which in all cases was shorter than the first, there was a defined increase in the ovarian maturation rate. The greatest increase corresponded with the shortest photoperiod.

Observations on the ovarian cycle of females at Witless Bay revealed that decreasing photoperiod probably stimulated initiation of rapid ovarian maturation (vitellogenesis). The experiments performed in the laboratory confirmed this theory. The longest photoperiod available was 14 hours light and it showed a marked inhibitory effect on maturation while complete darkness had a stimulatory effect, resulting in successive reproductive cycles. Those photoperiods between the two extremes inhibited ovarian maturation in proportion to the day length.

The oogonia of *G. setosus* do not normally develop to any great degree while the embryos are in the brood pouch. After release of the young and the subsequent post-reproductive moult, the females at Witless Bay enter resting stage. This condition is characterized by the loss of the ovigerous setae from the oostegites and a lull in reproductive activity evidenced by minimal ovarian development.

Approximately 95% of the females in the photoperiod experiments had no setae on their oostegites when sampled. This may indicate that the pre-reproductive moult, as well as ovulation, is dependent upon the presence of the male.

Both ovarian development and incubation period for the embryos in *G. setosus* are influenced by temperature. By comparing females kept in the laboratory at 10°C to those kept at the MSRL and subjected to seasonal sea water temperatures during the year, it could be seen that low temperatures retarded both ovarian and embryonic development. Differences in reproductive timing can also be seen by comparing the reproductive activity and the incumbent temperatures for two successive breeding years at Witless Bay (figs. 103, 109 and tables 2, 3 & 4). The difference between the peaks of brood production for these two years was derived from figure 102 and was about one month later in 1973. The results suggest that if the female is kept in temperate water and exposed to a shorter photoperiod, more than one brood per year can be induced.

NEUROSECRETION AND REPRODUCTION:

NEUROSECRETORY CELLS OF THE BRAIN, SUBOESOPHAGEAL MASS AND VENTRAL GANGLIA:

Examination of the brain, suboesophageal mass and ventral ganglia of females during various months of their annual cycle revealed a seasonal variation of activity in the neurosecretory cells of the glomerular layers. Stain intensity and number of stainable cells were the criteria used to determine the degree of neurosecretory activity at the various intervals.

NEUROSECRETORY CELLS OF THE BRAIN:

NEUROSECRETORY CELLS OF THE PROTOCEREBRUM:

The majority of neurosecretory cells in the protocerebrum are found in the anterior inferior medial glomeruli and the anterior inferior medial glomerular bridge in the region between the fibrous humps of the protocerebrum (figs. 110a-f) and are concentrated in the posterior dorsolateral portion of this bridge (figs. 110a,b). The most constant features of this region are the two large B cells of the anterior inferior medial glomerular bridge (aimgb). Neurosecretory B cells are also common along the borders of this bridge.

Neurosecretory A cells are dispersed throughout the anterior inferior lateral (ail) and anterior superior lateral (asl) glomeruli (figs. 110a-c) and are occassionally seen in the optic lobe glomeruli (olg) extending from the optic lobes of the protocerebrum to the eye (fig. 110c). A few are seen in the ventral part of the anterior inferior medial glomeruli (aimg), (figs. 110d-f). The greatest accumulation of neurosecretory neurons appears to be localized in the dorsoposterior portion of the anterior superior medial glomeruli (asmg). B cells are relatively scarce in this glomeruli but those present are scattered throughout as well as around the periphery. Figure 111a shows the location and type of neurosecretory cells present in the protocerebrum of *G. setosus* at peak periods of activity.

NEUROSECRETORY CELLS OF THE DEUTOCEREBRUM:

Compared to the protocerebrum, the deutocerebrum is relatively poor in glomerular layers and also in numbers of neurosecretory cells. The posteriorly located superior lateral posterior glomeruli (slpg) contain a few cells of both types. The A cells are more numerous (figs. 110g-h). The posterior part of the olfactory lobe glomeruli (oflg) have the largest concentration of neurosecretory cells in this brain region (figs. 110i-l). These glomeruli contain fair numbers of both A and B cells. The inferior lateral glomeruli (ilg) have very few neurosecrerory cells and those present are type A (figs. 110 l-h). Figure 111b shows the location and type of neurosecretory cells present in the deutocerebral glomeruli of *G. setosus* at periods of peak activity.

NEUROSECRETORY CELLS OF THE TRITOCEREBRUM:

In the tritocerebrum the neurosecretory cells are confined to the inferior medial (img) and inferior lateral (ilg) glomeruli. A cells predominate in the inferior medial glomeruli (figs. 110m,n) and in the inferior posterior glomeruli (ipg) where they are arranged in a row along the lateral aspect of the tritocerebral connectives (fig. 110o). B cells are rare and only seen in the inferior medial glomeruli. Figure 111c shows the location and type of neurosecretory cells present in the tritocerebral glomeruli of *G. setosus* at periods of peak activity.

NEUROSECRETORY CELLS OF THE SUBOESOPHAGEAL MASS:

The neurosecretory cells in the dorsolateral, ventral and segmental nerve root glomeruli of the suboesophageal mass were identified as type A and not exceeding 11 microns in diameter (fig. 119b). The majority of these A cells are smaller ranging from 2.5-7.0 microns in diameter. There were no neurons present large enough to be classified as B cells and those larger than 11 microns were designated A'. The A' neurosecretory neurons exhibit a larger amount of stainable NSM (fig. 119b) and are located in the dorsolateral glomeruli region surrounding the root of the segmental nerve where it arises from the ganglionic mass.

NEUROSECRETORY CELLS OF THE VENTRAL THORACIC GANGLIA:

The cellular glomeruli are located on the ventral and dorsolateral aspects of the ventral thoracic ganglia. These layers are richly endowed with neurosecretory cells of various types. In routine paraffin sections the neurons show greater detail than those of the brain and suboesophageal mass.

The neurons of the ventral glomeruli were classified into one of several types: (1) Non-neurosecretory, with little cytoplasm and no stainable NSM, 7-15 microns in diameter with variable cytoplasmic:nuclear ratios. (2) Neurosecretory: Type A - small unipolar neurons 7-11 microns in diameter with the nucleus occupying about 90% of the perikaryon. The NSM forms a thin black ring filling the space between it and the cell membrane (fig. 124b). These cells comprise approximately 50% of the glomerular layer.

Type A' - small, bipolar neurons with the nucleus filling the center of this fusiform cell leaving two NSM-filled triangular regions at either end (fig. 126b). They contribute about 5% of the total neuronal complement. Type B - medium-sized neurons 11.5-15.0 microns in diameter, the nucleus occupying about 66% of the perikaryon. The NSM is found throughout the cytoplasm in varying intensity (fig. 124b). These neurons compose about 30% of the ventral glomeruli.

Type C - large neurons, 15.5 microns or greater. The largest C cell examined measured 35 microns in diameter. The nucleus occupies 50% or less of the perikaryon and the NSM is present in various intensity dependent upon the physiological state of the female (fig. 124b). These neurons comprise about 15% of the total neuronal composite of the ventral glomeruli. The proportion of smaller neurons (type A and A') to larger neurons (type B and C) in the dorsolateral glomeruli of the thoracic ganglion is about 2:1.

NEUROSECRETORY CELLS OF THE ABDOMINAL GANGLIA:

The ventral glomeruli of the abdominal ganglia are also heavily endowed with neurosecretory cells. The types of cells are as described in the thoracic ganglia but the number of smaller neurons (type A and A') in proportion to the larger neurons (type B and C) is higher - approximately 10:1 (fig. 127).

SEASONAL ACTIVITY OF NEUROSECRETORY CELLS IN THE CENTRAL NERVOUS SYSTEM:

The brain, suboesophageal mass and ventral ganglia are never completely free of neurosecretory cells and the greatest concentration of active cells appears in the period between major physiological events. In August, the neurosecretory cells exhibit the greatest amount of stainable NSM present at any point of the annual cycle (fig. 110). The location and type of neurosecretory cells showing stainable amounts of NSM at this point in the three brain sections have been shown in figure 111.

Figure 114-118 illustrate the comparative stainable neurosecretory activity in the brain of *G. setosus* throughout the female's annual physiological cycle. The number of active cells and staining intensity of the NSM increases through May (figs. 114-118a) and by the initiation of vitellogenesis in early August (figs. 114-118b), the brain shows an appreciable increase in both aspects.

In late August, when the female is in precopula and prior to ovulation, the neurosecretory cells show the greatest degree of activity (fig. 110). The brains of females immediately following ovulation are noticeably free of significant amounts of stainable NSM and the number of active neurosecretory cells is much reduced (figs. 114-118c).

By the time the embryos are in late A-B stages of development, the neurosecretory cells of the brain are few and faintly discernable (figs. 114-118d). At later stages of development, the number of neurosecretory cells, amount and intensity of stainable NSM increases visibly, indicating resumed synthetic activity (figs. 114-118e).

The cycle of neurosecretory activity appears to be similar in the neurons of the suboesophageal mass (fig. 119) and the dorsolateral and ventral glomeruli of the thoracic and abdominal ganglia (figs. 120-127). The neurons of the ventral ganglia however, exhibit a slight degree of neurosecretory activity after ovulation when the brain and suboesophageal mass appear free of neurons engaged in synthetic activity (fig. 123).

The sinus gland exhibits a stainable NSM cycle similar to that encountered in the glomeruli of the central nervous system. The bulk of the NSM appears to be localized in the more distal portion of the gland. Actual release of NSM from this gland was not observed in either paraffin or plastic sections (fig. 112).

The glomerular layer in the ventral regions of the protocerebrum, referred to by Gabe (1954) as a probable amphipod X organ, was located in *G. setosus* and seen to contain stainable amounts of NSM (fig. 113). This glomeruli is the ventral portion of the anterior superior lateral glomeruli (aslg) and has a secretory cycle similar to that of the other brain glomeruli (fig. 113).

In an attempt to correlate the secretory cycle of the neurosecretory cells in the central nervous system to the physiological processes of the female, the following facts were considered: the buildup of stainable NSM until the time of the preovulatory moult and its absence after ovulation for a short period of time and then its subsequent buildup in the neuron perikarya once again.

These observations suggest that the cells constantly release NSM and its production approaches levels too great to be compensated by its release. The quantity of NSM continues to build up until its production ceases, sometime before the pre-ovulatory moult, but the release continues until the cells are free of any stored NSM. This type of cycle could have either an inhibitory effect on the moult and ovulation or a stimulatory effect on gonad maturation and development. These physiological processes are very closely related in *G. setosus* during the fall and determination of the individual or isolated effect of these cells is difficult to assess by ordinary histological examination.

VITELLOGENESIS AND NEUROSECRETION:

In view of the presence of NSM granules within the neurons of the frontal organ, the possibility that this organ functions as a neurohemal site in *G. setosus* arises. After examining frontal organs from females sampled throughout their annual physiological cycle, a correlation was found between the cyclic release phenomena of the type I neurons and certain phases of the reproductive cycle. Figure 128 illustrates the type I frontal organ neurons at various times during the annual female reproductive cycle.

From May until August there is a steady increase in the amount of NSM present in the form of CHP and PF-positive granules ~~(figs. 128a,b).~~ In early August the neurons are empty of granules at the time of initiation of vitellogenesis in the ovary (figs. 128c, 129). This occurs during the period of decreasing day length at Witless Bay (fig. 103).

By late August the cells have once again accumulated a substantial amount of NSM (fig. 128d). The granules increase in number rapidly and by late September the eggs are packed with large

CHP-positive granules (figs. 128e,f). At the time of the preovulatory moult the type I frontal organ neurons contain fewer granules than they did in late September, indicating either increased speed of release or cessation of NSM granule production (fig. 128g). Immediately after the moult, while the female is still in precopula, ovulation occurs. One day after ovulation and separation from the male, with cleaving A stage embryos in the brood pouch, the neurons appear empty of granules (fig. 128h). During brooding of the developing embryos the quantity of NSM granules steadily increases within the perikarya (128i-l).

After December females could not be obtained from the ice-covered rocky beach until May, but by examining animals kept at the MSRL at Logy Bay, a third granule release from the frontal organ was observed (fig. 130). This last release occurs after the release of the hatched young and coincides with the post-reproductive moult into resting stage. After this the NSM granules are produced at a much slower rate. In May the cells are about one half full of granules which is probably a result of the physiological slowdown encountered over the winter months caused by the low incumbent temperatures.

The observations on the cycle of storage and release of NSM in the type I frontal organ neurons (fig. 128), suggests that the granules may control, or partially control vitellogenesis and moulting. It is extremely difficult to isolate the exact significance of the release because the two physiological events occur within a short period of time, *ie.* moulting and ovulation. If the NSM is an inhibitory substance, its release may control moulting by letting it proceed when the level of NSM in the frontal organ falls below a certain threshold value. Its total absence may stimulate release of the oocyte at ovulation.

As it was impossible to identify empty vesicles in paraffin sections, it was uncertain whether there was a slow continual release of NSM or a simultaneous release. Thin plastic sections of the frontal organ at periods when the cells appeared full of granules in paraffin sections, showed that vacuoles resembling empty granules were present within each cell (fig. 64). This suggests a slow continual release of the complex neurosecretory vesicles seen by electron microscopy from these type I frontal organ neurons. The ultrastructural observations also suggest that these cells produce and receive NSM faster than they release it accounting for the accumulation of granules between major physiological events.

The production of vesicles must eventually cease, but the stored vesicles continue to be released. At the time when the cells are emptied, vitellogenesis on one hand, moulting and ovulation on the other, occur. The production and build up of NSM vesicles begins soon after the above functions have transpired. It would seem logical to concluded that the NSM released from the type I frontal organ neurons is inhibitory in nature.

At this time nothing can be said about the function of the neurosecretory vesicles produced, stored and released from the type II frontal organ neurons. These vesicles must function in the control of some other physiological phenomena as they appear filled with stored vesicles at periods when the type I neurons are empty (fig. 66). It can be concluded that release of neurosecretory vesicles stored within these type II neurons is gradual as well.

DISCUSSION:

THE CENTRAL NERVOUS SYSTEM:

The study of external and internal brain morphology in Amphipoda, especially *Gammarus*, has been limited. Dahl (1956) correlated the topography of the central nervous system with the position of the various anatomical structures such as the mouth, eyes, and head appendages. In *Gammarus* the eyes are located laterally but are functionally directed dorsoventrally, the head appendages are positioned anterodorsal and anteroventral, while the mouth opening is ventral. The axis of the nervous system therefore, is deflected rather abruptly upwards in the posterior part of the tritocerebrum. The brain does not bend over backwards and the protocerebrum lies directly above the deutocerebrum.

Gräber (1933) alone investigated the amphipod brain in great detail in *Gammarus pulex* and *Gammarus fluviatilis*. Others such as Hanström (1929, 1933, 1947) and Madsen (1960) studied the brains of related amphipods or reviewed amphipod brain morphology in general. Thore (1932) and Ståhl (1938) touched briefly on the anatomy of the brain in *Gammarus* while describing the accessory cephalic structures.

The brain of *G. setosus* has the three characteristic crustacean divisions: the protocerebrum, deutocerebrum and tritocerebrum. It is remarkably similar in external morphology to that of *G. fluviatilis*, a freshwater species, as described by Gräber (1933). The protocerebrum is laterally elongated with no curving of the outermost portions as seen in *G. pulex* (Thore, 1932). The brain of *G. locusta* (Thore, 1932) is far more laterally compressed in comparison with that of *G. setosus*.

The deutocerebrum of amphipods is generally simpler than that of higher malacostracans (Hanström (1947). The antenna and olfactory lobes are well developed but the parolfactory lobes are small and relatively undeveloped. Both the deutocerebrum and tritocerebrum of *G. setosus* resemble those of *G. fluviatilis* (Gräber, 1933) in morphology and proportion and differ from those of *G. pulex* and *G. locusta* as described by Thore (1932).

The distribution of the superficial glomeruli forming the cellular rind of the *Gammarus* brain had been previously investigated to an even lesser degree. Gräber (1933) included a thorough description of the various glomeruli covering areas of the brain surface in *G. fluviatilis* and it appears to be the only description of its kind in the literature for *Gammarus*. The great similarity of external brain morphology in these two gammarids facilitated the comparative study of the glomeruli.

All the cellular glomeruli described by Gräber (1933) were identified in *G. setosus* with some degree of variation in location and size. The inferior anterior medial glomerulus (iamg) and dorsal extension of the inferior medial glomeruli (img) are reduced in length and the inferior posterior glomeruli (ipg) extend a great distance further back along the tritocerebral connectives. The olfactory lobe glomeruli (oflg) have increased in size and a glomerular bridge (aimgb) is present in the anterior region of the anterior inferior medial glomeruli (aimg). This formation is the greatest deviation in cellular distribution between the two gammarids and forms a small canal between the fibrous humps of the protocerebrum. This bridge is not present in the description of *G. fluviatilis* by Gräber (1933). The functional significance of this cellular bridge is unclear and except for the presence of two extremely large neurosecretory cells in the posterior dorsolateral region of the bridge, it is simply an additional aggregation of neuron perikarya.

The location and description of the neuropile masses present in the fiber core of the *Gammarus* brain were again most extensively studied by Gräber (1933) in *G. fluviatilis*. It is in this aspect that the brains of these two gammarids differ the most. The three optic neuropiles are distinctly separate bodies with no overlap as shown by Gräber (1933) in *G. fluviatilis*. The compound eyes have a varying structure throughout the Amphipoda and this in turn influences the size of the three primary optic centers of the protocerebrum (Bullock & Horridge, 1965). The most characteristic feature here is the poorly developed state of the medulla interna. The connection between it and the medulla externa is not developed as a chiasma like that between the lamina gangliaris and medulla externa.

The protocerebral bridge in the brain of *G. setosus* is not as distinct as that present in *G. fluviatilis*, being only barely distinguishable from the surrounding fibrous mass of the protocerebrum. The central body is homogeneous and not divided into seven subunits like that of *G. pulex* (Gräber, 1933). The central body of most gammarids is well developed compared to that of decapods where it is reduced with a corresponding enlargement of the antennal association centers (Bullock & Horridge, 1965).

A fairly well developed neuropile located in the dorsal portion of the protocerebrum, the medulla terminalis, receives nervous innervation from the paired statocysts as well as deeper areas of the brain. This neuropile was not described as being distinguishable in the brain of *G. fluviatilis* by Gräber (1933). The antennal I and antennal II neuropiles of *G. setosus* are well developed and compare favourably to those of *G. fluviatilis*. A tegumentary neuropile can be vaguely differentiated in the upper region of the tritocerebrum of *G. setosus* which was also not described in *G. fluviatilis*.

The morphology of the suboesophageal mass is similar to that described by Rosenstadt (1888) and has the typical amphipod trait where the first four ganglia fuse to form one mass. The general morphology of the ventral nerve cord is similar to that of *Gammarus neglectus* as described by Sars (1867). Apart from these two accounts, no recent material on the subject could be found in the literature for *Gammarus*. The morphology, however, appeared to resemble that described in the lower Crustacea by Bullock and Horridge (1965).

ACCESSORY CEPHALIC STRUCTURES:

Earlier investigations focused on the sensory structures within the head of amphipods, especially the statocysts. Závadsky and Prag (1914) described the presence of these structures in the head of *G. pulex*. Langenbuch (1928) studied the statocysts of several amphipods including *G. locusta* and *G. pulex*, but used the terms 'statocyst' and 'frontal organ' somewhat synonomously and the work of these two authors on the statocysts of *G. pulex* did not coincide. Hanström (1933) and Gräber (1933) recorded observing statocysts in the head region of several families of Amphipoda. Recent histological observations on the structure of the statocyst in the gammarids or related amphipods could not be found.

Thore (1932) distinguished between the statocysts and frontal organ in his study of *G. pulex* and the statocysts of the two gammarids studied, *G. pulex* and *G. locusta*, proved to be very distinct and different structures. The statocyst of *G. setosus* resembles that of *G. locusta* described by Thore (1932). The statolith is also fusiform although its overall structure in *G. setosus* is broader but still retains the dorsal and ventral tapering points of attachment. Thin sections have given a clear picture of the cellular and acellular aspects of this structure. It is evident that the statolith is a secretory product enveloped by an outer cellular layer.

There has been a great deal of confusion over the identity of the organs of Bellonci (X organs) and the frontal organs as well as their function throughout Crustacea. Claus (1886) first described the dorsal frontal organs in *Artemia* and regarded them as sensory structures. Hanström (1939) regarded the X organ as a transformed group of sensory cells of a rudimentary eye papilla that had moved inwards and taken over a new secretory function. In higher Crustacea, this eye papilla exists in the form of a papilla or sensory pore. The X organ has been found in many groups of crustaceans including Leptostraca and Cumacea (Ståhl, 1938), Anaspidacea, Mysidacea, Stomatopoda and Decapoda (Hanström, 1931, 1933, 1934, 1937).

The X organ does not appear to be present in Amphipoda although Gabe (1954) described a structure similar to the organ of Bellonci (X organ) in Isopoda on the ventral aspect of the protocerebrum in some amphipods. This was characterized by an aggregation of a number of strongly NSM-positive neurons. In *G. setosus* this particular glomerular group was found in the mid portion of the posterior superior lateral glomeruli (pslg). The aggregation of neurosecretory cells here had cyclic pattern of activity corresponding with that of the remaining brain glomeruli.

The frontal organs of Amphipoda were first described as being paired structures in *Gammarus* by Zavadský and Prag (1914) and in *Caprella* by Hanström (1924) although with reservation. Thore (1932) and Gräber (1933) found an unpaired medial dorsal frontal organ in *G. pulex* and *G. locusta*. Gräber discounted the presence of paired organs in *G. pulex* and claimed the structures represented something other than frontal organs. The frontal organ in *G. setosus* is also medial and unpaired being quite similar in morphology to that described by Thore (1932) in *G. locusta*.

The frontal organs of the lower crustaceans were attributed a secretory function by Hanström (1931, 1934) and regarded as precursors to the higher malacostracan X organ. Hanström (1939) found that the medial frontal organ of the advanced members of the lower Crustacea showed the same structural transformation as the lateral frontal organ of the lower crustaceans. The lateral frontal organ represents the eye papilla of these forms but its function is unknown. Hanström (1939) noted obvious signs of secretory activity in the cells of the medial frontal organ. He concluded that this organ represented the transformation of a sensory organ into a secretory one. He did not consider these cells to be true neurosecretory cells as they are derived from sensory rather than nervous tissue.

Menon (1962), Elofsson (1966) and Lake (1969a) suggested the the frontal organs were associated with the nauplius eye center in Anostraca and other forms exhibiting a nauplius stage in their development. Elofsson (1965) disputed the existence of frontal organs in the Amphipoda claiming those stated were little more than either the nervus tegumentarius or a cluster of cells surrounding the ramifications of the anterior aorta that could be found in decapods, syncarids and mysids. This study shows that the frontal organ of *G. setosus* is a localized group of loosely arranged, but apparently highly specialized, cells that synthesize and release neurosecretory material.

Baid and Dabbagh (1972) described paired frontal organs in *Rivulogammarus syriacus* that were associated with neurosecretory release and possibly its synthesis. Although their written description of these organs coincides with that generally accepted in other species of *Gammarus*, the photographs indicate a misnomer. The structures labelled as paired frontal organs in *R. syriacus* appear to be located too low in the head region and have a core with a texture similar to that of the adjacent protocerebral fiber mass. These structures appear to be the antennal I nerves in cross section before they join the deutocerebrum at a location just ventral to this. Therefore, the existence of paired frontal organs in Amphipoda is doubtful and awaits the presentation of some solid evidence.

The secretory nature of the frontal organs is not a new concept as this function has already been attributed to them in some groups: Copepoda (Carlisle & Pitman, 1961), Anostraca (Hanström, 1934; Menon, 1962 and Elofsson, 1965) and Amphipoda (Baid & Dabbagh, 1972). This would perhaps give the frontal organ a secretory function analogous to that of the X organ of higher malacostracans.

Dahl (1965) considered the homology between the frontal organs and sensory pore X organs of Crustacea suggested by many authors *ie.* Hanström (1939). Other authors such as Barrington (1963) and Knowles (1963) treated this subject with some caution. Dahl (1965) however, states that this homology is improbable.

The various types of neurosecretory cells in the X organ of Crustacea form a final pathway terminating in a non-neural organ called the sinus gland. This structure was recognized as a hormonal source by Hanström (1935, 1937a) and is present in all malacostracans so far examined except for Leptostraca, Syncarida and Cumacea (Hanström, 1948). Hanström (1931) briefly mentioned the existence of a sinus gland in Crustacea and later described it in greater detail (1933). After a survey of the decapods, Hanstrom (1937) noted that there were many anatomical variations of this gland.

There is confusion with respect to the sinus gland and sensory pore X organ in the Isopoda. Two structures have been observed in the optic region: the organ of Bellonci (1881) and the pseudofrontal organ (Gräber (1933). Amar (1948, 1950, 1953), Gabe (1952, 1954) and Oguro (1960) homologize the pseudofrontal organ to the sinus gland and the organ of Bellonci to the sensory pore X organ. In Amphipoda, as well as some species of isopods and decapods, Hanström (1947, 1948) was unable to find a sensory pore.

The sinus gland in *Gammarus* was described by Gräber (1933) in *G. pulex* and *G. fluviatilis* as the pseudofrontal organ. Other workers found structures they termed pseudofrontal organs or sinus glands in many lower malacostracan crustaceans: Koller (1930), Walker (1936), Hanström (1933), Oguro (1959a, 1959b, 1960), Baid and Dabbagh (1972). Gabe (1952) equated the pseudofrontal organs described by some authors to the sinus glands of the higher malacostracans.

The sinus gland nerve connecting it with the X organ was located by Hanström (1931, 1933) but the transport of NSM along the fibers was detected by Bliss (1951), Bliss and Welsh (1952) and Passano (1951, 1952), and observations by Enami (1951) indicated its migration. Nucleated cells are present in all malacostracan sinus glands while distinct zones with differing tinctorial properties have been reported in those of higher malacostracans (Baid & Dabbagh, 1972). The sinus gland is the most constant component of the malacostracan neurosecretory system and its bulk is composed of an aggregation of axonal terminals filled with NSM stored for release from this neurohemal organ.

The sinus gland of *G. setosus* contains nucleated cells as well as large areas of fiber core composed of axons and their terminals. Observations suggest a cyclic pattern of neurosecretory activity corresponding with the rest of the brain glomeruli. This gland has an ideal location to function as a neurohemal organ being projected out from the brain mass and suspended in an area bathed in blood. However, actual release of NSM was not observed in the sections examined.

THE NEUROSECRETORY SYSTEM:

The phenomenon of neurosecretion is found in almost every metazoan animal wherever a central nervous system exists along with a degree of cephalization (Bullock & Horridge, 1965). In these areas some nerve cells with secretory activity can be found. The occurrence of these cells can be reasonably expected in representatives of all invertebrates although some of the smaller invertebrate phyla have yet to be examined (Gabe, 1966).

The generalized neurosecretory system found in metazoan animals consists of a source of secretion in the form of neurosecretory cells and a tract of secretion-bearing fibers which terminate in close association with a neurohemal organ for storage and release of NSM. Although a great deal of the research conducted on invertebrate neurosecretory systems has been based on that of insects, evolutionary convergence has resulted in the occurrence of neurosecretory systems that closely resemble those in other major invertebrate groups (Hanström, 1947, 1948, 1953, 1957; B. Scharrer, 1959 and E. Scharrer, 1959).

The neurosecretory systems in the Malacostraca are complex and their components are wide-spread throughout the central nervous system. Neurons of secretory function have been found in most ganglia examined including: the ganglia of the optic centers, the brain, the connective ganglia, the tritocerebral commissure of natantians and the thoracic ganglia of brachyurans, natantians, isopods and amphipods (Bullock & Horridge, 1965).

There are three components of the crustacean neuroendocrine system: neurosecretory cells, neurohemal organs and non-endocrine glands.

NEUROSECRETORY CELLS:

The central nervous system of *G. setosus* is well endowed with neurosecretory cells. In Crustacea the neurosecretory cells have been classified into as many as 11 types within one individual based on size of the cells, mode of discharge and nature of the secretory material (Matsumoto, 1958). The neurosecretory cells of crustaceans have been studied in a wide variety of species including *Sesarma* (Enami, 1951), *Eriocheir* (Matsumoto, 1954), *Chionectes* (Matsumoto, 1956), *Pachigrapsus* (Inoue, 1957), *Armadillidium* (Matsumoto, 1959), *Potamon, Chionectes, Neptuns* and *Sesarma* (Miyawaki, 1960), *Tecticeps japonicus* (Oguro, 1960), *Streptocephalus* sp. (Menon, 1962), *Metapenaeus* sp. (Dall, 1965), *Artemia salina* (Baid & Ramaswamy, 1965), *Chirocephalus* and *A. salinus* (Hentschel, 1965), *Scylla serrata* (Nagabhushanam & Rango Rao, 1966), *Chirocephalus diaphanus* (Lake, 1969a); *Daphnia magnus* (Halcrow, 1969), *Diogenes bichristimanus* (Nagabhushanam & Sarojini, 1969), *Podon intermedius* (van den Bosch Aguilar, 1971), *Porcellio dilatatus, P. laevis, Protrocheaniscus asiaticus* (Vitez, 1971), *Rivulogammarus syriacus* (Baid & Dabbagh, 1972), *Talorchestia martensii* and *Orchestia platenus* (Shyamasundari, 1973).

Baid and Dabbagh (1972) classified the neurosecretory cells in the central nervous system of the amphipod *R. syriacus* into 6 types based on the size, mode of NSM discharge and nature of the secretory granules, of which only 4 were located in the brain. Shyamasundari (1973) analyzed the neurosecretory cells of two talitrids *T. martensii* and *O. platensis*, and identified 3 types in the brains of these two amphipods.

Maynard (1961) pointed out that the previous methods of neurosecretory cell classification were both unsatisfactory and confusing. Miyawaki (1960) was among the first authors to adopt the simple size basis for classification - small, medium and large. In *G. setosus* the neurosecretory cells of the brain and suboesophageal mass were classified solely on the basis of size. The morphology of these relatively small cells, in comparison to those in the ventral ganglia, was too vague to make elaborate descriptions. The NSM staining varied considerably in intensity and during the active phase the cytoplasm had a uniform dark color. The chosen size classification encompassed the types of neurosecretory cells present. Observations on the morphology of the NSM within the cells proved difficult and inconsistent as it commonly appeared as a homogeneous mass of varying intensity.

There were only two types of neurosecretory cells identified in light microscope sections of the brain of *G. setosus* and these were classified type A and type B. Electron micrographs revealed that there were two types of A cells but the distinction was made on the presence of two different types of neurosecretory granules that could not be distinguished on the light microscope level. The suboesophageal mass also contained two types of neurosecretory cells, type A and A'. Although these cells are within the size limits of the A cells in the brain, they are present here in two distinct size ranges and have been classified accordingly.

Many of the neurosecretory cells of the ventral ganglia in Crustacea were included in the classification of the entire nervous system by some of the above authors. However, other investigators have focused their attention on the ganglia alone; *ie.* Carlisle and Knowles (1959) in natantians, Matsumoto (1956) in *Chionectes opilio, Idothea baltica* and *Oniscus*, Matsumoto (1959) in *Armadillidium vulgare*, Legrand and Johnson (1961) in *Ligia oceanica*, Matsumoto (1962) in *Hemigrapsus*, Johansson and Schreiner (1965) in *Homarus vulgaris*, Teodorescu *et al.*, (1965) and Prunesco (1970) in *Chilpod* sp., Baid *et al.*, (1967, 1968) in *Potamon magnum magnum* and Schreiner *et al.*, (1969) in *Homaris vulgaris*. Baid and Dabbagh (1972) located 3 of the 6 neurosecretory cell types in the ventral ganglia of *R. syriacus* and Shyamasundari (1973) found 3 of the 4 cell types present in the ventral ganglia of the two talitrid amphipods.

In *G. setosus* very few of the brain and suboesophageal mass cell types could be found in the glomeruli of the ventral ganglia. The neurons, especially those of the ventral glomeruli, of the ventral ganglia are seen in much greater detail probably due to the lack of underlying cells. Of the 4 cell types described here, only type A' is not recognized on the basis of size, being the only example of a bipolar neuron in this amphipod. Types A-C are arranged in increasing perikaryon dimensions.

In comparison to the ganglion neurons of higher crustaceans *ie.* decapods (Johansson & Schreiner, 1965), the neurons of *G. setosus* are much smaller in proportion and lack the occurrence of "giant" cell types. These observations correspond in general with Maynard's (1961) method of classification. The ventral ganglion neurons all ultimately acquire a uniformly dense accumulation of NSM and at other times they are in the process of synthesis or release. These observations were confirmed by electron microscopy.

NEUROHEMAL ORGANS:

There are three classical neurohemal organs in different orders of Crustacea: the sinus gland, postcommissure organ and pericardial organ (Bullock & Horridge, 1965). The latter two are found only in the higher malacostracans and of these three *G. setosus* possesses only the sinus gland. The presence of a neurohemal organ is not a necessary component of a functional neurosecretory system as many neurosecretory axons do not terminate in a neurohemal association but mingle with the ordinary axons extending out to the peripheral areas of the animal (Carlisle, 1959). Huddart and Bradbury (1972) found neurosecretory axons terminating in crustacean skeletal muscle.

The cephalic neurosecretory system of *G. setosus* consists of a frontal organ that produces and releases NSM, as well a sinus gland that exhibits cyclic storage of varying amounts of NSN, although actual release of the material was not observed on the light microscope level. Many authors recognized, or theorized, a secretory function for the frontal organ (Hanstrom, 1939) but little was actually described about its secretory cycle or mechanism. Ultrastructural studies in *G. setosus* have shown the actual release of thousands of minute elementary particles contained within the secretory vesicle of the type I frontal organ neurons. Actual release of the vesicles from the type II frontal organ neurons was not observed but is hypothesized. These clusters of NSM-containing cells, suspended in a blood sinus fed by the anteriorly emptying dorsal aorta, constitutes an additional neurohemal organ in *G. setosus*.

The presence of neurohemal organs within the ventral ganglia of an orthopteran insect *Schizodactylus monstrous* was reported by Khatter (1972). In this animal the external fibrous connective tissue capsule is invaginated forming a sinus, but Gundevia and Ramamurty (1972) found intraganglionic neurohemal sites in the coleopteran insect *Hydrophilus olivaceus*. Neurohemal organs of this type were not seen in the ventral ganglia of *G. setosus*.

NON-NEURAL ENDOCRINE ORGANS:

Invertebrate hormones are not exclusively neurosecretory in origin and some arise from epithelial secretory tissues (non-endocrine organs) but these seem to play only minor roles (Bullock & Horridge, 1965). A main source for this type of hormone is the Y organ first described by Gabe (1953a). It was shown to have control over the moulting process in a large number of higher malacostracans. The Y organ is a pair of glands lying in the antennary or second maxillae segment, depending upon the location of the excretory organs. It is similar to the ecdysial gland of insects and both are derived from ectodermal ventral glands.

In *Gammarus* the paired Y organs are located in the antennary region as the excretory organs are located in the maxillary segment. The gland has a foliaceus appearance and is composed of small, uniform cells averaging 10 microns in diameter (Tombes, 1970). The gland is innervated by nervous extensions of the suboesophageal mass and they are the true secretors of the moult inducing hormone which is inhibited by the secretions of the X organ-sinus gland complex in higher malacostracans (Karlson & Skinner, 1960).

The Y organ of *Carcinus maenus* (Arvy *et al.*, 1956) affects the immature male and female gonads by hormonal influence on cell division. Removal of the Y organs results in blockage of oogonial growth and yolk deposition in the ovary. Carlisle and Knowles (1959) found that the Y organ controlled gonadal development in juvenile females but after puberty removal had no effect.

The androgen gland was first described by Charniaux-Cotton (1956) and is located near the genital pore of most male crustaceans. This organ determines testicular development and male secondary sex characteristics. The androgen gland anlage does not develop into a functional organ in the female and through auto-differentiation in the absence of a hormone, the gonad developes into an ovary (Charniaux-Cotton, 1959). Implantation of the gland into the female causes transformation of the ovaries into testes (Charniaux-Cotton, 1960).

Development of oostegites is induced by the release of an ovarian hormone (Charniaux-Cotton, 1955, 1957). The moult hormone is responsible for the formation of the juvenile hairs on the oostegites that resemble those found elsewhere on the animals body but when the ovarian hormone is added, the trichogenic matrix stretches out and an ovigerous hair (long seta) is formed (Charniaux-Cotton, 1957). If the hormone is not secreted in a threshold level (*ie*. after a partial ovariectomy), the hairs reach an intermediate length. Any portion of the ovary in stages of vitellogenesis can induce the formation of long ovigerous setae. This indicates that the source of the hormone is well distributed throughout the ovary (Charniaux-Cotton, 1960). The follicular cells would be the most likely source as they are the only components of the ovary outside of the germ cells themselves (Vevers, 1962).

The formation of the brood pouch in *Gammarus* is also under ovarian control and the X organ-sinus gland complex produces a hormone that inhibits the ripening of the ovary and yolk deposition outside the breeding season in higher malacostracans (Charniaux-Cotton, 1960). The NSM produced and released by the type I frontal organ neurons in *G. setosus* may have this function. At initiation of vitellogenesis in the ovary these cells are empty of the ovary-inhibiting NSM and the ovary enlarges and vitellogenesis begins. With the appearance of the yolk, the follicle cells have undergone a morphological change and the ovarian hormone influencing the production of the ovigerous hairs may be produced (Vevers, 1962).

NEUROSECRETORY CELL ULTRASTRUCTURE:

The ultrastructure of invertebrate neurosecretory cells is a relatively young field and investigations on crustaceans are few and those on amphipods even rarer. Some of the crustacean invesigators include Malhotra and Meek (1961), Wendelaar Bonga (1970, 1971), Fernandez and Fernandez (1972), Yahata (1972), Herman and Preus (1973) and Roubos (1973).

As in other areas of invertebrate neuroendocrine re-research, the bulk of the information has been collated on insects.

These studies however, are valuable as reference and work by authors such as Nishiitsutsuji-Uwo (1960, 1961), Beattie (1971), Scharrer (1971), Sandifer and Tombes (1972), McLaren (1972). O' Leary *et al.*, (1973), Borg and Marks (1973), Marks *et al.*, (1973), Girardie (1973), Kono (1973) and Borg *et al.*, (1973) have proved to be useful in this study on *G. setosus*.

The most distinctive feature of the crustacean neurosecretory cell is the large nucleus, the chromatin content of which is variable and appears to be correlated to the degree of NSM synthetic activity. Sandifer and Tombes (1972) also note this as well as the difference of chromatin distribution between the neurosecretory neuron and the adjacent chromatin-laden glial cell nuclei. Both these features were seen in the neurosecretory neurons of *G. setosus*.

Malhotra and Meek (1961) describe another distinctive feature of these cells in *Leander serratus*, the agranular membrane systems of the neuron perikarya, the crescent-shaped dictysomes. Bullock and Horridge (1965) equate these structures with Golgi and attribute their shape to fixation techniques.

Similar structures resembling flattened groups of Golgi cisternae arranged in a fingerprint configuration are also found in the perikaryon. Lake and Ong (1972) termed these structures "phaosomes" in the onion cell bodies of the organ of Bellonci. Fahrenbuch (1964) and Dudley (1969) found them in photoreceptor cells associated in some locations with rough ER. Lai-Fook (1973) most recently described these structures and called them residual bodies. These structures were also seen in *G. setosus* surrounded by an isolation membrane. Residual bodies of another form were also seen, large bag-like bodies containing assortments of fibrillar and granular debris. The significance and function of these structures is uncertain but in *G. setosus*, the larger variety appear to be the "garbage collectors" of the perikaryon and have been observed forming pores through the cell membrane as if dumping their contents into the glial cell processes.

Large accumulations of mitochondria are present in most actively secreting neurons and tend to be massed in the region of the axon hillock and extend out along the axon. Yahata (1972) termed this arrangement a "mitochondrial lump". Although Malhotra and Meek (1961) discounted the presence of elongated mitochondria, stating previous authors mistook the trophospongia for these organelles, such were undoubtedly present and a dominant feature in the neuron perikarya and axon of *G. setosus*. Other authors including Nishiitsutsuji-Uwo (1961), Sandifer and Tombes (1972), Herman and Preus (1973) and Borg and Marks (1973) also noted their presence as well as their endless variation in both configuration and dimensions.

Lamellated stacks of rough ER were not encountered in the neurosecretory neurons of *G. setosus*, the majority of which was present in scattered short cisterns dilated to various degrees. The non-neurosecretory neurons contain rough ER in longer, but randomly arranged cisterns. Large aggregates of these membrane systems corresponding to vertebrate Nissl bodies were not seen, as was the case in the perikarya of *L. serratus* (Malhotra & Meek, 1961).

Trophospongium, a characteristic feature of crustacean neurons were also described by Malhotra and Meek (1961). These structures penetrate the neurons for varying distances, branching mainly at the innermost portion and usually for short distances only. The tubular and fibrillar structures of the cell were somewhat similar in configuration to those described by David *et al.*, (1973). There was no definite arrangement and their overall dimensions differed slightly from those described by David *et al.*, (1973) working in vertebrate tissue.

NSM PRODUCTION:

Theories on the production of secretions by neurosecretory cells are based on the morphological observations of some earlier workers in the field (E. Scharrer and W. Bargmann). There have been many theories put forth including: nuclear secretion of NSM (Palay, 1943; Ortmann, 1958), related to the fact that the chromatin content decreases as synthetic activity increases. This was observed in the neurosecretory cells of *G. setosus* but actual implementation of the mode was not seen. Scharrer *et al.*, (1945) and Palay and Wissig (1953) associated NSM production with Nissl substance, Edstrom and Eichner (1958) found it had an association with cytoplasmic RNA, while others such as Pardoe and Weatherall (1955) and Nishiitsutsuji-Uwo (1960, 1961) suggested an association with mitochondria.

NSM production in *G. setosus* still remains to be clarified as there are at least two possible modes to be considered. Green and Maxwell (1959) claim that mitochondria may transform into neurosecretory granules while Nishiitsutsuji-Uwo (1960, 1961) stated that mitochondria fragment into these granules and Knowles (1958) felt that the granules were manufactured along the course of the axon by mitochondrial activity. The mitochondrion-like NSM-positive granules described in the type I frontal organ, protocerebral and ganglionic neurons are very similar to those described by Green and Maxwell (1959) and Nishiitsutsuji-Uwo (1960, 1961).

Mitochondria can undergo morphological changes including fragmentation into granules followed by lysis and dispersion, as well as intense swelling with transformation into large vacuoles. The internal configuration of these organelles can also be altered between two extreme states. The orthodox conformation appears with the inner membrane organized into the characteristic crests and the matrix filling the entire inner volume of the mitochondrion, giving it a granular appearance. The other extreme is the condensed state in which the inner compartment becomes shrunken and fluid accumulates in the outer compartment (DeRobertis *et al.*, 1970). Mitochondria in orthodox conformation are usually found to be related to glandular activity *ie.* in the adrenal cortex where they are engaged in the synthesis of steroid hormones (DeRobertis *et al.*, 1970). The neurosecretory vesicles in the type I frontal organ neurons of *G. setosus* bear a striking resemblance to mitochondria in this morphological state.

Although mitochondria originate *de novo* from simpler building blocks or by fragmentation of elongated "parent" organelles into smaller ones (DeRobertis *et al.*, 1970), an interesting relationship may exist within neurosecretory cells. There is a noted depletion of chromatin (RNA) within the neurosecretory cell nucleus as NSM synthetic activity increases. It is widely accepted that the rough ER system is continuous with the outer, ribosome-studded, membrane component of the nuclear membrane system (DeRobertis *et al.*, 1970). Ruby *et al.*, (1969) noted a close morphological relationship between mitochondria and rough ER, in many cases the outer mitochondrial membrane being continuous with the reticular membranes. These continuities were observed in mammalian ovaries and may function in the transfer of proetin from the rough ER to the mitochondria.

Mitochondria possess the necessary machinery for the synthesis of proteins from amino acids but the recognition of true ribosomes within the mitochondria is difficult even at the electron microscope level, mitochondrial ribosomes being smaller than those of the cytoplasm and are similar in size to bacterial ribosomes (DeRobertis *et al.*, 1970). This could mean that the RNA granules are passed from the nucleus via the rough ER to the mitochondria, possibly undergoing elaboration along the way. In the mitochondrion they are finally made into proteins and/or lipoprotein secretory substance. This could also explain the close association of the rough ER with the maturing mitochondrion-like neurosecretory vesicles observed in *G. setosus*.

The most commonly accepted theory on NSM synthesis associates the neurosecretory vesicles with the Golgi membranes (Palay, 1960; Miyawaki, 1960; Bern *et al.*, 1961; Steinnon & Drochmans, 1961; Murakami, 1961, 1962; Bern, 1963). This mode of synthesis has been elucidated for some species with the electron microscope and the presumed pathway involved in the formation of proteinaceous NSM is the synthesis of material in the rough ER, its transport to the proximal face of the Golgi complex and final condensation at the distal or mature face of the Golgi. Scharrer and Brown (1961), Scharrer (1963) and Borg *et al.*, (1973) reported a pathway similar to this in invertebrates. Continuity of secretory vesicles with the Golgi membranes has been observed in many invertebrate endocrine cells (Scharrer, 1963, 1971; Norman, 1965; Bloch *et al.*, 1966; Wendelaar Bonga, 1971), but evidence of continuities with both the rough ER and Golgi have been reported only by Borg *et al.*, (1973).

Type I neurosecretory granules produced in a number of the protocerebral neurosecretory A cells were clearly Golgi-formed and the formation of a solid periphery thought to designate granule maturity as in those of the insect *Pieris rapae crucivora*, distinguished by Kono and Kobayashi (1972). The type II vesicles of the type II frontal organ neurons also appear to have a similar formation-maturation process.

Borg *et al.*, (1973) noted the common occurrence of multivesicular bodies (MVB) in the neurosecretory cells of *Manduca sexta* and their association with the opaque neurosecretory granules. Scharrer (1971) reported the incorporation of Golgi-formed vesicles into MVBs. These bodies had small Golgi vesicles inside and outside the limiting membrane. Scharrer (1971) noted that these organelles seemed to reflect a process of transformation to dense bodies perhaps due to a gradual incorporation of a component of low electron density during growth and maturation.

The occurrence of MVBs was also noted in the neurons of *G. setosus* and like Scharrer (1971), a maturation process involving the transformation of these organelles into neurosecretory vesicles was a possibility but more study is needed in this area before a definite conclusion can be reached. The question of mitochondrial or Golgi production of NSM in *G. setosus* also cannot be answered at this time and experimentation at the electron microscopic level is the only technique available to solve the problem.

Although there is a problem correlating the secretory granule in light and electron microscopy, the stainable NSM is not a fixation artifact. Passano (1954) observed living neurosecretory cells in crustaceans and the material produced by these cells had a blue-white opacity. A distinction has to be made between the neurosecretory granules and synaptic vesicles sometimes found in the same nerve endings. In *G. setosus*, this is no problem due to the larger size and configuration of the elementary and mature vesicles.

Fingerman and Aoto (1959) found electron dense neurosecretory granules in *Cambarellus* ranging from 300-3000Å in diameter depending upon their location. Those of the sinus gland were 300-1650Å in diameter. Passano (1954) found that the neurosecretory granules in the X organ of *Sesarma* were composed of elementary granules with dimensions in the range of 1000Å. These in turn form large granules 300 nm in diameter grouped together to form granular spheres of 2-4 microns in diameter. These spheres finally form the large light microscope NSM granules 7 microns wide and 13 microns long. The size of the NSM granules in *G. setosus* was intermediate between those of *Sesarma* and *Cambarellus*. It varies from 2.6 microns in the type I frontal organ neurons to 195 nm in the protocerebral and ganglion neurons. The size of the secretory granules appear to differ from species to species.

Detailed examination of the elementary neurosecretory granules at high magnification reveals a degree of internal structure. The apparently homogeneous granule in the pericardial organ of *Squilla*, is a vesicle filled with ultraparticles about 50Å in diameter (Knowles, 1960). The neurosecretory vesicles in the frontal organ of *G. setosus* are similar to those of *Squilla*. These vesicle have an internal core composed of slightly larger ultraparticles, 60-100Å in diameter.

The vesicle membrane may not simply serve as an inactive limiting membrane but may possess dynamic properties to facilitate the modification of the vesicle content after it passes from its site of origin (Gerschenfield *et al.*, 1960). The NSM contained within the vesicle may increase in quantity or quality as it moves towards the axon hillock and out along the axon (Matsumoto, 1956; Lake, 1969a). This modification may continue up until the point of release (Bullock & Horridge, 1965).

MIGRATION AND RELEASE OF NSM:

Burgen (1959) considers the migration of NSM from the perikaryon to the axon terminal to be the major problem in the concept of neurosecretion. There are three principal facts that provide evidence for the existence of axon-travelling secretions: (a) the existence of stainable materials along the axons of neurosecretory cells; (b) the accumulation of secretory materials at the cut end of neurosecretory axons (Hild, 1951); and (c) *in vivo* observation of secretions moving along the axons of crustacean neurosecretory cells by Carlisle (1953, 1959). Axonal migration of NSM was observed in the suboesophageal connectives stained with Hubschman's Azan in *G. setosus*.

Axoplasmic flow itself is a generally accepted phenomenon and can be attributed to pressure causing changes in fiber diameter with the moving cytoplasm accelerating as it enters the narrow axon. The rate of movement is controlled by the cell body and is consistent with fiber growth or regeneration rate, establishing a balance between central synthesis and peripheral destruction. Neurosecretory transport and storage in the axon terminal may be just a special case of a phenomenon occurring in all neurons. Instead of being continually replaced, as in the case of the transmitter substance, the NSM is allowed to pile up due to interrupted release or inability to release the material as fast as it is being produced (Bullock & Horridge, 1965).

The majority of workers in the field accept the axonal transport theory but a few such as Green and Maxwell (1959), Knowles (1959) and Bodian (1951) suggest that NSM is synthesized throughout the neuron. The growth of the elementary granule while en route from the perikaryon implies continued synthesis. Goslar and Schultze (1958) found a concentration of structural elements in the axons of the neurosecretory cells. The peripheral axoplasm however, does not have the essential prerequisites for substantial biosynthesis as there are no ribosome concentrations in the axoplasm (Schmitt, 1959).

After synthesis and transport of NSM occur, release is imperative and is generally thought to occur at the axon terminal. However, it can take place along the axon as well as from the perikaryon itself, either alone or in combination with release from the axon terminals (Matsumoto, 1958). In insects the moult hormone is released from the brain itself.

Tombes (1970) summarized three modes of neurohormone release; (1) release of the intact granules into the vascular system by disruption of the cell membrane in some manner, (2) release of the contained material by exocytosis or reverse pinocytosis when the vesicular and cell membranes come into contact, and (3) diffusion of the active principle across the axonal membrane.

Neurosecretory release of the vesicles in the protocerebral and ganglion neurons of *G. setosus* was only observed in the perikaryon but this does not eliminate axonal release as this aspect was not investigated. The vesicles pass through a disintegrated portion of the cell membrane, usually in the region of the trophospongia, into the glial cell processes intact. The neurosecretory vesicles of the type I frontal organ neurons liberated their contents through a rupture in the cell membrane but release of the granular contents of the type II vesicles was not observed.

THE OVARY AND VITELLOGENESIS:

The female reproductive organs in *G. setosus* are similar to those described for *G. duebeni* by LeRoux (1933) and Steele (1964) and those of *O. gammarella* by Charniaux-Cotton (1960) and Meusy (1963). Oostegite and long setae development is controlled by an ovarian hormone of uncertain origin (LeRoux, 1933; Charniaux-Cotton, 1960). When no yolk is deposited between moults, the long setae are lost and this condition was induced by removal of the ovaries in *O. gammarella* by Charniaux-Cotton (1960) and by radium irradiation that suppressed yolk deposition in *G. duebeni* by LeRoux (1933).

Steele (1964) found that in *G. oceanicus* unfertilized eggs were not deposited into the brood pouch by females isolated from precopula with males and they therefore did not moult.

Sexton (1924) had similar results with *G. pulex* and *G. chevreuxi* and observations on the females in the photoperiod experiments indicate that *G. setosus* behave in the same manner. However, some species such as *G. duebeni* (LeRoux, 1933) and *G. locusta* (Sexton, 1924), lay unfertilized eggs.

The maturation cycle of male gametes was not studied in *G. setosus* as Steele (1964) determined that the male does not have a definite cycle and will seize females with ripe gonads at any time of the year. This indicates that the female cycle is more definitive and is responsible for regulation of the breeding cycle.

The vitelline membrane of the oocyte is formed during oogenesis by a hardening of the outer layer of ooplasm and in species where it is thick (*ie.* worms, molluscs and echinoderms), a zona radiata is present (Raven, 1961). The zona radiata is not continuous being perforated by pores through which pass cytoplasmic extrusions (connections) linking the cytoplasm of the follicle cell with that of the oocyte (Kemp & Hibbart, 1957). These extrusions were seen in the oocyte of *G. setosus* but the zona radiata is relatively thin.

Yamamoto (1956) noted the appearance of fine granules beneath the vitelline membrane, in the zona radiata, at the initiation of vitellogenesis forming a dense cortical layer. Beneath this layer is a vacuolated zone that gradually disappears as the cortical layer thickens. This process also occurs in the oocyte of *G. setosus* where the appearance of peripheral polysaccharide granules eventually lead to obliteration of the vacuolated ooplasm.

The formation of lipid globules was not studied in *G. setosus* although some were seen en route from the hepatopancreas in the direction of the ovary. In the crustaceans

Cambarus (Kater, 1928), *Palaemon* and *Paratelphusa* (Bhatia & Nath, 1931) lipid yolk globules arise from Golgi bodies. The fatty yolk is originally rich in phospholipid while the neutral fats (triglycerides) predominate in the final stages. The full term oocyte is composed almost entirely of saturated and fatty acids (Raven, 1961). Nath *et al.*, (1958) found that in *Pheretima*, the fat globules had an inner core of phospholipid enveloped by a triglyceride cortex whereas *Periplaneta*, had triglyceride centers. The phospholipid later disappears leaving a solid tryglyceride fat droplet. Electron micrographs of the yolk in *G. setosus* show some lipid globules with a core of different density, but this may be the result of insufficient osmification. The yolk globules however, have a jig-saw-like arrangement facilitating the compacting of the oocyte,

The protein granules are not often exclusively protein, but are associated with various proportions of fats and lipids. Usually they are bound to protein as lipoprotein while polysaccharides are also admixed to the protein yolk granules (Raven, 1961). Telfer (1961) showed that in some insects the yolk proteins have extraovarian origin and are immunologically similar to proteins found in the hemolymph. The female-specific vitellogenic proteins have been shown to originate in the fat body of some insect species and enter the oocytes through the intrafollicular spaces (Brooks, 1970).

The oocyte of *G. setosus* is mainly polysaccharide in composition with both lipid and protein fractions also present. These components are probably extraovarian in origin and the neighbouring hepatopancreas is the major supplier as lipid globules, PAS-positive polysaccharide areas and PF-positive protein granules are all found within its cells and usually concentrated near their bases adjacent to the ovary.

The follicular epithelium must function normally in order for yolk deposition to occur. Laurence and Simpson (1974), working with four species of mosquitoes, found that there were mitotic divisions resulting in an increase in the number of follicle cells and without this step there was no further development of the oogonia. A numerical increase in follicular cells was also noted in *G. setosus* at initiation of vitellogenesis. Bell and Barth (1971) showed that the presence of the juvenile hormone was required for morphological changes in the follicular epithelium prior to vitellogenesis in insects after Deloof and Lagasse (1970) found that these changes were necessary for successful yolk deposition. Anderson (1971) showed that if the follicular cells were stripped off the oogonia in culture, they failed to absorb the vitellogenic proteins from the surrounding media.

Sahota (1973) found that the juvenile hormone in the Douglas Fir beetle influences RNA synthesis in the follicle cells and without this yolk deposition is inhibited. Yolk deposition may also be controlled by similar means in *G. setosus* as morphological changes were noted in the follicle cells prior to vitellogenesis.

THE HEPATOPANCREAS:

Yonge (1924) described glands in the body cavity of crustaceans opening via ducts of varying length and regarded them to be actively secreting mucus and/or amylase. The granule-laden, gland-like accumulation of cells in the region of the hepatopancreas and ovary of *G. setosus* may also function in the secretion of mucus. These structures are morphologically similar to the Bowman's mucus-producing glands of vertebrate olfactory epithelium and their ducts infiltrate the invaginations of the hepatopancreas. The released granules penetrate the hepatopancreas by pinocytosis and may be elaborated by these cells or passed directly through into the gut to serve as a protective lubricant against the caustic enzymes produced by the secretory cells of the hepatopancreas. The collecting ductules funnel these secretions into the midgut behind the stomach in *G. setosus*. Roche (1953) found that in *Asellus* the midgut played an accessory role in the secretion of the digestive juices, while in decapods, these secretions are produced almost entirely by the hepatopancreas (Vonk, 1960).

The inner wall of the blind tubules is composed of a simple epithelium with special structure and function. There are generally two types of cells present: storage cells (R cells) and secretory cells (B cells), (Yonge, 1924). The hepatopancreas also serves in absorbing nutrients as well as in the secretion of digestive juices that include proteases, lipases and carbohydrases. The R cells of *Nephrops* absorb iron (Yonge, 1924) while those of *Atya* store lipids (van Weel, 1955). The hepatopancreas of *G. setosus* contain stored lipid globules, and massive rough ER complexes and large numbers of mitochondria account for the presence of PF-positive protein and PAS-positive polysaccharide material. These cells had extensive canalicular networks weaving through their cytoplasm, especially in the region nearest the ovary.

The hepatopancreas of crustaceans (analogous to the liver of vertebrates and fat body of insects) is a major site for bulk storage, synthesis and transformation of a variety of organic and inorganic substances. Adiyodi and Adiyodi (1970, 1971, 1972), working with *Paratelphusa hydrodromous*, established that the hepatopancreas reserves were maximal in intermoult and become mobilized to meet the demands of somatic and reproductive growth. Hepatopancreatic phospholipids, especially phosphotidylethanalamine and phosphatidylcholine, were depleted by the oogonial maturation process. Free sugars and unsaturated fatty acids varied in quality and quantity suggesting utilization in yolk formation. Fluctuations also occurred with the organic and inorganic substances associated with the moult. Although the chemical components of the hepatopancreas were not extensively studied in *G. setosus*, a marked depletion of lipid globules in these cells was noted during vitellogenesis in the ovary and the other yolk constituents probably had similar cycles. The synthesis of proteins in the hepatopancreas related to the moult and reproductive activity, vitellogenesis, appears to be inhibited during the intermoult by some eyestalk principle (Adiyodi & Adiyodi, 1972).

EFFECT OF PHOTOPERIOD ON REPRODUCTION:

In evaluating the effect of photoperiod on the ovarian cycle it was necessary to take into consideration that not all oogonia and oocytes in an ovary pass through similar stages simultaneously. Some oocytes appear healthy and normal while the initial stages of resorption are occurring in the ones adjacent. Determining the state of the ovary was based on the number of oogonia or oocytes that are being simultaneously affected.

Photoperiod duration does not influence the frequency of the cycle in any portion of the population but rather causes resorption of the oocytes instead of ovulation. It does however, influence the amplitude of the ovarian cycle in regard to the number of oogonia or oocytes affected simultaneously in a given animal. There are varying thresholds of light sensitivity in the animals and the longer the period of exposure to a certain photoperiod, the greater the number of animals influenced. Stephens (1952) found that with *Orconectes virilis*, 20 hours of light per day synchronized the responses of an entire experimental sample.

O. virilis (Stephens, 1952), *Cambarellus shufeldti* (Lowe, 1961) and *Procambarus simulans* (Perryman, 1969), all boreosubtropical species, show that an increase in photoperiod caused rapid ovarian maturation and resorption cycles, the longer the photoperiod the faster the cycle. Decreased photoperiods resulted in a more rapid maturation process but stabilized the ovary in a mature condition with limited recycling after the majority of the oocytes attained maturity (Lowe, 1961), while in complete darkness no recycling was recorded (Perryman, 1969).

The decreasing temperature and shortening photoperiods in late fall stimulated proliferation of new oocytes but inhibited ovarian maturation. Gradually this inhibition is lost with the onset of spring with increasing temperatures and lengthening photoperiods, and the ovaries mature and ovulation follows (Lowe, 1961). Lowe found that even after yolk deposition is complete ovulation couldn't always be induced suggesting that additional changes occur after apparent histological maturity is reached.

Stephens (1952) suggested that total darkness stimulates the release of an inhibitory factor restricting proliferation of new oocytes. The medulla terminalis section of the X organ may produce this substance (Brown & Jones, 1947). Continuous exposure to 6 hours light causes the inhibitor, released in total darkness, to loose its effect and the cyclic process begins after initial rapid maturation is reached but can not be maintained in *O. virilis* (Stephens, 1952).

Aiken (1969) found that temperature alone would not permit complete ovarian maturation in *O. virilis* but would prevent growth and degeneration cycles and a temperature threshold of 10-11°C was established for ovulation. Below this, sustained maturation and degeneration cycles were reported (Stephens, 1952; Lowe, 1961). Growth is photoperiodically controlled in juvenile *O. virilis* but this was not proven in adults.

Segerstrale (1970) observed that the boreo-arctic amphipod *Pontoporeia affinis* breeds in the cold season and results suggested that it was the decrease in seasonal illumination that induced maturation of the gonads and controlled the reproductive cycle. Animals kept in complete darkness had ovaries far more mature than those exposed to seasonal photoperiods while constant illumination inhibited ovarian activity (Segerstrale, 1971). The difference in illumination that triggers this cycle may be due to an adaptive mechanism connected with the perception of light. When the animals live in water deeper than 100 meters, they also breed outside the period defined by those in shallower depths as at 100 meters constant darkness prevails (Segerstråle, 1970).

H. Barnes (1963) and Crisp and Patel (1969) found that illumination exerted an inhibitory influence on ovarian maturation in *Balanus*, delaying the onset of breeding. The decrease of light in late summer may also trigger the maturation in this species as they reproduce in November. *P. affinis* shares this feature of winter reproduction with other marine animals living at high latitudes. It has been suggested that this is an adaptation to the marked seasonal fluctuations in temperature, food supply and so on, typical of this region where conditions are favourable in the spring for survival of the new generation (H. Barnes, 1963).

Temperature has been excluded as a regulatory mechanism in *P. affinis* because of the marked difference between that of the shallow and deeper waters of its range before and at the onset of gonad maturation in late summer (Segerstrale, 1937).

In the subarctic waters of Newfoundland, *G. setosus* has a well defined reproductive cycle resulting in one brood per year. Since the rate of development in *Gammarus* depends largely on the temperature (Sexton, 1924; Steele & Steele, 1973), the gonads of the larger (older) females mature earlier in the year than those of the developing young. This spreads their breeding period over several months and females releasing their young in early winter are prevented from having a second brood by the low incumbent temperatures that prolong the physiological processes and the female enters the resting stage (Steele, 1967).

The resting stage is considered by Steele (1967) to be the mechanism regulating the reproductive cycle in *G. setosus* that prevents the animal from getting out of phase with its environment which is most favourable for survival of the young. Lowe (1961) found that the ovaries in *C. shufeldti* had an inherent late summer decline that may have been linked to a general metabolic factor as the animals showed the least body weight increase at this time. This may be a phenomenon analogous to the resting stage of *G. setosus*.

Reproductive timing in *G. setosus* has been found to be largely dependent upon photoperiod (Steele, personal communication) and to a lesser degree upon temperature. The timing for release of the young and their embryonic development has been found to be based upon environmental temperatures and occurs earlier the further south the animal lives in its range (Steele & Steele, 1973). The females enter the resting stage earlier but the next ovarian cycle does not proceed any faster unless induced by altering the photoperiod. Based on the observations in this study, the resting stage is probably a phenomenon brought on by the animals physiological slow down after release of the young in a period of low incumbent temperatures. At 10°C in the laboratory, the resting stage duration was not as long but it cannot be ruled out as it could have been reduced to the period during which the stage 5 oocytes were resorbed in the ovary prior to the initiation of the successive cycle.

Because *G. setosus* reproduces from late fall to early winter, it may be assumed that acceleration of ovarian development is triggered by the seasonal decrease in illumination. Results from the photoperiod experiments in this study coincide with the hypothesis elucidated by Segerstråle (1970). The shorter the duration of the photoperiod, the faster the animals pass through their ovarian cycle. Complete darkness stimulates successive cycles, 14 hours light prolongs the cycles while constant illumination probably inhibits ovarian development as in the case of *P. affinis* (Segerstråle, 1971) or may arrest the oocytes in a stage of maturity as in *P. simulans* (Perryman, 1969) and *O. virilis* (Aiken, 1969).

Bliss (1966) noted that females kept in long day photoperiods and unsuccessful in sexual maturation had high mortality rates possibly explained by antagonism between the processes leading to somatic and reproductive growth. This could also be the cause of the higher mortality rates observed among female *G. setosus* exposed to 14 hours light in this study.

G. setosus and *P. affinis* (Segerstråle, 1970, 1971) are subarctic species and live at different latitudes than the three crayfish species, *C. shufeldti*, *P. simulans* and *O. virilis*, are subtropical. The photoperiods that trigger their reproductive cycles and response to the various experimental photoperiods are opposite.

NEUROSECRETORY EFFECT ON REPRODUCTION:

The reproductive activity of female crustaceans is dependent upon both environmental and hormonal action but the complete picture is still vague. Panouse (1943, 1944) was the first to observe an acceleration of ovarian growth, vitellogenesis and ovulation in a resting stage *Leander serratus* female after eyestalk removal. Otsu and Hanaoka (1951) stated that ovarian development was controlled by two antagonistic factors in Crustacea, one inhibitory and the other stimulatory. Brown and Jones (1947) confirmed the presence of an ovary-inhibiting hormone in *Cambarus*, Brown and Jones (1949) in *Uca*, Demeusy and Veillet (1952) in *Carcinus* and Carlisle (1953) in *Lysmata*. Carlisle (1953) also indicated that the ovary-inhibiting hormone was produced in the X organ. Of the three endocrine factors thought to influence ovarian development, two were from the eyestalk and the third from the suboesophageal ganglion.

The eyestalk hormones control moulting, oogenesis, vitellogenesis and the secretion of sex hormones. The reproductive hormones influence the synthesis and accumulation of a lipoprotein utilized in vitellogenesis. This substance was found in adult female *Libinia* by Hinsch (1972) but not in juvenile animals. The eyestalk hormones regulate ovulation but after removal there is a delay before ovulation occurs, suggesting the involvement of another factor also under the control of the eyestalk. This substance could be stimulatory and be produced by the neurosecretory cells of the cerebral and/or thoracic ganglia.

Otsu (1960) discovered the presence of the ovary-stimulating hormone secreted by the neurosecretory cells of the thoracic ganglia in *Potamon dehaani*. Otsu (1963) showed that implantation of a thoracic ganglion mass into a female crab with eyestalks induced ovarian development. Gómez (1965) demonstrated acceleration of gonadal development after brain implantation in *Paratelphusa hydrodromous*. Hinsch and Bennett (1973) showed that implantation of the thoracic ganglion of adult female spider crabs into immature females resulted in hormonal stimulation of vitellogenesis. The endocrine centers of the eyestalk inhibit the reproductive cycle of decapod crustaceans while thoracic ganglion implants induce the same acceleration of ovarian growth shown after removal of the eyestalks.

The sinus gland of *Uca pugilator* inhibits reproduction and its removal accelerates ovarian growth, maturation of oocytes and ovulation during the period when the oocytes are normally quiescent (Brown & Jones, 1949). Carlisle (1953) suggested that sex reversal in *Lysmata seticaudata* was inhibited by this same hormone produced in the ganglionic X organ and released from the sinus gland. Rangnecker *et al.* (1971) found that the hormones from the eyestalk also inhibit the activity of the androgen gland in male crabs which in turn inhibits gonadal development. Gonadal development in females requires less ovary-stimulating hormone from the eyestalks and more ovary-stimulating hormone from the brain and thoracic ganglia.

Destalked immature decapods do not attain sexual maturity, suggesting hormonal control from locations other than the X organ-sinus gland complex. In some crustaceans the Y organ may be the source of the maturation factor (Hinsch, 1972). Demeusy (1962) showed that *Carcinus maenus* underwent ovarian enlargement after removal of the moult-inducing Y organ. Gonadal development may also require an increase in the amount of moult-inhibiting hormone and a decrease in Y organ moult-inducing hormone. In *Paratelphusa* and *Caridina* liberation of the moult hormone at the time of the intra-brood moult stimulates vitellogenesis in the ovary (John, 1967). The gonadotropic hormone controlling vitellogenesis is distinct from the moult-inhibiting hormone as the rate of yolk deposition cannot be attributed to the acceleration of the intermoult periods after eyestalk removal. Premature vitellogenesis prolongs the intermoult period in normal intermoult females (Drach, 1955).

The moult-inducing and ovary-stimulating hormones are both produced in the eyestalk of higher malacostracans and are antagonistic to one another. When the eyestalk is removed the animal somehow determines which of the two phenomena should be expressed. The answer seems to depend upon the time of year during which the destalking occurred. The animal is more physiologically equipped at one time for moulting and at another for reproductive development (Bliss, 1966). The fact that oogenesis does not always occur is based on whether the oogonia have reached the point permitting vitellogenesis to proceed. Its removal prior to the breeding season usually causes acceleration of the event (Charniaux-Cotton, 1960).

The intensity of neurosecretory activity in the eyestalk corresponds with that of the oocytes. The difference in histological appearances have been used to show that neurosecretory cells do influence reproduction and neurosecretory control of ovarian maturation and ovulation has been established in many insect species (Highnam, 1962; Ittycheriah, 1967; Mouton, 1971; Foster, 1972 and Kupferman, 1972). Kratzsch (1951), Ortmann (1951) and Andersson and Jewell (1957) recognized a correlation between the physiological state of the animal and the quantity and quality of NSM. Matsumoto (1958) found that the secretory activity of the alpha and beta neurosecretory cells of the optic peduncle to be higher during peak periods of reproductive activity in *Sesarma, Potamon, Neptunas* and *Chionectes*. Perryman (1969) related morphological changes in the neurosecretory cells identified by Bliss *et al*., (1954) and Durand (1956) in *P. simulans* with the reproductive cycle. At different periods of the ovarian cycle there were varying amounts of NSM in cells located in the suboesophageal ganglion and eyestalk. Of the four basic cell types, two were in the medulla terminalis X organ and could both be related to the reproductive cycle.

Cell type one from the medulla terminalis X organ of the eyestalk produced an inhibitory secretion that restricted proliferation of new oogonia until the mature oocytes had been either ovulated or resorbed. The NSM granules accumulate while the oocytes developed reaching a peak at time of ovulation or resorption. Cell type three, also in the medulla terminalis X organ, produced a substance that accelerated ovulation or resorption of the mature oocytes. More granules were present when vitelloegenesis occurred.

Besse (1968) found that in the isopod *Porcellio dilatatus*, ablation of the medial protocerebral region of the adult female brain, induced ovarian maturation and aborted the occurrence of the moult. Mocquard *et al.*, (1971) showed that one or more neurohemal centers inhibiting growth, moulting and vitellogenesis were present in the protocerebrum of the isopod *Ligia oceanica*. The ventral ganglion chain stimulated water resorption at moulting but had no effect on sexual physiology. The inhibitory effect of the protocerebrum on the moult and growth are far more marked when the nervous system connections are intact, suggesting the necessity of contact with the target organ.

G. setosus is a sessile-eyed crustacean and the X organ-sinus gland complex of the higher malacostracan eyestalk is nonexistent. The sinus gland may still be an integral neurohemal release site for the regulation of the reproductive cycle by liberating an undesignated hormone. The secretory activity of the gland is cyclic, appearing empty of NSM at the time of ovulation. As actual release of NSM from the gland was not observed, the hormone could be inhibitory if released continually up until a point of depletion, or stimulatory if released all at once at the time of the preovulatory moult, inducing ovulation.

The frontal organ however, appears to play an inhibitory role in the reproductive cycle, similar to that exhibited by the X organ-sinus gland complex of higher malacostracans. In early August, when the type I frontal organ neurons appear empty of NSM, vitellogenesis is initiated in the ovary. After another accumulation and release cycle the neurons empty again, at time of precopula, and ovulation occurs. These cells may also inhibit moulting as it occurs when the frontal organ neurons contain only a small quanity of NSM. The role of the Y organ was not investigated in *G. setosus* but its moult-inducing role exhibited throughout Crustacea was assumed with the possibility that the latter observation on the frontal organ was coincidental. The Y organ could also exhibit its reported stimulatory effect on vitellogenesis as at this point its moult-inducing hormones are being suppressed. However, at ovulation its secreted hormone is dominant due to the coinciding preovulatory moult and its presence could stimulate ovulation. Inhibition of oogonial proliferation after ovulation and up until time of release of the hatched young could also be under the hormonal influence of the type I frontal organ neurons. They continue to release NSM again after the occurrence of ovulation and do not cease until the postovulatory moult at which time the oogonia may be stimulated into growth only to be inhibited by the low temperatures at the initiation of the resting stage. When the temperature rises again in the spring the oogonia automatically begin to grow without the appearance of any additional or lack of neurosecretory activity.

The neurosecretory cells of the brain and ventral ganglia also appear to effect reproduction and undergo an increase in activity as the cycle proceeds. By the time the female enters precopula, the neurosecretory cells stain intensely, indicating a large accumulation of NSM in the perikarya. After ovulation the cells appear empty but a minimal amount is still present in some neurons of the ventral ganglia. The results of the investigation are hard to interpret without ablation experiments to observe the reproductive activity in their absence. However, at present it appears that they function in a manner similar to that described by Besse (1968) and Mocquard *et al.*, (1971) in two isopod species, as inhibitory. The apparent build-up of NSM in the neurons may be the result of a faster production than release and at a point around the time of precopula, the cells cease production depleting themselves of NSM and ovulation occurs. The activity of the protocerebral neurons may be linked to that of the frontal organ through the medial frontal organ nerve that originates in this region and neurosecretory vesicles have been seen along the axons of the frontal organ neurons. The ovary-stimulating hormone may be produced by the cells of the thoracic ganglia when the frontal organ depletes itself of granules at the onset of vitellogenesis.

PHOTOPERIOD EFFECT ON NEUROSECRETION:

The first indications of cyclic changes in neurosecretory elements were described by Pyle (1943) studying the sinus gland of higher malacostracans. These have since been confirmed and amplified by several authors including Stephens (1952) and Suko (1958), relating changes in the neurosecretory pathway to the moult cycle as well as photoperiod. Stephens (1952) suggests that ovarian maturation and ovulation in *O. virilis* are controlled by four hormones that are in turn regulated by photoperiod. Aiken (1969) claims that the Stephen's theory (1952) does not stress temperature enough. There was however, evidence that neurosecretory cells in the central nervous system secrete an ovary-stimulating substance that regulates reproductive activity in *O. virilis* (Aiken, 1969). Although photoperiod influences ovarian maturation and ovulation partly through the X organ-sinus gland complex, the balance of the endocrine control, as well as the many environmental parameters that influence the endocrine system remain to be explained.

Photoperiod control of the endocrine system and photoperiod influence over it has been most thoroughly investigated in insects by Lees (1964), Highnam (1965), Geldiay (1966, 1967), Williams and Adkisson (1969) and others. They collectively established the direct action of light on endocrine system receptors influencing brain hormone secretions that control pupal diapause as well as long-day photoperiod stimulation of cerebral neurosecretory cells and their effect on ovarian development:

Parker (1966) established that reproduction was controlled in *Daphnia* by a neurohormone influence whose production is regulated by photoperiod. The quantity of NSM in the central nervous system of *Daphnia schødleri* is affected by photoperiod. The NSM may be an antimoult hormone activated and released into the bloodstream which in turn causes release of a second hormone produced by other glandular tissue. Since *Daphnia*, like *G. setosus*, usually moults each time it releases a brood; either hormone could be related to reproductive activity.

Tighe-Ford (1967) found that the breeding cycle of *Balanus balanoides* was controlled by both light and temperature. Critical values of 10°C and 12 hours light below which the barnacle could breed, were established. Neurosecretory cells were located in the subsupraoesophageal ganglion, and illumination caused the photoreceptor cells to generate a sustained depolarization inhibiting the second order neurons in this ganglion. Neurosecretory fibers were found in the median photoreceptor nerve by Fahrenbuch (1965).

Actual effect of photoperiod on the neurosecretory cells was not evaluated due to the limitation on time in this study. It stands to reason by extrapolation of the effect of photoperiod on the ovarian cycle, that a speed up of all the neurosecretory activities related with ovarian development occurs. In regard to the mechanism of resorption, this phenomenon has not been investigated in Crustacea and is a question worthy of future probing.

CORRELATION OF NEUROSECRETORY ACTIVITY WITH PHYSIOLOGICAL PROCESSES:

Staining reactions alone cannot provide an adequate basis for conclusions regarding the occurrence of neurosecretion. Bullock and Horridge (1965) employed the following criteria in making the assumption: (1) the observation of stainable materials in the neuron indicating the possibility of neurosecretion, (2) if changes in quantity or quality of presumed NSM can be correlated with seasonal changes or physiological condition the occurrence of a secretory cycle indicates the existence of neurosecretion is probable and (3) if the presumed NSM can be associated in quantity and in location with the occurrence of a hormonal factor, the neurosecretion can be considered established.

When the staining cell has been established as being neurosecretory, the interpretation of the physiological significance requires caution. There are at least two alternate explanations: (1) the cell is actively releasing hormone into the blood stream but is producing the secretion faster than it can liberate it or (2) the rate of release is slight or even nil so that a low rate of synthesis causes accumulation of secretion in the axon and perikaryon (Bullock & Horridge, 1965).

Holms and Knowles (1960), Norman (1965), Smith and Smith (1966), Scharrer (1968) and Kono (1973) consider secretion to be occurring constantly and neurosecretory activity to consist of two phases: (1) synthesis of NSM in the perikaryon and (2) the release of NSM. Thw quantity of NSM in the cytoplasm changes accordingly with the relative activities of these two processes.

Staining as a criterion for secretory activity has different meanings in different forms. In some insects the neurosecretory cells contain the most secretion during periods when there is little or no hormone being liberated as release is not occurring but synthesis continues. This leads to an accumulation of NSM in the cells (Bell *et al.*, 1974). A situation such as this would completely reverse that stated previously about the neurosecretory significance in reproduction in *G. setosus*. This can only be clarified by further ultrastructural study.

The function of the neurosecretory cells is to form a system that is central to the operation of endocrine mechanisms wherever they exist among metazoan animals. There are many non-neural endocrine organs in invertebrates and they also have their functioning closely regulated by the nervous system through hormonal or nervous pathways. Neurosecretion is a specialized activity of neurons that are carrying out a type of secretory process distinct from the neurohemal role of the ordinary neuron (Bullock & Horridge, 1965). Major questions concerning neurosecretion still exist in regard to the nature, both structural and chemical, synthesis, transport and release of NSM as well as the neuronal properties of the neurosecretory neuron.

SUMMARY AND CONCLUSIONS:

The central nervous system of *G. setosus* consists of a brain, suboesophageal ganglion and a ventral ganglion chain. The organization of the nervous elements show the characteristic crustacean core/rind arrangement and both the central fibrous neuropiles and the peripheral cellular glomeruli show good differentiation. The glomeruli of the brain contain two types of neurosecretory cells, A and B, based on perikaryon size. The medial glomeruli of the protocerebrum contain the largest accumulation of neurosecretory cells while the glomeruli of the deutocerebrum and tritocerebrum contain relatively fewer cells and the majority of these are A cells. The glomeruli of the suboesophageal ganglion contain two types of neurosecretory cells, A and A', based on perikaryon size and these cells are found mainly in the dorsolateral glomeruli at the root of the segmental nerves. The glomeruli of the ventral thoracic and abdominal ganglia contain four types of neurosecretory cells, A, A', B and C, based on perikaryon size with A' being bipolar. These cells are found evenly distributed throughout the dorsolateral and ventral glomeruli of the thoracic ganglia but mainly in the ventral glomeruli of the abdominal ganglia.

The accessory cephalic structures of the anterior head region include the sinus gland, statocyst and frontal organ, all three of which have a nervous connection with the brain. The sinus gland has both cellular and acellular areas, containing variable quantities of NSM. The statocysts are large and well developed and the neurons of the frontal organ are of two types, I and II, based on the size of the neurosecretory vesicles they produce and release in a cyclic pattern. There is no X organ present.

The ovaries of *G. setosus* are paired and located dorsolateral to the digestive tract. The female has one brood per year at Witless Bay, Newfoundland, with the ovaries beginning steady growth in May. In early August they undergo vitellogenesis resulting in rapid enlargement and final maturation of the ovaries. Ovulation occurs in late fall and the female enters a resting stage after release of the hatched young in early winter. Oogonial growth is weak during this period, probably the result of low ambient temperatures. The hepatopancreas appears to function in supply of the vitellogenic materials to the ovary and the peripheral follicular epithelial layer of the oocytes, undergoes major morphological changes to facilitate this process. The yolk of the oocyte has three fractions: polysaccharide, lipid and protein, deposited in that order. Photoperiod appears to be the main environmental factor influencing the reproductive cycle and the decrease in illumination of late summer is the stimulus for vitellogenesis. The photoperiod experiments show that longer photoperiods (14 hours light) prolong the ovarian cycle, while shorter ones (12 and 8 hours light) accelerate it. Complete darkness induces successive cycles after resorption of the mature oocytes produced by each maturation cycle.

Synthesis of NSM was directly associated with the Golgi regions in the type II frontal organ neurons and the A cells of the brain glomeruli producing type I neurosecretory granules. Production of the larger, mitochondrion-like neurosecretory vesicles found in the type I frontal organ neurons and the remaining neurosecretory neurons of the brain and ventral ganglia, has not been definitely established. Mitochondrial fission and enlargement, or transformation of Golgi-formed multivesicular bodies were the two alternatives suggested in this study.

The continual release of NSM from the type I frontal organ neurons appears to have an inhibitory effect on ovarian development. The cells first appear empty in early August when vitellogenesis is intitiated. The cells then produce and liberate more NSM becoming empty again at the time of ovulation. The neurosecretory activity cycle of the cells of the brain, suboesophageal and ventral ganglia is difficult to interpret and could be either stimulatory or inhibitory pending further investigation. The cells have an accumulation of NSM that builds up until the time of ovulation after which they appear empty. If the mode of release is gradual, the material is inhibitory; if the release is all-out, it is stimulatory. A number of neurons in the ventral ganglia exhibit stainable NSM at all times and these may be the source of an ovary-inhibiting hormone. The role of the Y organ was not investigated but it may also have an inhibitory effect when in dominance.

FIGURES

LEGEND OF ABBREVIATIONS USED IN FIGURES

A

a,A - axon
act - adipose connective tissue
ag - antennal glomeruli
ailg - anterior inferior lateral glomeruli
aimg - anterior inferior medial glomeruli
aimgb - anterior inferior medial glomerular bridge
al - accessory lobe
alc - accessory lobe commissure
an - antenna II nerve
anb - antennal nerve branch
ann - antenna II neuropile
ant - antenna I nerve
antn - antenna I neuropile
aslg - anterior superior lateral glomeruli
asmg - anterior superior medial glomeruli

B

b - blood
bl - basal lamina

C

c - connective
C - mitochondrial crest
cb - central body
CE - cytoplasmic extrusion
CM - cell membrane
cp - capsule
cr - core
cs - connective tissue strand
ct - connective tissue
Cy - cytoplasm

D

d - dorsal
DC - dense core vesicle
DG - dense granule
dnl - dorsolateral neuronal layer
ds - distal portion
dt - deutocerebrum

E

e - eye
eg - empty granule
es - extracellular space
EV - empty vesicle

F

fc,FC - follicle cell
fct - fibrous connective tissue
Fm - flocculent material
fo - frontal organ
foc - frontal organ cells
fr - fiber core
FR - free ribosome

G

g - granule
G - Golgi
gb - ganglion body
gc,GC - glial cell
gg - ghost granule
Gg - glycogen granule
gp - gap
GP - glial process
gs,GS - glial sheath
Gt - gliotubule
GV - Golgi vesicle

H

h - hypodermis

hp, Hp - hepatopancreas

I

i - integument
iamg - inferior anterior medial glomeruli
ilag - inferior lateral anterior glomeruli
ilg - inferior lateral glomeruli
img - inferior medial glomeruli
ipg - inferior posterior glomeruli

L

l.L - lipid
lg - lamina ganglionaris
lgn - lateral ganglionic neuropile
lm - limiting membrane
lt - light area
lu - lumen
LV - lucent vesicle

M

m - muscle
M - mitochondrion
mc - mucus cell
md, MD - mucus droplet
me - medulla externa
mfo - medial frontal organ nerve
mgn - medial ganglionic neuropile
mi - medulla interna
mp - mucus plug
mpgn - medial parallel ganglionic neuropile
mt - medulla terminalis
MV - mitochondrion-like vesicle
MVB - multivesicular body

N

n, N - nucleus
nc - neuron
Nf - neurofilament
nl - neuronal layer
NM - nuclear membrane
np - neuropile
NP - nuclear pore
ns - nucleolus
NS - nuclear space
Nt - neurotubule
NV - neurosecretory vesicle

O

o - ovary
oe - ovarian epithelium
oflg - olfactory lobe glomeruli
og - optic ganglia
ol - optic lobe
olf - olfactory lobe
olg - optic lobe glomeruli
on - optic nerve
oo, OO - oogonia/oocyte
ot - olfactorio-globularis tract

P

p - perikaryon
pb - protocerebral bridge
pg - protein granule
PG - pale granule
po - primary oogonium
pol - parolfactory lobe
pr - protocerebrum
ps - pseudopodia
pslg - posterior superior lateral glomeruli
PV - pale vesicle
px - proximal portion
py - protein yolk

R

r - rupture
R - ribosome
RB - residual body
RER - rough endoplasmic reticulum
rg - ruptured granule
RV - ruptured vesicle

S

s - statocyst
S - synapse
sg - sinus gland
sk - stalk
sl - statolith
sn - segmental nerve
so - secondary oogonium
stn - statocyst nerve

T

t - tract
T - trophospongium
TB - tubular structure
tn - tegumentary nerve
tnb - tritocerebral neuropile bridge
tnn - tegumentary nerve neuropile
tr - tritocerebrum
trc - tritocerebral connective
tso - tegumentary sensory organ

V

v - vacuole
V - large vesicle
vl - ventral
VM - vesicular membrane
vnl - ventral neuronal layer

X

Xo - X organ

Y

y - yolk

Z

ZR - zona radiata

Figure 1: Sagittal view through the head region of *G. setosus* showing the various nervous elements in relation to one another.

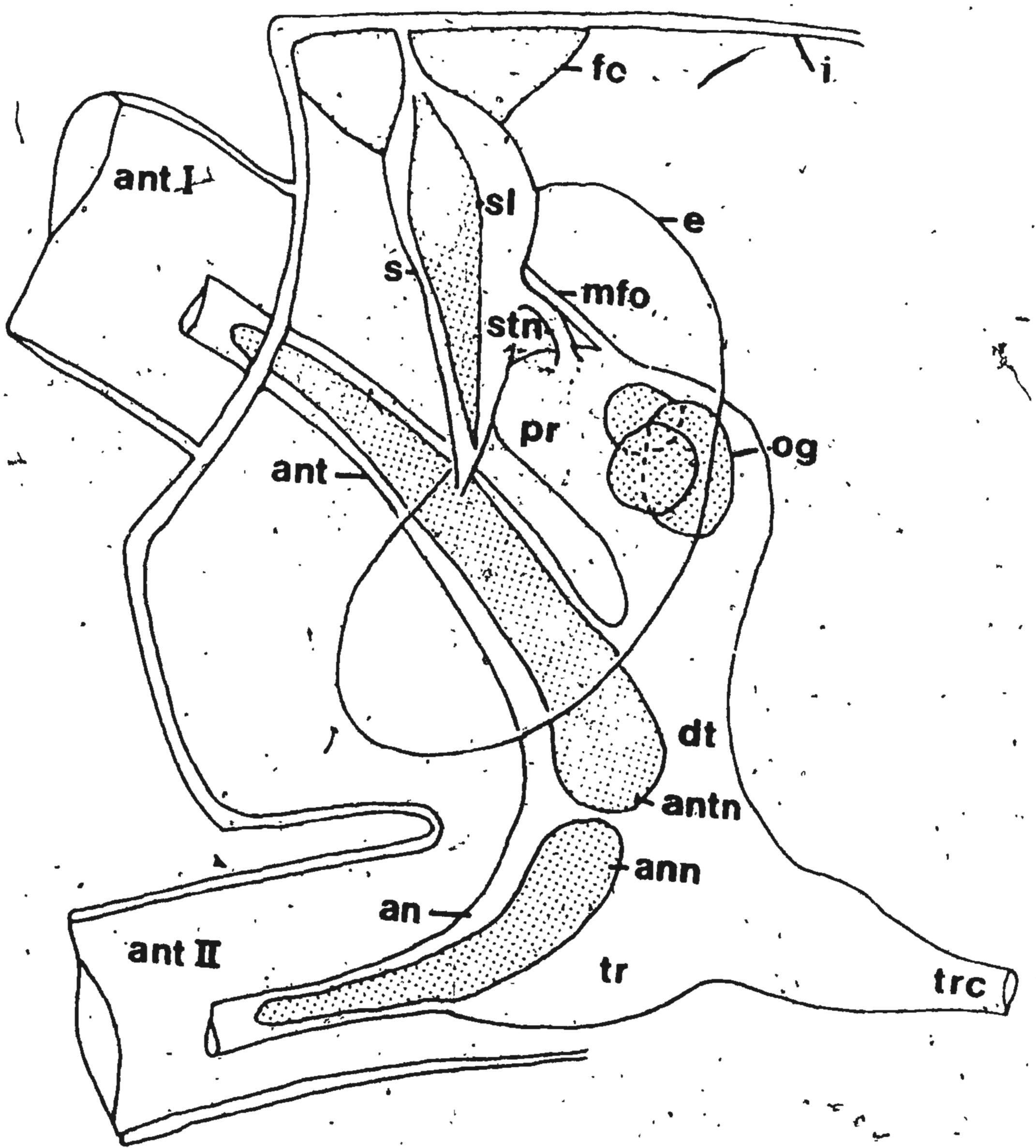
fc
i
ant I
sl
e
s
mfo
stn
pr
og
ant
dt
antn
ann
an
ant II
tr
trc

Figure 2: Anterior vertical view of the brain of *G. setosus* showing the location of the various neuropiles (modified from Gräber, 1933).

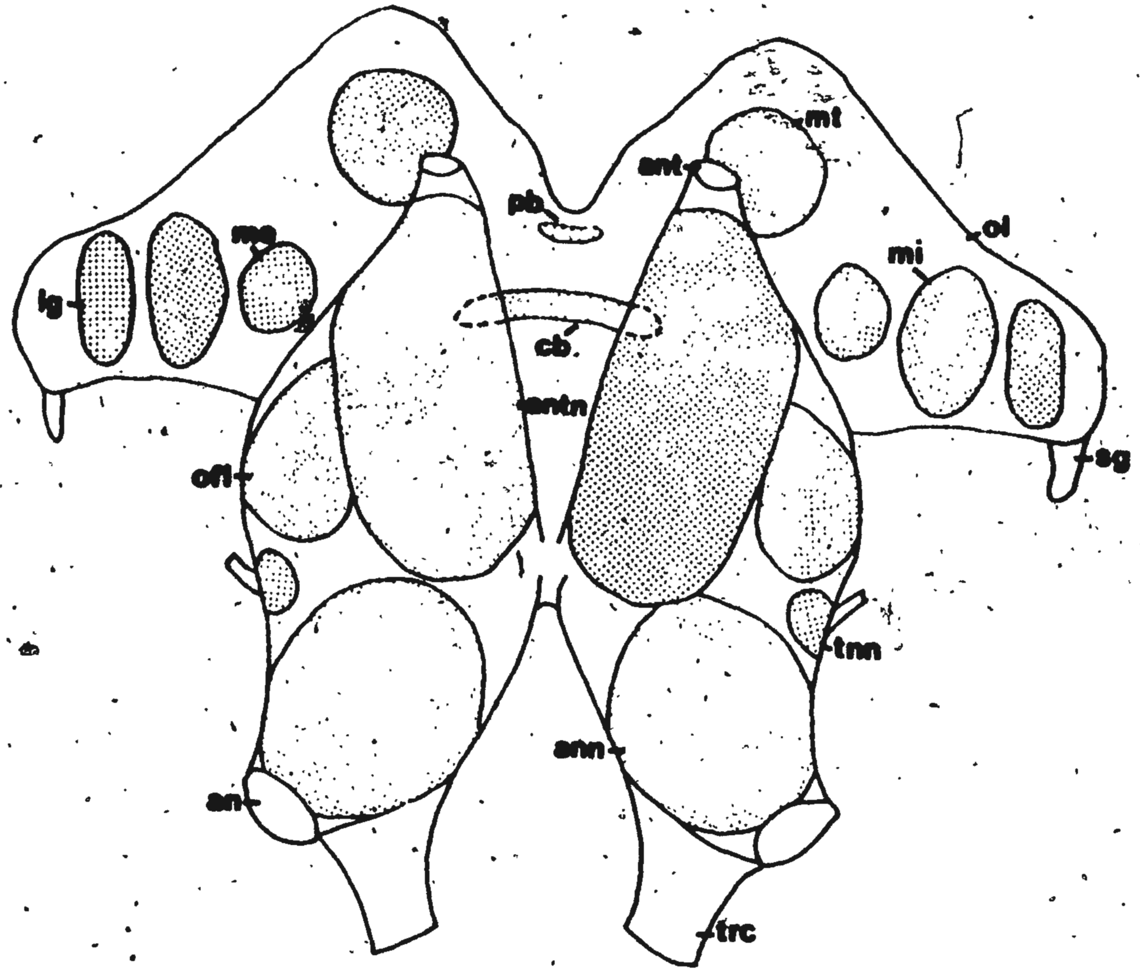
mt
ant
pb
ol
mi
mg
lg
cb
antn
sg
ofl
tnn
ann
an
trc

Figure 3: Vertical view of the anterior side of the brain of *G. setosus* showing the ganglionic cell layers (modified from Gräber, 1933).

Figure 4: Vertical view of the posterior side of the brain of *G. setosus* showing the ganglionic cell layers (modified from Gräber, 1933).

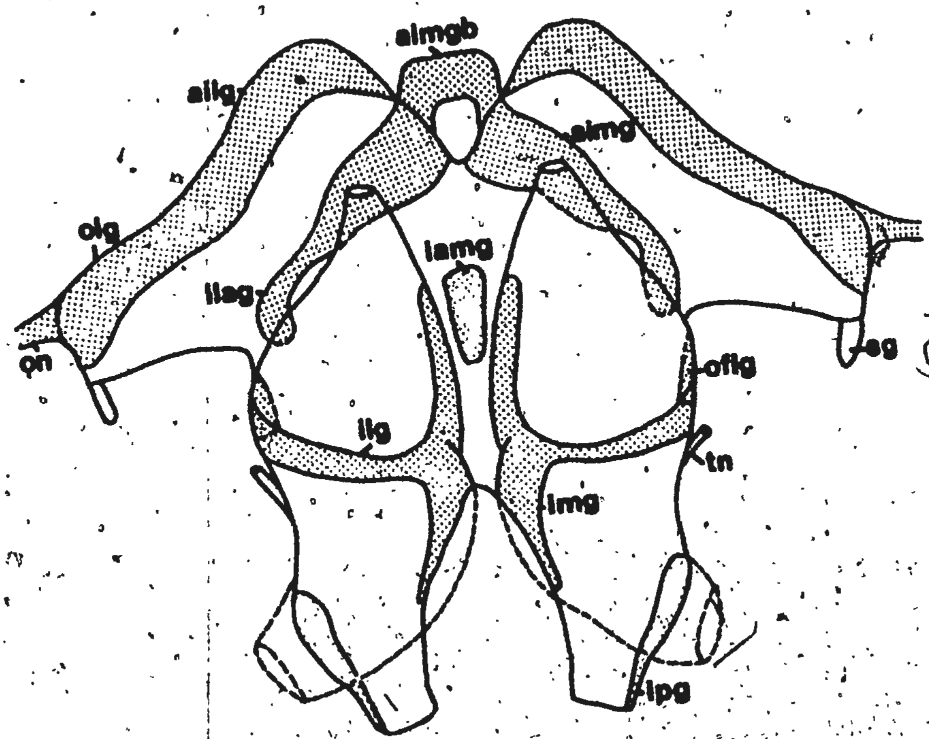
almgb
alig
almg
olg
lamg
llsg
on
eg
oflg
llg
tn
lmg
lpg

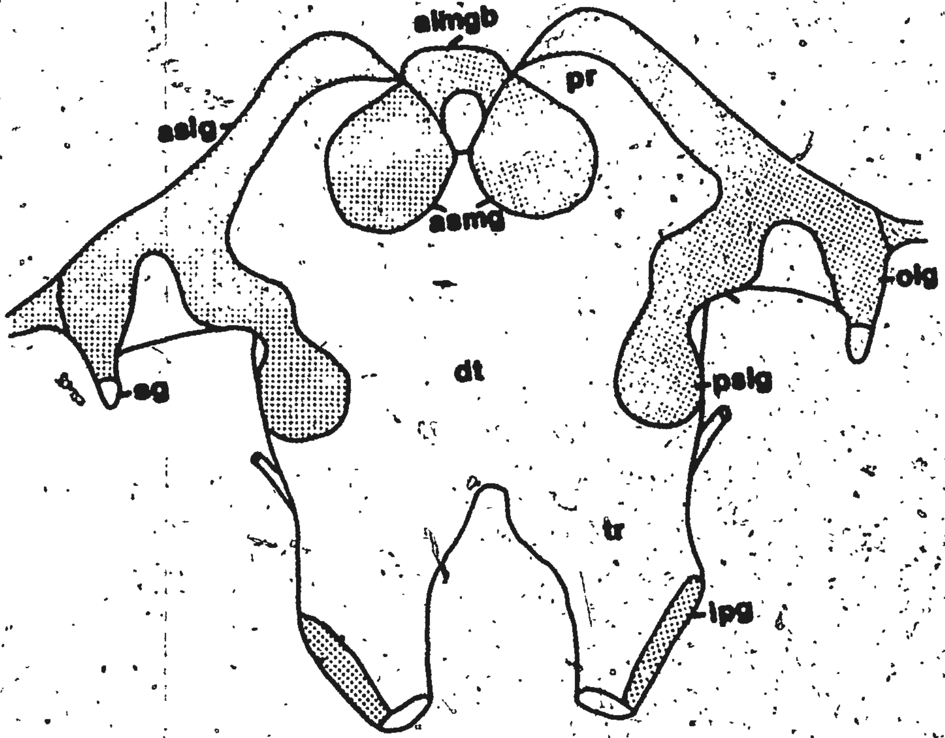
almgb
pr
asig
asmg
olg
dt
eg
psig
tr
lpg

Figure 5: (A) Structure of the adipose connective tissue found in the head region of *G. setosus* surrounding the brain mass (epon, toluidine blue pH 11.1, 1420X).

(B) Adipose connective tissue strands adhering to the fibrous connective tissue capsule of the brain mass functioning in support, holding the brain in a fixed position (epon, toluidine blue pH 11.1, 1420X).

Figure 6: Thin frontal section of the dorsal part of the protocerebrum of *G. setosus* (epon, toluidine blue pH 11.1, 70X).

Figure 7: Thin frontal section of the mid-protocerebral region of the brain of *G. setosus* (epon, toluidine blue pH 11.1, 70X).

Figure 8: Thick section of the mid-protocerebral region in the brain of *G. setosus* showing the various neuropiles (paraffin, PF, 50X).

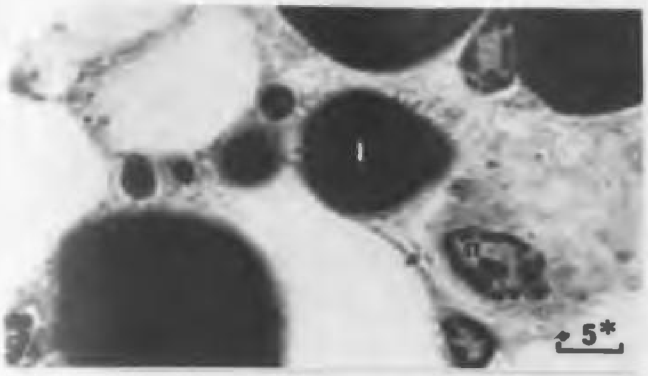
l
n
5*

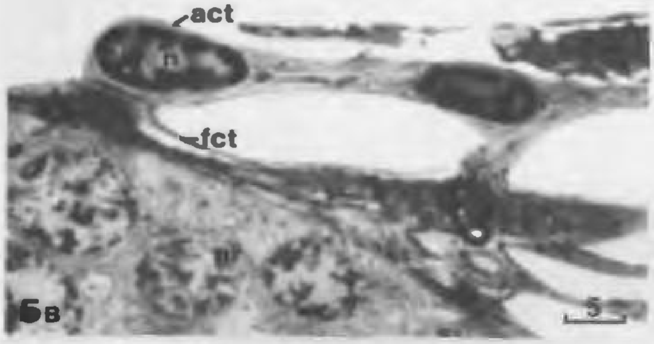
act
n
fct
n
5B
5

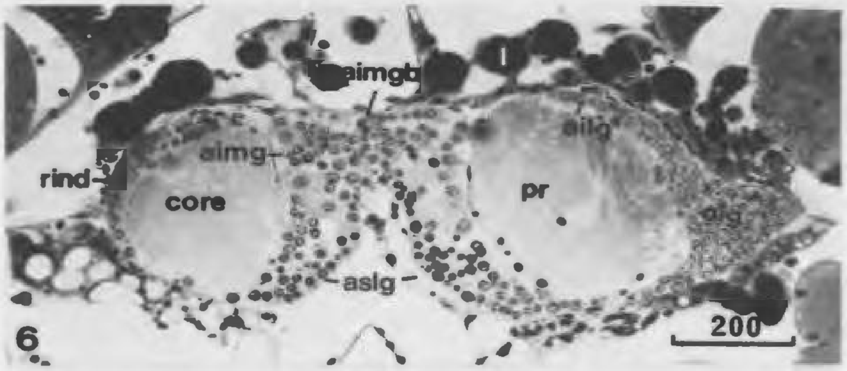
l
aimgb
ailg
aimg
rind
core
pr
olg
aslg
6
200

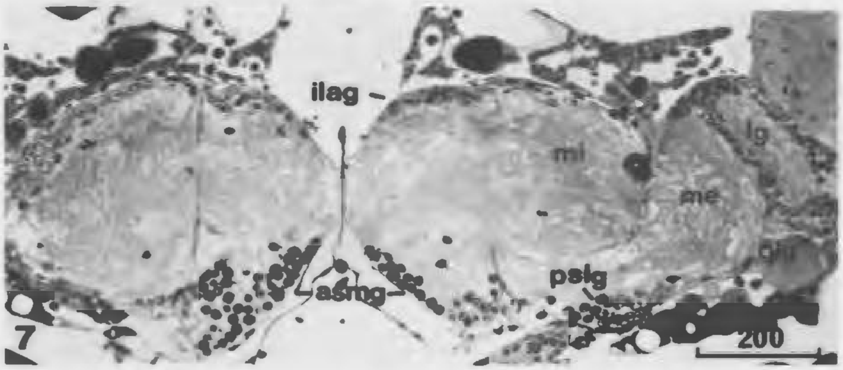
ilag
ml
lg
me
glo
pslg
asmg
7
200

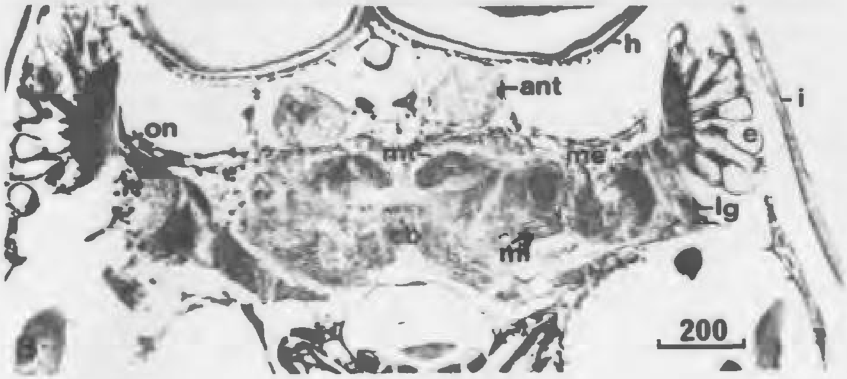
h
ant
i
on
mt
me
e
lg
cb
ml
200

Figure 9: Thin frontal section of the lower deutocerebral region of the brain of *G. setosus* showing the various neuropiles, tracts and cellular glomeruli (epon, toluidine blue pH 11.1, 64X).

Figure 10: Frontal section of the lower tritocerebrum of the brain of *G. setosus* just above the region where the antenna II nerves and tritocerebral connectives originate (epon, toluidine blue pH 11.1, 110X).

Figure 11: Frontal section through the upper tritocerebral region showing the neuropile bridge (epon, toluidine blue pH 11.1, 110X).

Figure 12: Thin cross section through the brain of *G. setosus* in the region of the central body showing its homogeneity (epon, toluidine blue pH 11.1, 500X).

Figure 13: Higher magnification of the neuropile constituting the central body (epon, toluidine blue pH 11.1, 2600X).

Figure 14: Cross section of the antenna I nerve in antenna I of *G. setosus* showing the origin of peripheral antennal nerve branches (epon, toluidine blue pH 11.1, 225X).

Figure 15: Thin frontal section of the upper head region of *G. setosus* showing the tegumentary sensory organ innervated by the tegumentary nerve of the mid-tritocerebral region (epon, toluidine blue pH 11.1, 225X).

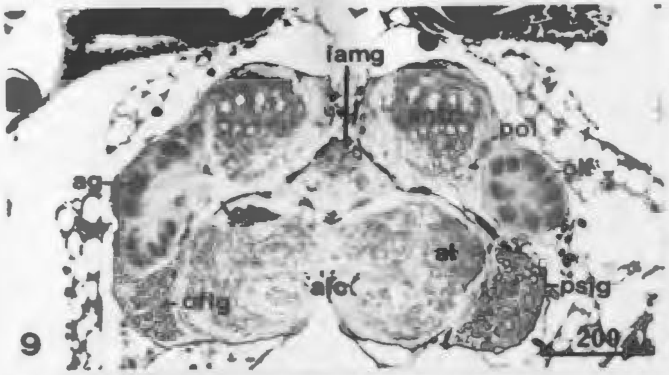
iamg
pol
ol
ag
at
afc
cflg
psig
9
200

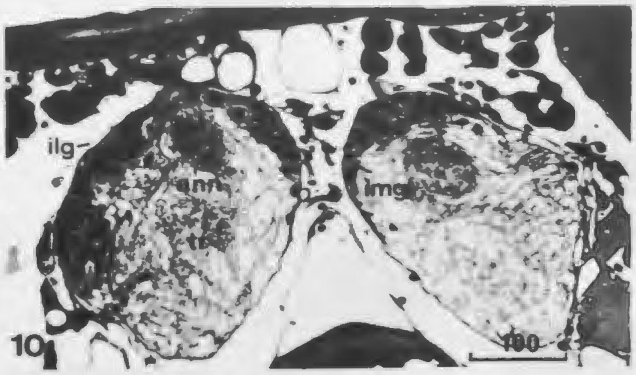
ilg
anm
tr
img
10
100

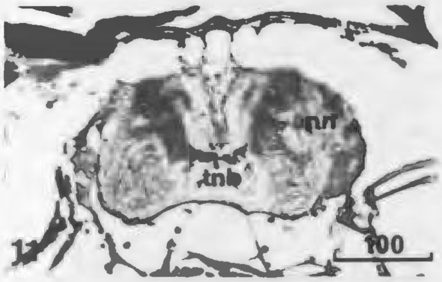
nm
tnb
11
100

12
25

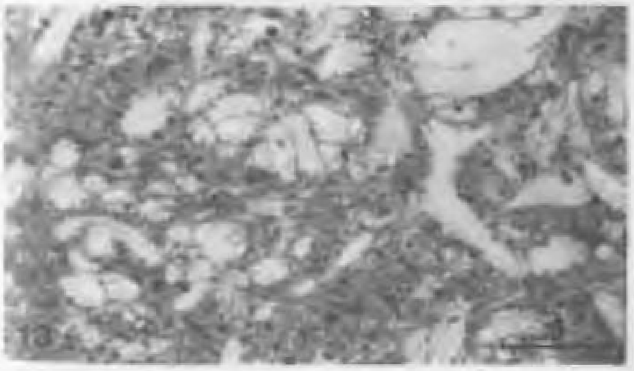
13

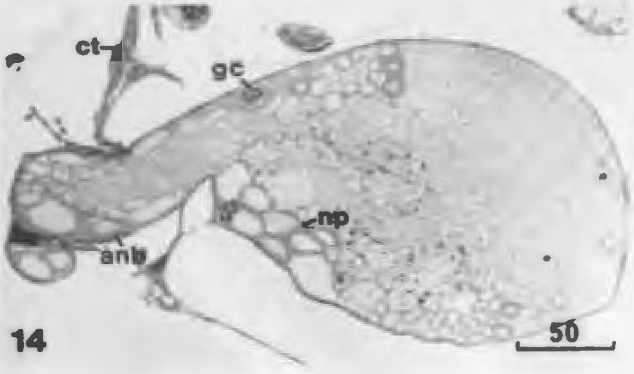
ct
gc
np
anb
14
50

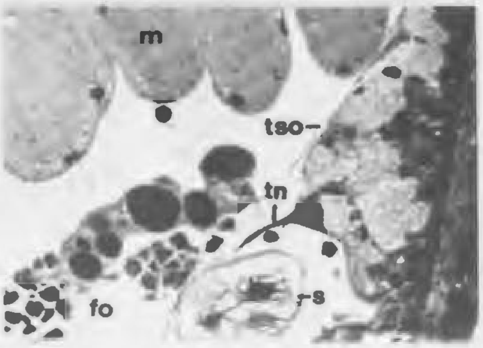
m
tso
tn
fo
s

Figure 16: Longitudinal section through the ganglionic fiber core. Note the elongated mitochondria that are common in this region. The majority of the tubular structures found in the axons are identified (epon, uranyl acetate/lead citrate, 20,840X).

Figure 17: Cross section of the protocerebral fiber core in the brain of *G. setosus*. Note the mitochondria with extremely swollen crests (arrow). The various types of vesicles found throughout the fiber core are identified (epon, uranyl acetate/lead citrate, 20,840X).

Figure 18: Cross section through the protocerebral fiber core. The mitochondria have swollen crests and a spiral configuration in the synaptic regions (arrow) (epon, uranyl acetate/lead citrate, 20,840X).

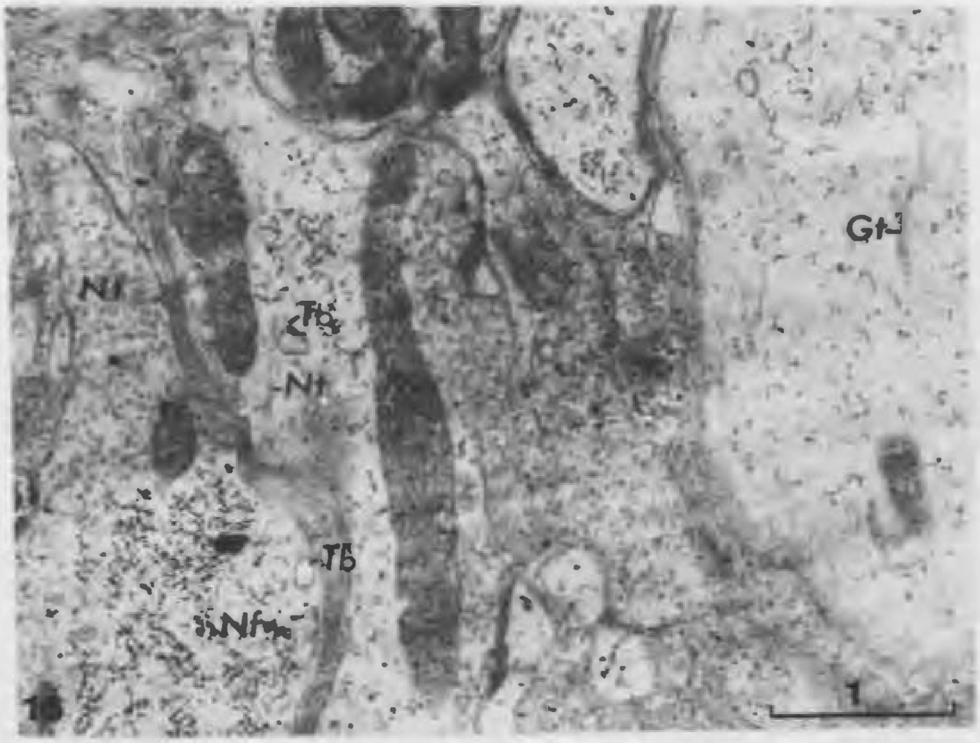
Nt
Tb
Nt
Tb
Nfm
Gt
1
16

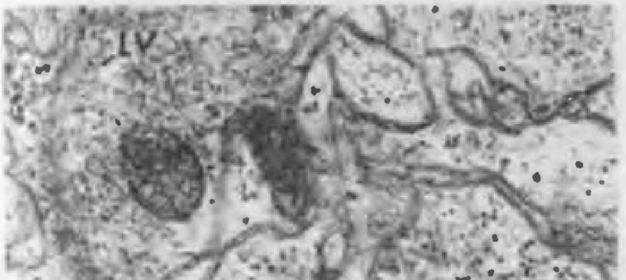
LV
A
V
S
Gc
1

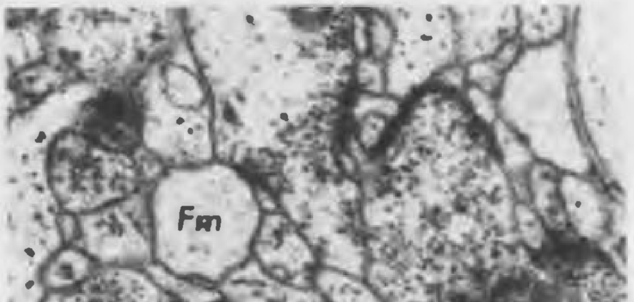
Fm
Gg
DV
S
1
18

Figure 19: Frontal section through the suboesophageal ganglion showing the fusion of the four single ganglion bodies (paraffin, PF, 99X).

Figure 20: Sagittal section through the suboesophageal ganglion showing the position of the neuropiles and cellular aggregations (paraffin, CHP, 156X).

Figure 21: Dissected thoracic ganglion seen in ventral view (gluteraldehyde-fixed, slightly osmicated, 50X).

Figure 22: Frontal sections (A,B,C,) through a thoracic ganglion from dorsal to ventral side showing the location of various neuropiles and cellular groups (paraffin, PF, 45X).

Figure 23: A portion of the ventral ganglion chain with the abdominal ganglia in lateral view (gluteraldehyde-fixed, slightly osmicated, 33X).

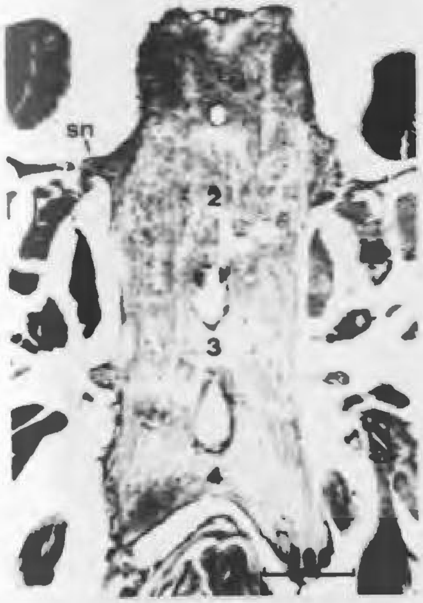

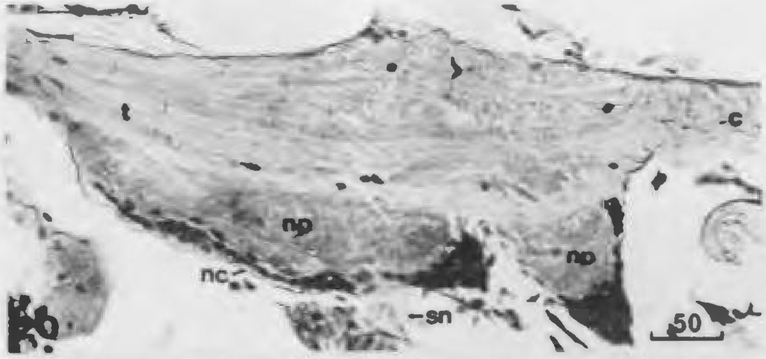
t
c
np
nc
np
sn
50

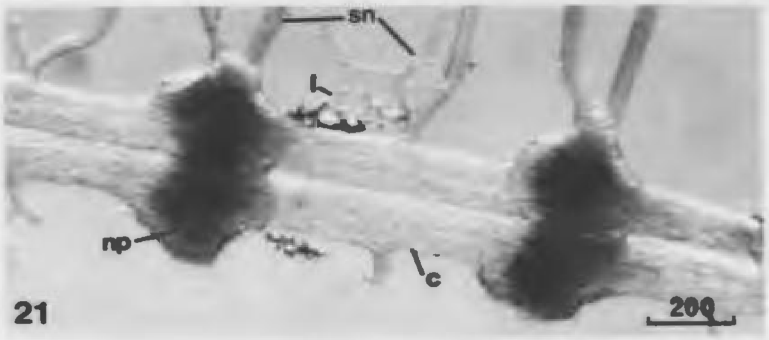

21

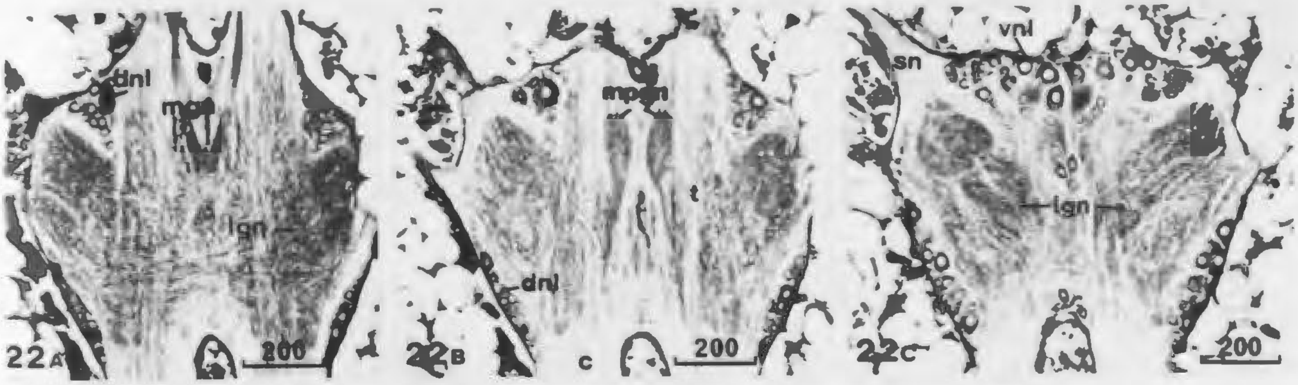
dnl
mpn
lgn
200
mpn
t
dnl
c
200
vnl
sn
lgn
200

22A 22B 22C

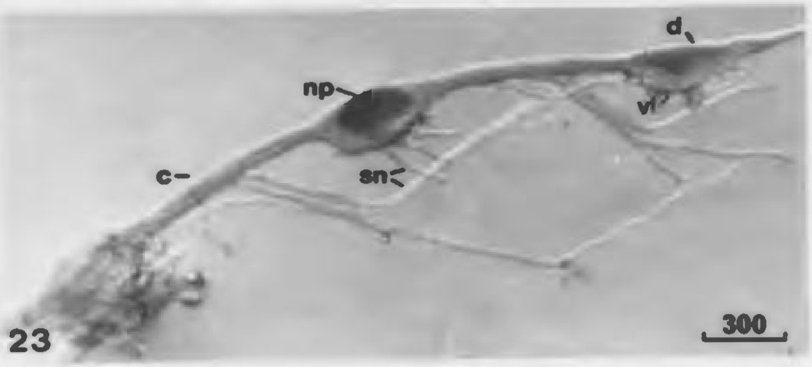
d
np
vl?
c
sn
300

23

Figure 24: Scanning electron micrographs of a thoracic ganglion dissected from a *G. setosus* female.

(A) Ventral aspect of the thoracic ganglion (45X).

(B) Frayed end of a segmental nerve showing individual axons (80X).

(C) Cut end of a connective in the ganglion chain with axons removed in the cutting process (485X).

(D) Core area of the ganglion (fiber) showing the glial cell wrappings around displaced axons (1200X).

(E) Split in the fibrous connective tissue capsule allows a look into the interior of the ganglion body passing through the neuron layer into the fiber mass (370X).

(F) Higher resolution photomicrograph of the same area seen in (E) but concentrated on the neuron layer (950X).

(gluteraldehyde-fixed, gold coated).

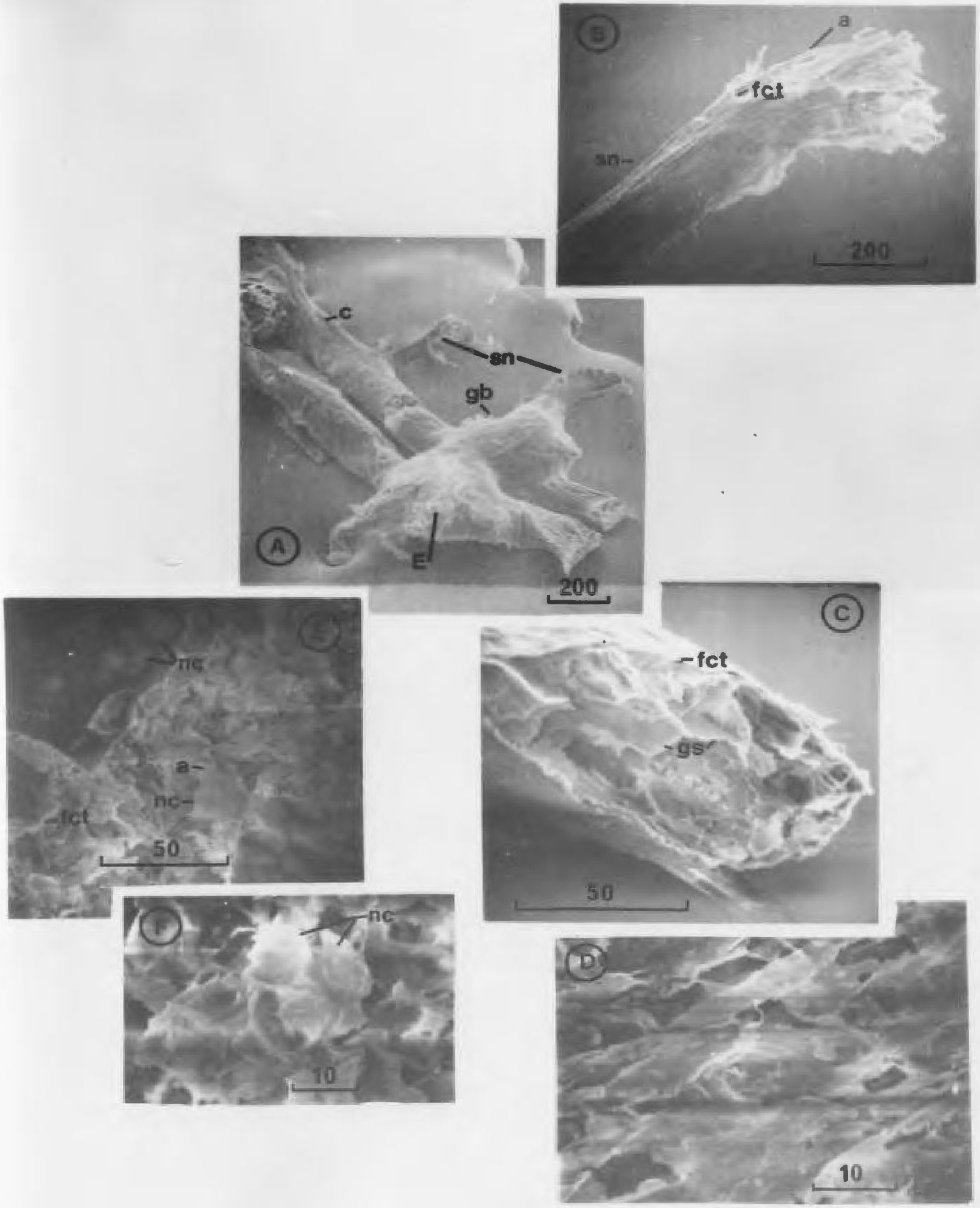
B
a
fct
sn
200
c
sn
gb
E
A
200
E
nc
a
nc
fct
50
C
fct
gs
50
F
nc
10
D
10

Figure 25: Scanning electron micrographs of a cross section through the body of a thoracic ganglion. Arrows indicate the location of the ventral neuronal groups (345X).

(A) Area A of center picture at increased magnification. Note the defined "gap" between the neuron group and the fiber core (1930X).

(B) Area B of center picture at increased magnification. The "gap" is again visible (960X).

(epon-embedded, NaOH/methanol treated to remove epon, gold coated).

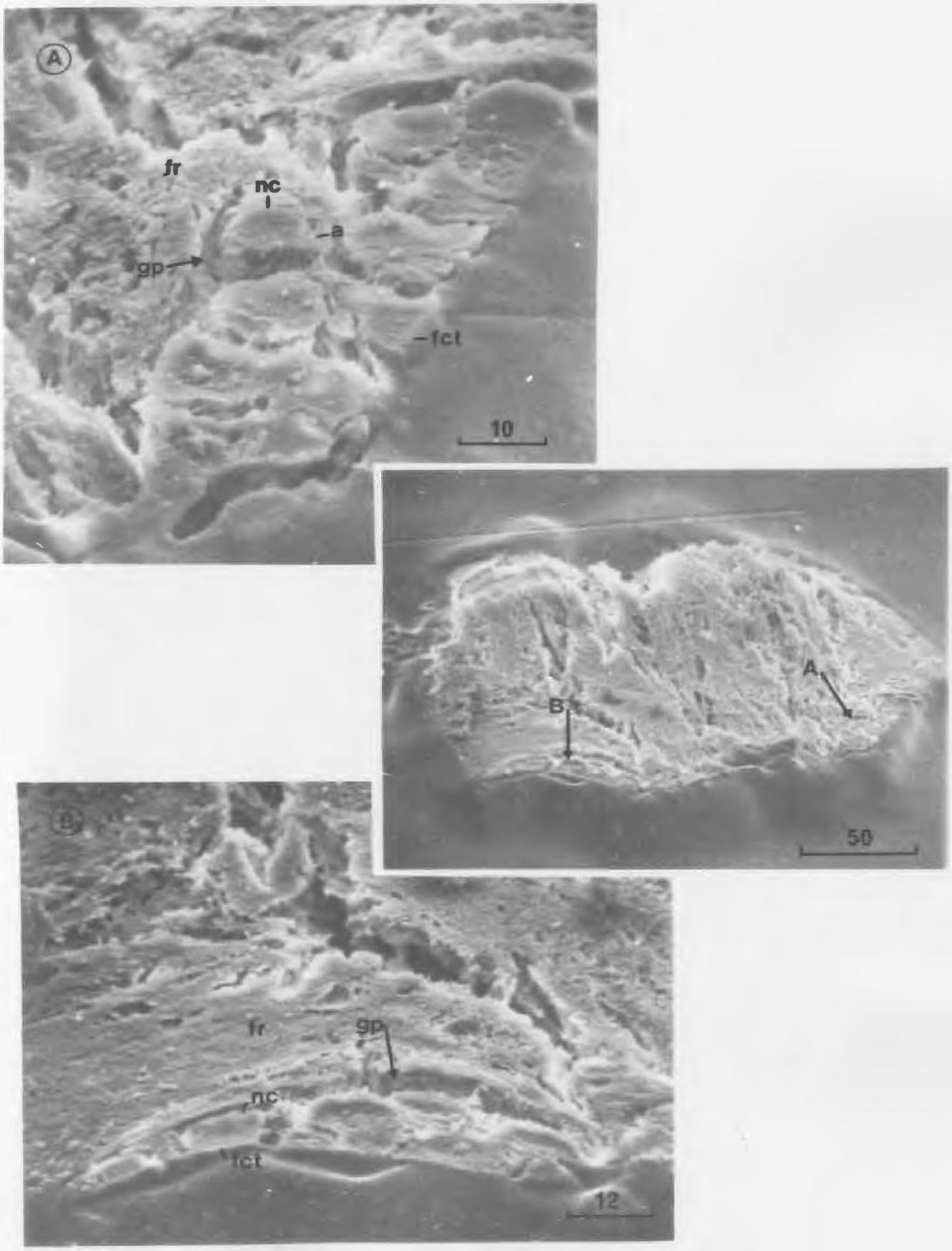
A
fr
nc
a
gp
fct
10
A
B
50
B
fr
gp
nc
fct
12

Figure 26: Thin frontal section through the mid region of the first abdominal ganglion showing the neuropile arrangement (epon, osmium stained, 180X).

Figure 27: Ventral neuronal layer of the first abdominal ganglion in *G. setosus* (paraffin, PF, 130X).

Figure 28: Arrangement of the unipolar neurons in the anterior superior medial glomeruli (asmg) of the brain. Note large extracellular spaces present in this region (epon, toluidine blue pH 11.1, 580X).

Figure 29: Four adjacent B cells in the anterior superior medial glomeruli (asmg) of the brain positioned along the periphery of the glomeruli with numerous A cells clustered within it (epon, epoxy PF, 580X).

Figure 30: (a) Note absence of chromatin in the nucleus of the large B cell found in the dorsoposterior region of the anterior inferior medial glomerular bridge (aimgb) as well as the presence of epoxy PF-positive regions throughout the wispy cytoplasm (epon, epoxy PF, 1475X).

(b) Section through another region of the same B cell stained with toluidine blue. Note presence of fairly large, deeply staining granules (arrow) in the extensively vacuolated cytoplasm (epon, toluidine blue pH 11.1, 1475X).

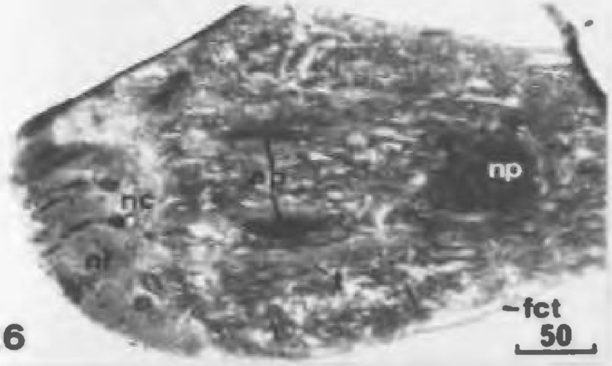
26
nc
np
np
nf
fct
50

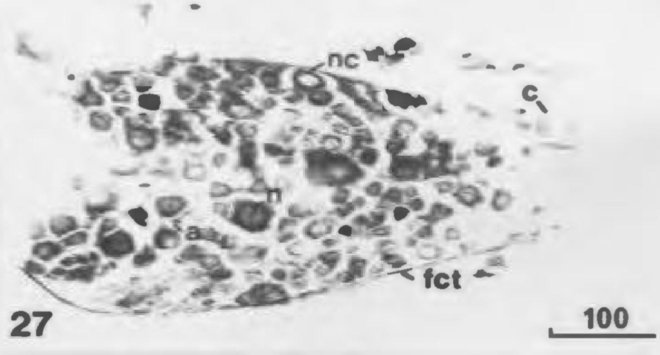
27
nc
c
n
a
fct
100

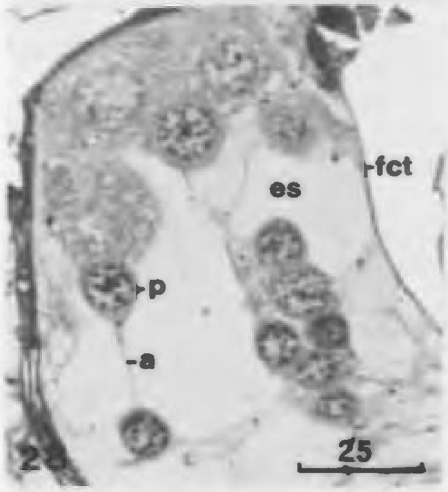
28

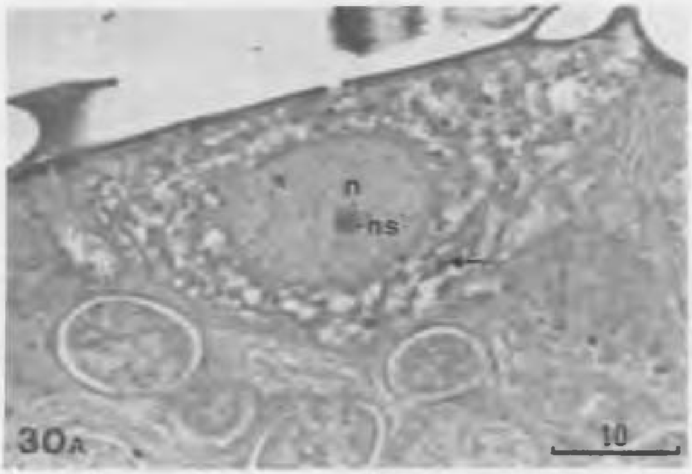
30A

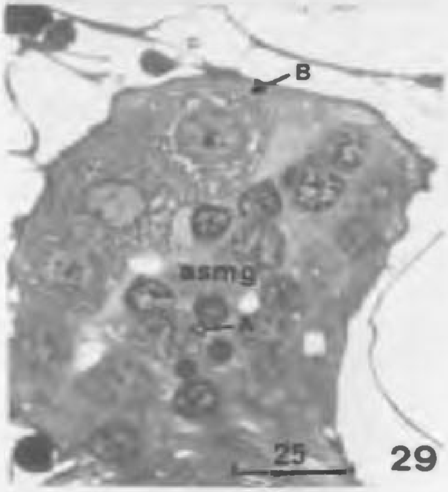
29

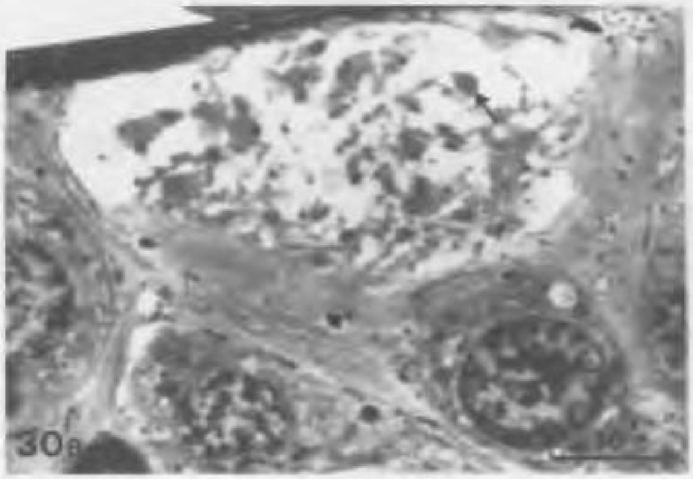
30B

Figure 31: Ultrastructure of a brain glomeruli containing neurosecretory and non-neurosecretory neurons. The presence of granules in the cytoplasm and chromatin-poor condition of the nucleus indicates neurosecretory activity in the neuron on the lower right. Several layers of glial cell membranes and cytoplasm fill the spaces between neurons. Note the large residual body (RB) present in the glial cell (GC) process in the center of the picture (epon, uranyl acetate/lead citrate, 4,750X).

Figure 32: Nucleus and ramifying perikaryon of a glial cell. Note the presence of large spherical mitochondrion-like vesicles (small arrow) and dense chunks of material resembling chromatin (large arrow) in the cytoplasm. The chromatin is localized around the inside of the nuclear membrane (epon, uranyl acetate/lead citrate, 4,750X).

Figure 33: A large mitochondrion that appears to be dividing transversely. The close association of the two smaller organelles on the right suggest they have been formed in a similar manner. The configuration of the crests differs greatly in each portion. Note the extremely dilated cistern that appears to be rough ER (arrow) as the limiting membrane is ribosome-studded in places (epon, uranyl acetate/lead citrate, 17,900X).

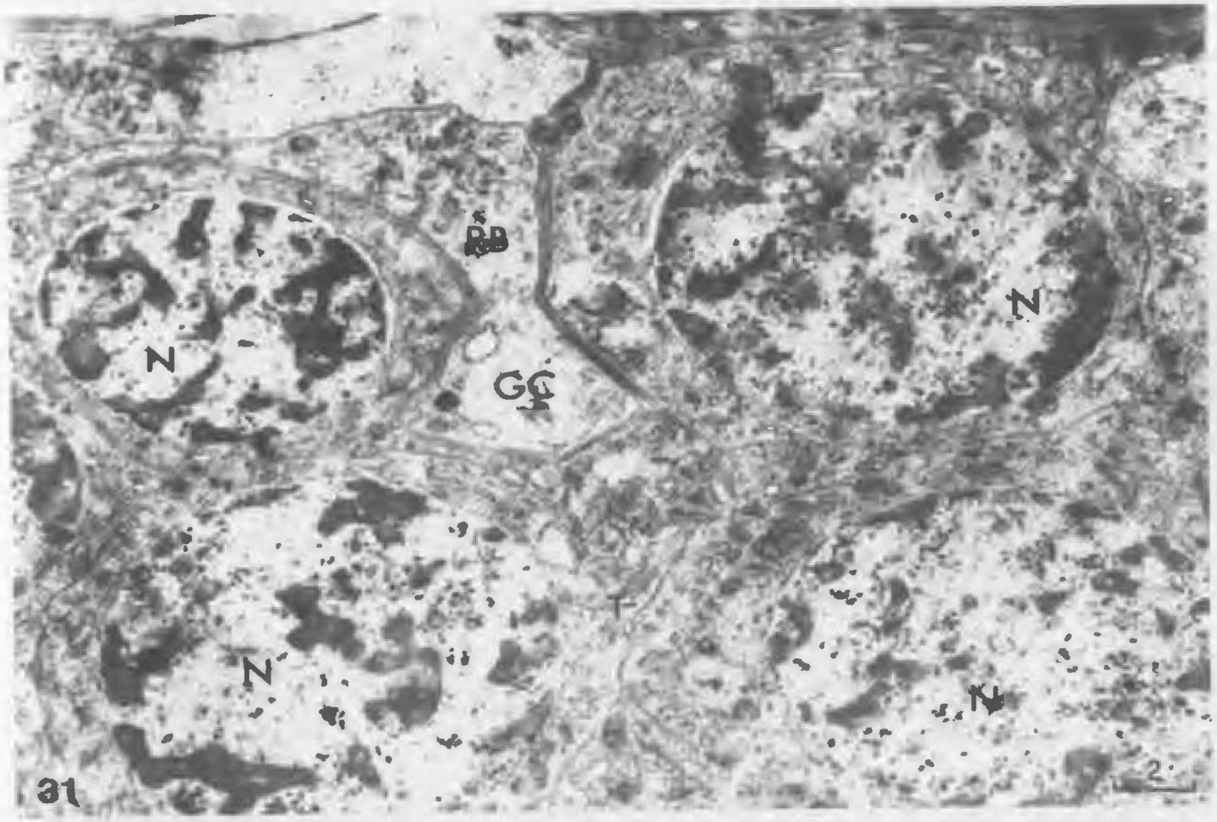
RB
N
GC
N
N
N
31
2

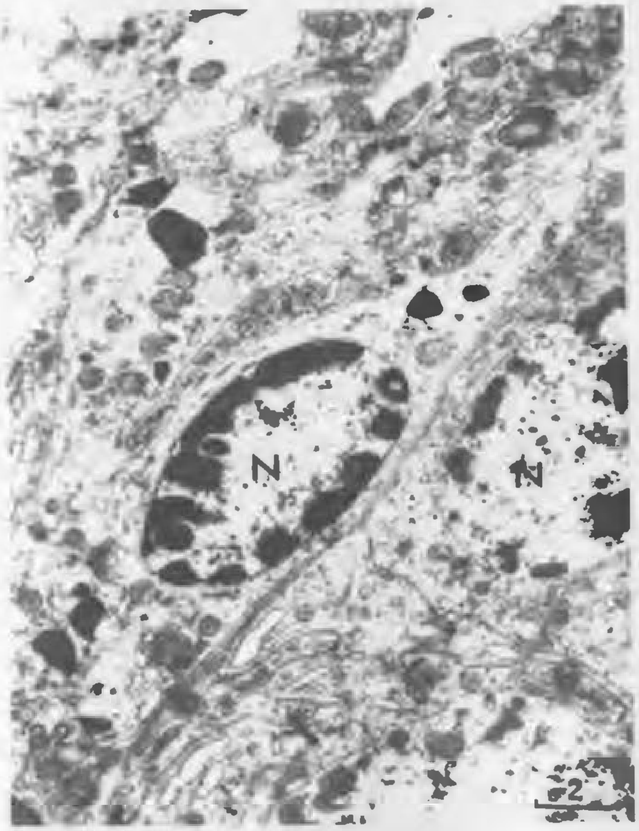
N
N
32
2

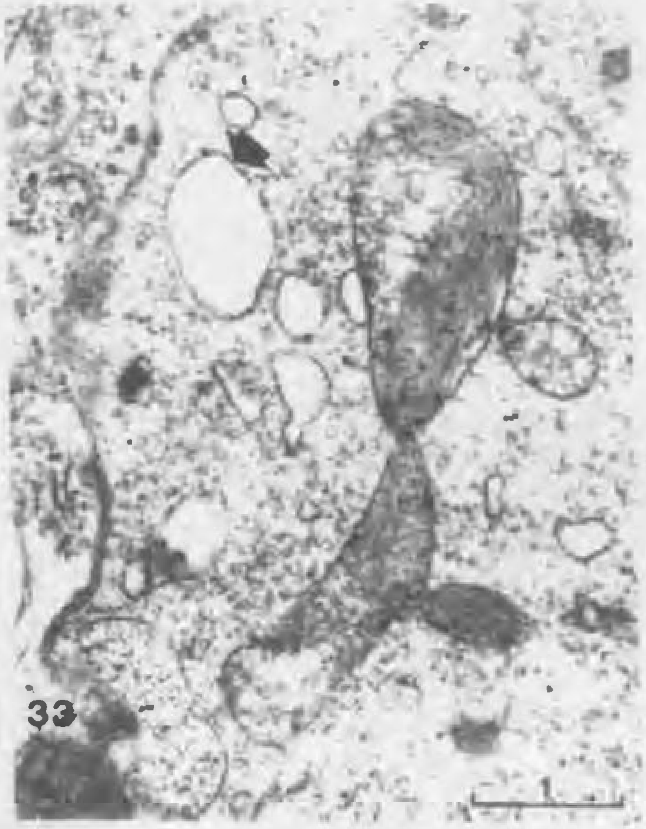
33
1

Figure 34: An A cell containing type I neurosecretory granules scattered throughout the perikaryon in clusters (solid arrow). The nucleus contains small amounts of chromatin and cisterns of Golgi and rough ER appear to be extremely dilated (hollow arrow), some having a flocculent matrix (epon, uranyl acetate/lead citrate, 17,000X).

Figure 35: A Golgi complex actively producing type I neurosecretory granules (epon, uranyl acetate/lead citrate, 17,000X).

Figure 36: Dilated cisterns of smooth ER (Golgi) filled with a finely granulated matrix. Some of the cisterns contain denser more aggregated particles that may be the precursor of the type I neurosecretory granules present (epon, uranyl acetate/lead citrate, 17,000X).

Figure 37: An active Golgi region producing large numbers of Golgi vesicles which radiate from its distal face. Note the close association of the rough ER with its proximal face and the slightly modified multivesicular body (MVB) in the lower right (epon, uranyl acetate/lead citrate, 17,000X).

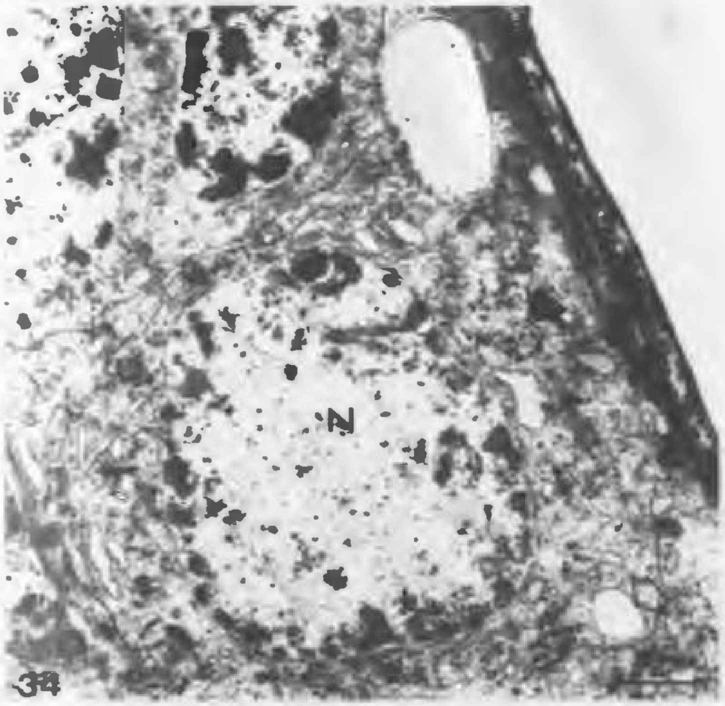
34

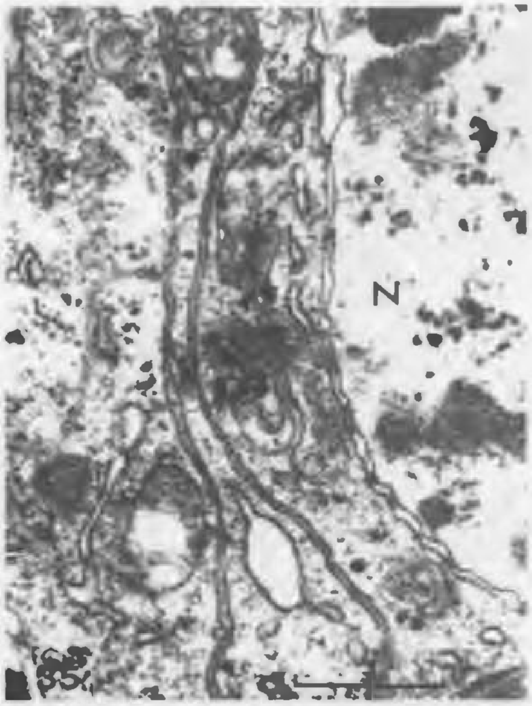
35

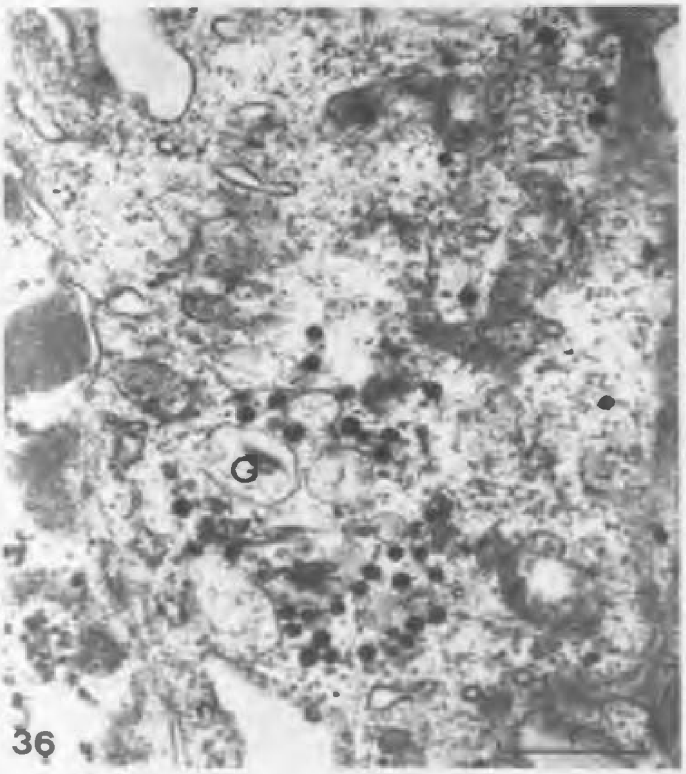
36

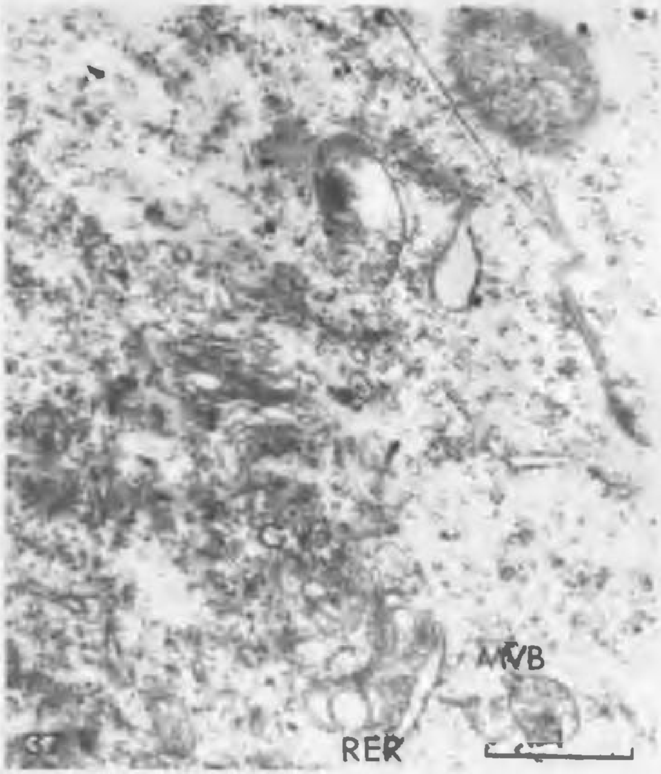
37

Figure 38: Portion of a neurosecretory B cell containing a number of MVBs as well as mitochondrion-like type II neurosecretory vesicles. The rough ER cisterns in the neuron on the right are dilated and contain a flocculent matrix while those in the adjacent neuron are dilated but contain little matrix (arrows), (epon, uranyl acetate/lead citrate, 15,900X).

Figure 39: Migration of a type II neurosecretory vesicle out of the neuron perikaryon into a glial cell process via a trophospongia. The cell membranes have disintegrated at the bottom of the invagination allowing free passage of the vesicle (arrow), (epon, uranyl acetate/lead citrate, 15,900X).

Figure 40: An aggregation of type II neurosecretory vesicles that bear a striking resemblence to mitochondria. Mitochondrial fission appears to be occuring in the lower left and another example is shown in the upper right insert. Note the small vesicle in the indentation of the lower right mitochondrion (hollow arrow). Residual bodies (RB) are also present in both compact lamellate and debris-filled vesicle forms (epon, uranyl acetate/lead citrate, 15,900X).

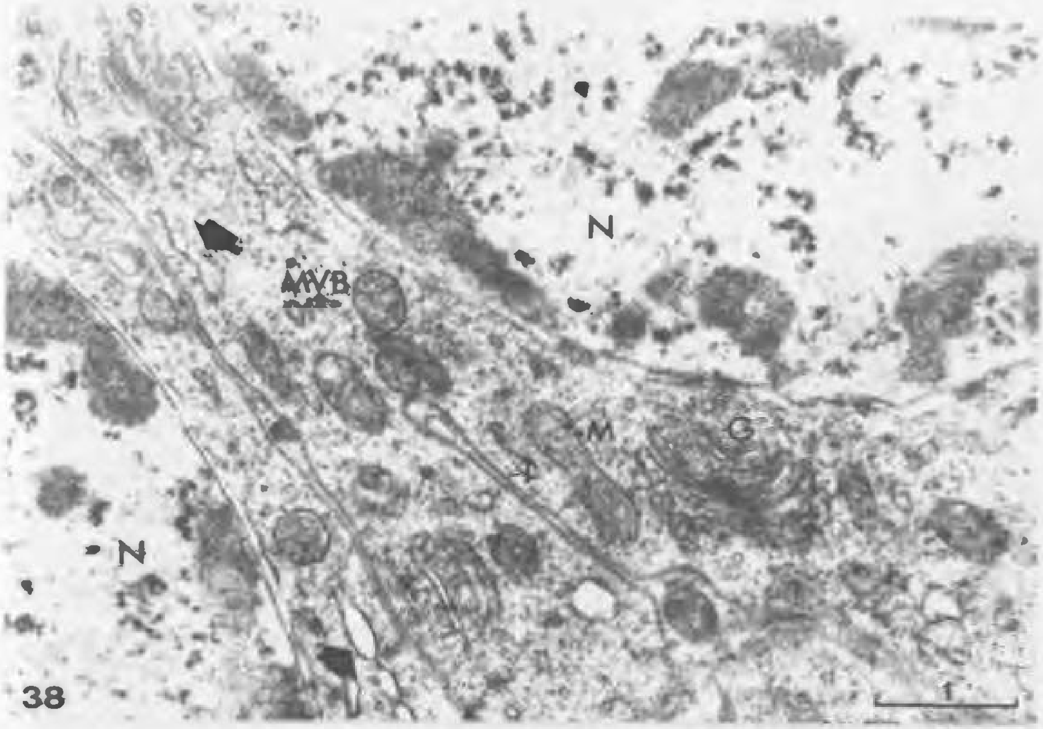

38

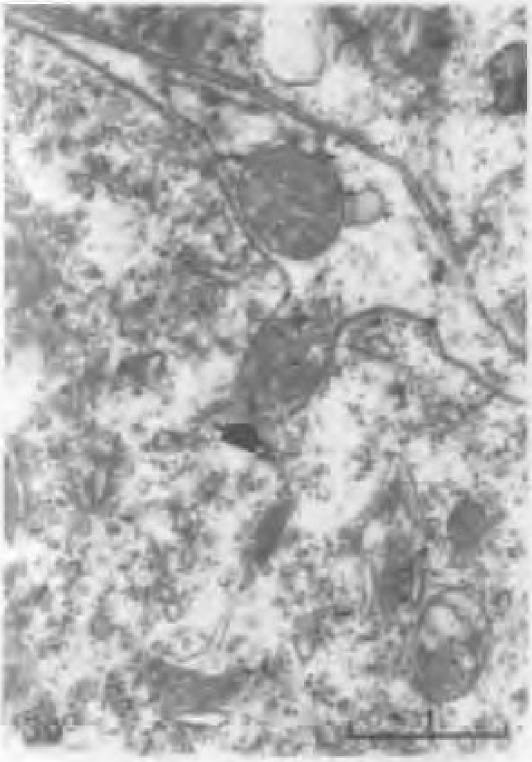

39

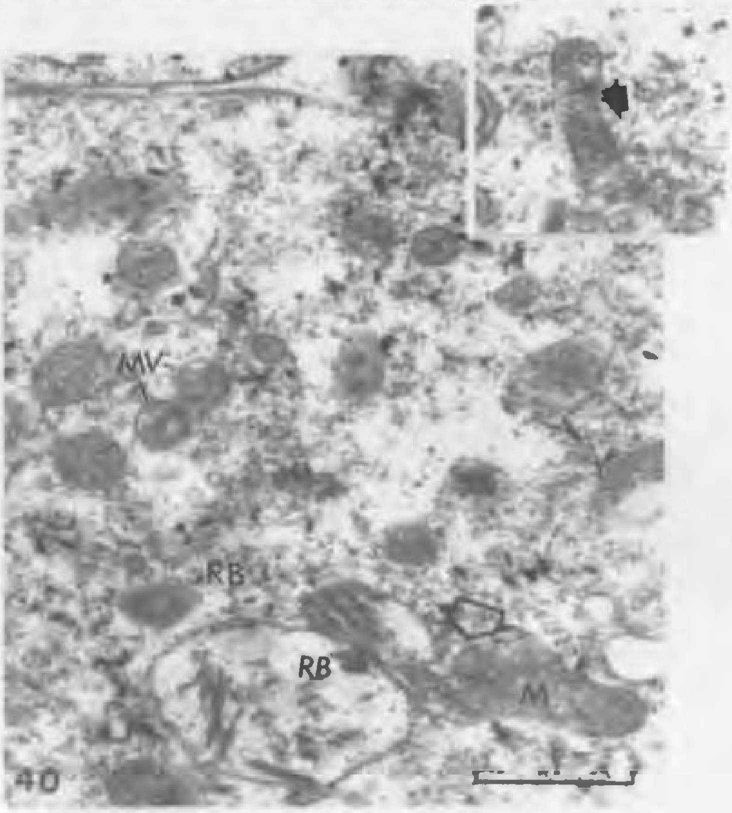

40

Figure 41: Synthesis of type II neurosecretory vesicles involving multivesicular body transformation (epon, uranyl acetate/lead citrate, 20,500X).

(a) Active Golgi regions producing large numbers of Golgi vesicles.

(b) A number of these small vesicles encapsuled by a single limiting membrane, the structure now comprising an MVB.

(c) and (d) The space between the vesicles becomes electron dense and a double membrane appears.

(e) A single membraned MVB and a double membraned mitochondrion-like vesicle within a neurosecretory neuron. Note the double membraned vesicle has a denser matrix although smaller in size.

Figure 42: An axon hillock of a neurosecretory neuron in the dorsolateral glomeruli of a thoracic ganglion. Note the presence of elongated mitochondria in the adjacent neuron (solid arrow) as well as a long cistern that appears to be composed of rough ER at one end and agranular ER (Golgi) at the other. The rough ER segment (on the left) contains dark granules. The small solid and hollow arrows indicate tubular and transverse mitochondrial crests respectively. The axon hillock contains numerous large mitochondrion-like neurosecretory vesicles, an active Golgi complex and dense core vesicles. The single membraned vesicles containing flocculent material may be rough ER and Golgi cisterns (epon, uranyl acetate/lead citrate, 20,500X).

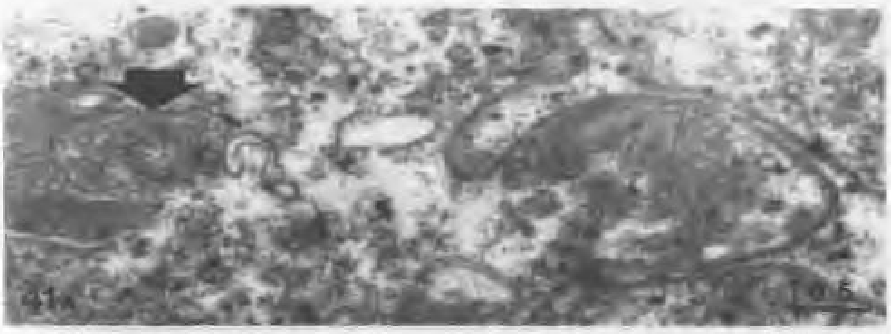
41A
0·5

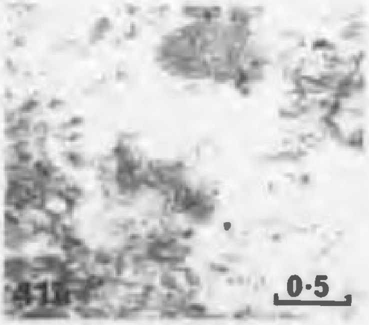
41B
0·5

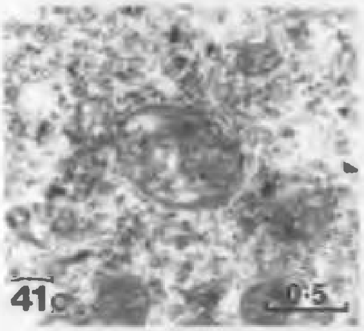
41C
0·5

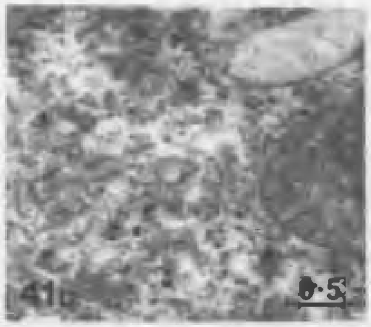
41D
0·5

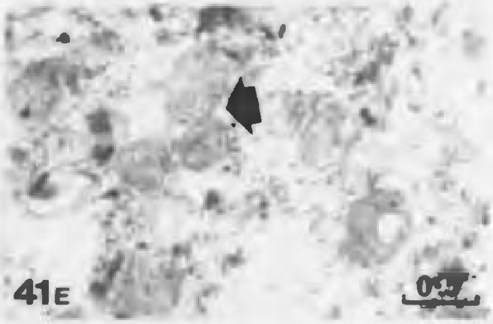
41E
0·5

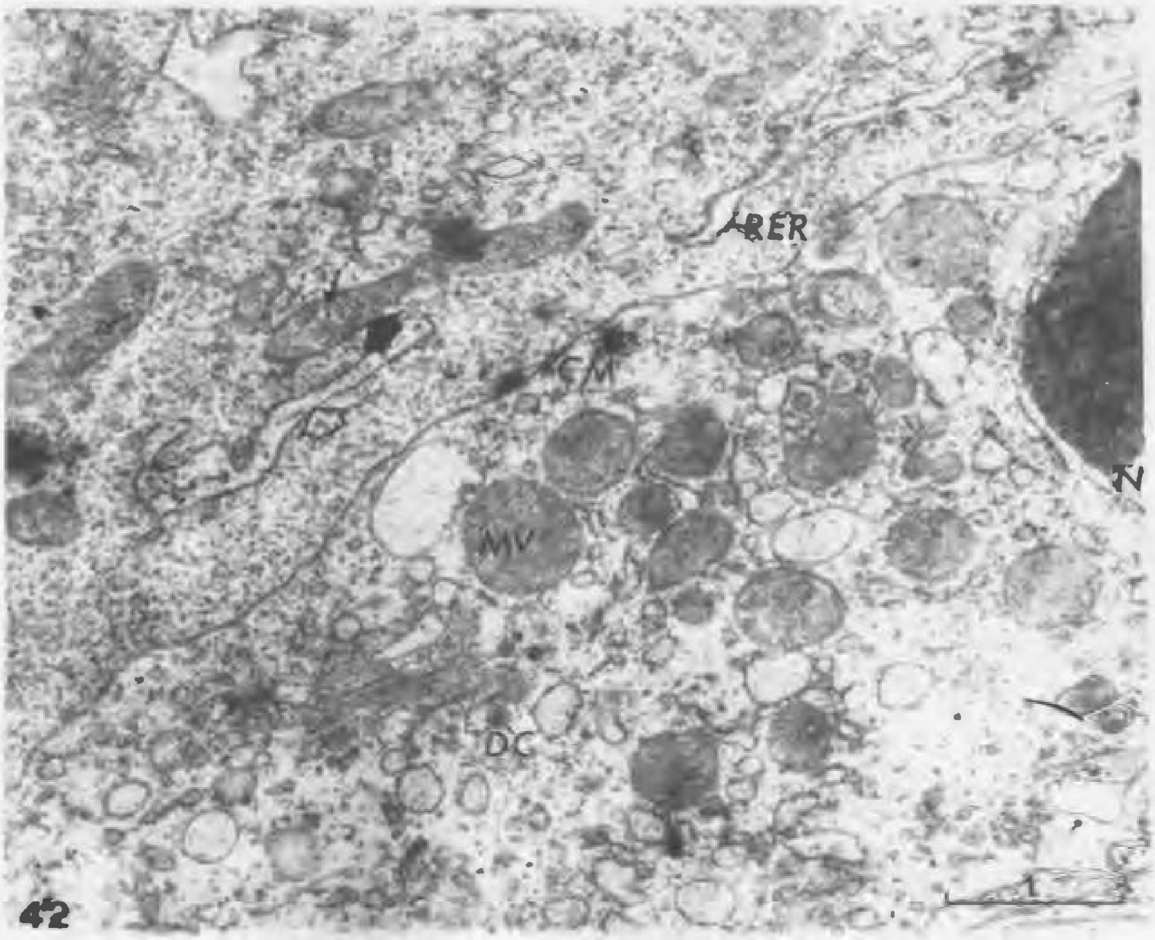
RER
CM
N
MV
DC
1
42

Figure 43: A neurosecretory neuron in the dorsolateral glomeruli of a thoracic ganglion. There is an active Golgi region producing both electron lucent and semi-opaque Golgi vesicles. Note the presence of single membraned MVBs (arrow) as well as mitochondrion-like double membraned vesicles with denser matrix (epon, uranyl acetate/lead citrate, 18,500X).

Figure 44: Portion of another neurosecretory neuron in the ventral glomeruli of a thoracic ganglion showing the presence of MVBs (large arrow), dense core vesicles (small arrow), and double membraned mitochondrion-like vesicles with a dense matrix. These vesicles are also found in the trophospongium (epon, uranyl acetate/lead citrate, 18,500X).

Figure 45: A thoracic ganglion neurosecretory neuron in the dorsolateral glomeruli containing elongated mitochondria in many configurations. The arrow indicates a possible point of fission producing two smaller mitochondria (epon, uranyl acetate/lead citrate, 18,500X).

Figure 46: A neurosecretory neuron in the mid stages of neurosecretory vesicle formation. Note the absence of MVBs and that the mitochondrion-like, double membraned vesicles have become more electron dense with the vesicles contained inside becoming distended. Note the rough ER is dilated and contains a flocculent matrix (epon, uranyl acetate/lead citrate, 18,500X).

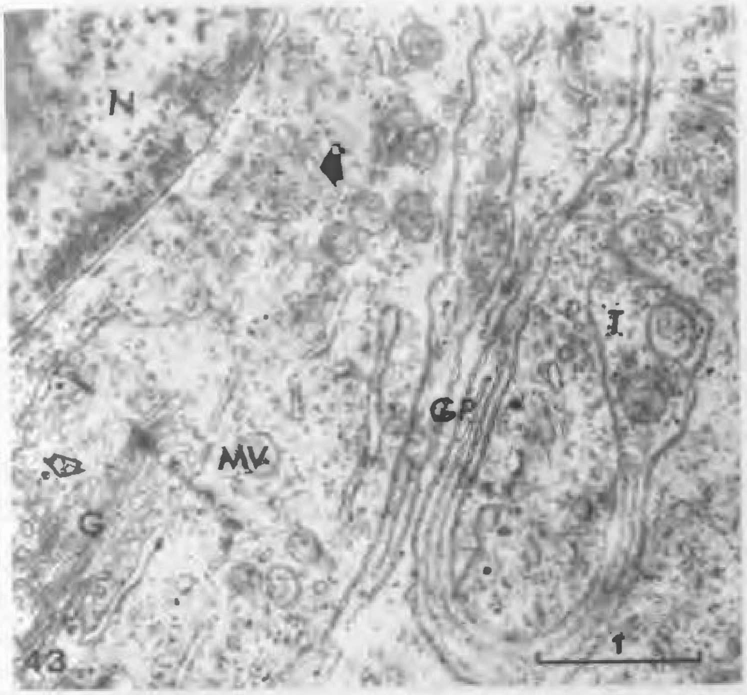

43

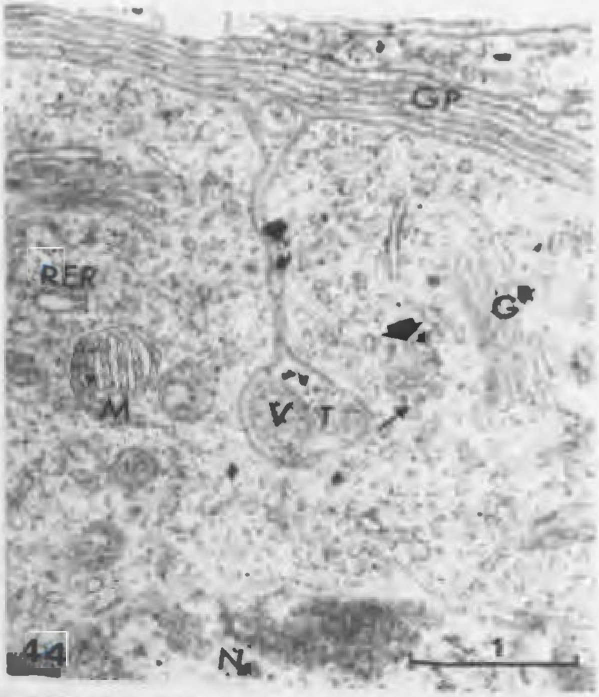
GP
RER
G
M
V
T
N
1

44

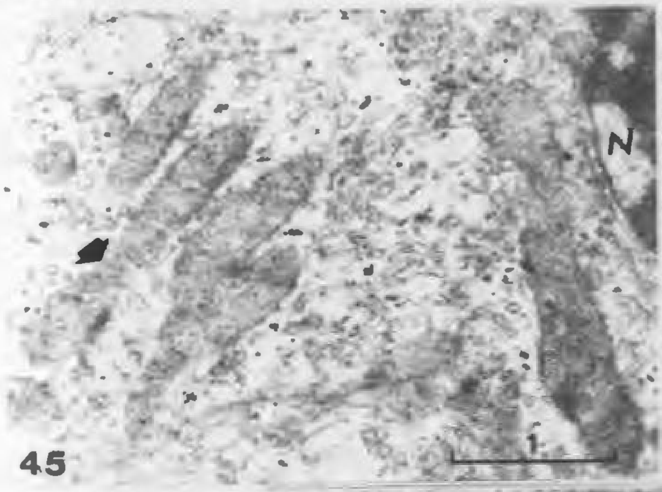

45

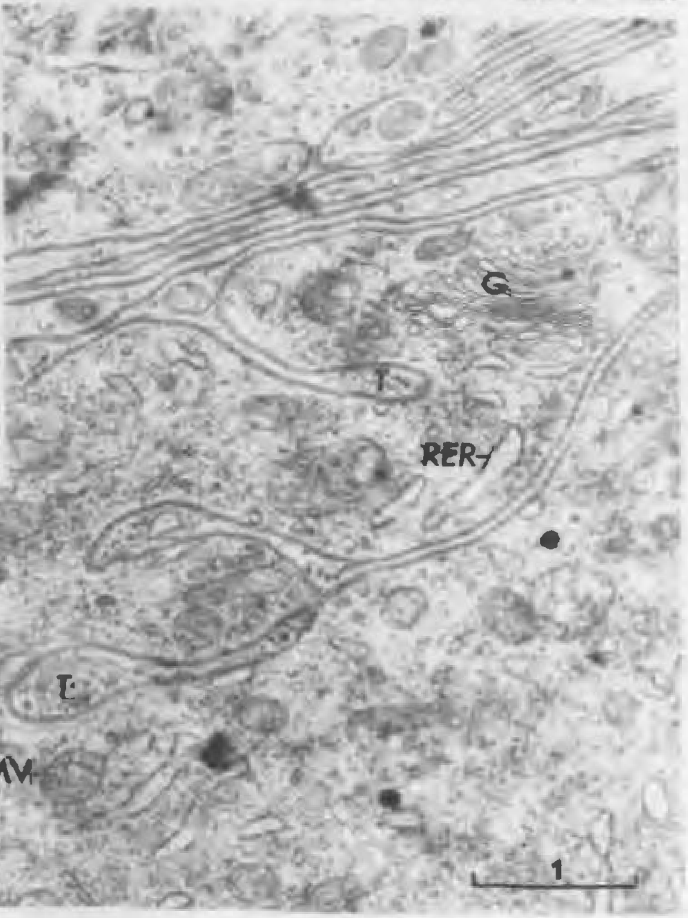

46

Figure 47: Position of the sinus gland in relation to the brain in *G. setosus* (epon, toluidine blue pH 11.1, 45X).

Figure 48: Frontal section of the sinus gland showing its cellular stalk, fiber mass and presence of granules in the neuron perikarya in the distal end (paraffin, CHP, 45X).

Figure 49: Fine structure of the sinus gland showing the distribution of the cellular and fibrous portions as well as presence of supporting tissue anchoring it in place (epon, toluidine blue pH 11.1, 165X).

Figure 50: Thin frontal section of the sinus gland delineating the cellular and fibrous portions (epon, toluidine blue pH 11.1, 115X).

Figure 51: Sagittal section through the head region showing the nervous connection between the protocerebrum of the brain and the medial frontal organ (paraffin, Mallory's triple, 45X).

Figure 52: Cross-section of the mid protocerebral region of the brain showing one of the paired roots of the medial frontal organ nerve originating from the anterior superior medial glomeruli (asmg),(paraffin, Hubschman's Azan, 225X).

Figure 53: Frontal organ of *G. setosus* in cross-section showing the clusters of neurons on the vine-like strands of connective tissue (paraffin, PF, 100X).

Figure 54: Longitudinal section of the statocyst and frontal organ showing their proximity in the cephalic region of *G. setosus* (paraffin, PF, 115X).

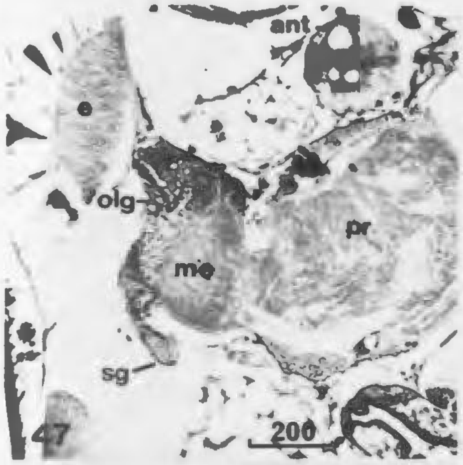
47
ant
e
olg
pr
me
sg
200

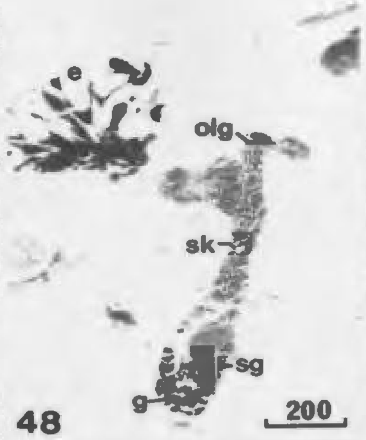
48
e
olg
sk
sg
g
200

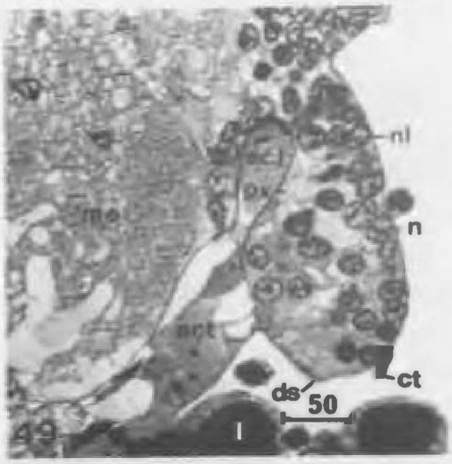
49
nl
me
n
act
ds
50
ct
l

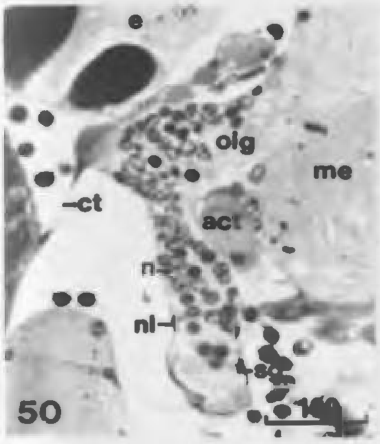
50
e
olg
me
ct
act
n
nl
s
100

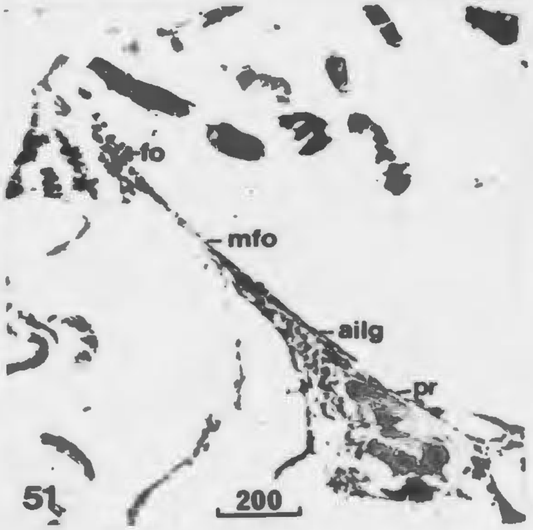
51
fo
mfo
ailg
pr
200

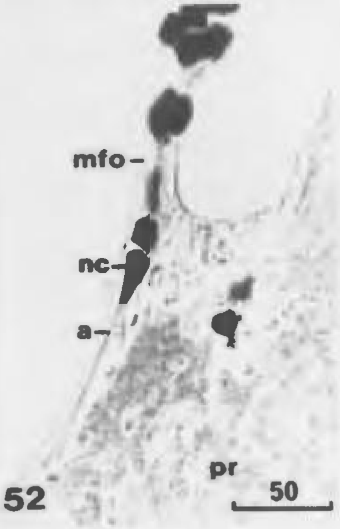
52
mfo
nc
a
pr
50

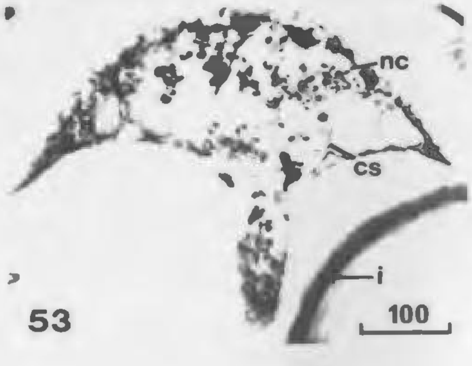
53

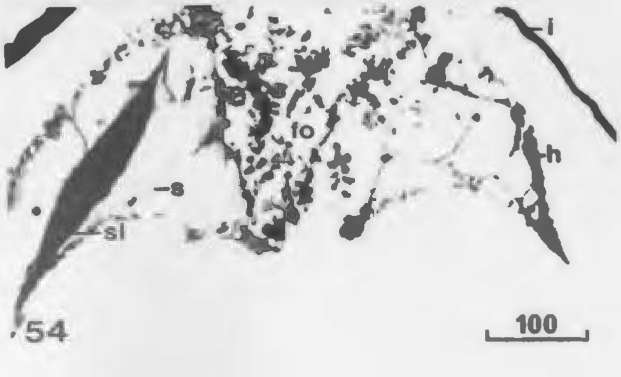
54
i
fo
h
s
sl
100

Figure 55: Thin cross section of the frontal organ showing the chromatin-rich nuclei of the neurons arranged in a vine-like manner (epon, toluidine blue pH 11.1, 160X).

Figure 56: Paraffin section through the frontal organ showing the granule-laden neurons surrounded by a granular matrix with tinctorial properties similar to that of blood found within the animal (paraffin, CHP, 160X).

Figure 57: Sagittal sections through the anterior cephalic region of *G. setosus* showing the nervous innervation of the statocyst. Note the large nerve arising from the anterior inferior lateral glomeruli (ailg) of the protocerebrum and extending to the dorsally located statocyst (paraffin, Mallory's triple, 65X).

Figure 58: Thin cross section through the basal root of the statocyst nerve where it arises from the anterior inferior lateral glomeruli (ailg), (epon, toluidine blue pH 11.1, 540X).

Figure 59: Frontal section through the upper head region showing the position of the various accessory cephalic structures (paraffin, CHP, 120X).

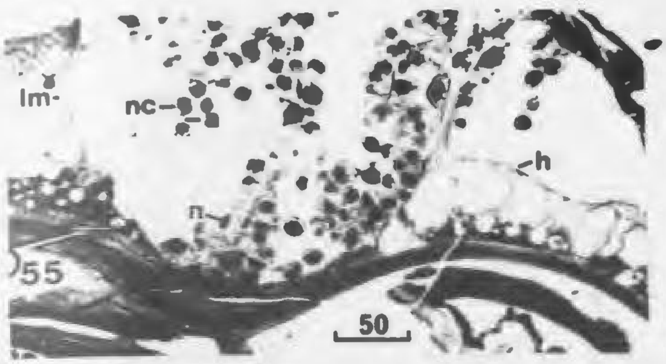
lm
nc
h
n
55
50

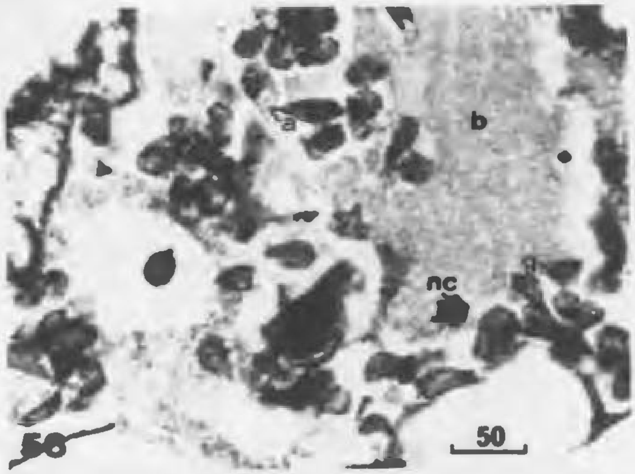
a
b
nc
56
50

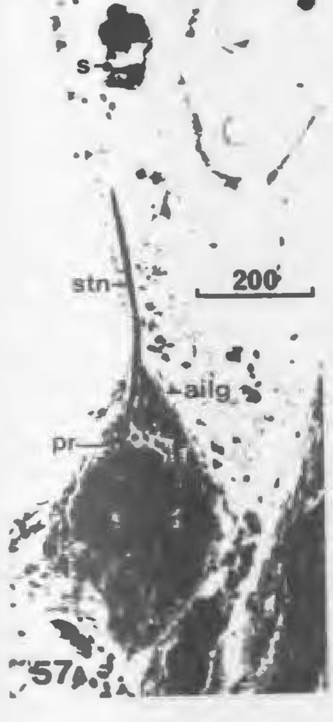
s
200
stn
ailg
pr
57

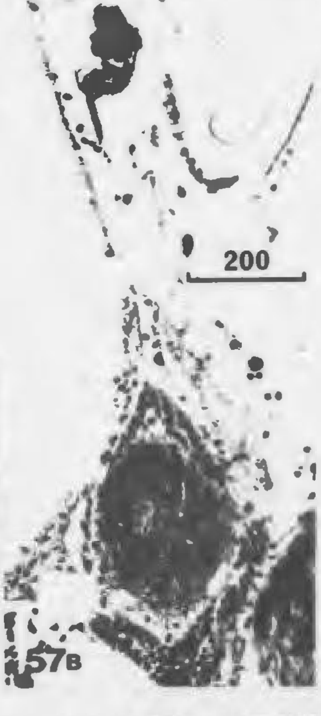
200
57B

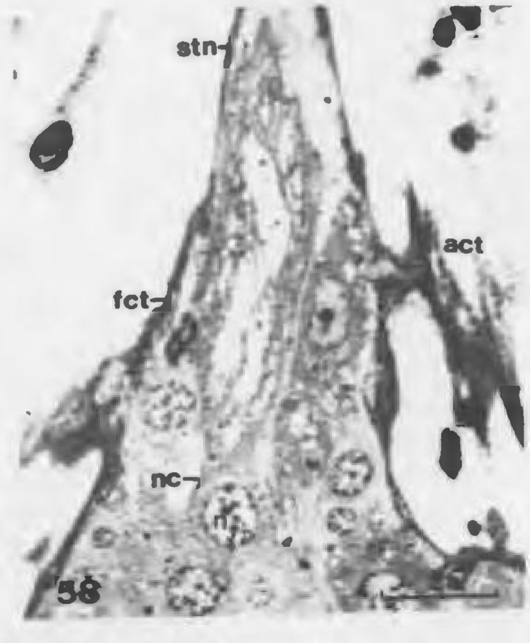
stn
act
fct
nc
n
58

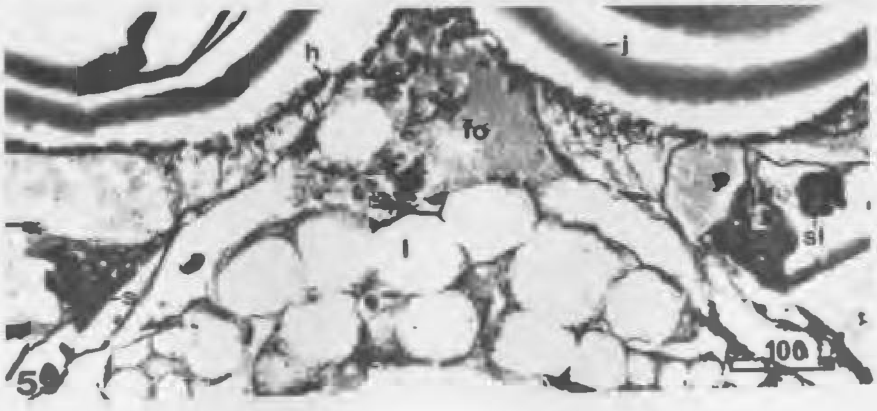
h
j
fo
l
sl
100
59

Figure 60: Thin cross-section through the dorsal cephalic region of *G. setosus* passing longitudinally through the statocyst showing its structure (epon, toluidine blue pH 11.1, 250X).

Figure 61: Cross-section through the statocyst as seen in paraffin section. Note the encapsulated appearance of the neuron perikarya in the neuronal layer (paraffin, PF, 560X).

Figure 62: Thin frontal section through the dorsal cephalic region cutting the statocyst into cross sections (epon, toluidine blue pH 11.1, 250X).

(a) Dorsal end of the statocyst just below the attachment of the stalk.

(b) Mid-section showing the statocyst nerve arising from the neuronal layer.

(c) Section just ventral to the origin of the statocyst nerve showing the attachment of the statolith with the neuronal layer.

(d) Section of the statocyst at its ventral tip.

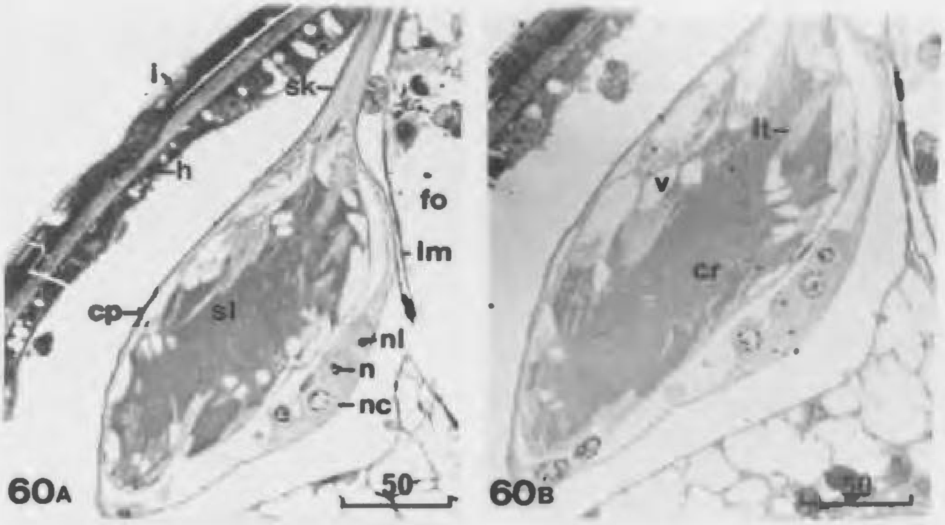
i
sk
h
fo
lm
cp
sl
nl
n
nc
60A
50
lt
v
cr
60B
50

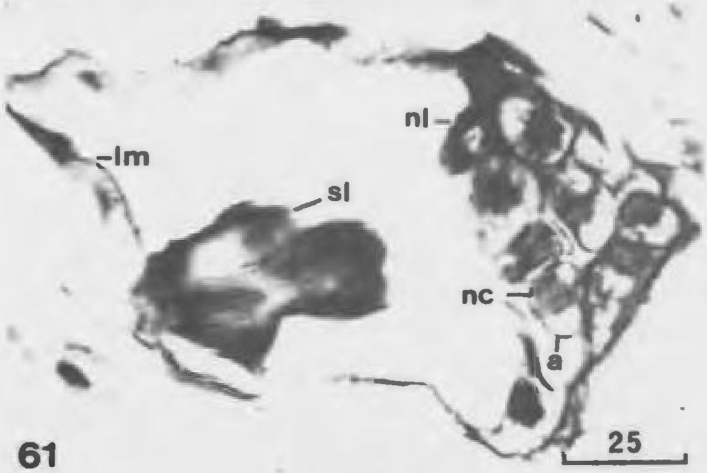
nl
lm
sl
nc
a
61
25

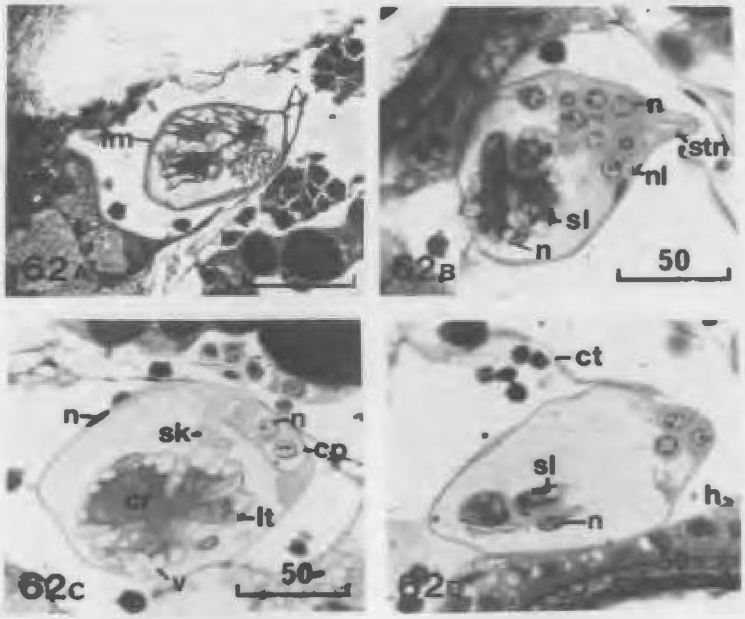
lm
62A
n
str
nl
sl
n
62B
50
n
sk
n
cp
cr
lt
v
62C
50
ct
sl
n
h
62D

Figure 63: Demonstration of NSM within the neurons of the frontal organ (epon, 265X).

(a) Routine toluidine blue pH 11.1 stained section showing apparent granules and nuclear chromatin.

(b) Epoxy PF-positive staining reaction exhibited by the granules. Note non-reactive nature of the chromatin.

(c) Epoxy PF control section from the same animal (permanganate oxidation omitted). The granules are not exhibited but the chromatin is.

Figure 64: The frontal organ of *G. setosus* in its full condition.

(a) Frontal organ in cross-section with the majority of the neurons loaded with granules (epon, toluidine blue pH 11.1, 185X).

(b) Type I frontal organ neurons loaded with granules Note the presence of scattered vacuolated vesicles within these cells (epon, toluidine blue pH 11.1, 1500X).

Figure 65: The frontal organ of *G. setosus* in the empty condition.

(a) Frontal organ in cross-section showing the majority of the neurons to be empty of granules. Note presence of type II neurons still loaded with granules (epon, epoxy PF, 185X).

(b) Type I frontal organ neurons in an extremely vacuolated state after release of the granules (epon, toluidine blue pH 11.1, 1500X).

Figure 66: Appearance of the type II frontal organ neurons among the empty type I's in the frontal organ of a female *G. setosus*. Note the presence of large numbers of neurosecretory granules packing the cytoplasm (epon, epoxy PF, 600 & 1500X).

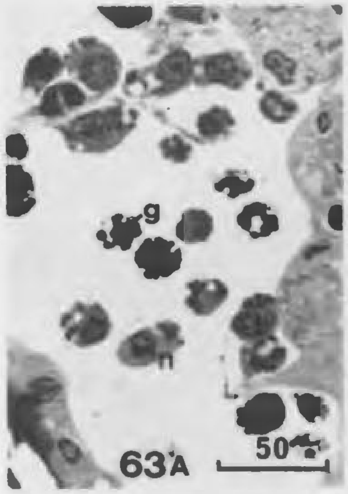
g
n
63A
50

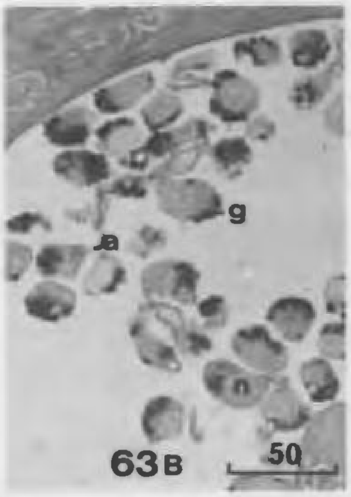
g
a
n
63B
50

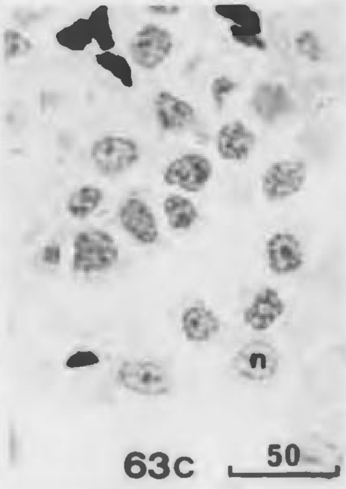
n
63C
50

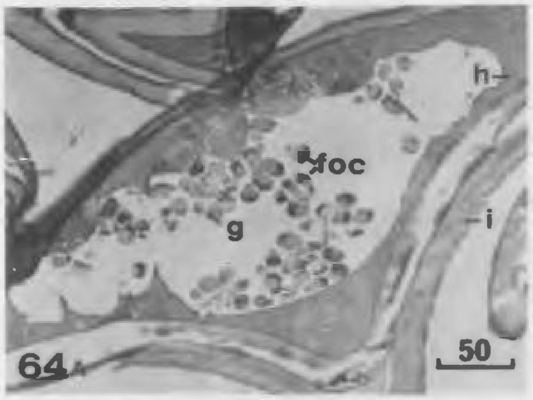
h
foc
g
i
64A
50

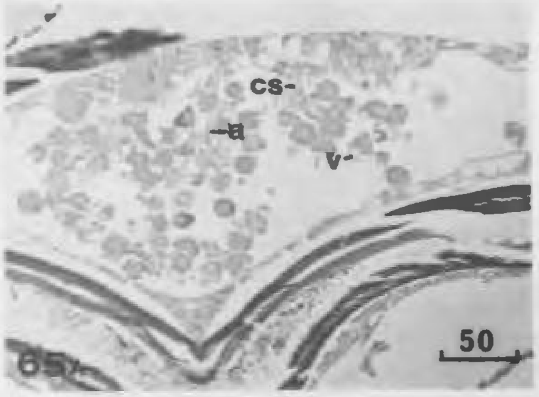
cs
a
v
65A
50

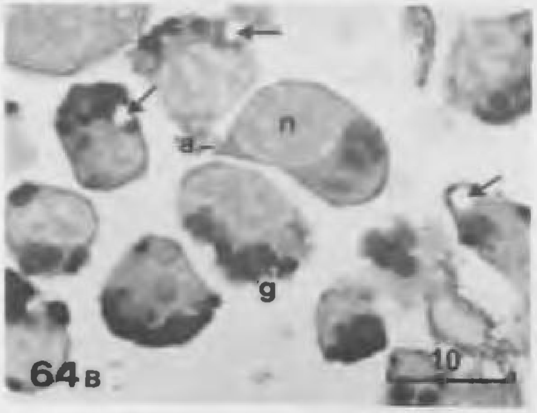
n
a
g
64B
10

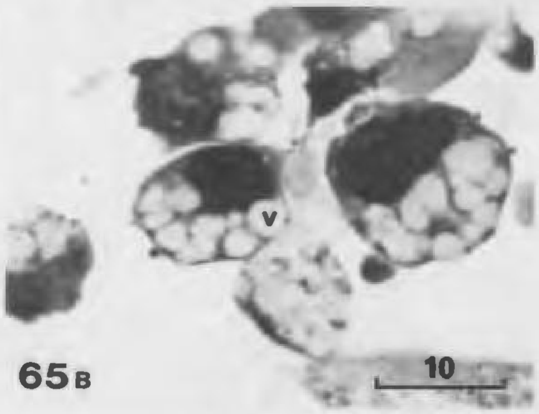
v
65B
10

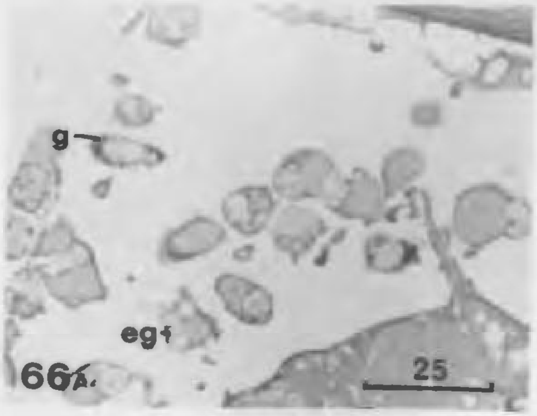
g
eg
66A
25

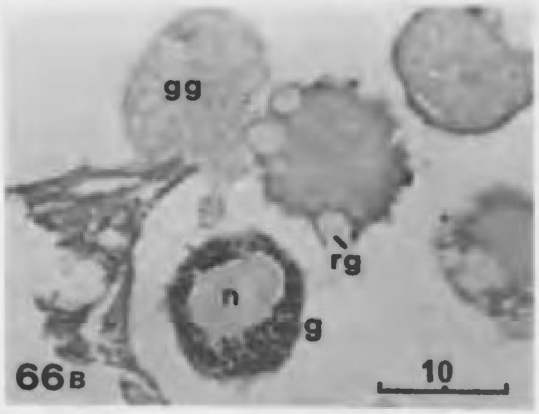
gg
rg
n
g
66B
10

Figure 67: The two types of frontal organ neurons identified in thin sections and verified here by electron microscopy. The cells are classified by neurosecretory vesicle size (epon, uranyl acetate/lead citrate, 4,115X).

(a) Type I frontal organ neuron with large mitochondrion-like vesicles present in the peripheral region of the cytoplasm.

(b) Type II frontal organ neuron containing many of the smaller neurosecretory vesicles.

Figure 68: Axon projecting from a type I frontal organ neuron in longitudinal section showing a large mitochondrion-like vesicle en route. Rough ER is in close association with the vesicle in a number of locations (epon, uranyl acetate/lead citrate, 19,980X).

Figure 69: Synthesis of neurosecretory vesicles in a type I frontal organ neuron. Shrinking empty vesicles can be seen near the periphery and are flanked by small stacks of rough ER. Mitochondria are in the region and a number of active Golgi are producing numerous Golgi vesicles filled with a finely reticulated matrix (arrow), (epon, uranyl acetate/lead citrate, 19,980X).

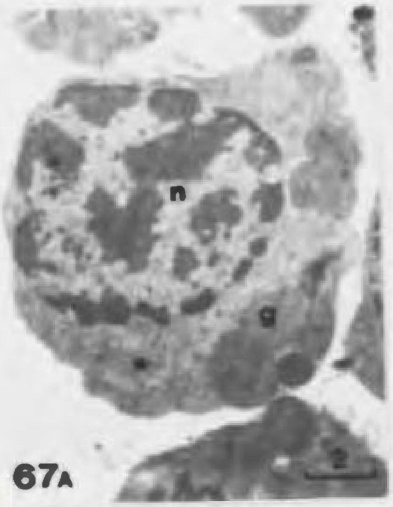

67A

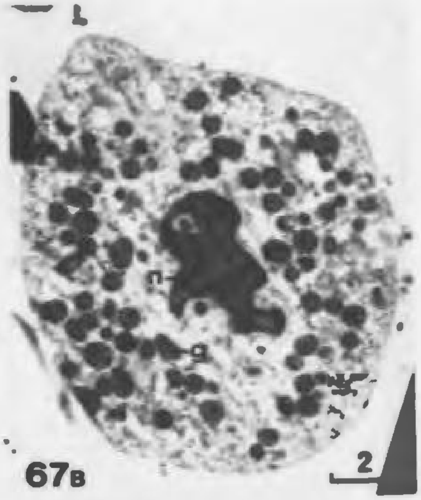

67B

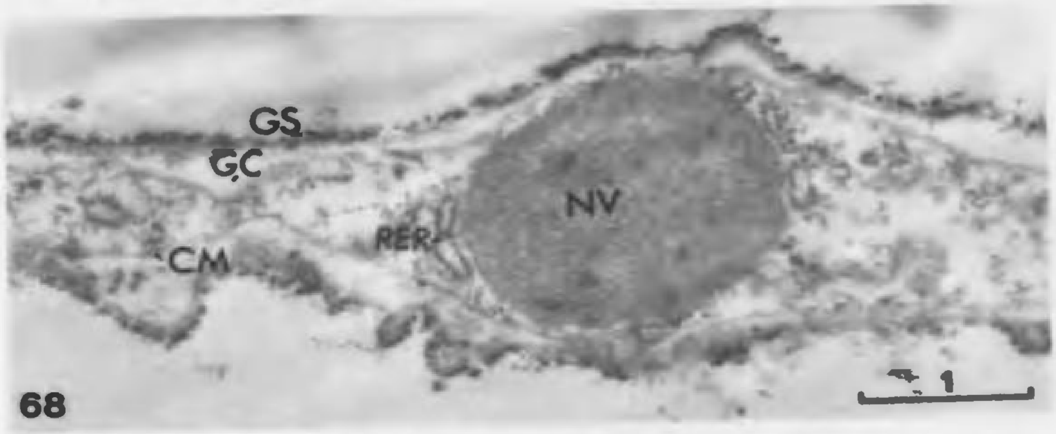
GS
GC
CM
RER
NV
1

68

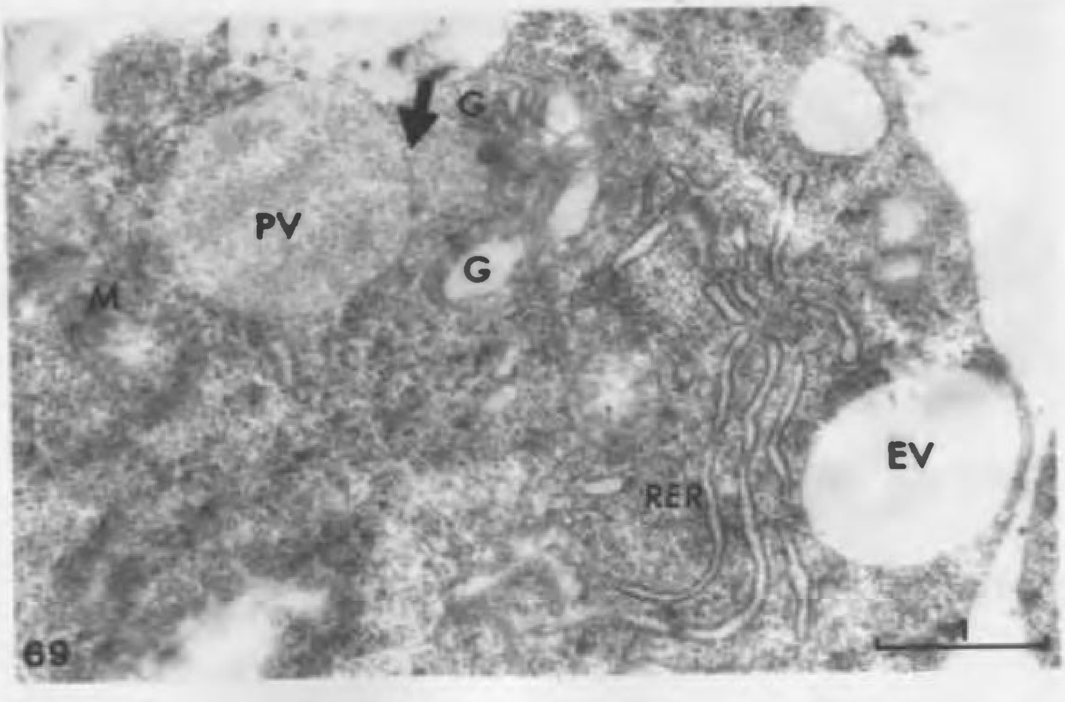
G
PV
G
M
RER
EV

69

Figure 70: Axon of a type I frontal organ neuron containing large mitochondrial-like vesicles. The mitochondrial crests (C) can be clearly distinguished and rough ER is closely associated with the vesicles. Some is dilated and filled with a finely flocculated material (arrow). The glial sheath can be distinguished in this region and thin trophospongia extend into the axon (epon, uranyl acetate/lead citrate, 18,855X).

Figure 71: Vesicle in close proximity with the nucleus. Note the double membrane of the vesicle as well as the mitochondrial-like crest extending a short distance into the granular matrix (epon, uranyl acetate/lead citrate, 63,000X).

Figure 72: (a) Cell membrane of a type I frontal organ neuron during periods of neurosecretory vesicle accumulation. Note definite configuration of the membrane (epon, uranyl acetate/lead citrate, 54,165X).

(b) Granule as it approaches the cell boundary of a type I frontal organ neuron. The double membrane of the granule is now absent and the cell membrane has become indistinct (epon, uranyl acetate/lead citrate, 63,000X).

Figure 73: Type I frontal organ neuron with neurosecretory vesicles in various stages of maturation. Note the lamellated stack of rough ER and the large mitochondria (epon, uranyl acetate/lead citrate, 18,855X).

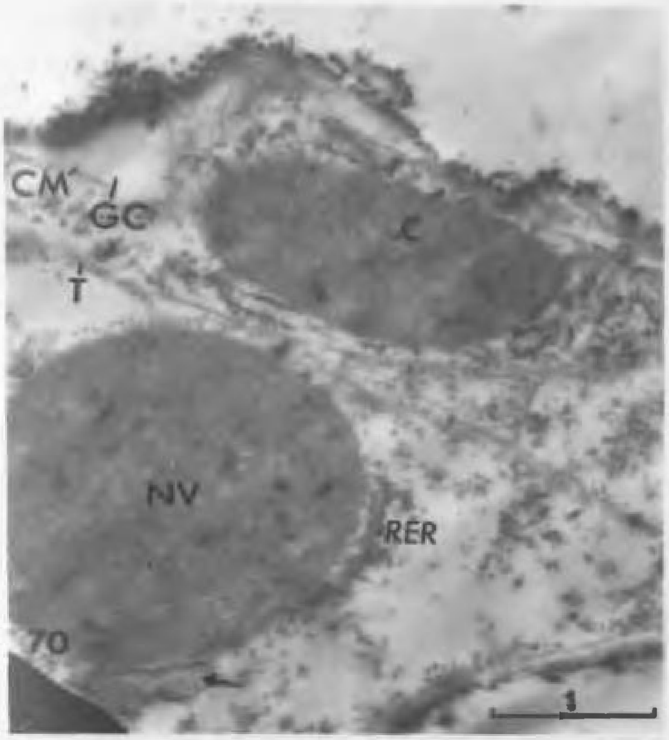
CM
GC
T
C
NV
RER
70
1

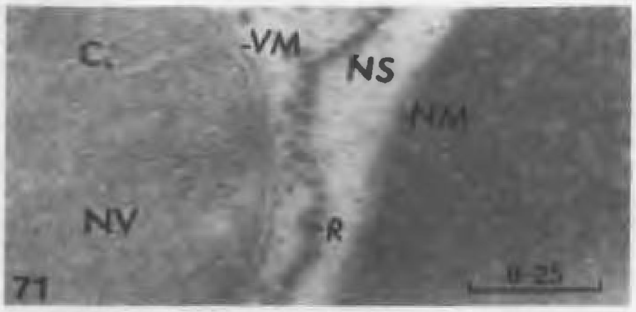
C
VM
NS
NM
NV
R
71
0.25

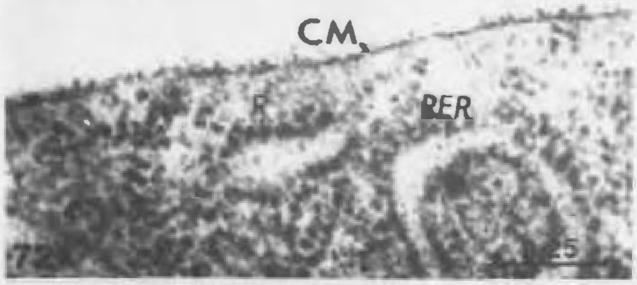
CM
R
RER
72
0.25

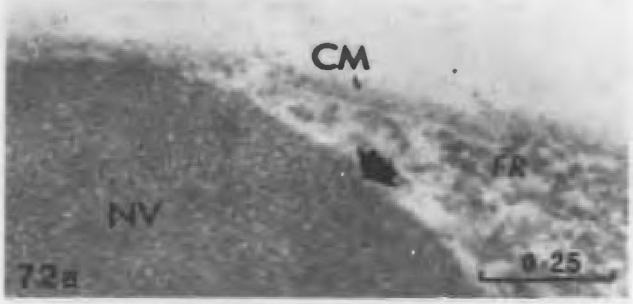
CM
FR
NV
72a
0.25

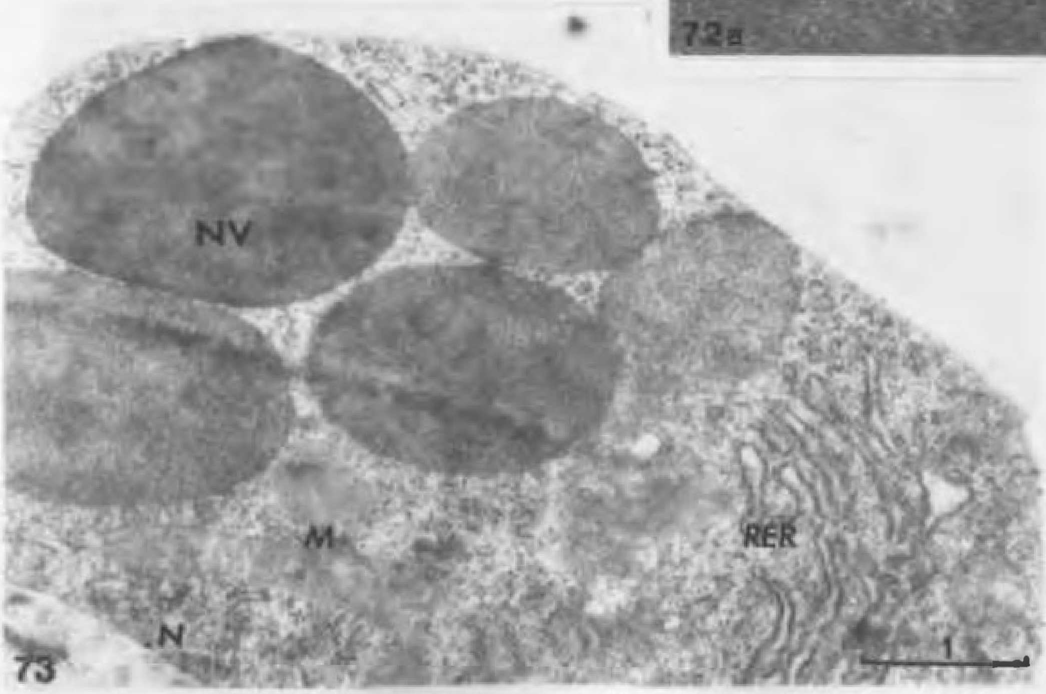
NV
NV
M
RER
N
73
1

Figure 74: Lysis of the cell boundary of a type I frontal organ neuron and expulsion of the vesicles granular contents. The rough ER is in a scattered arrangement close to the nucleus and large mitochondria with flocculent matrix are also in this region (epon, uranyl acetate/lead citrate, 18,720X).

Figure 75: Restoration of cell boundary continuity of a type I frontal organ neuron and formation of turgid empty vesicles following release of the granular contents. An active Golgi complex is close to the nucleus with numerous Golgi vesicles of varying diameter radiating from it (epon, uranyl acetate/lead citrate, 18,720X).

Figure 76: Empty type I frontal organ neuron after vacuole resorption prior to active neurosecretory vesicle accumulation. The mitochondria are present in many configurations (arrow) and the rough ER is near them. Note the nuclear pores, large space between the paired membranes delineating the nucleus and the chromatin-rich nucleus (epon, uranyl acetate/lead citrate, 18,720X).

Figure 77: Type I frontal organ neuron at an early phase of neurosecretory vesicle accumulation (epon, uranyl acetate/lead citrate, 18,720X).

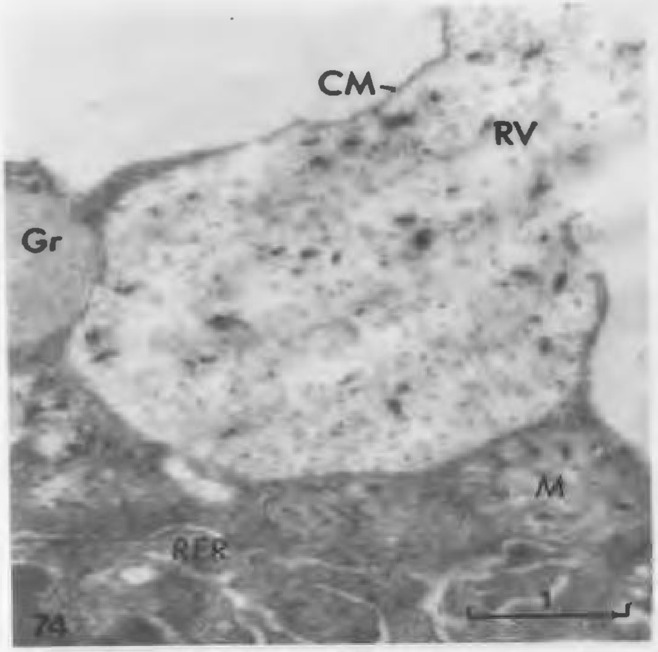
74
CM
RV
Gr
M
RER
1

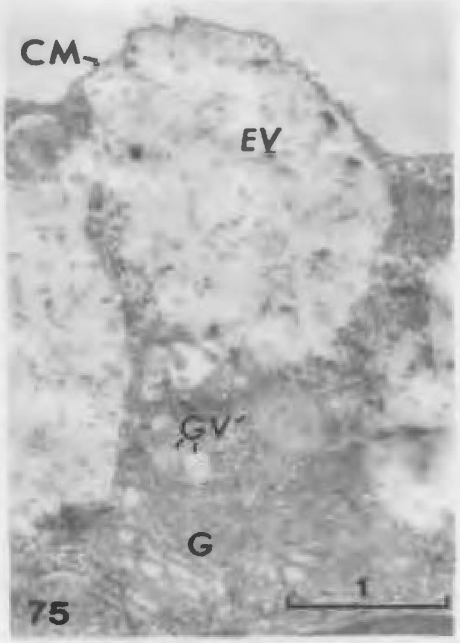
75

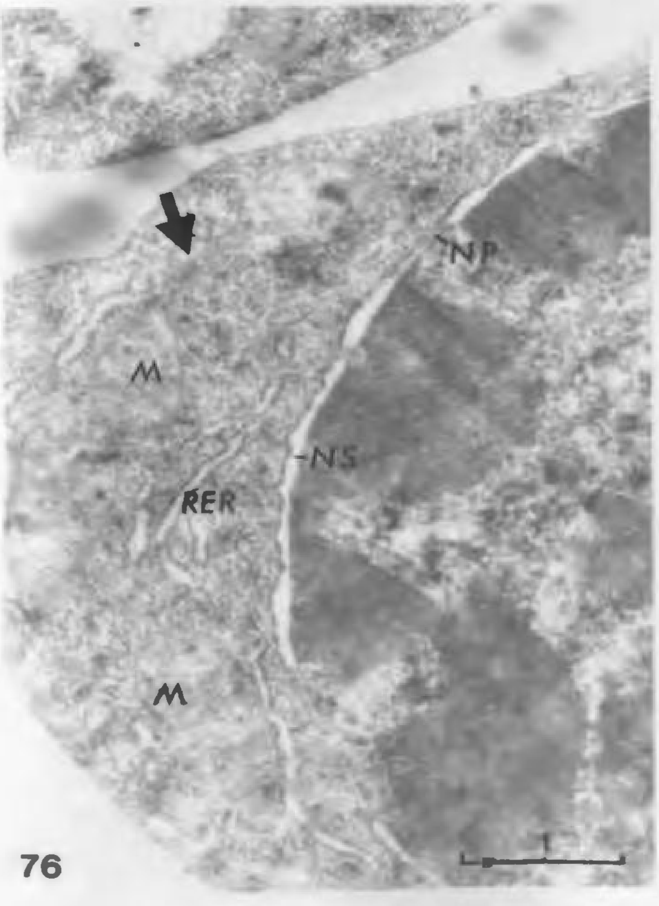
76
NP
M
NS
RER
M
1

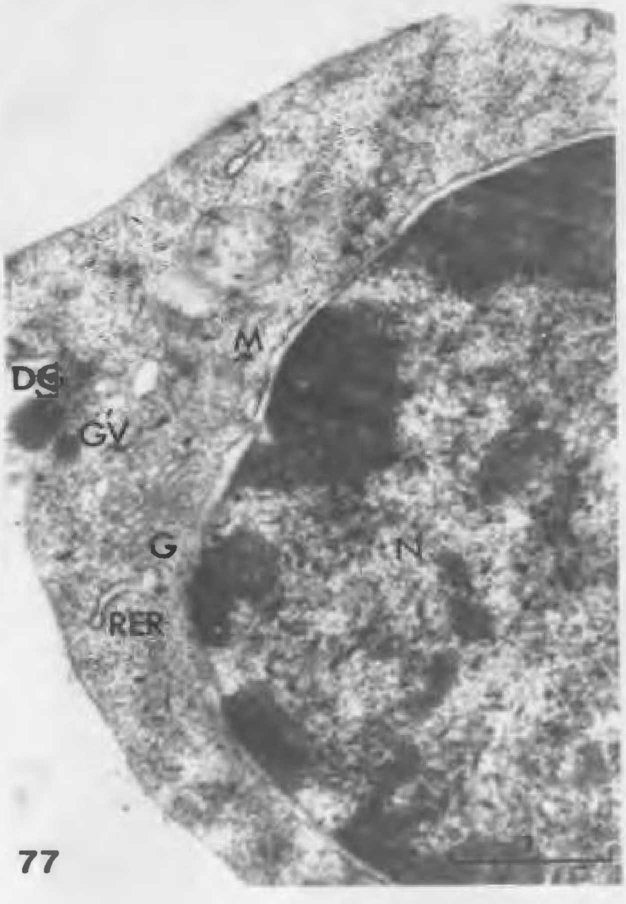
77
M
DG
GV
G
N
RER

Figure 78: Ultrastructural aspects on neurosecretory vesicle formation in type II frontal organ neurons. Note the apparent formation of a pale vesicle (PV) in (c) from the distal face of a Golgi complex. Double membrane formation coincides with an increase in vesicle density. 78(b) contains a vesicle attaining a double membrane in the section where the matrix is denser (arrows). This suggests that the acquistion of the double membrane is a step in the maturation process of the vesicle (epon, uranyl acetate/lead citrate, 18,850X).

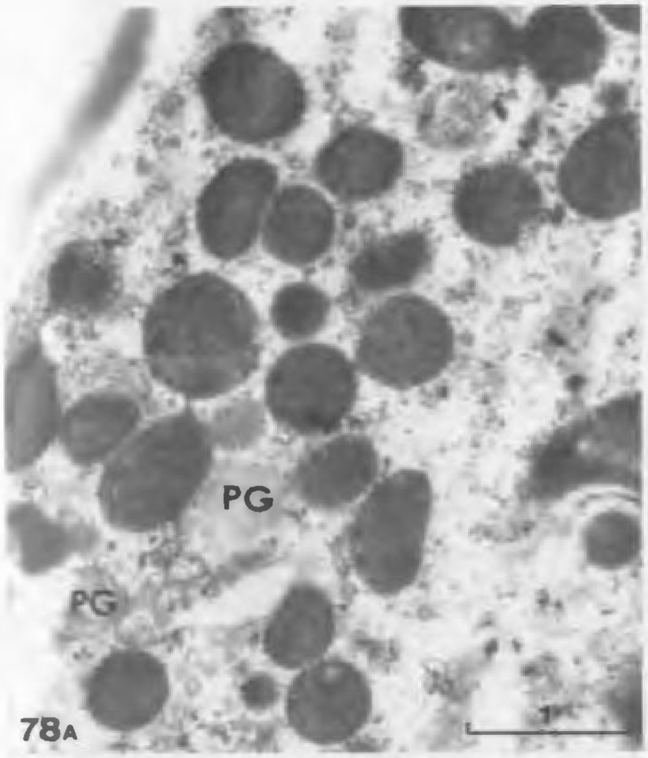
78A

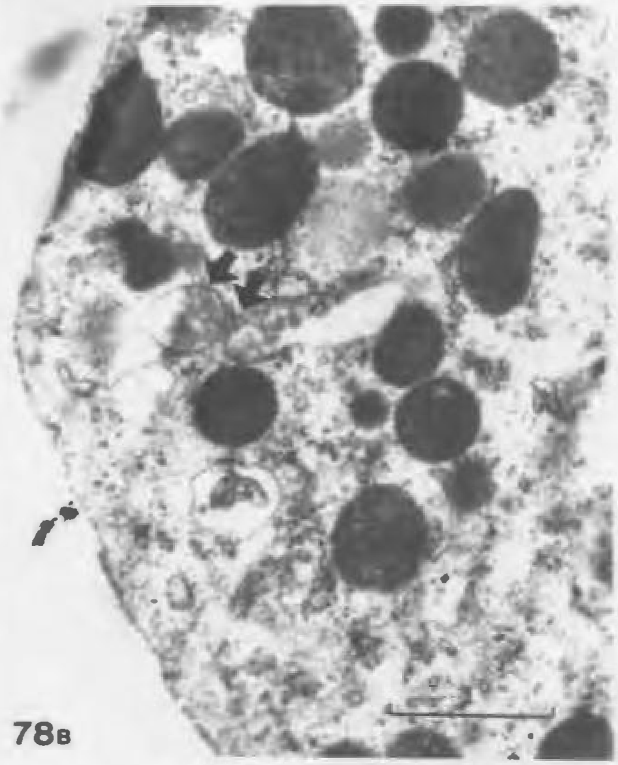
78B

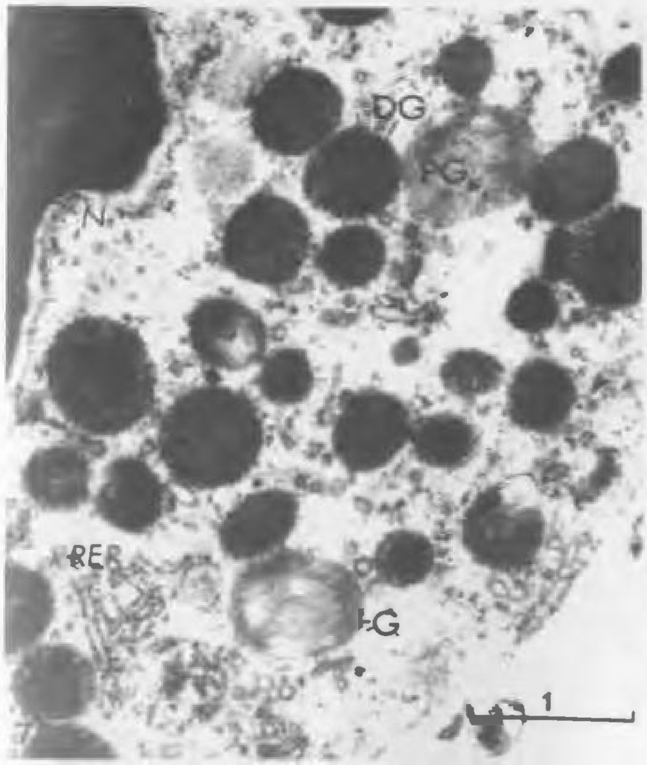
7
DG
PG
N
RER
G
1

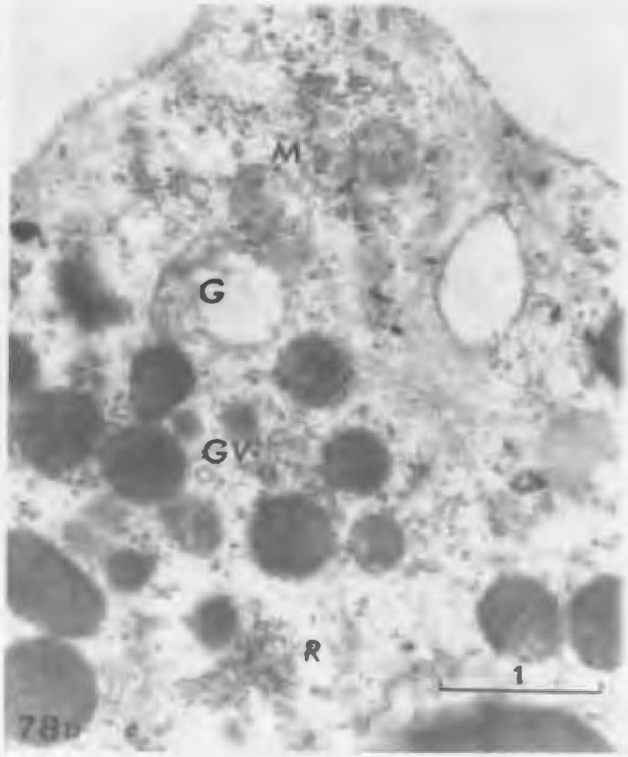
78D

Figure 79: Some histological aspects of the hepatopancreas illustrating its synthetic capacity.

(a) Arrangement of the cells in the simple blind tubules. Note presence of lipid globules (black), (epon, toluidine blue pH 11.1, 85X),

(b) Hepatopancreatic cells with villi-like projections on their outer border adjacent to the lumen (epon, epoxy PF, 850X).

(c) Dense aggregations of mitochondria of various configuration in these cells (epon, uranyl acetate/lead citrate, 16,000X).

(d) Ultrastructure of the villi-like border of the hepatopancreatic cells (epon, uranyl acetate/lead citrate, 16,000X).

(e) Inner membrane of the hepatopancreas cells nearest the ovary showing the invagination of the mucous gland duct. Note the network of canaliculi perforating this edge of the cell (arrow), (epon, uranyl acetate/lead citrate, 16,000X).

(d) Section through the mid region of these cells showing the dense rough ER accumulations, flattened Golgi cisternae and the larger probable portions of the canaliculi (arrow), (epon, uranyl acetate/lead citrate, 16,000X).

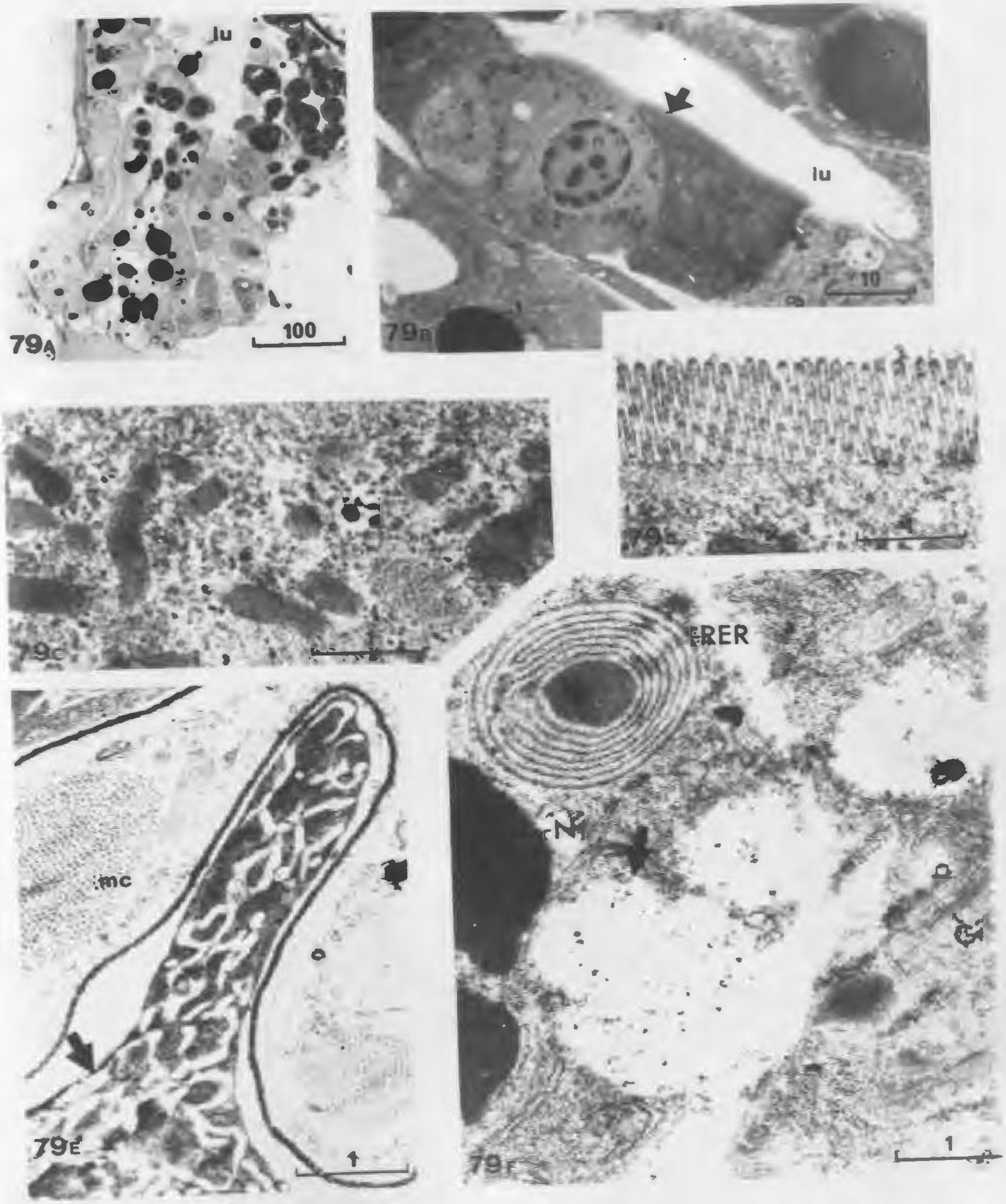
lu
100
79A
lu
10
79B
79C
1
79D
RER
N
G
mc
1
79E
1
79F

Figure 80: Cross section through the anterior portion of the oviduct in the region of the mucous gland. The duct is blocked with a mucous plug (paraffin, CHP, 455X).

Figure 81: Connective tissue wedge between two developing oocytes. The nuclei here are prominent but the cell boundaries are indistinct (epon, toluidine blue pH 11.1, 560X).

Figure 82: Connective tissue wedge of more irregular composure with different cell types readily visible. The cell bodies are distinct and contain a varying quantity of granules (epon, toluidine blue pH 11.1, 560X).

Figure 83: A PF-positive reaction (arrow) of the granules within the cells found in the connective tissue wedges of the ovary. Pseudopodia-like processes can be seen arising from a number of these cells. The chromatin does not react (hollow arrow), (epon, epoxy PF, 1450X).

Figure 84: Localization of the mucous cell aggregations in the region of the ovary and hepatopancreas. They bear resemblance to Bowman's glands of vertebrate olfactory epithelium (epon, toluidine blue pH 11.1, 145X).

Figure 85: Mucous cells releasing their granules in the concavities along the basal lamina of the hepatopancreas. The cell can be seen rupturing through the membrane of the duct and vacuolated cells are also present (epon, toluidine blue pH 11.1, 1450X).

Figure 86: Released mucous droplets being taken into the hepatopancreas by invagination of the basal lamina (epon, toluidine blue pH 11.1, 1450X).

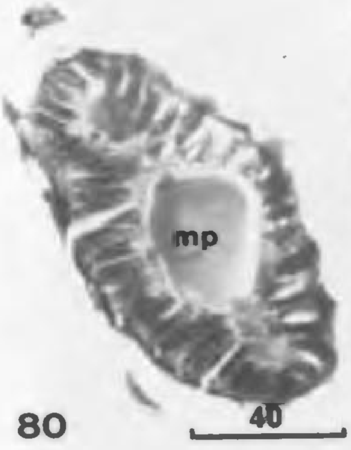

80

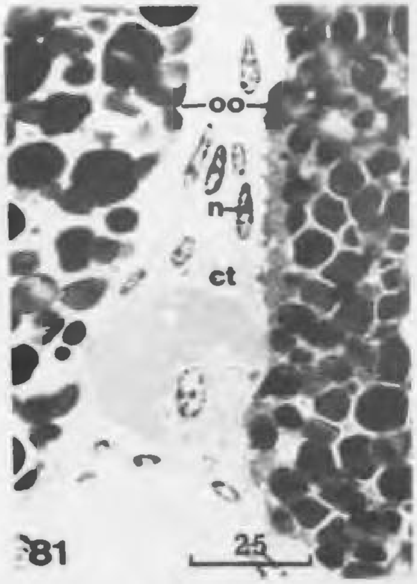

81

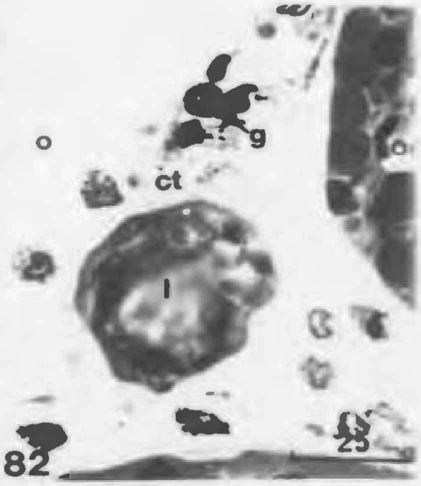

82

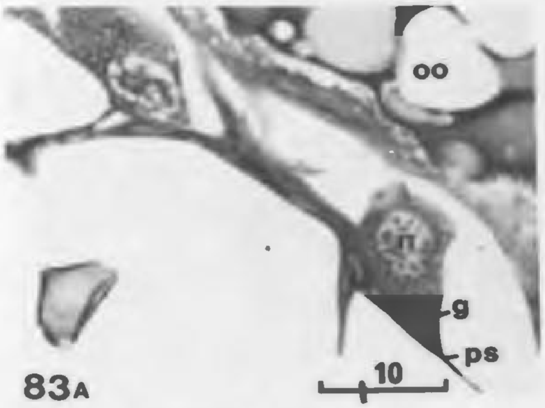

83A

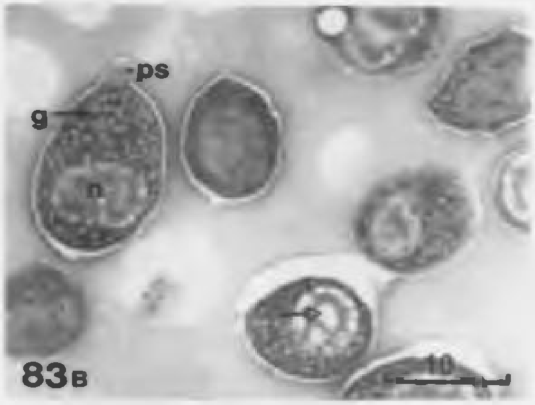

83B

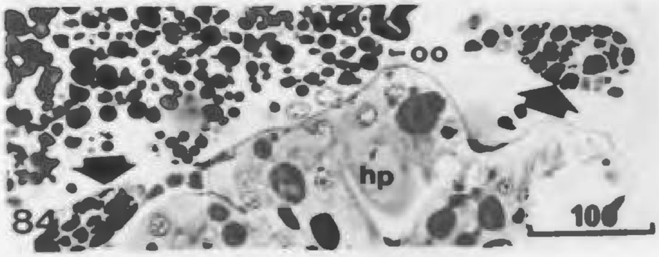

84

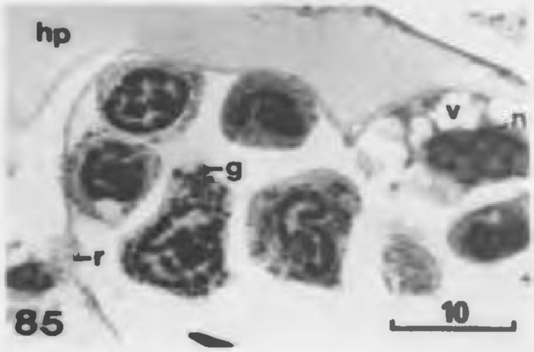

85

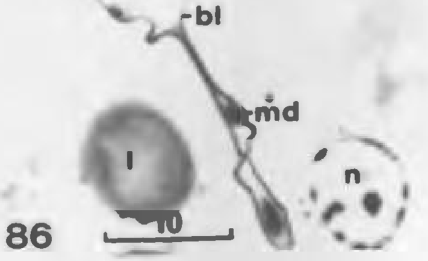

86

Figure 87: Ultrastructural aspect of the mucous cells showing the large homogeneously dense mucous granules, relatively organelle-poor, finely reticulated cytoplasm (epon, uranyl acetate/lead citrate, 20,235X).

Figure 88: Cross-section of the ovary of *G. setosus* showing the slowly developing oogonium en route into the lumen of the ovary. The ovarian epithelium appears irregularly thickened and wispy (epon, toluidine blue pH 11.1, 145X).

Figure 89: Cross-section through the germinal part of the ovary showing the developing primary and secondary oogonia (epon, toluidine blue pH 11.1, 1450X).

Figure 90: Frontal section through the ovary showing a maturing oocyte (stage 4-5) and the different morphological stages of the follicle cells. They first become confluent with indistinct boundaries (hollow arrow) then regain their membranes (short white arrow) and finally become extremely stetched just before ovulation (long white arrow), (epon, toluidine blue pH 11.1, 245X).

Figure 91: Low power electron micrograph of the homogeneous follicular cells mass surrounding the developing oocyte. Both cell membranes have broken down (arrows) and great cytoplasmic activity is evident. Many mitochondria, dilated rough ER and Golgi accumulate in the area nearest the ooplasm (epon, uranyl acetate/lead citrate, 4,170X).

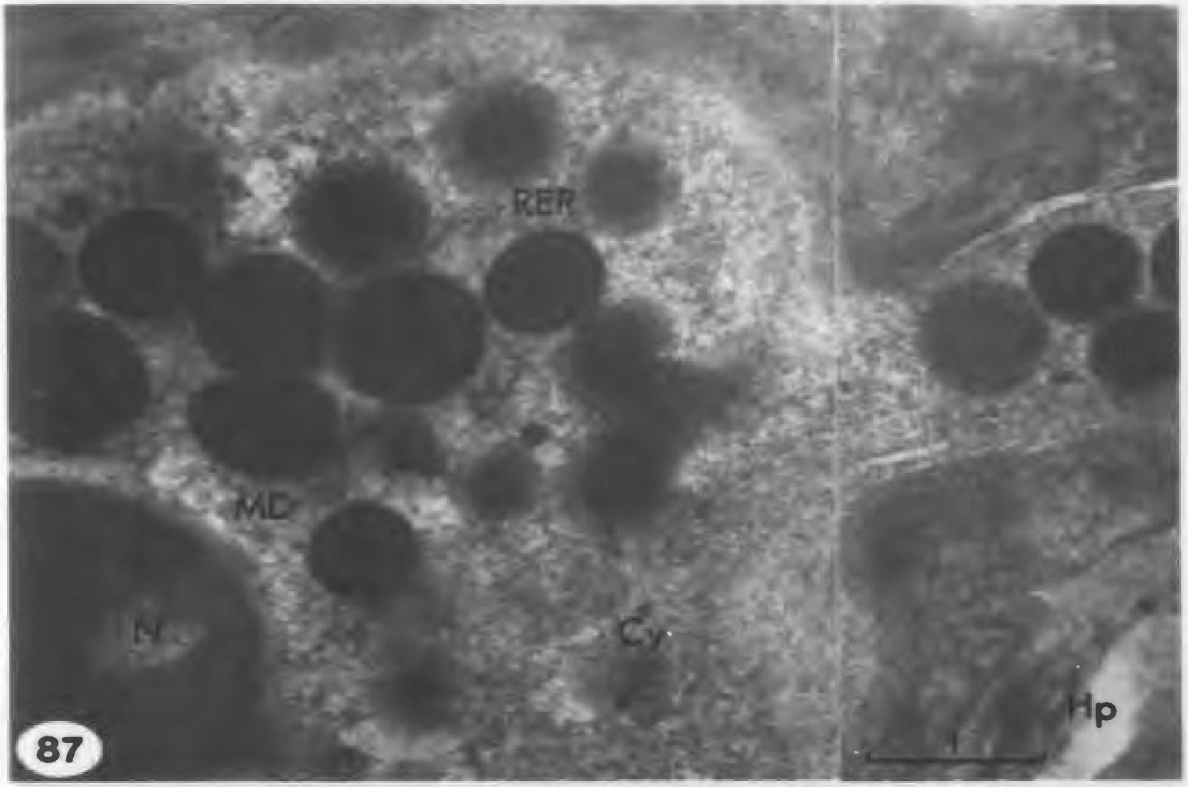
RER
MD
N
Cy
Hp
1
87

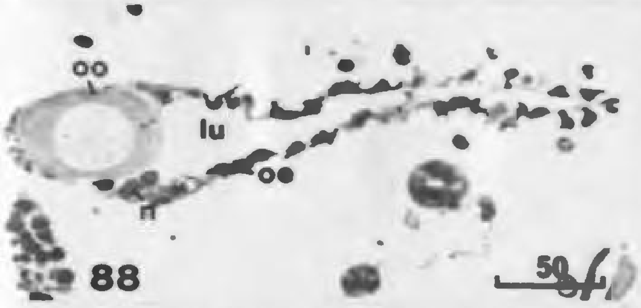
oo
lu
oe
n
50
88

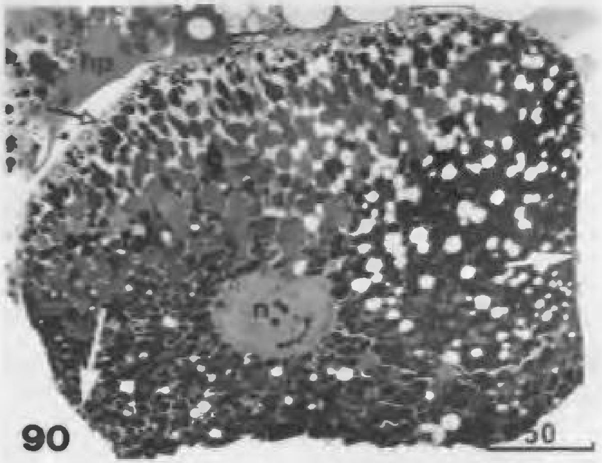
hp
n
50
90

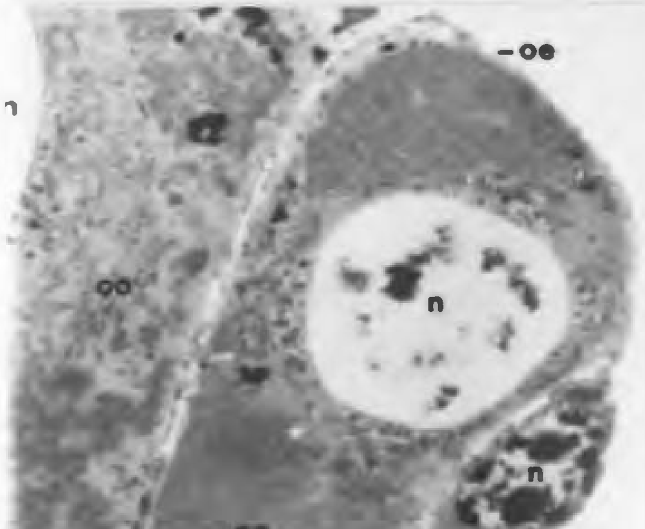
oe
n
oo
n
so
po
fc
10
89

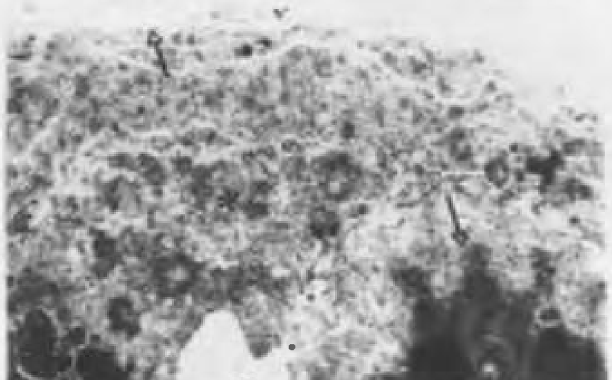
2
91

Figure 92: The inner portion of a follicle cell nearest the ooplasm. The cell membrane is partially disentigrated (hollow arrow). No cytoplasmic extrusions are apparent at this point (epon, uranyl acetate/lead citrate, 21,335X).

Figure 93: Deteriorated follicle cell boundary (arrow) during vitellogenesis. Note the cytoplasmic extrusion from the cytoplasm of the follicle cell into the zona radiata of the oocyte (epon, uranyl acetate/lead citrate, 21,335X).

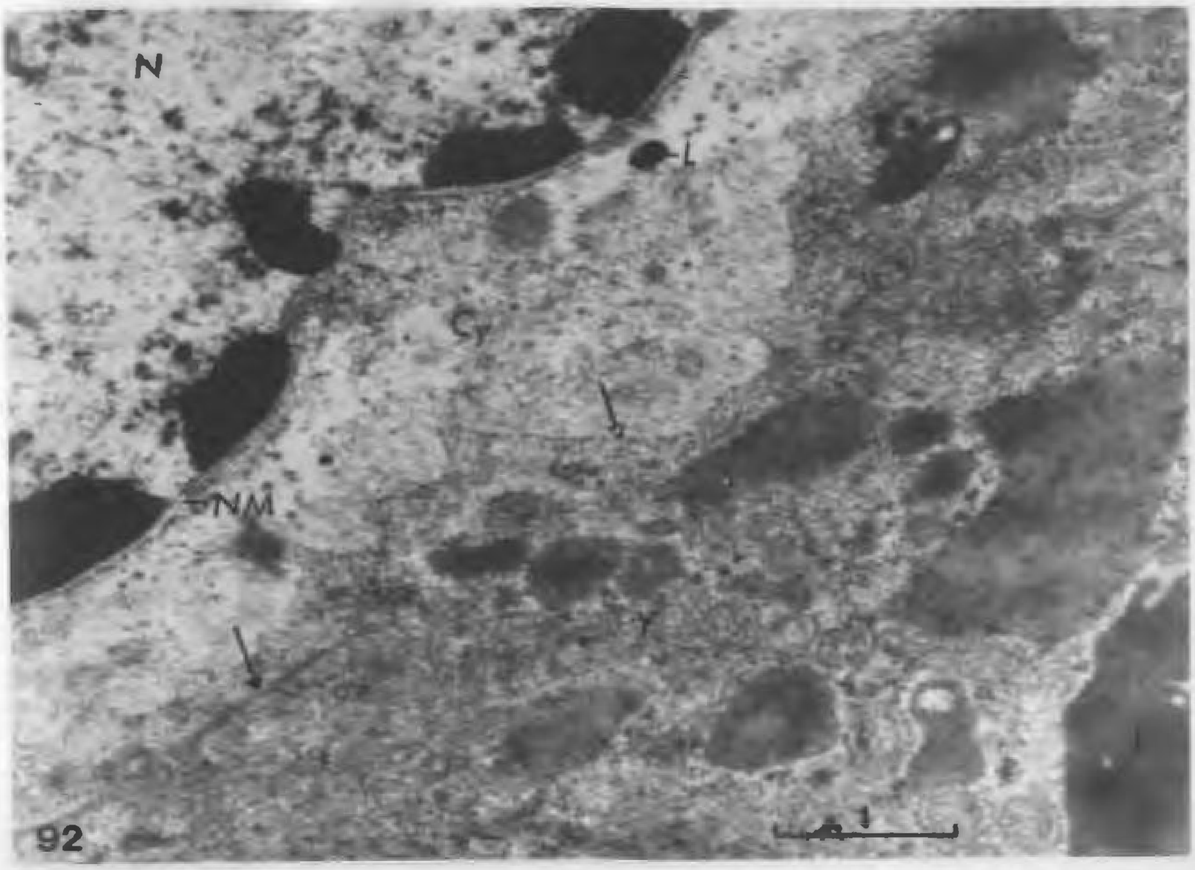
N
L
Cr
NM
Y
1
92

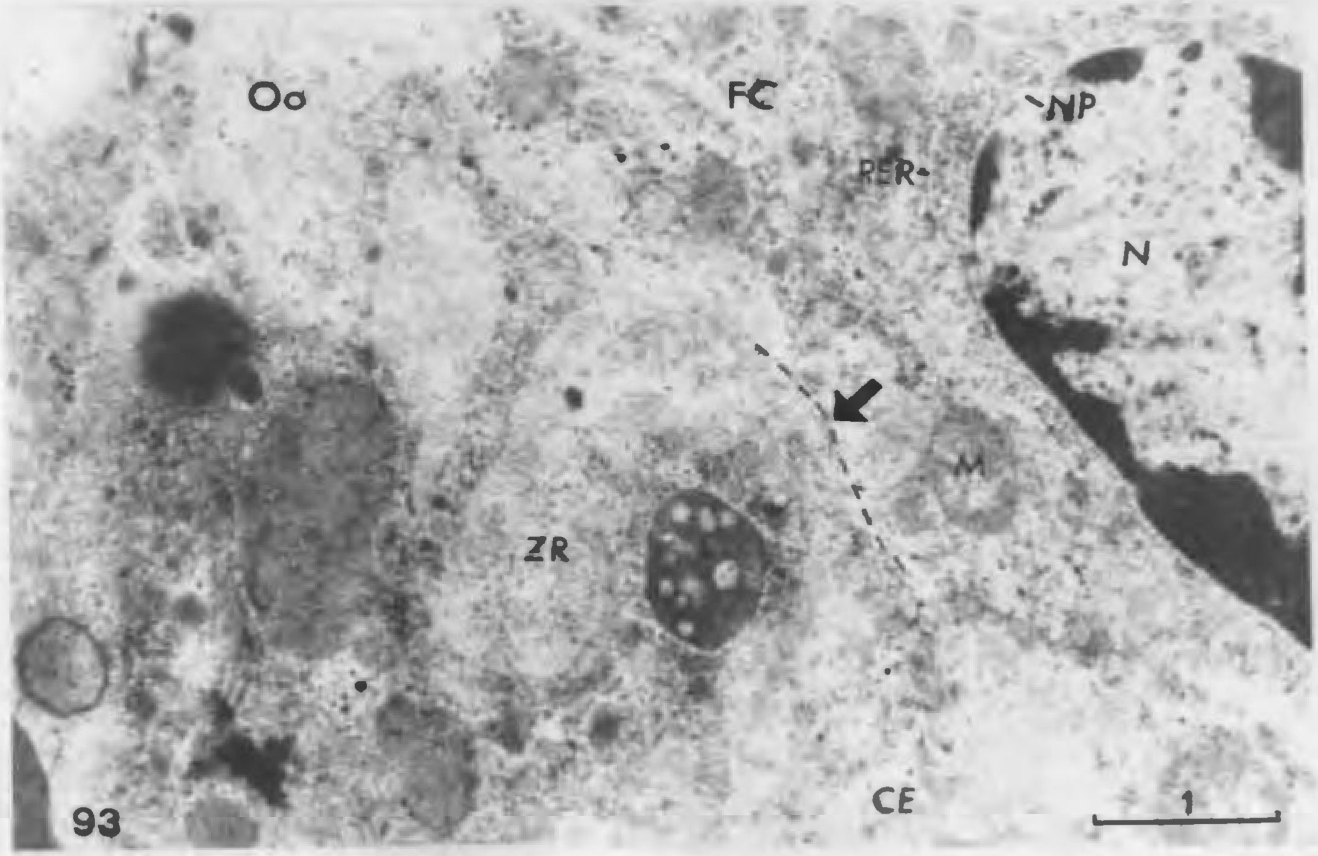
Oo
FC
NP
RER
N
M
ZR
CE
1
93

Figure 94: Frontal section through the viscera of the animal showing the proximity of the gut and hepatopancreas to the ovary. Note the absence of lipid globules in the section of the hepatopancreas opposite the fully mature section of the oocyte (small arrow) opposed to the anterior portion still undergoing vitellogenesis (large arrow), (epon, toluidine blue pH 11.1, 140X).

Figure 95: Proximity of the ovary and hepatopancreas with emphasis on the location of the lipid globules in the hepatopancreas (epon, toluidine blue pH 11.1, 1400X).

Figure 96: A lipid globule penetrating the basal lamina of the hepatopancreas (arrow) moving into the space between it and the ovary (epon, toluidine blue pH 11.1, 1400X).

Figure 97: Deposition of the protein fraction of the yolk occuring during the final stages of vitellogenesis in the oocyte of *G. setosus* (epon, epoxy PF, 1400X).

(a) Initial stages of protein granule infiltration (*).

(b) Latter stages when the granules become packed into a solid protein mass (*) and the follicle cell appears devoid of granules. The lipid material appears as empty vacuoles due to processing.

Figure 98: Proteinaceous granules accumulated in the posterior region of the hepatopancreas cells (epon, epoxy PF, 1400X).

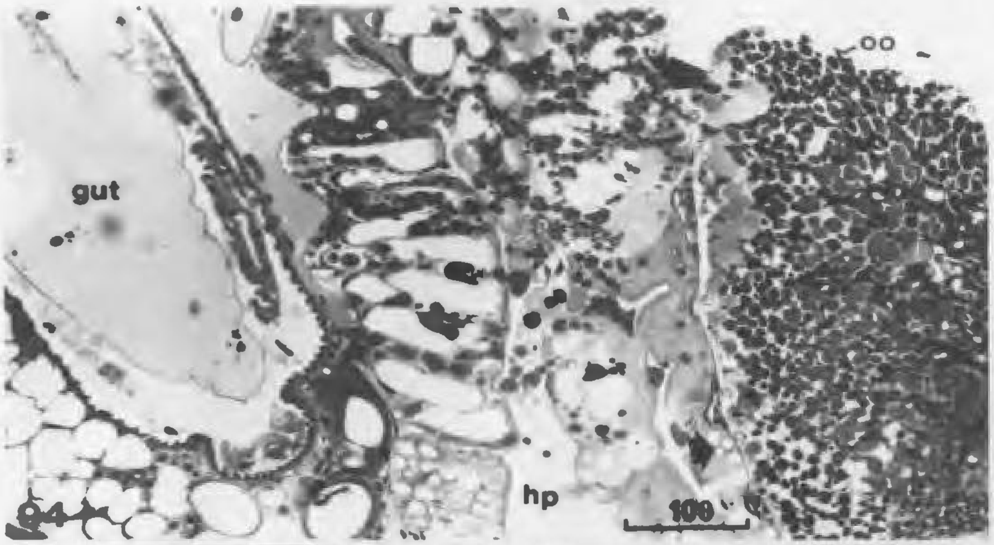
oo
gut
hp
100
94

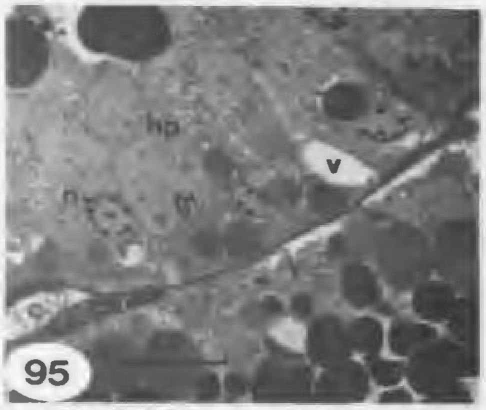
hp
v
n
m
95

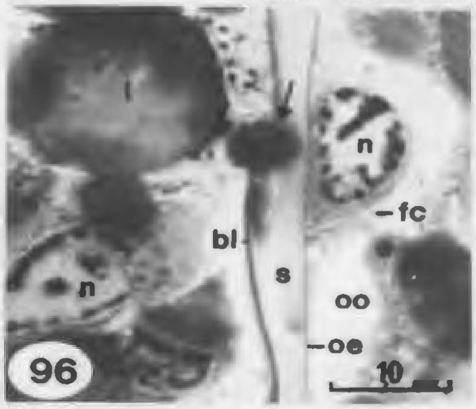
l
n
fc
bl
s
n
oo
oe
96
10

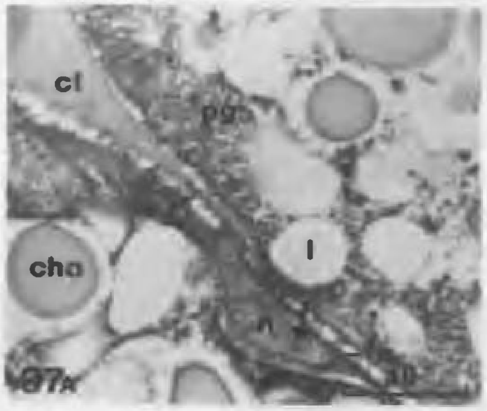
cl
pg
cho
l
n
97A

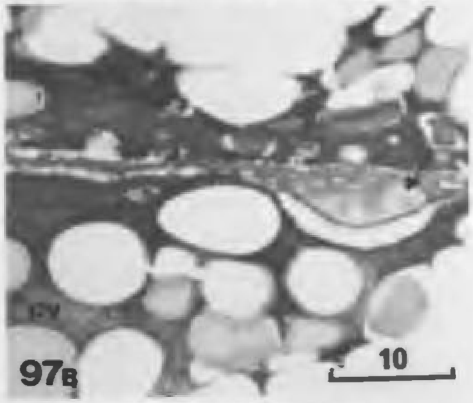
pv
97B
10

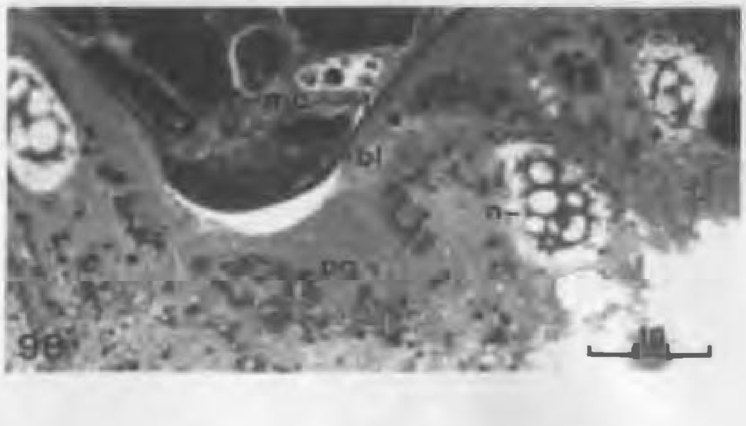
mb
bl
n
pg
98
10

Figure 99: Stages of vitellogenesis in the oocytes of *G. setosus* (paraffin, CHP, 120X).

- (a) Large stage 1 oogonia prior to initiation of vitellogenesis.
- (b) Stage 2 oogonia with ooplasmic vacuolation beginning (solid arrow) as well as initiation of nuclear activity (hollow arrow).
- (c) Stage 2 oocytes with yolk granule deposition occurring around the periphery (hollow arrow). The nucleolus (solid arrow) becomes enlarged.
- (d) Stage 3 oocytes with a great increase of ooplasmic vacuolation and more extensive yolk granule deposition.
- (e) Stage 3 oocytes with severe ooplasmic vacuolation and invasion of yolk granules deep into the oocyte.
- (f) Heavy deposition of yolk granules in a stage 4 oocyte with only a small amount of ooplasm remaining unvacuolated.
- (g) Complete deposition of yolk in late stage 4 oocytes and accumulation of additional granules results in size enlargement.

Figure 100: Stages of yolk resorption and oocyte destruction in female *G. setosus* kept in constant darkness (paraffin, CHP, 53X).

- (a) Vacuolation of yolk granules in a stage 5 oocyte begins (arrow).
- (b) Ovary filled with scattered yolk granules and other debris from the degrading oocytes.
- (c) Majority of the degraded material has been resorbed and ooplasmic vacuolation has begun in oogonia present (large arrow) as well as nuclear activity (hollow arrow).

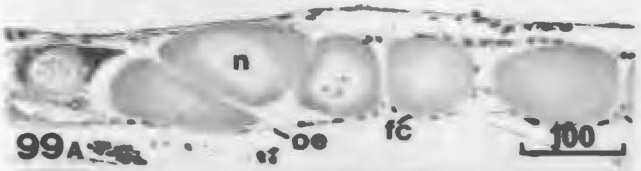
99A
n
oe
fc
100

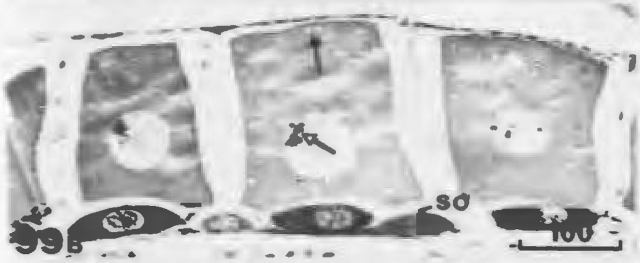
99B
so
100

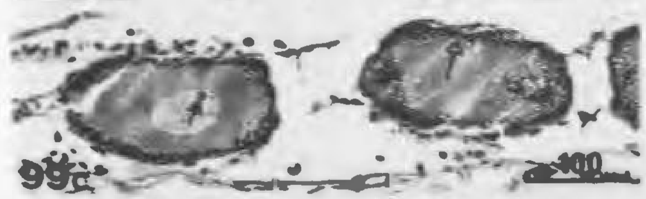
99C
100

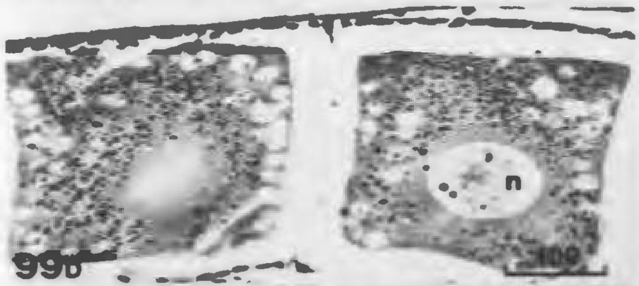
99D
n
100

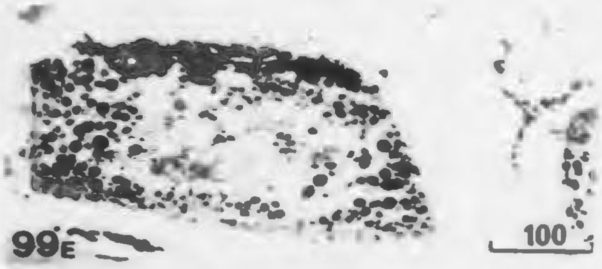
99E
100

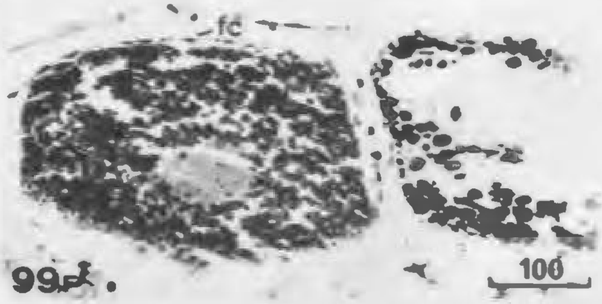
fc
99F
100

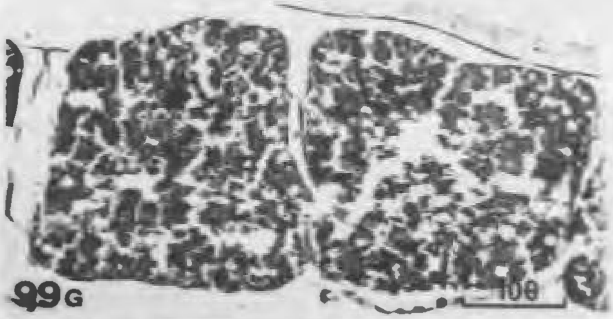
99G
100

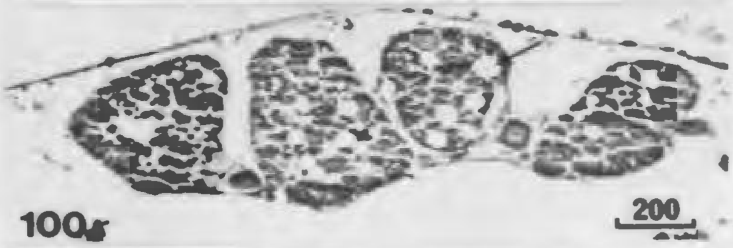
100A
200

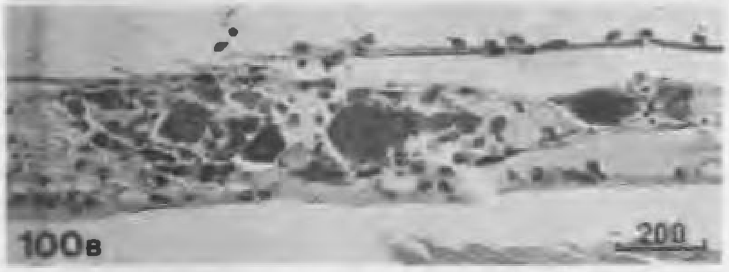
100B
200

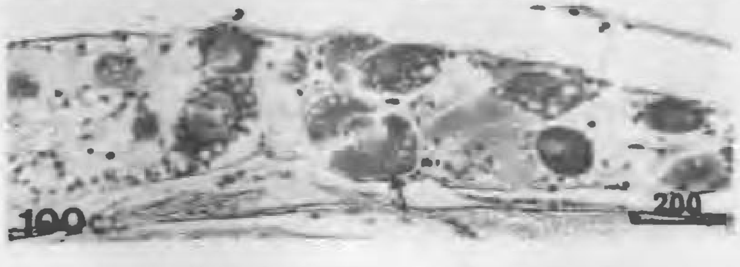
100C
200

Figure 101: Annual ovarian cycle of female *G. setosus* at Witless Bay, Newfoundland. The figures represent average size of oogonia and oocytes in each dated sample (paraffin, CHP, 52X).

(a) OCTOBER 21st, 1971. Oogonia from female with A-B stage embryos (Stage 1, 0.086 mm).

(b) NOVEMBER 20th, 1971. Oogonia from female with B-C stage embryos (Stage 1, 0.091 mm).

(c) DECEMBER 9th, 1971. Oogonia from female with C-D stage embryos (Stage 1, 0.097 mm).

(d) JANUARY 6th, 1972. Oogonia from female with D-H stage embryos (Stage 1, 0.105 mm).

(e) MAY 4th, 1973. Oogonia from resting stage female with no setae (Stage 1, 0.125 mm).

(f) MAY 29th, 1973. Oogonia from resting stage female with no setae (Stage 1, 0.152 mm).

(g) JUNE 1st, 1972. Oogonia from female in resting stage with no setae (Stage 1, 0.189 mm).

(h) JULY 12th, 1972. Oogonia from female with no setae (Stage 1, 0.197 mm).

(i) JULY 12th, 1972. Oocytes from female with no setae. Arrow indicates initiation of vitellogenesis (Stage 2, 0.230 mm).

(j) AUGUST 12th, 1972. Oocytes from female with no setae (Stage 3, 0.343 mm).

(k) AUGUST 26th, 1972. Oocytes from female with no setae (Stage 3, 0.359 mm).

(l) SEPTEMBER 8th, 1972. Oocytes from female with no setae (Stage 4, 0.406 mm).

(m) SEPTEMBER 25th, 1972. Oocytes from female with no setae and in precopula (Stage 4, 0.483 mm).

(n) OCTOBER 7th, 1972. Oocyte from female with no setae and in precopula (Stage 5, 0.526 mm).

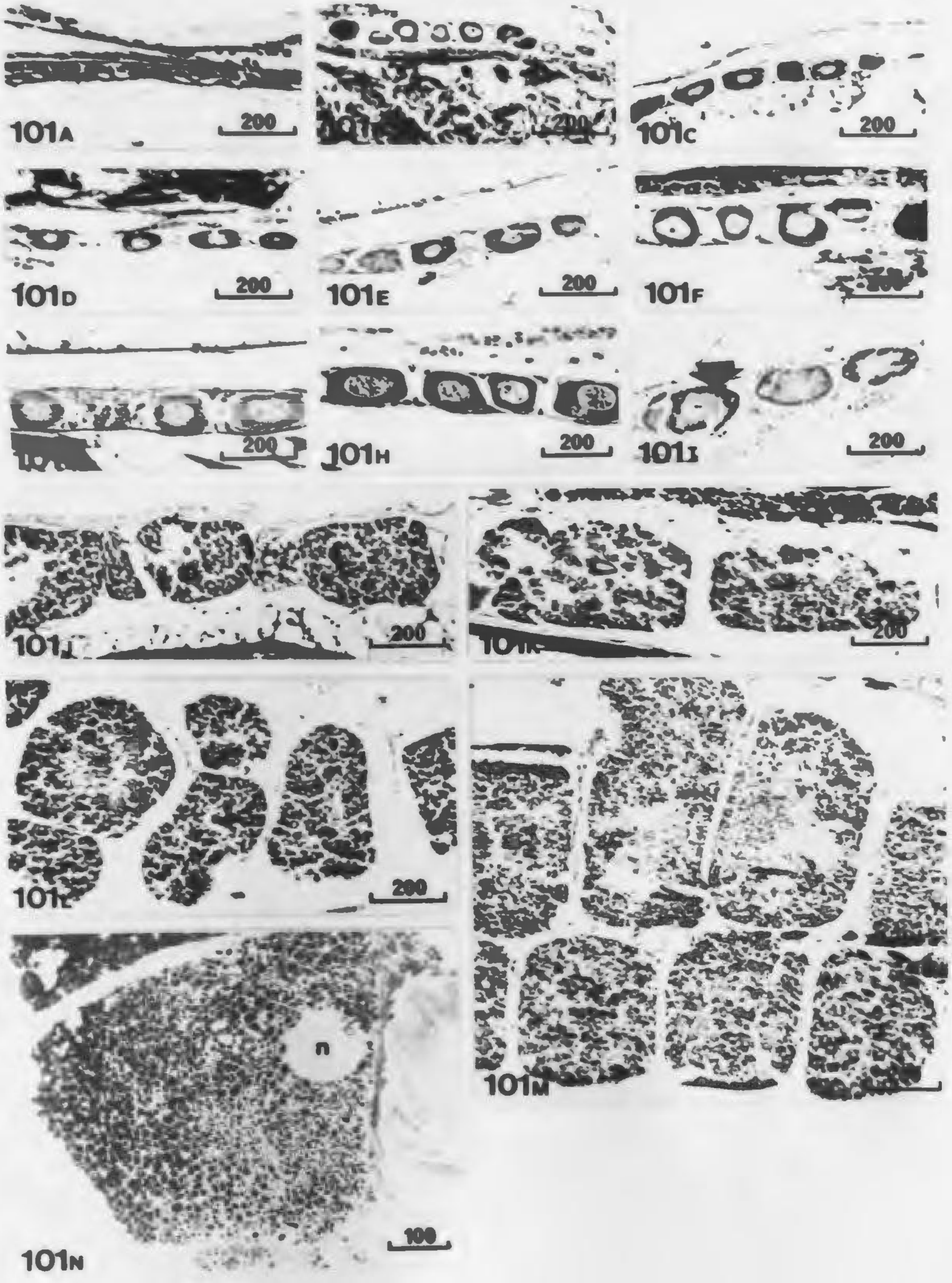
101A
200
200
101C
200
101D
200
101E
200
101F
200
101H
200
101I
200
200
200
200
101M
n
100
101N

Figure 102: Stages of oogonia, oocytes and embryos of *G. setosus* at Witless Bay, Newfoundland. The number in the sample is shown in the upper box of each year. Criteria for determining stages of oogonial and embryo development were adopted from Steele and Steele (1969).

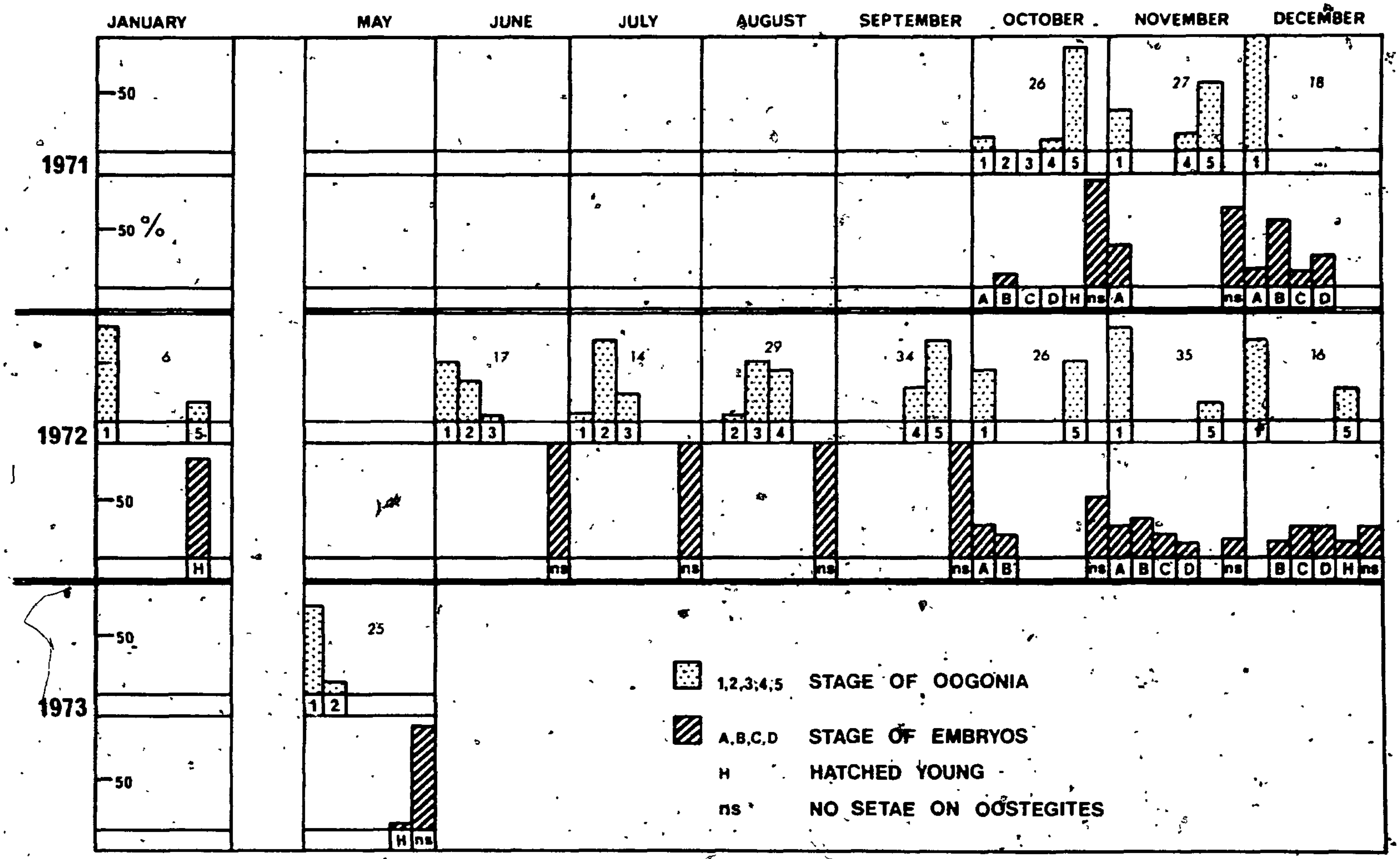
JANUARY
MAY
JUNE
JULY
AUGUST
SEPTEMBER
OCTOBER
NOVEMBER
DECEMBER
1971
1972
1973
50
50 %
26
27
18
6
17
14
29
34
26
35
16
25
1 2 3 4 5
A B C D H ns
1,2,3,4,5 STAGE OF OOGONIA
A,B,C,D STAGE OF EMBRYOS
H HATCHED YOUNG
ns NO SETAE ON OOSTEGITES

Figure 103: Correlation between photoperiod (Dominion Observatory) and sea water temperature (MSRL, Logy Bay, Newfoundland) and size of oogonia/oocytes in *G. setosus* for the 1972 breeding season at Witless Bay, Newfoundland. The arrows indicate the point at which the majority of the females ovulate.

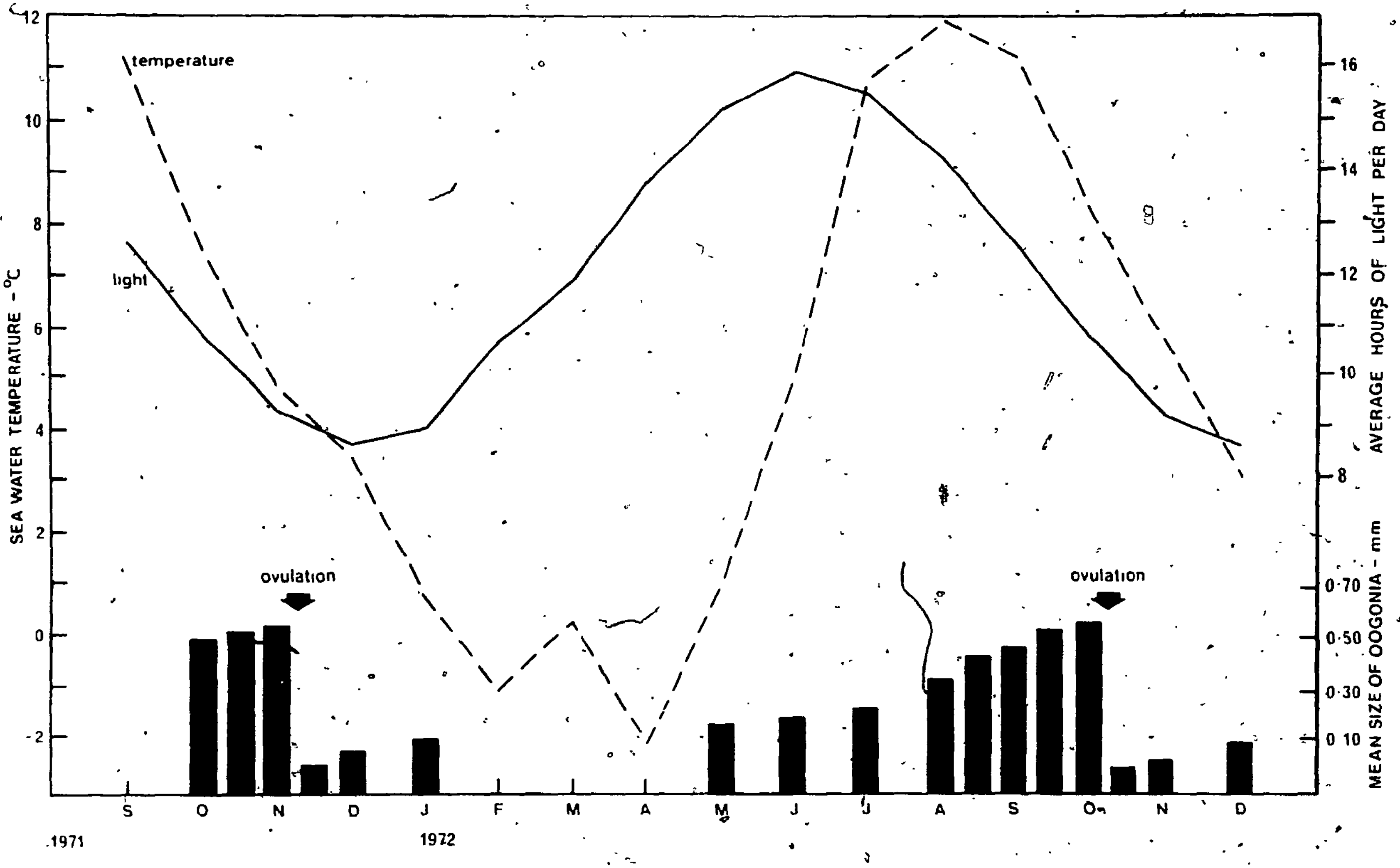
temperature
light
ovulation
ovulation
SEA WATER TEMPERATURE - °C
12
10
8
6
4
2
0
-2
AVERAGE HOURS OF LIGHT PER DAY
16
14
12
10
8
MEAN SIZE OF OOGONIA - mm
0·70
0·50
0·30
0·10
S
O
N
D
J
F
M
A
M
J
J
A
S
O
N
D
1971
1972

Figure 104: Mean stage of oogonial/oocyte development in *G. setosus* females placed into a designated photoperiod during resting stage and sampled at stated intervals. Thirty-five (35) females were placed initially into each and the sample size is shown in the circles.

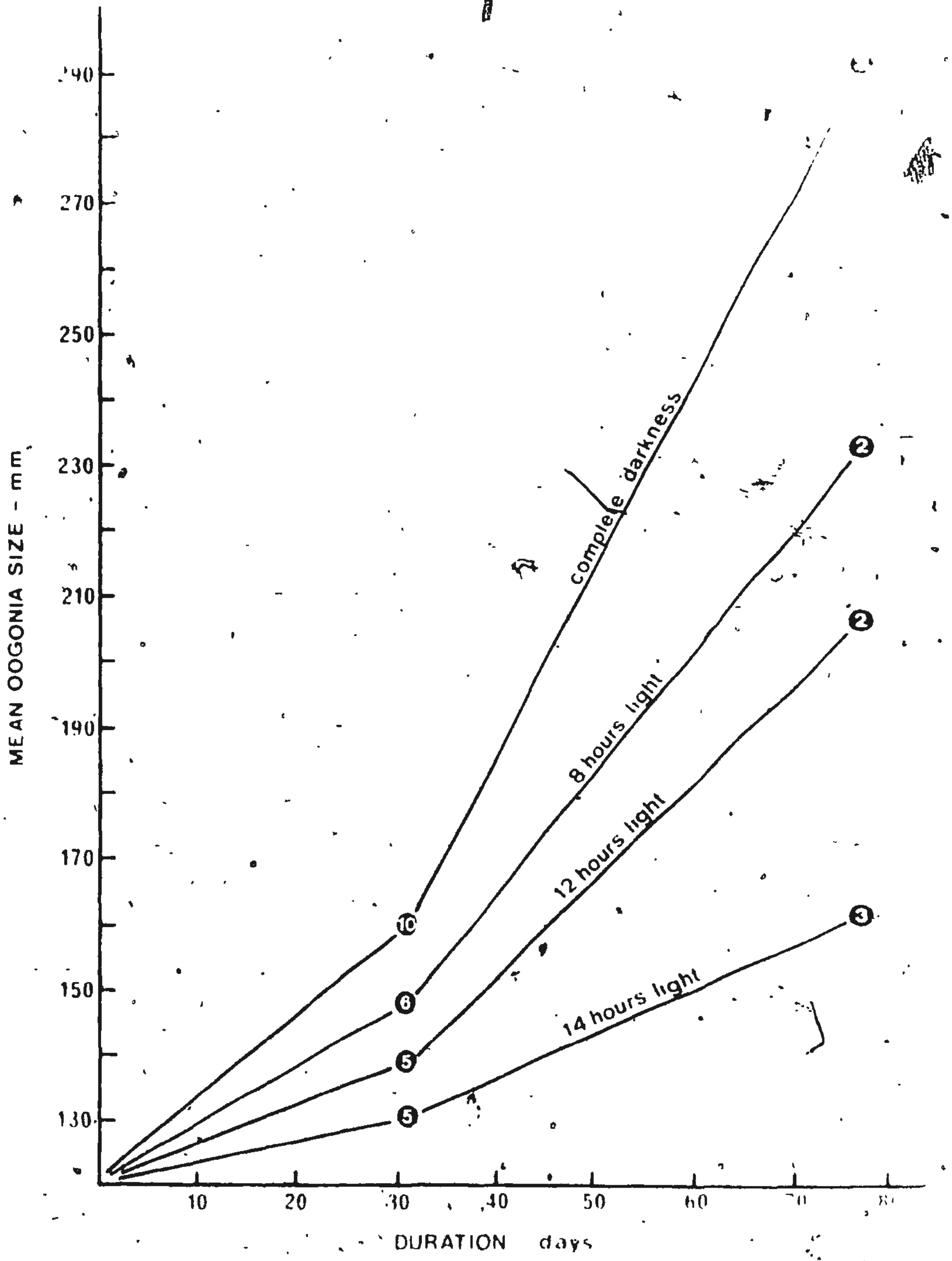
MEAN OOGONIA SIZE - mm
290
270
250
230
210
190
170
150
130
complete darkness
8 hours light
12 hours light
14 hours light
⑩
⑥
⑤
⑤
②
②
③
10
20
30
40
50
60
70
80
DURATION days

Figure 105: Mean oogonial/oocyte size in female G. *setosus* kept in either complete darkness or 14 hours light per day. Fifty (50) females entered the experiment in late stages of ovarian maturation (S_{4-5}) and were sampled at the intervals stated. The figure in the circle represents the number of animals in each sample. R on the ordinate signifies ovarian resorption.

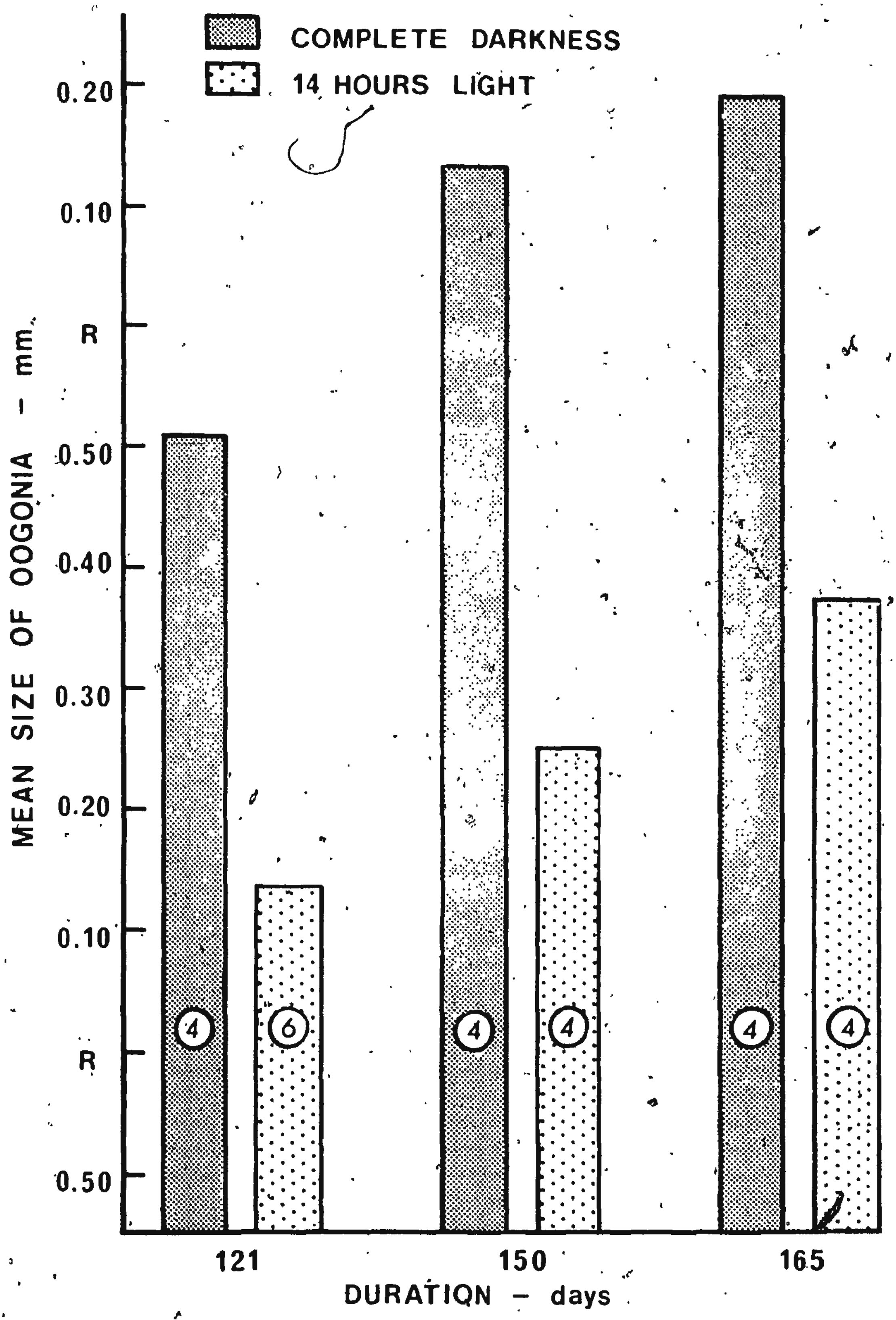
COMPLETE DARKNESS
14 HOURS LIGHT
MEAN SIZE OF OOGONIA - mm.
0.20
0.10
R
0.50
0.40
0.30
0.20
0.10
R
0.50
4
6
4
4
4
4
121
150
165
DURATION - days

Figure 106: Meam size of oogonia/oocytes after 165 days exposure to one of the photoperiods. Initial sample size in each photoperiod was 35 females and the number in the circle represents the survivors sampled at the end of the experiment. The number in the square is the average size of all oogonia or oocytes measured in each sample in mm. The arrow indicates the position of the value in the square in the reproductive cycle and the range of the sample means is delineated by the horizontal bars.

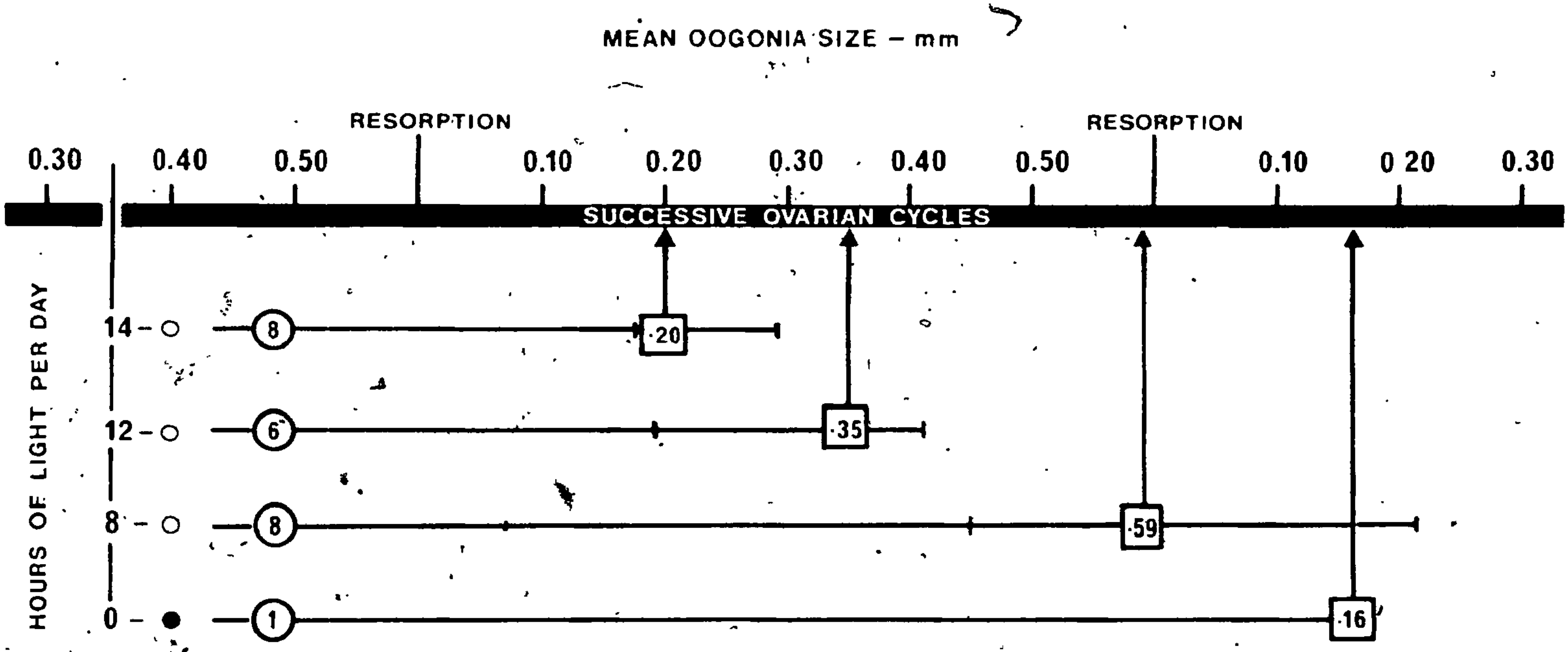

MEAN OOGONIA SIZE – mm
RESORPTION
RESORPTION
0.30
0.40
0.50
0.10
0.20
0.30
0.40
0.50
0.10
0 20
0.30
SUCCESSIVE OVARIAN CYCLES
HOURS OF LIGHT PER DAY
14 – ○
12 – ○
8 – ○
0 – ●
8
6
8
1
·20
·35
·59
·16

Figure 107: The effect of a photoperiod change on mean size of oogonia or oocytes in the reproductive cycle of female *G. setosus*. Fifty (50) females were placed into the experiment in late stages of ovarian maturation (S4-5) and after 117 days in complete darkness the surviving animals (31) were divided into three groups and each placed in a different photoperiod for 14 days. R on the ordinate represents oocyte resorption and the number in each sample is shown in the circle.

Figure 108: The effect of a photoperiod change on mean size of oogonia or oocytes in the reproductive cycle of female *G. setosus*. Fifty (50) females were placed into the experiment in late stages of ovarian maturation (S4-5) and after 117 days in a 14 hour photoperiod the survivors (27) were divided into three groups and each placed into a different photoperiod for 14 days. R on the ordinate represents oocyte resorption and the number in each sample is shown in the circle.

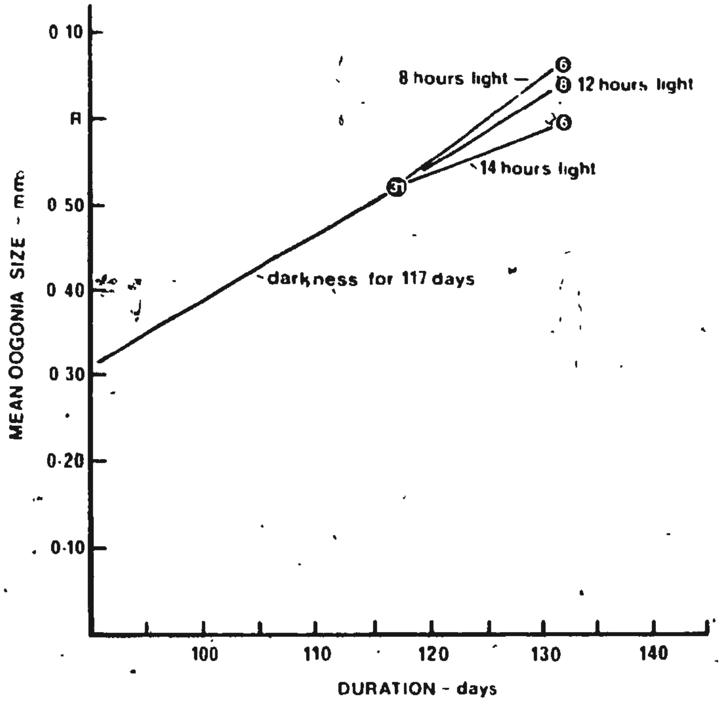

MEAN OOGONIA SIZE - mm
0·70
0·60
0·50
0·40
0·30
0·20
0·10
100
110
120
130
140
DURATION - days
darkness for 117 days
31
8 hours light
6
8
12 hours light
6
14 hours light

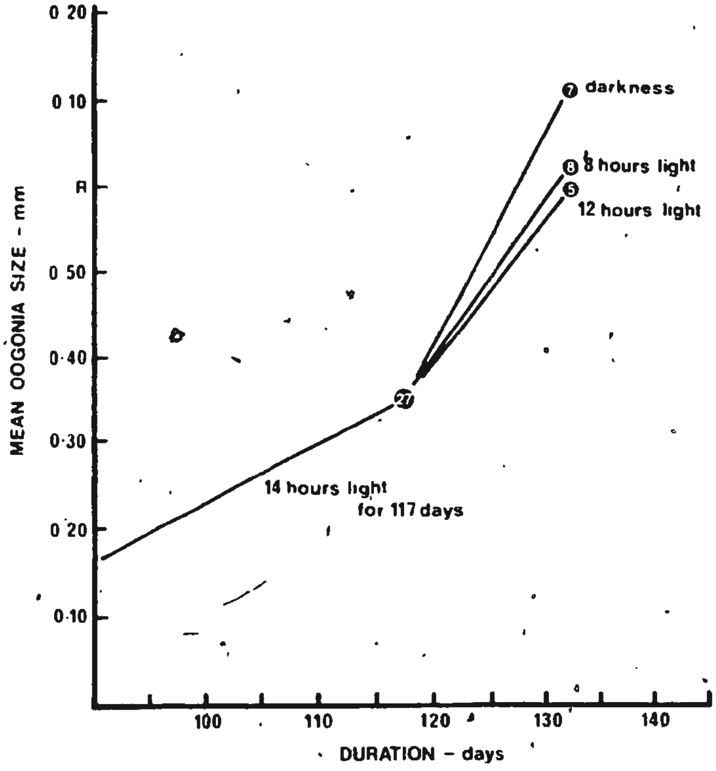

MEAN OOGONIA SIZE - mm
0·80
0·70
0·60
0·50
0·40
0·30
0·20
0·10
100
110
120
130
140
DURATION - days
14 hours light for 117 days
27
7
darkness
8
8 hours light
5
12 hours light

Figure 109: Annual variation in air (Monthly Record) and sea water (MSRL, Logy Bay, Newfoundland) temperature expressed as mean monthly values. The solid bars indicate the period during which *G. setosus* at Witless Bay, Newfoundland ovulated. The vertical line through each bar indicates the peak period of reproduction.

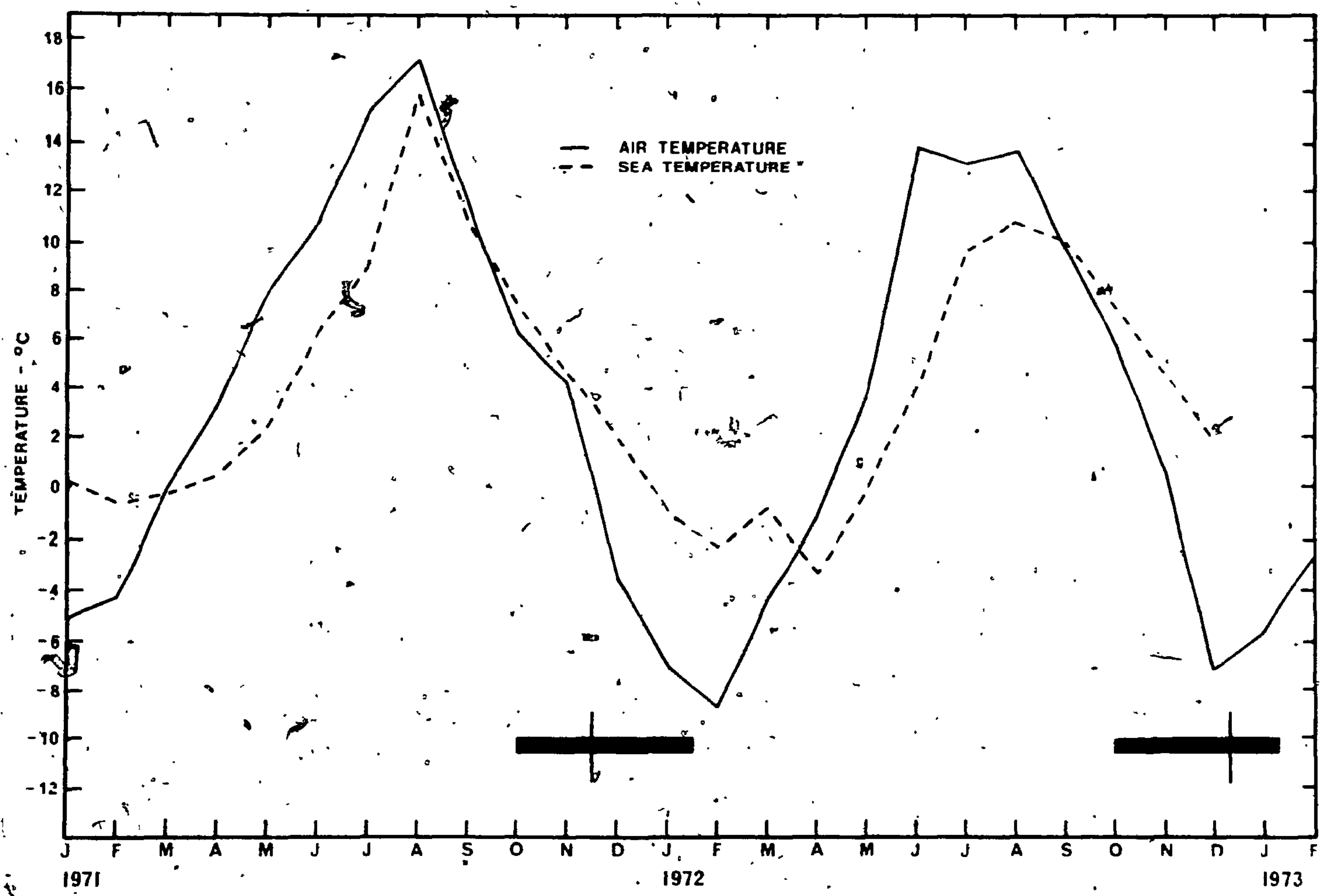

AIR TEMPERATURE
SEA TEMPERATURE
TEMPERATURE - °C
18
16
14
12
10
8
6
4
2
0
-2
-4
-6
-8
-10
-12
J
F
M
A
M
J
J
A
S
O
N
D
J
F
M
A
M
J
J
A
S
O
N
D
J
F
1971
1972
1973

Figure 110: (a) to (f) Neurosecretory activity in the cellular glomeruli of the protocerebral region of the brain of a late August female *G. setosus* in precopula. The solid arrows indicate appearance of NSM in the A cells while the hollow arrows represent that in the B cells (paraffin, PF, 205X, Kodak Wratten filter #22).

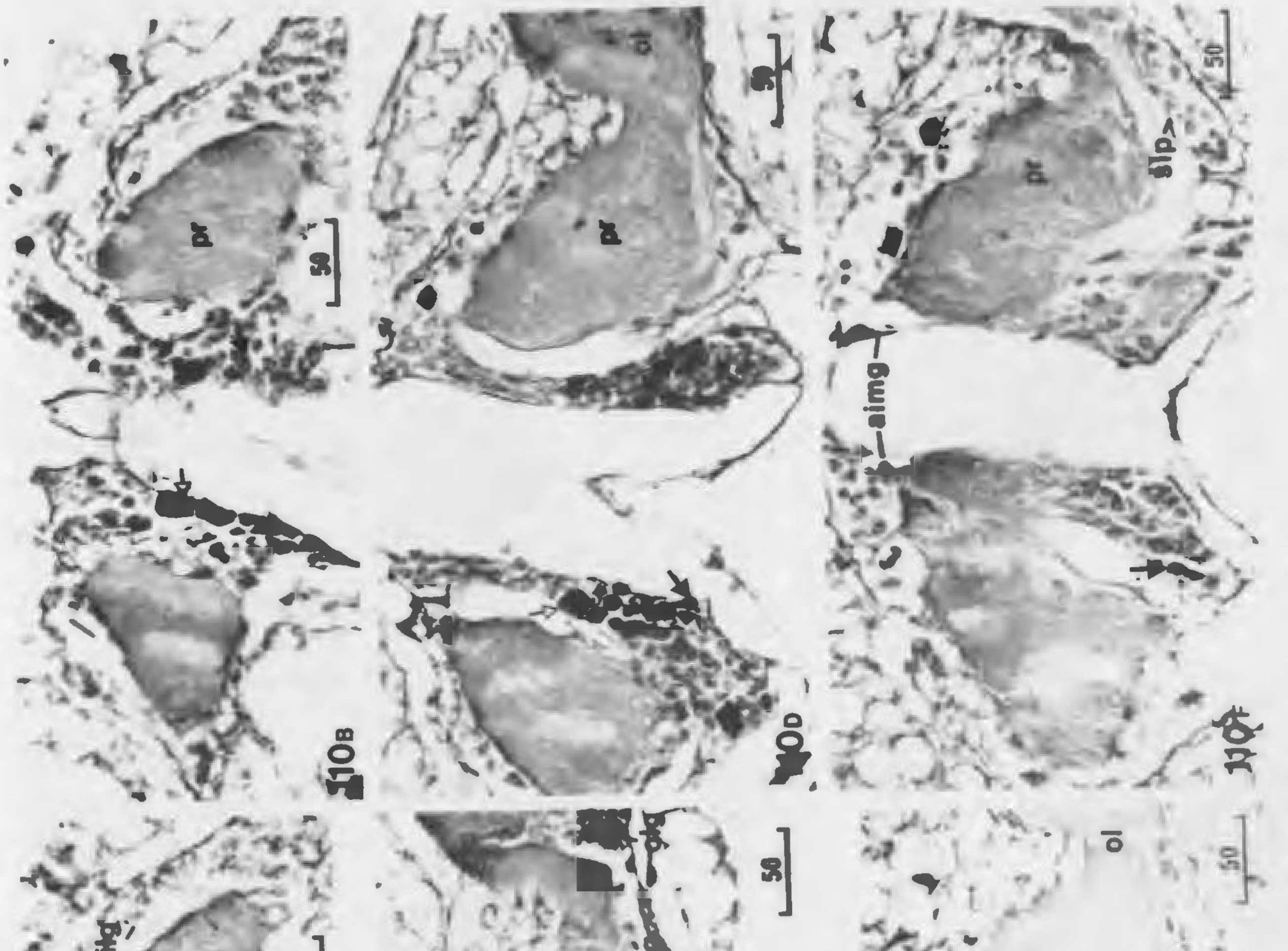
110A
aimg
aimg
aisg
pr
50
110B
pr
50
110C
aimg
asmg
pr
aslg
50
110D
pr
ol
50
110E
asmg
aslg
pr
ol
50
110F
aimg
pr
slp
50

Figure 110: (g) to (l) Neurosecretory activity in the cellular glomeruli of the deutocerebral region of the brain of a late August female *G. setosus* in precopula. The solid arrows indicate the appearance of NSM in the A cells while the hollow arrows represent that in the B cells (paraffin, PF, 205X, Kodak Wratten filter #22).

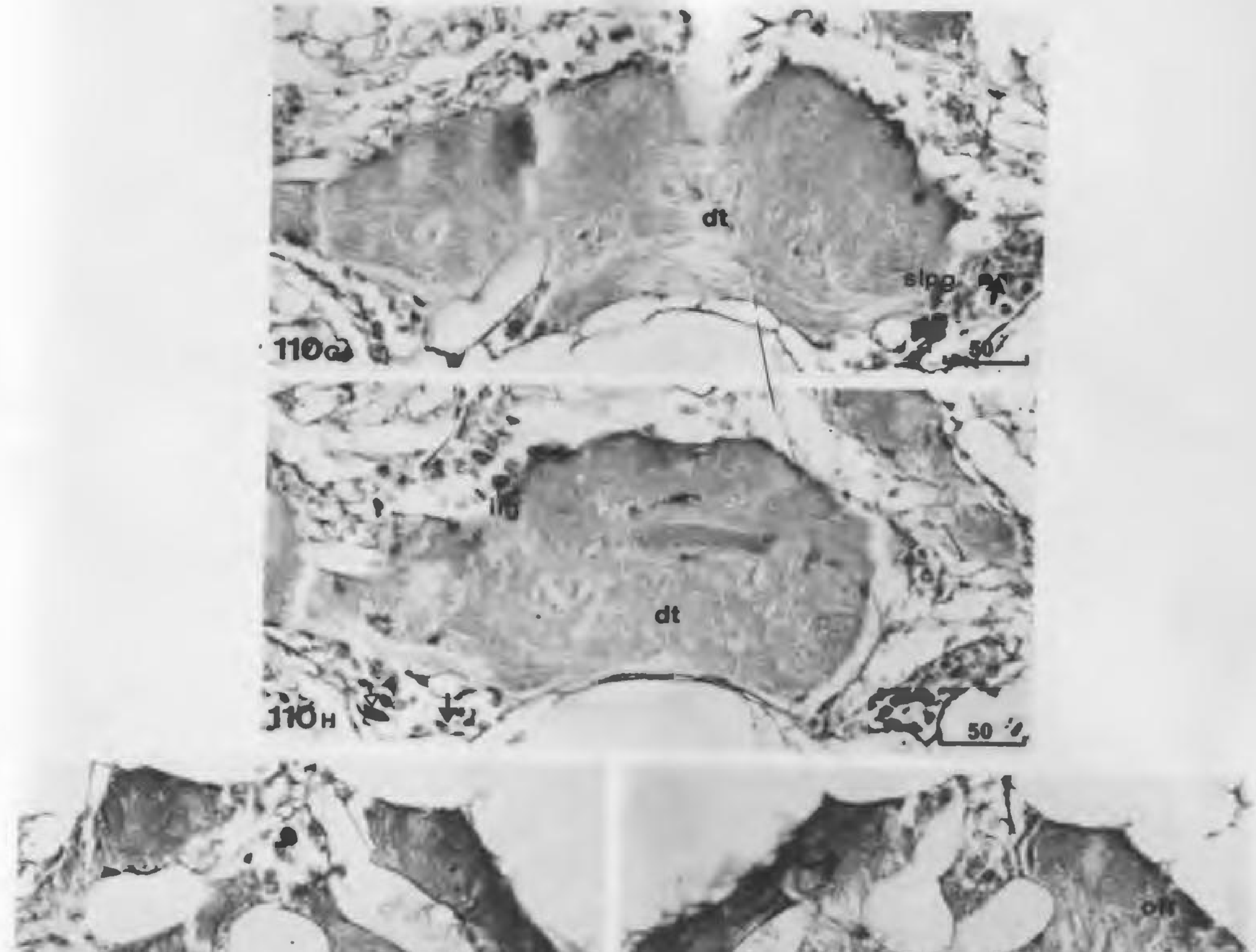
dt
slpg
110G
50
llg
dt
110H
50
dt
110I
50
ofl
dt
-oflg
110J
50
dt
-oflg
110K
50
dt
110L
50

Figure 110: (m) Neurosecretory activity in the cellular glomeruli along the upper region of the tritocerebrum of a late August female *G. setosus* in precopula (paraffin, PF, 195X, Kodak Wratten filter #22).

(n) Neurosecretory activity in the cellular glomeruli located in the lower region of the tritocerebrum of a late August female *G. setosus* in precopula (paraffin, PF, 260X, Kodak Wratten filter #22).

(o) Neurosecretory activity in the cellular glomeruli along the tritocerebral connectives of a late August female *G. setosus* in precopula (paraffin, PF, 260X, Kodak Wratten filter #22).

Figure 111: (a) Location and type of neurosecretory cells in the protocerebral regions of the brain of a late August female *G. setosus* in precopula. The solid dots represent A cells while the hollow triangles indicate B cells.

(b) Location and type of neurosecretory cells in the deutocerebral regions of the brain of a late August female *G. setosus* in precopula. The solid dots represent A cells while the hollow triangles indicate B cells.

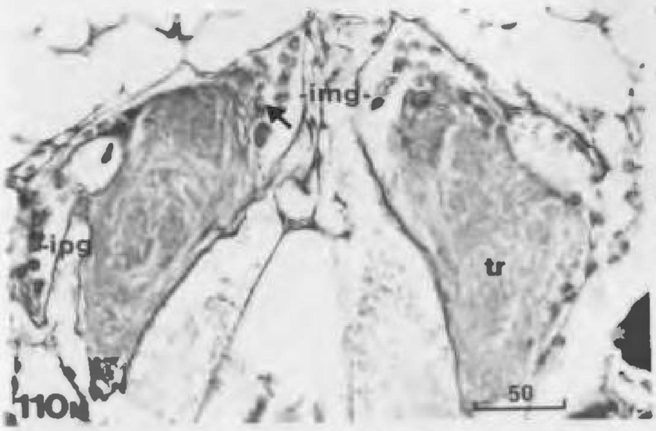
img
ipg
tr
50

110M

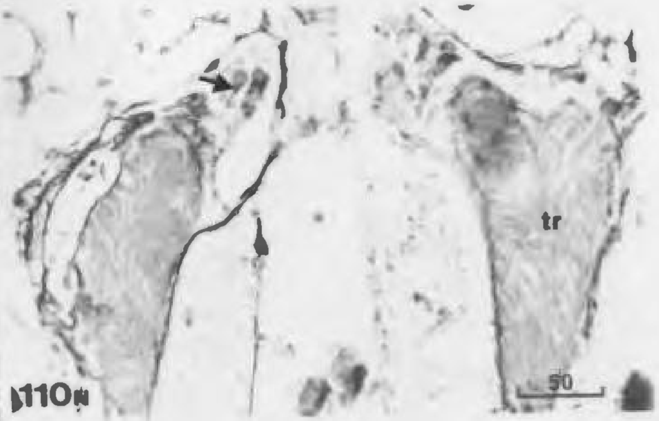

110N

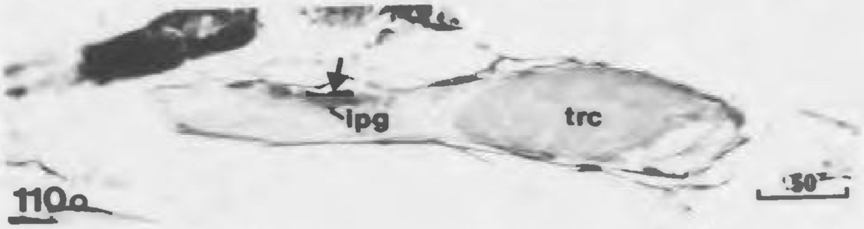

110O

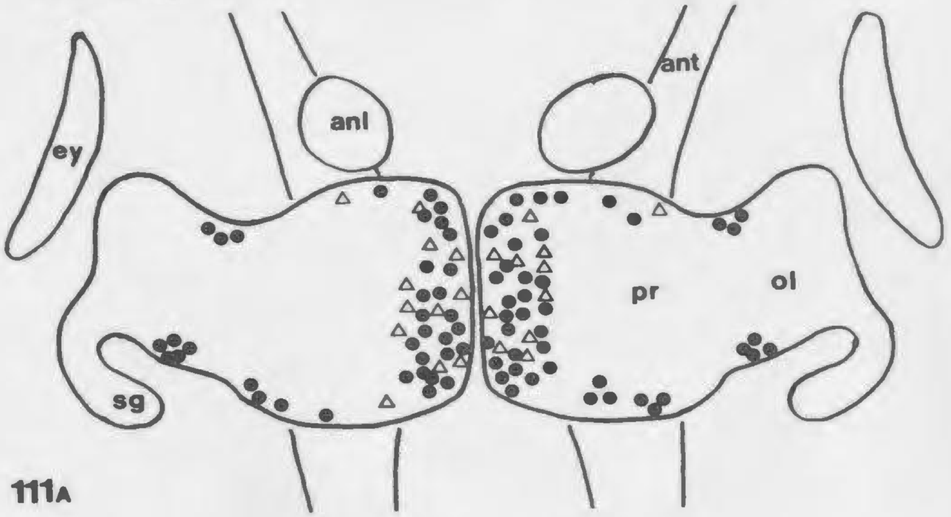
ant
anl
ey
pr
ol
sg

111A

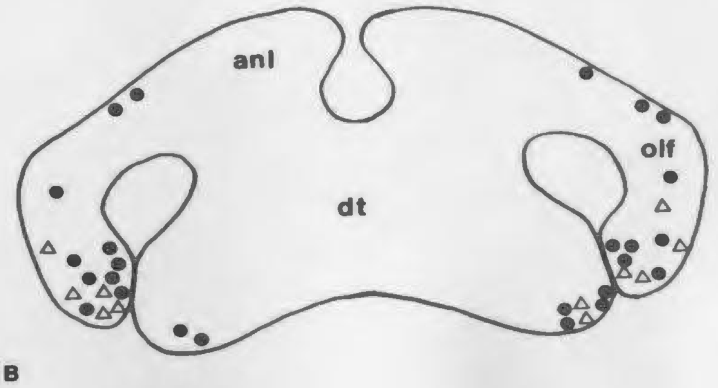

111B

Figure 111: (c) Tritocerebrum of *G. setosus* females in precopula showing the location and types of neurosecretory cells in the peripheral glomeruli. The solid dots indicate A cells while the hollow triangles represent B cells.

Figure 112: Sinus gland of a December female brooding B-C stage embryos with stainable amounts of NSM visible in the neuron perikarya (arrow), (paraffin, PF, 190X, Kodak Wratten filter #22).

Figure 113: (a) Ventral portion of the anterior superior medial glomeruli (asmg) of a December female brooding B-C stage embryos and showing neurosecretory activity in some neuron perikarya (arrow), (paraffin, PF, 190X, Kodak Wratten filter #22).

(b) Sinus gland and ventral portion of the anterior superior medial glomeruli (asmg) of an October female just after ovulation with A cleavage stage embryos. Note absence of stainable NSM in significant amounts in the neuron perikarya (paraffin, PF, 190X, Kodak Wratten filter #22).

Figure 114: Variation in neurosecretory activity of the anterior inferior medial glomerular bridge (aimgb) of the protocerebrum of female *G. setosus*. The solid arrow indicates appearance of NSM in typical A cells while the hollow arrow represents that of the B cells (paraffin, PF, 190X, Kodak Wratten filter #22).

(A) May female in resting stage.

(B) Early August female at initiation of vitellogenesis.

(C) October female with A cleavage stage embryos.

(D) November female with A-B stage embryos.

(E) December female with B-C stage embryos.

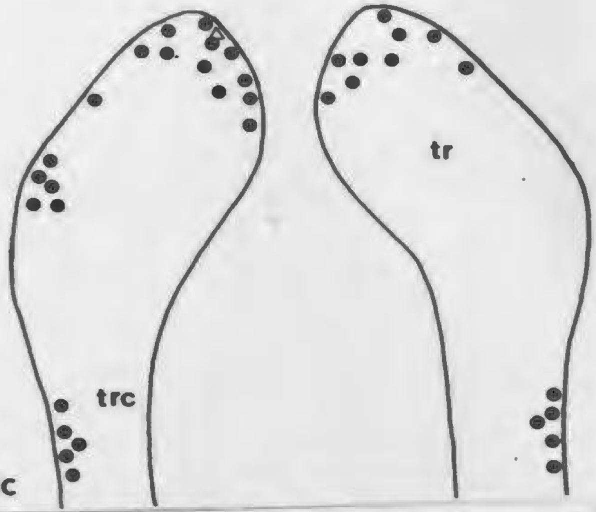

111c

olg
act
sk
sg
50

112

dt
ol
olg
asmg (Xo)
50

113A

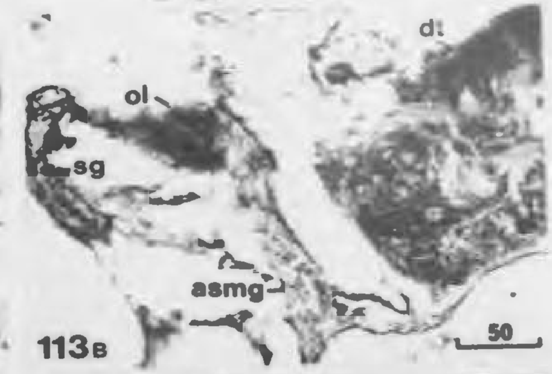
dt
ol
sg
asmg
50

113B

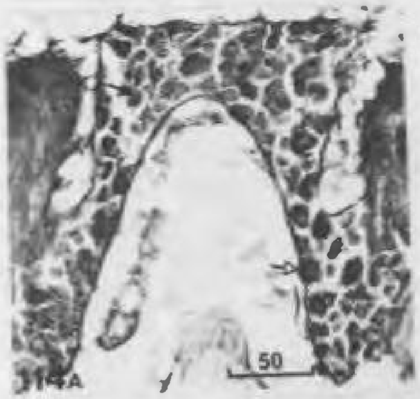

114A

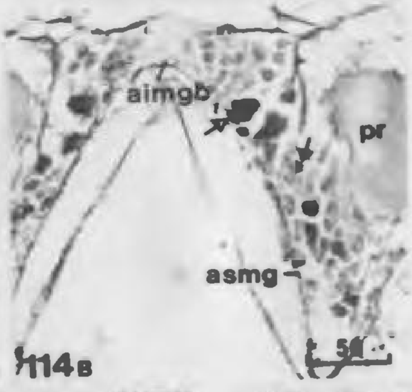
aimgb
pr
asmg
50

114B

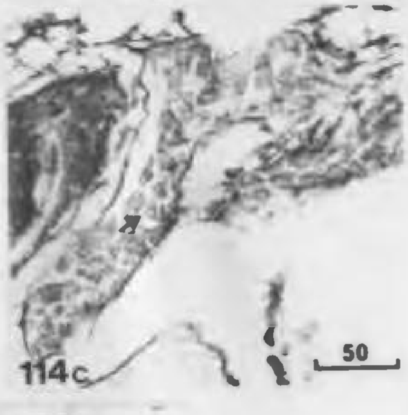

114C

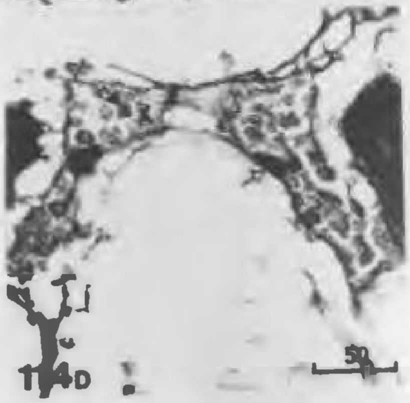

114D

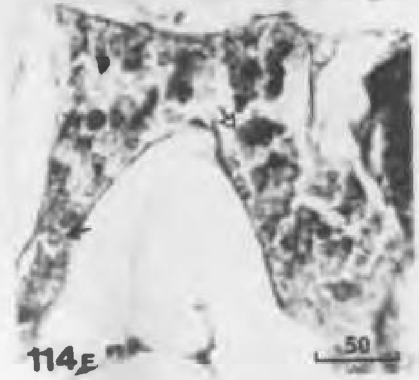

114E

Figure 115: Variation in neurosecretory activity in the anterior inferior medial (aimg) and anterior superior medial glomeruli (asmg) of the lower protocerebrum of *G. setosus*. Solid arrows indicate appearance of NSM in A cells while hollow arrows designate that of B cells (paraffin, PF, 170X, Kodak Wratten filter #22).

(A) May female in resting stage.
(B) Early August female at initiation of vitellogenesis.
(C) October female with embryos in A cleavage stage.
(D) November female with A-B stage embryos.
(E) December female with B-C stage embryos.

Figure 116: Variation in neurosecretory activity in the olfactory lobe glomeruli (oflg) of the deutocerebrum. Solid arrows indicate appearance of NSM in the predominantly A cell population (paraffin, PF, 170X, Kodak Wratten filter #22).

(A) May female in resting stage.
(B) Early August female at initiation of vitellogenesis.
(C) October female with A cleavage stage embryos.
(D) November female with A-B stage embryos.
(E) December female with B-C stage embryos.

Figure 117: Variation in neurosecretory activity in the inferior medial glomeruli (img) of the tritocerebrum. Solid arrows indicate appearance of NSM in the A cells (paraffin, PF, 170X, Kodak Wratten filter #22).

(A) May female in resting stage.
(B) Early August female at initiation of vitellogenesis.
(C) October female with A cleavage stage embryos.
(D) November female with A-B stage embryos.
(E) December female with B-C stage embryos.

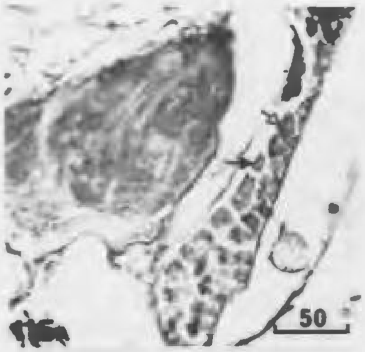
115A

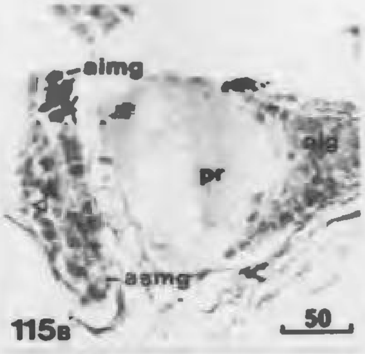
115B
aimg
pr
oig
asmg
50

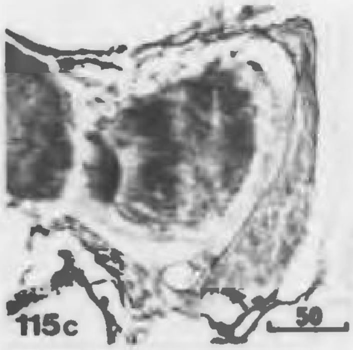
115C

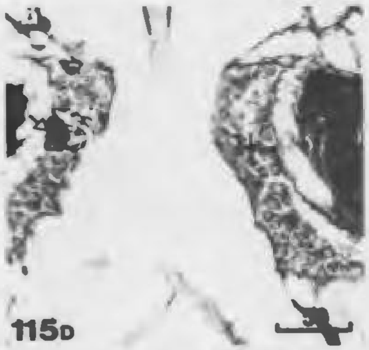
115D

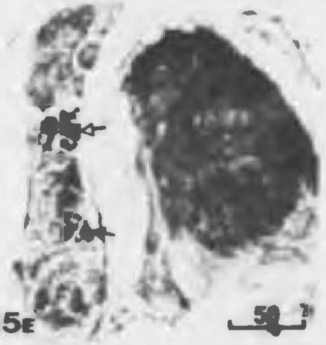
115E

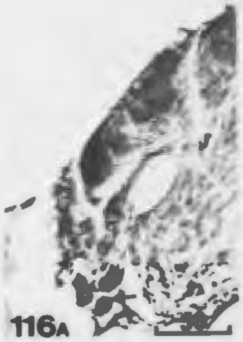
116A

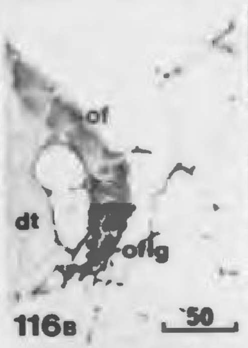
116B
of
dt
ofig
50

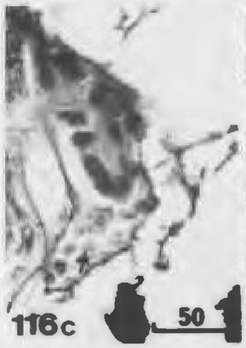
116C

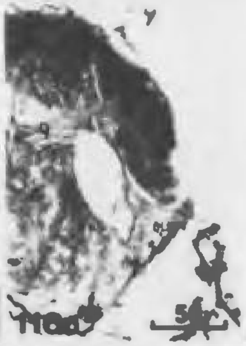
116D

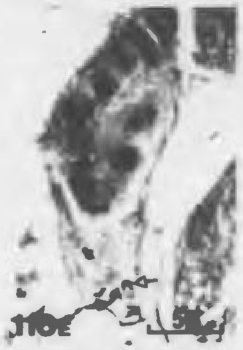
116E

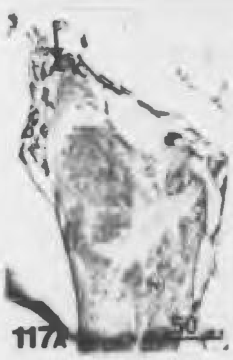
117A

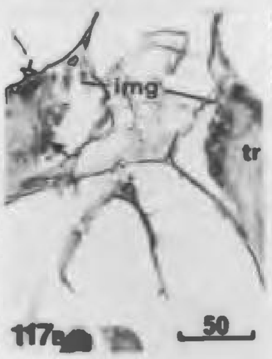
117B

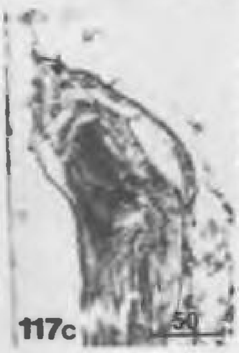
117C

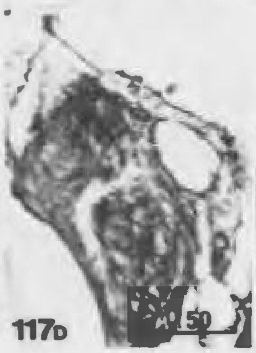
117D

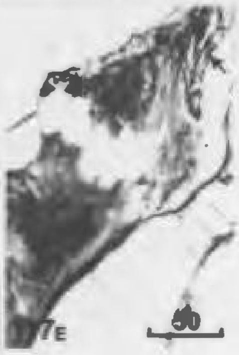
117E

Figure 118: Variation in neurosecretory activity in the neurons of the inferior posterior glomeruli (ipg) of the tritocerebral connectives. Solid arrows indicate appearance of stainable NSM (paraffin, PF, 190X, Kodak Wratten filter #22).

(A) May female in resting stage.
(B) Early August female at initiation of vitellogenesis.
(C) October female with A cleavage stage embryos.
(D) November female with A-B stage embryos.
(E) December female with B-C stage embryos.

Figure 119: Variation in neurosecretory activity in the main glomeruli of the suboesophageal mass in female *G. setosus*. Solid arrows indicate appearance of NSM (paraffin, PF, 190X, Kodak Wratten filter #22).

(A) May female in resting stage.
(B) Early August female just after initiation of vitellogenesis (hollow arrow indicates A' neurosecretory cell type).
(C) Late August precopula female.
(D) October female with A cleavage stage embryos.
(E) November female with A-B stage embryos.
(F) December female with B-C stage embryos.

Figure 120: Neurosecretory activity in the neurons of the dorsolateral and ventral glomeruli of the thoracic ganglia of a May female in resting stage. Solid arrows indicate the appearance of NSM (paraffin, PF, 190X, Kodak Wratten filter #22).

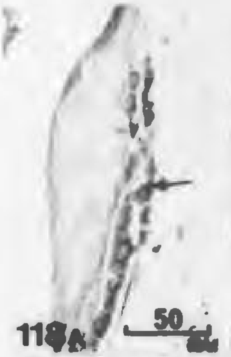

118A

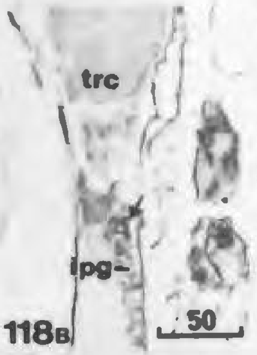

118B

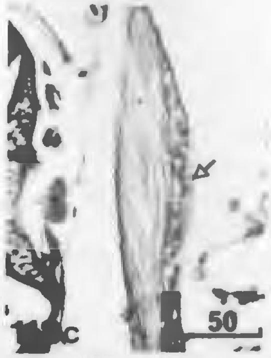

118C

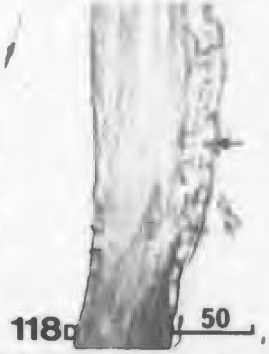

118D

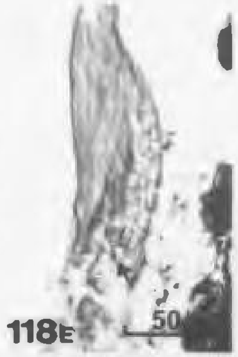

118E

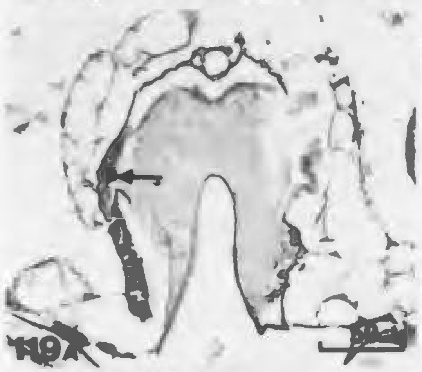

119A

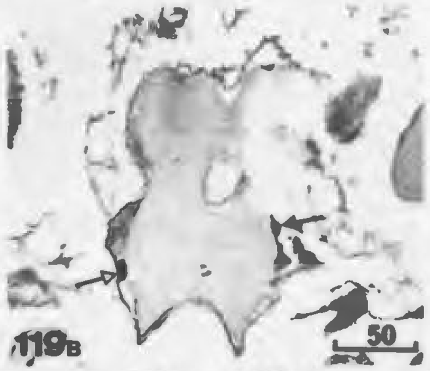

119B

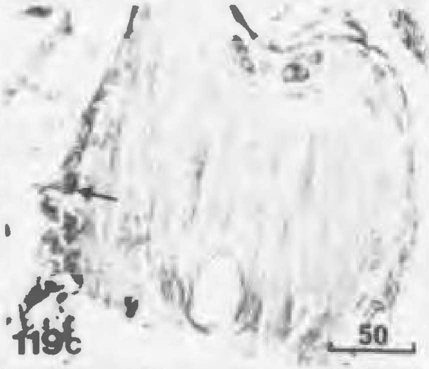

119C

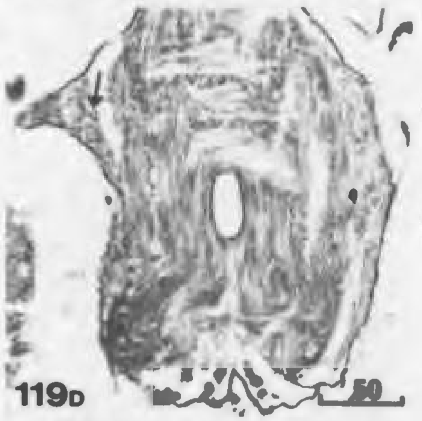

119D

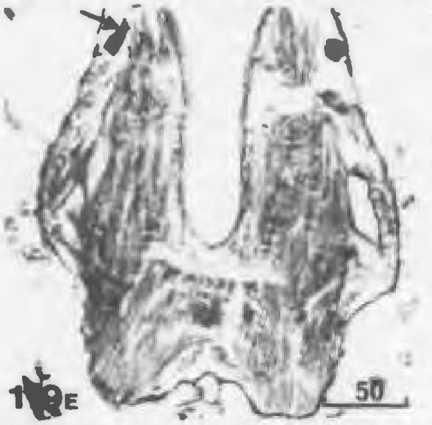

119E

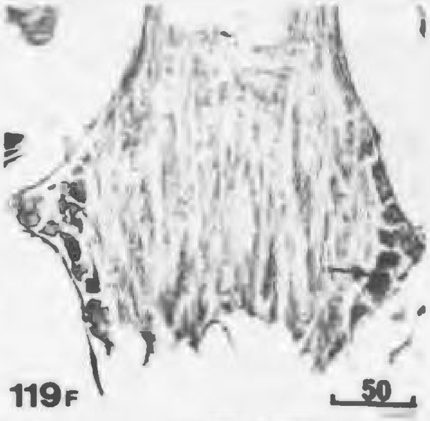

119F

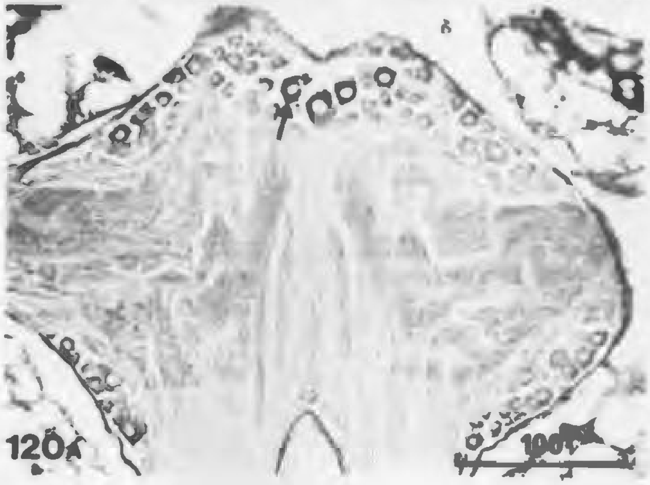

120A

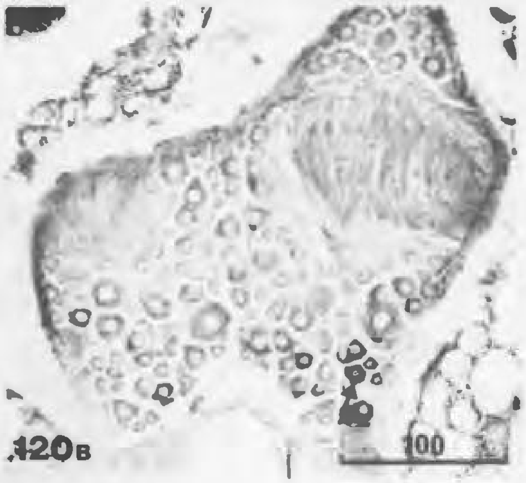

120B

Figure 121: Neurosecretory activity in the neurons of the dorsolateral and ventral glomeruli of the thoracic ganglia of an early August female just after initiation of vitellogenesis. Solid arrows indicate appearance of NSM (paraffin, PF, 190X, Kodak Wratten filter #22).

Figure 122: Neurosecretory activity in the neurons of the dorsolateral and ventral glomeruli of the thoracic ganglia of a late August precopula female. Solid arrows indicate appearance of NSM (paraffin, PF, 190X, Kodak Wratten filter #22).

Figure 123: Neurosecretory activity in the neurons of the dorsolateral and ventral glomeruli of the thoracic ganglia of an October female just after ovulation with A cleavage stage embryos in the brood pouch. Hollow arrows indicate meager amounts of NSM present (paraffin, PF, 190X, Kodak Wratten filter #22).

Figure 124: Neurosecretory activity in the neurons of the dorsolateral and ventral glomeruli of the thoracic ganglia of a November female with A-B stage embryos in the brood pouch. Solid arrows indicate appearance of NSM (paraffin, PF, 190X, Kodak Wratten filter #22).

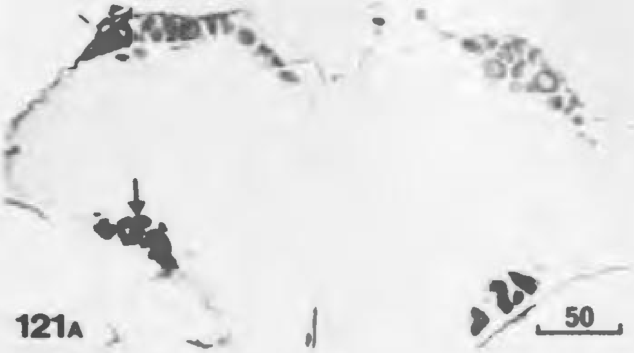
121A

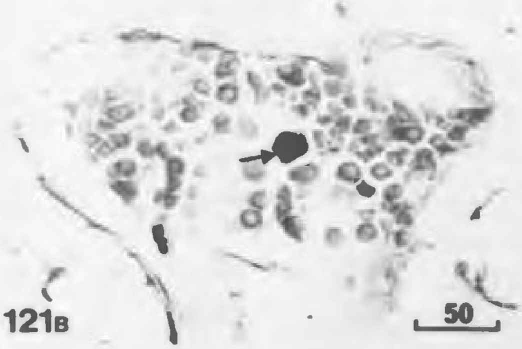
121B

122A

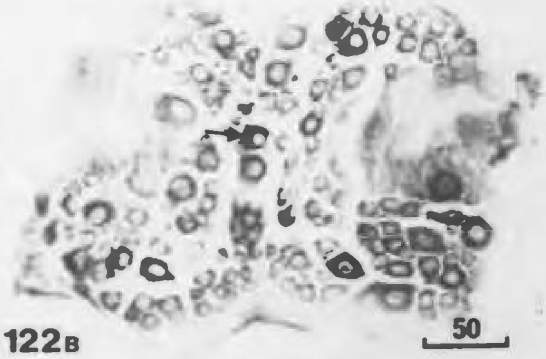
122B

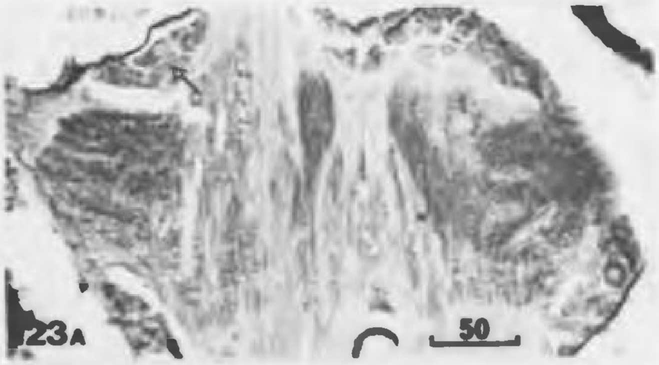
23A

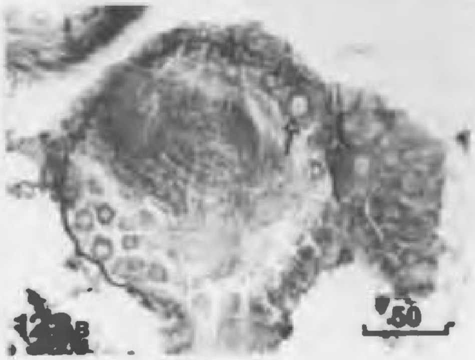
12[illegible]B

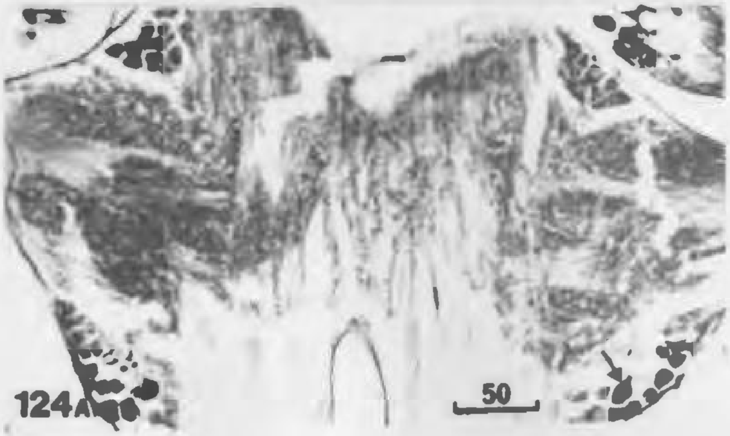
124A

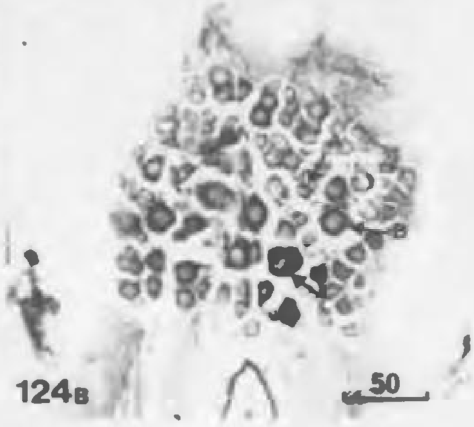
124B

Figure 125: Neurosecretory activity in the neurons of the dorsolateral and ventral glomeruli of the thoracic ganglia of a December female brooding B-C stage embryos. Solid arrows indicate the appearance of NSM (paraffin, PF, 200X, Kodak Wratten filter #22).

Figure 126: Neurosecretory activity in the neurons of the dorsolateral and ventral glomeruli of the thoracic ganglia of a January female in resting stage. Note presence of large amounts of NSM (small arrow) and presence of bipolar A' neurosecretory neurons (large arrow), (paraffin, PF, 200X, Kodak Wratten filter #22).

Figure 127: Neurosecretory activity in the ventral glomeruli of the abdominal ganglia in *G. setosus*.

(A) Note presence of NSM (solid arrows) in the various sized neurons (type C uppermost and type A below) of a May female in resting stage (paraffin, PF, 200X, Kodak Wratten filter #22).

(B) Note absence of significant amounts of stainable NSM in the abdominal ganglion of an October female with A cleavage embryos (paraffin, PF, 200X, Kodak Wratten filter #22).

(C) Note presence of chromatin in the nucleus of the NSM-poor neuron (solid arrow), (paraffin, PF, 560X, Kodak Wratten filter #22).

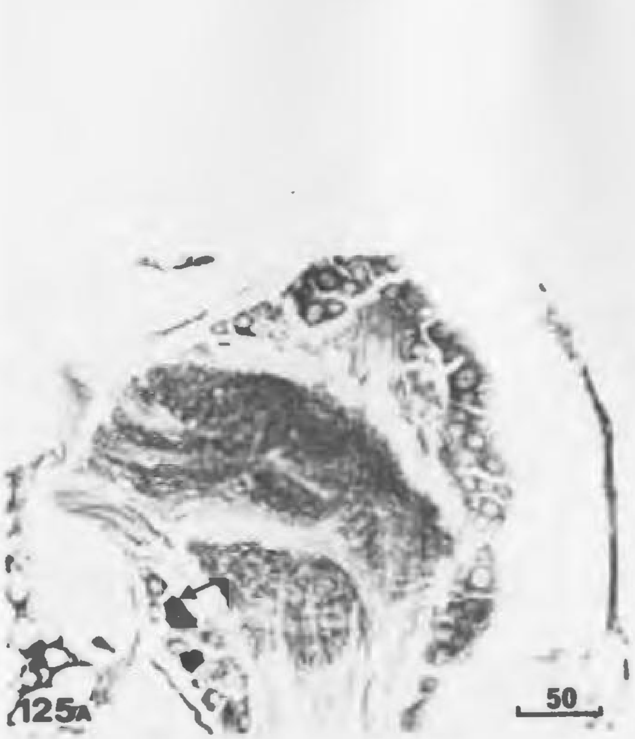

125A

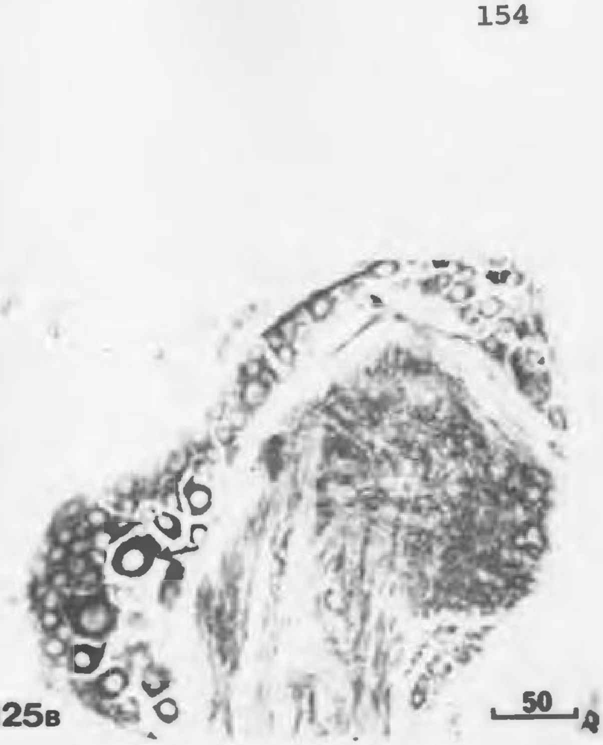

125B

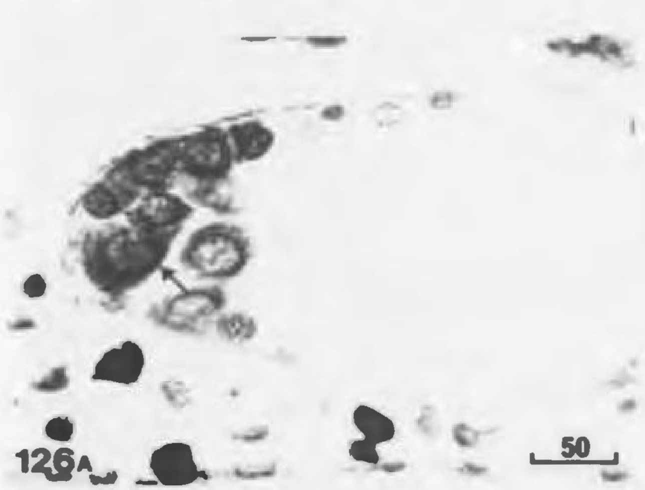

126A

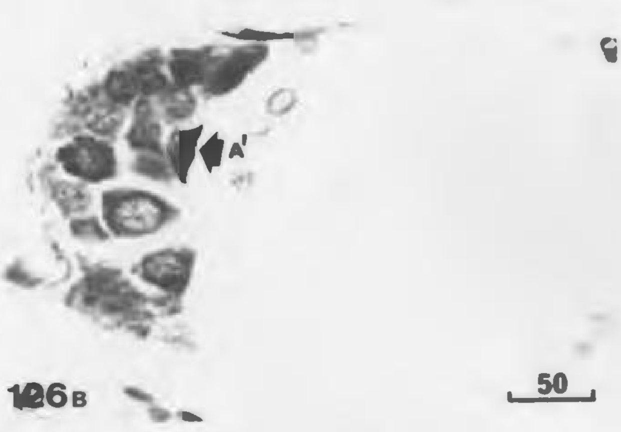

126B

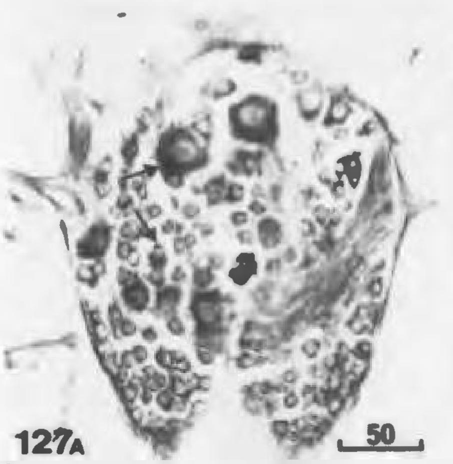

127A

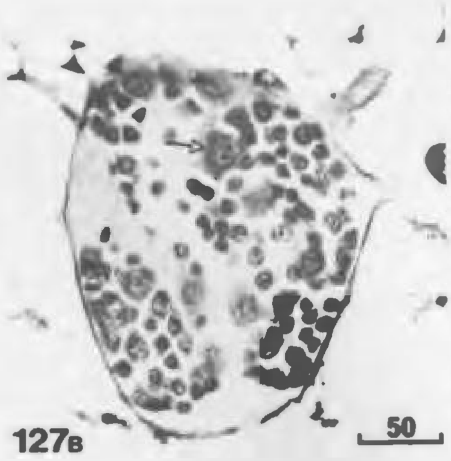

127B

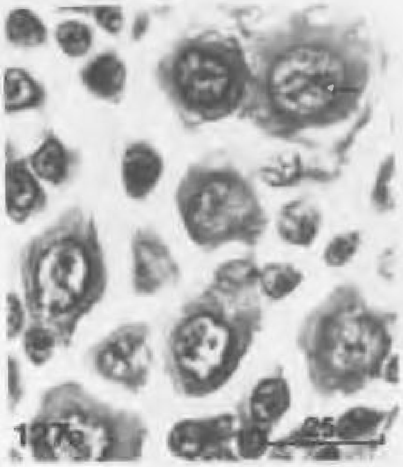

127C

Figure 128: Annual storage and release cycle of NSM in type I frontal organ neurons in female *G. setosus*. The arrow indicates appearance of NSM granules (paraffin, CHP, 560X, Kodak Wratten filter #25).

(a) MAY female in resting stage; NS*, 45%+, S_1'.
(b) JULY female in resting stage; NS, 60%, S_2.
(c) Early AUGUST female at initiation of vitellogenesis. Note absence of granules in the cells (hollow arrow); NS, 0%, S_3.
(d) Late AUGUST female; NS, 50%, S_4.
(e) SEPTEMBER female; NS, 70%, S_4.
(f) Late SEPTEMBER female in precopula; NS, 90%, S_5.
(g) OCTOBER female just after preovulatory moult. Note presence of fewer granules; LS, 50%, S_5.
(h) OCTOBER female less than 1 day after ovulation. Note extreme scarcity of granules; LS, less than 5%, S_1 oogonia, A cleavage stage embryos.
(i) OCTOBER female 4 days after ovulation; LS, 20%, S_1 oogonia, A stage embryos.
(j) OCTOBER female; LS, 40%, S_1 oogonia, A-B stage embryos.
(k) NOVEMBER female; LS, 60%, S_1 oogonia, B-C stage embryos.
(l) JANUARY female; LS, 80%, S_1 oogonia, hatched young in brood pouch.

* NS - no setae; LS - long setae on oostegites.
+ Percent of cell cytoplasm filled with granules.
' Stage of development of oogonia and oocytes.

Figure 129: Oocyte in early August female at initiation of vitellogenesis. Note vacuolation of ooplasm (v) and peripheral distribution of yolk granules (yg). At this point the type I frontal organ neurons appear devoid of granules (see figure 128c), (paraffin, CHP, 265X).

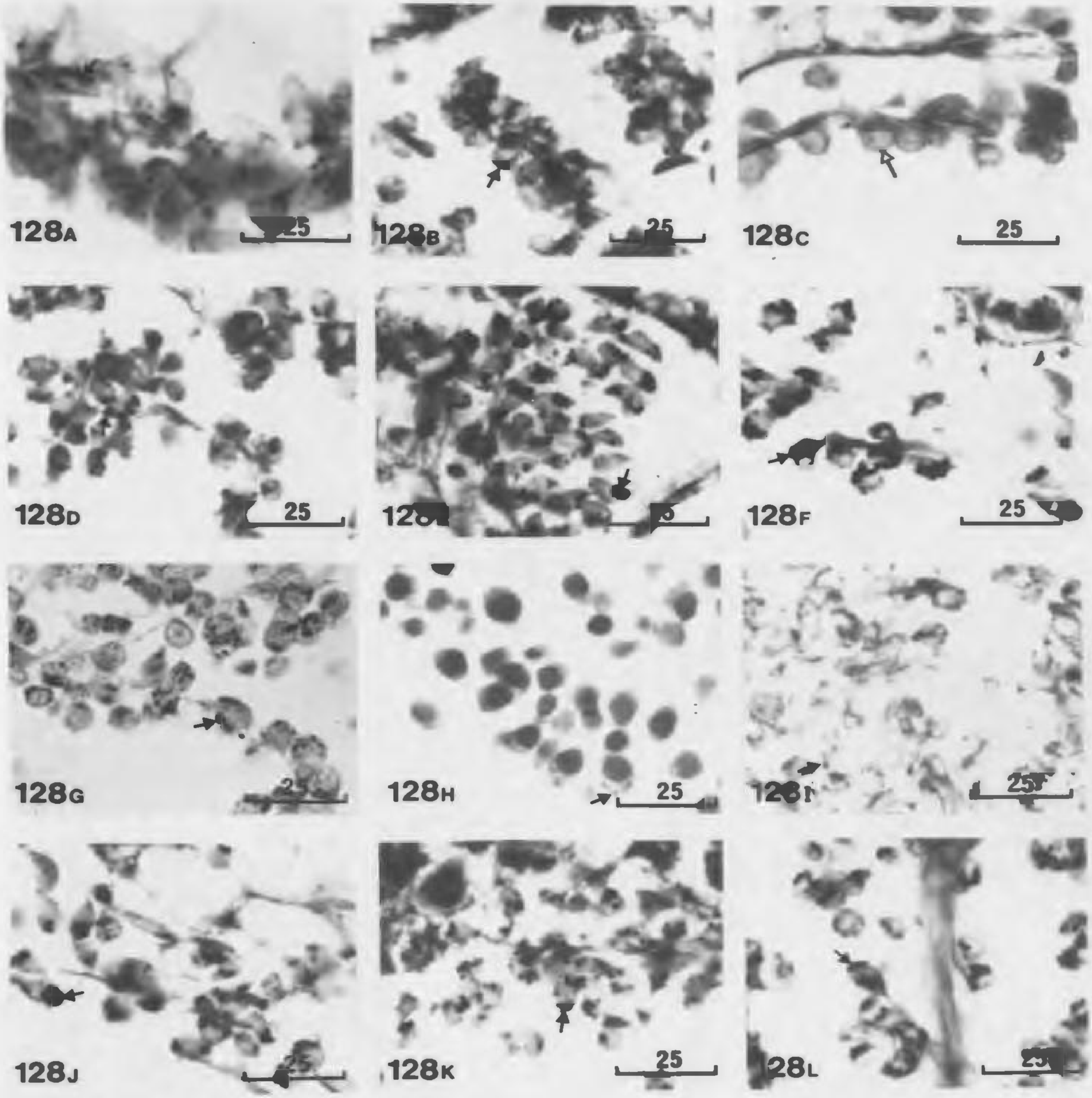
128A
25
128B
25
128C
25
128D
25
128E
128F
25
128G
25
128H
25
128I
25
128J
25
128K
25
128L
25

50
129

Figure 130: The cyclic release of NSM from frontal organ type I neurons correlated with oogonial development in *G. setosus*. The dashed line represents buildup and release of NSM.

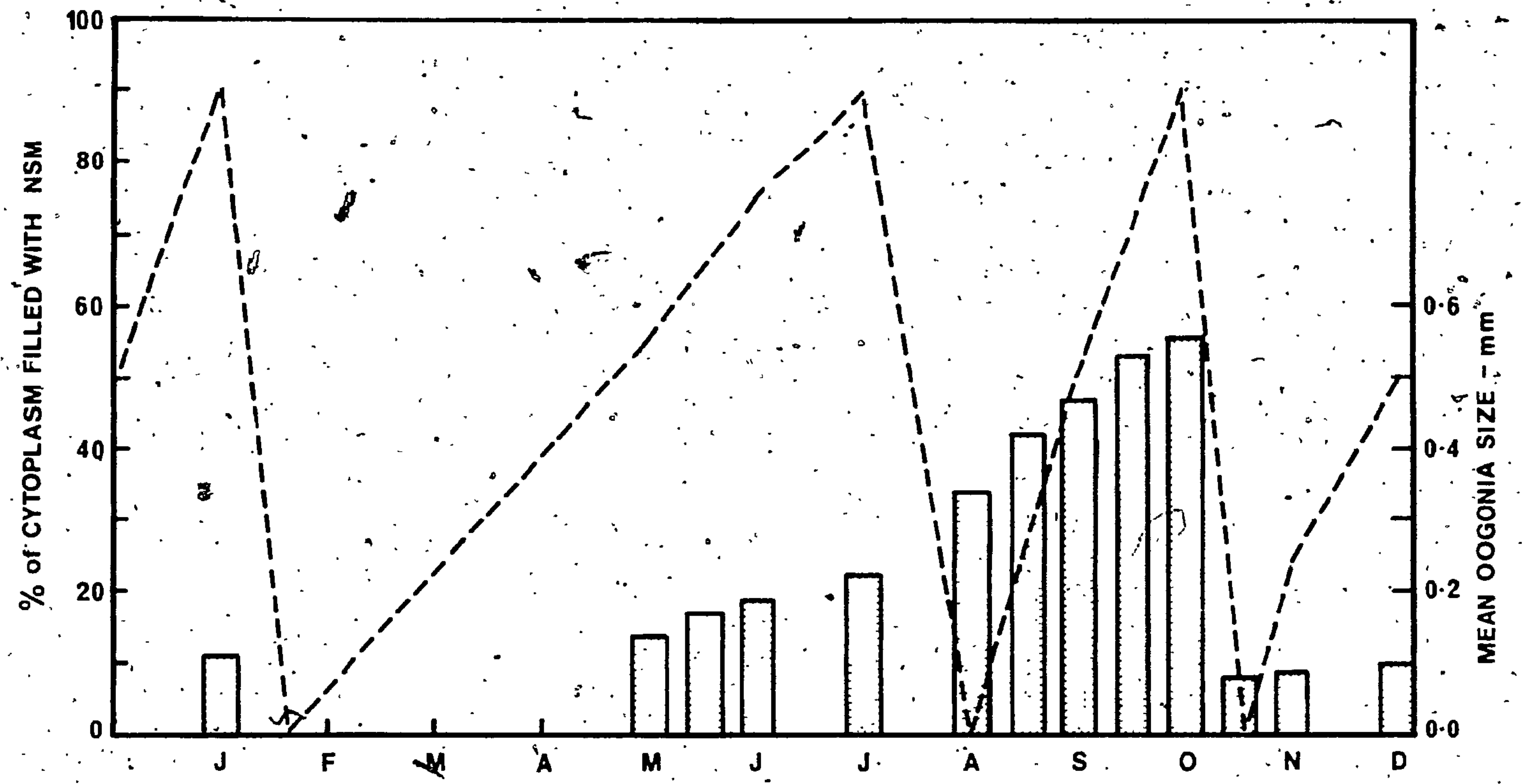
% of CYTOPLASM FILLED WITH NSM
100
80
60
40
20
0
J
F
M
A
M
J
J
A
S
O
N
D
0·6
0·4
0·2
0·0
MEAN OOGONIA SIZE – mm

TABLES

Table 1: Size class and stages of oogonia and oocytes of *G. setosus*.

Stage	Mean size range - mm.	Description*
S_1 (oogonia)		
small	0.02-0.10	Large nucleus surrounded by a dense, uniform ooplasm and thin epithelium.
medium	0.11-0.14	
large	0.15-0.19	
S_2 (oocytes)+	0.20-0.29	Yolk deposition around periphery and small vacuoles appear in the ooplasm.
S_3 (oocytes)	0.30-0.39	Vacuolation of ooplasm is severe and yolk granules appear in the vacuoles and along the ooplasmic webbing. Yolk deposition becomes progressively denser.
S_4 (oocytes)	0.40-0.49	Oocyte is filled with large yolk granules and the nucleus is still in a central position.
S_5 (oocytes)	0.50-	Nucleus moves to the periphery of the oocyte to facilitate fertilization.

* From 8 micron paraffin sections stained with CHP or PF.

+ Size ranges for stages 2 and up have been adopted from Steele and Steele, 1969.

Table 2: Mean oogonia/oocyte size in *G. setosus* collected at Witless Bay, Newfoundland determined by averaging the size of the oogonia or oocytes for each female in the sample from paraffin sections.

Year	Date	Number in sample	Mean oogonia size - mm.	Stage	Standard error of the mean
1971	October 4	12	.500	S_5	.0071
	October 19	12	.535	S_5	.0054
	November 3	12	.550	S_5	.0035
	November 20	12	.087	S_1	.0013
	December 2	12	.095	S_1	.0017
1972	January 6	6	.102	S_1	.0011
	June 1	17	.181	S_1	.0015
	July 12	14	.220	S_2	.0018
	August 12	14	.344	S_3	.0028
	August 26	15	.426	S_4	.0043
	September 8	16	.465	S_4	.0016
	September 25	17	.532	S_5	.0038
	October 7	13	.552	S_5	.0016
	October 21	13	.085	S_1	.0009
	November 20	20	.092	S_1	.0012
	December 9	16	.098	S_1	.0015
1973	May 4	12	.133	S_1	.0019
	May 29	13	.162	S_1	.0017

Table 3: Total hours between sunrise and sunset at Witless Bay, Newfoundland.*'

Latitude	47°N	
Month	Hours/month	Hours/day
January	278.5	8.95
February	299.0	10.65
March	371.0	11.90
April	409.5	13.55
May	468.0	15.10
June	475.0	15.80
July	479.0	15.45
August	438.5	14.10
September	375.5	12.50
October	336.5	10.85
November	281.0	9.25
December	266.0	8.60
Yearly average	372.9	12.25

* Computed from a table of total hours (leap year) between sunrise and sunset at various latitudes in the northern hemisphere (Dominion Observatory, Ottawa).

' Latitude of Witless Bay, Newfoundland is approximately 47° 17'N.

Table 4: Mean monthly air and seawater temperature expressed in degrees Centigrade.*

	1971		1972	
Month	Air	Seawater	Air	Seawater
January	-5.13	0.18	-6.00	0.86
February	-4.25	-0.49	-7.86	-1.09
March	0.25	0.09	-3.41	0.20
April	3.36	0.63	0.22	-2.12
May	8.19	2.57	4.88	1.00
June	10.88	6.22	14.88	4.87
July	15.27	9.00	14.22	10.73
August	17.27	16.16	14.77	11.89
September	11.63	11.23	10.66	11.19
October	6.38	7.54	6.72	8.31
November	4.16	4.83	1.50	5.68
December	-3.60	2.38	-6.55	2.96
Average	5.36	5.02	3.66	4.16
Sub-average'	2.31	4.92	0.55	5.65

* Mean monthly air temperatures were taken for St. John's from the Monthly Record (Anonymous, 1971, 1972) while seawater values were those recorded at the Marine Sciences Research Laboratory, Logy Bay, Newfoundland.

' The average for the last three months of the year.

Table 5: Mean stage of oogonial development in *G. setosus* females placed in a designated photoperiod during the resting stage and sampled at stated intervals. The animals were collected from Witless Bay in November and kept at the MSRL. The oogonia averaged 0.120 mm at the beginning of the experiment.

	31 days			79 days		
Photoperiod	Number in sample'	Average oogonia size per female in mm.*	Mean oogonia size in mm.	Number in sample	Average oogonia size per female in mm.	Mean oogonia size in mm.
Darkness	10	$10S_1$ - 0.11 0.13 0.13 0.14 0.16 0.17 0.18 0.18 0.18 0.19	0.16	3	$2S_2$ - 0.26 0.29 $1S_3$ - 0.32	0.29
8 hours light	6	$6S_1$ - 0.11 0.13 0.14 0.16 0.17 0.17	0.15	2	$2S_2$ - 0.21 0.25	0.23
12 hours light	5	$5S_1$ - 0.11 0.11 0.12 0.17 0.18	0.14	2	$2S_1$ - 0.18 0.19	0.19
14 hours light	5	$5S_1$ - 0.09 0.10 0.11 0.15 0.16	0.13	3	$3S_1$ - 0.14 0.16 0.18	0.16

* Arranged in size and position in cycle.

' Initial sample size was 25 females per photoperiod.

Table 6: Mean stage of oogonial development in *G. setosus* females placed into either constant darkness or 14 hours light during the final stages of their ovarian maturation (S_{4-5}) and sampled at various intervals.

	Complete darkness			14 hours light		
Duration in days	Number in sample'	Average oogonia size per female in mm.*	Mean oogonia size in mm.	Number in sample	Average oogonia size per female in mm.	Mean oogonia size in mm.
121	4	$1S_4$ - 0.46 $3S_5$ - 0.51 0.52	0.50	6	$6S_1$ - 0.11 0.12 0.13 0.13 0.14 0.15	0.13
150	4	$4S_1$ - 0.12 0.13 0.14 0.15	0.14	4	$1S_1$ - 0.19 $3S_2$ - 0.25 0.28 0.29	0.25
165	4	$2S_1$ - 0.17 0.18 $2S_2$ - 0.20 0.21	0.19	4	$3S_3$ - 0.34 0.36 0.37 $1S_4$ - 0.44	0.38

* Arranged in size and position in cycle.

' Initial sample size was 50 females per photoperiod.

Table 7: Mean stage of oogonial development in *G. setosus* females placed into a designated photoperiod during the mid-stages of their ovarian maturation (S_{3-4}) and then sampled after 165 days exposure.

Photoperiod	Number in sample'	Average size of oogonia per female in mm.*	Mean oogonia size in mm.
Darkness	1	$1S_1$ - 0.16	0.16
8 hours light	8	$2S_4$ - 0.45	0.59$^+$
		0.47	
		$5S_1$ - 0.07	
		0.09	
		0.10	
		0.14	
		0.16	
		$1S_2$ - 0.22	
12 hours light	6	$1S_1$ - 0.19	0.35
		$1S_2$ - 0.20	
		$2S_3$ - 0.33	
		0.36	
		$2S_4$ - 0.41	
		0.42	
14 hours light	8	$6S_1$ - 0.18	0.20
		0.18	
		0.18	
		0.19	
		0.19	
		$2S_2$ - 0.23	
		0.29	

* Arranged in size and position in cycle.

' Initial sample size was 50 females per photoperiod.

$^+$ Sample range used in this instance.

Table 8 : Mean stage of oogonial development in *G. setosus* females kept in complete darkness for 117 days and then transferred to one of the remaining photoperiods for 14 days. They entered the experiment in late ovarian maturation stages (S_{4-5}) and after 117 days the mean oogonial size was 0.52 mm.

Photoperiod	Number in sample'	Average size of oogonia per female in mm.*	Mean oogonia size in mm.+
8 hours light	6	$1S_5$ - 0.53	0.07
		$2S_1$ - 0.18	
		0.19	
		$3S_2$ - 0.21	
		0.22	
		0.24	
12 hours light	8	$2S_4$ - 0.44	0.05
		0.48	
		$3S_5$ - 0.52	
		0.56	
		0.53	
		$1S_1$ - 0.13	
		$2S_2$ - 0.22	
		0.23	
14 hours light	6	$2S_4$ - 0.46	0.01
		0.48	
		$1S_5$ - 0.53	
		$3S_1$ - 0.12	
		0.14	
		0.15	

* Arranged in size and position in cycle.

' Initial sample size of 50 females.

+ Sample range used in calculating mean.

Table 9: Mean stage of oogonial development in *G. setosus* females kept in 14 hours light for 117 days and then transferred to one of the remaining photoperiods for 14 days. They entered the experiment in late maturation stages (S_{4-5}) and after 117 days the mean oogonial size was 0.35 mm.

Photoperiod	Number in sample'	Average size of oogonia per female in mm.*	Mean oogonia size in mm.+
Complete darkness	7	1S_5 - 0.55	0.10
		4S_1 - 0.13	
		0.15	
		0.15	
		0.16	
		3S_2 - 0.20	
		0.24	
8 hours light	8	3S_5 - 0.52	0.04
		0.52	
		0.53	
		5S_1 - 0.13	
		0.14	
		0.14	
		0.16	
		0.18	
12 hours light	5	2S_5 - 0.53	0.02
		0.55	
		3S_1 - 0.09	
		0.10	
		0.11	

* Arranged in size and position in cycle.

' Initial sample size of 50 females.

+ Sample range used in calculating mean.

LITERATURE CITED:

Adiyodi, R.G., and K.G. Adiyodi. 1970. Lipid metabolism in relation to reproduction and moulting in the crab *Paratelphusa hydrodromous* (Herbst). Phospholipids and reproduction. Indian J. Exp. Biol. 8: 222-223.

________. 1971. Lipid metabolism in relation to reproduction and moulting in the crab *Paratelphusa hydrodromous* (Herbst). Cholesterol and unsaturated fatty acids. Indian J. Exp. Biol. 9: 514-515.

________. 1972. Hepatopancreas of *Paratelphusa hydrodromous*, histophysiology and the patterns of proteins in relation to reproduction and moult. Biol. Bull. (Woods Hole). 142(3): 359-369.

Aiken, D.E. 1969. Ovarian maturation and egg laying in the crayfish *Orconectes virilis*, influence of temperature and photoperiod. Can. J. Zool. 47(5): 931-935.

Amar, R. 1948. Un organe endocrine chez *Idotea*. C.R. Acad. Sci. Paris. 227: 301-303.

________. 1950. Les formations endocrines cerebrales des Isopodes marins. C.R. Acad. Sci. Paris. 230: 407-409.

________. 1953. Sur l'existence de cellules neurosecretices dans le cerveau de *Rochinela*. Bull. Soc. Zool. Fr. 78: 171-173.

Anderson, L.M. 1971. Protein synthesis and uptake by isolated *Cecropia* oocytes. J. Cell. Sci. 8: 735-750.

Andersson, B., and P.A. Jewell. 1957. The effect of long periods of continuous hydration of the neurosecretory material in the hypothalamus of the dog. J. Endocrinol. 15: 332-338.

Arvy, L., G. Echalier, and M. Gabe. 1954. Modification de la gonade de *Carcinides (Carcinus) maenus* (Crustacea, decapode) apres ablation bilaterale de l'organe Y. C.R. Acad. Sci. Paris. 239: 1853-1855.

Baid, I.C., and S.A. Dabbagh. 1972. On the neurosecretory system of *Rivulogammarus syriacus* Chevreux. Biol. Bull. 142: 370-384.

________, R.A. Hafidh, and S. Dabbagh. 1967. Studies on the neurosecretory cells in the cerebral ganglion of *Potamon magnum magnum* (Pretzman). Experientia. 23: 564-565.

________, ________, and D. Suhayla. 1968. Studies on the neurosecretory cells of the thoracic ganglion of *Potamon magnum* (Pretzman). Zool. Anz. 180(1/2): 22-23.

________, and L.S. Ramaswami. 1965. Neurosecretory cell in *Artemia salina*. Experientia (Basel). 21(9): 528-529.

Bargmann, W. 1949. Uber die neurosekretorische von Hypothalamus und Neurohypophyse. Z. Zellforsch. Mikr. Anat. 34: 610-634.

Barnes, H. 1963. Light, temperature and the breeding of *Balanus balanoides*. J. Mar. Biol. Ass. U.K. 43: 717-727.

Barnes, R.D. 1963. Invertebrate zoology. W.B. Saunders Co., Philadelphia and NewYork. 632p.

Barrington, E.J.W. 1963. An introduction to general and comparative endocrinology. Claredon Press, Oxford. 387p.

Beattie, T.M. 1971. Histology, histochemistry and ultrastructure of neurosecretory cells in the optic lobe of the cockroach, *Periplaneta americana*. J. Insect Physiol. 17: 1843-1850.

Bell, W.J., and R.H. Barth. 1971. Initiation of yolk deposition by juvenile hormone. Nature, New Biol. 230: 220-221.

Bellonci, G. 1881. Sistema nervoso e organi dei sensi della *Sphaeroma serratum*. Mem. Accad. Lincei. 19(3): 91-104.

________. 1882. Nuove richerche sulla struttura del ganglio ottico della *Squilla mantis*. Mem. Accad. Sci. Bologna. 4(3): 419-424.

Bern, H.A. 1963. The secretory neuron as a doubly specialized cell, p. 349-366. *In* General physiology of cell specialization (D. Mazia and A. Tyler, eds.).

________, R.S. Nishioka, and I.R. Hagadorn. 1961. Association of elementary granules with the Golgi complex. J. Ultrastr. Res. 5: 311-320.

Besse, G. 1968. Contribution to the study of neurohumoral control of the ovarian maturation and moulting at partuition in the oniscoid *Porcellio dilatatus* Brandt. C.R. Acad. Sci. Paris. 266(9): 917-919.

Bhargava, S. 1972. Changes in the neurosecretory system of the female *Lethocerus*. Dtsch. Entomol. Z. 19(1-3): 141-149.

Bhatia, D.R., and V. Nath. 1931. Studies in the origin of yolk VI. The crustacean oogenesis. Quart. J. Micr. Sci. 74: 669.

Bliss, D.E. 1951. Metabolic effects of the sinus gland or eyestalk removal in the land crab *Gecarcinus lateralis*. Anat. Rec. 111: 502.

________. 1966. Neurosecretion of invertebrates other than insects Part 4. Physiological processes and neurosecretion as related to ecdysis and reproduction. Introduction: Relation between reproduction and growth in decapod crustaceans. Am. Zool. 6: 231-233.

________., J.R. Durand, and J.H. Welsh. 1954. Some decapod crustacean neurosecretory systems. Pubbl. Staz. Zool. Napoli. 24: Suppl. 68-69.

________., and J.H. Welsh. 1952. The neurosecretory system of brachyuran Crustacea. Biol. Bull. (Woods Hole). 103: 157-169.

Bloch, B., E. Thomsen, and M. Thomsen, 1966. The neurosecretory system of adult *Calliphora erythrocephala* III. Electron microscopy of the medial neurosecretory cells of the brain and some adjacent cells. Z. Zellforsch. Mikr. Anat. 20: 185-208.

Bodian, D. 1951. Nerve endings, neurosecretory substance and lobular organization of the neurohypophysis. John Hopkins Hospital Bull. 89: 354-376.

Borg, T.K., R.A. Bell, and D.J. Picard. 1973. Ultrastructure of neurosecretory cells in the frontal ganglion of the tobacco hornworm *Manduca sexta*. Tissue and Cell. 5(2): 259-267.

________., and E.P. Marks. 1973. Ultrastructure of the median neurosecretory cells of *Manduca sexta* in vivo and in vitro. J. Insect Physiol. 19(10): 1913-1920.

Bretschneider, K. 1914. Uber die Gehirne der Kuchenschabe und des Mehekafers. Jena. Z. Naturu. 52: 269-362.

Brown, F.A.Jr. 1944. Hormones in the Crustacea. Their sources and activities. Quart. Rev. Biol. 19: 118-143.

________., and G.M. Jones. 1947. Hormonal inhibition of ovarian growth in the crayfish *Cambarus*. Anat. Rec. 99: 657-668.

_________., _________. 1949. Ovarian inhibition by a sinus gland principle in the fiddler crab. Biol. Bull. (Woods Hole). 91: 228-232.

Bullock, T.H., and C.A. Horridge. 1965. Structure and function in the nervous system of invertebrates. W.H. Freeman, NewYork, 1719p.

Burgen, A.S.V. 1959. Introduction to symposium on neurosecretion. Can. J. Biochem Physiol. 37: 307-308.

Cameron, M.L., and J.E. Steele. 1959. Simplified aldehyde fuchsin staining of neurosecretory cells. Stain Technol. 34(5): 265-266.

Carlisle, D.B. 1953. Studies on *Lysmata seticaudata* Risso (Crustacea, decapoda) V. The ovarian inhibiting hormone and the hormonal inhibition of sex reversal. Pubbl. Staz. Zool. Napoli. 24: 355-372.

_________. 1959. On the sexual biology of *Pandalus borealis* (Crustacea, decapoda). I. Histology of the incretory elements. J. Mar. Biol. Ass. U.K. 38: 381-394.

_________, and E.G.H. Knowles. 1959. Endocrine control in crustaceans. Cambridge University Press, Cambridge. 120p.

_________., and W.J. Pitman. 1961. Diapause, neurosecretion and hormones in Copepoda. Nature 190: 827-828.

Charniaux-Cotton, H. 1955. Le determinisme hormonal des caracteres sexuels d'*Orchestia gammarella* (Crustace, Amphipode). C.R. Acad. Sci. Paris. 240: 1487-1489.

_________. 1956. Determinisme hormonal de la differenciation sexuelle chez les Crustacés. Ann. Biol. 32: 371-398.

_________. 1957. Croissance, regeneration et determinisme endocrinien des caractères sexuels d' *Orchestia gammarella* (Pallas) Crustace, Amphipode. Ann. Sci. Nat. Zool. et Biol. Animale. 19: 411-559.

_________. 1960. Sex determination, p. 411-447. *In* The physiology of Crustacea I. Metabolism and growth. (T.H. Waterman, ed.) Academic Press, NewYork.

Crisp, D.J., and B. Patel. 1969. Environmental control of the breeding of three boreo-arctic cirripedes. Mar. Biol. 2: 283-295.

Dahl, E. 1956. On the differentiation of the topography of the crustacean head. Acta Zool. 37: 123-197.

________. 1963. Main evolutionary lines among recent Crustacea, p. 1-26. *In* Phylogeny and evolution of Crustacea (H.B. Whittington, ed.). Museum of Comparative Zoology. Special Publication.

________. 1965. Frontal organs and protocerebral neurosecretory systems in Crustacea and Insecta. Gen. Comp. Endocrinol. 5: 614-617.

Dahlgren, U. 1914. On the electric motor nerve in the skates (*Rajidae*). Science. 40: 862-863.

Dall, W. 1965. Studies on the physiology of a shrimp, *Metapenaeus* sp. (Crustacea, decapoda). II. Endocrine control of moulting. Crust. J. Mar. Freshwat. Res. 16: 1-12.

David, G.F.X., J. Herbert, and G.D.S. Wright. 1973. The ultrastructure of the pineal ganglion in the ferrat. J. Anat. 115(1): 79-97.

DeLoof, A., and A. Lagasse. 1970. Ultrastructure of the follicle cells of the ovary of the Colorado beetle in relation to yolk deposition. J. Insect Physiol. 16: 211-220.

Démeusy, N. 1962. Rôle de la gland de mue dans l'évolution ovarienne du crabe *Carcinus maenus* Linne. Cahiers Biol. Marine. 3: 37-56.

________., and A. Veillet. 1952. Déclenchement de la ponte chez le crabe *Carcinus maenus* Pennant par l'ablation des pédoncles oculaires. C.R. Acad. Sci. 234: 1224-1226.

DeRobertis, E.D.P., W.W. Nowinski and F.A. Saez. 1970. Cell biology (fifth ed.). W.B. Saunders Co., Philadelphia, London, Toronto. p. 199-228.

Dogra, G.S., and B.K. Tandan. 1964. Adaptation of certain histological techniques for *in situ* demonstration of the neuroendocrine system of insects and other animals. Quart. J. Micro. Sci. 105(4): 455-466.

Drach, P. 1955. Système endocrinien pédonculaire, durée d'intermue et vitellogenèse chez *Leander serratus* (Pennant), Crustacé, Décapode. C.R. Soc. Biol. 149: 2079-2083.

Dudley, P.L. 1969. The fine structure and development of the nauplius eye of the copepod *Doropygus seclusus* Illg. Cellule. 68: 7-42.

Durand, J.B. 1956. Neurosecretory cell types and their secretory cativity in the crayfish. Biol. Bull (Woods Hole). 111: 62-76.

Edstrom, J.E., and D. Eicher. 1958. Quantitative Ribonuklein-säure-Untersuchungen an den Ganglienzellen des Nucleus supra opticus der Albino-Ratten unter experimentallen Bedingungen (Kochsalz-Belastung). Z. Zellforsch. Mikr. Anat. 48: 187-200.

Elofsson, R. 1963. The nauplius eye and frontal organs in Decapoda (Crustacea). Sarsia. 12: 1-68.

________. 1965. The nauplius eye and frontal organs in malacostraca (Crustacea). Sarsia. 19: 1-54.

________. 1966. The nauplius eye and frontal organs of the non-malacostraca (Crustacea). Sarsia. 25: 1-128.

Enami, M. 1951. The sources and activities of two chromatophotropic hormones in crabs of the genus *Sesarma*. II. Histology of incretory elements. Biol. Bull. (Woods Hole). 101: 241-258.

Erlandsen, S.L., A. Thomas, and G. Wendelschafer. 1973. A simple technique for correlating SEM with TEM on biological tissue originally embedded in epoxy resin for TEM. Scanning Electron Microscopy - 1973 (pt. III). Proc. of the workshop on SEM in pathology. p. 349-356.

Fahrenbach, W.H. 1964. The fine structure of the nauplius eye. Z. Zellforsch. Mikr. Anat. 62: 182-197.

________. 1965. The micromorphology of some simple photoreceptors. Z. Zellforsch. Mikr. Anat. 66: 233-254.

Fernandez, J., and M.S. Fernandez. 1972. Nervous system of the snail *Helix aspersa*. Part 3. Electron microscope study of neurosecretory nerves and endings in the ganglionic sheath. Z. Zellforsch. Mikr. Anat. 135(4): 473-482.

Fingerman, M., and T. Aoto. 1959. The neurosecretory system of the dwarf crayfish *Cambarellus schufeldti* revealed by electron and light microscopy. Trans. Amer. Micro. Soc. 78: 305-317.

________., and C. Oguro. 1967. The neuroendocrine system in the head of the crayfish *Faxonella clypeata*. Trans. Am. Micro. Soc. 86: 178-183.

________., ________, M. Miyawaki and P. McKinnell. 1964. The neurosecretory system in the head of the blind cave crayfish *Cambarus setosus* Faxon. Amer. Midl. Nat. 71: 415-421.

Foster, W.A. 1972. Influence of medial neurosecretory cells on reproduction in female *G. austeni*. Trans. R. Soc. Trop. Med. Hyg. 66(2): 322.

Gabe, M. 1952. Sur l'existence d'un cycle secretoire dans l'organe pseudofrontal (glande du sinus) chez *Oniscus asellus*. C. R. Acad. Sci. Paris. 235: 900-903.

________. 1953a. Sur l'existence chez quelques Crustaces malacostraces d'un organe camparable a la glande de la mue des insectes. C.R. Acad. Sci. Paris. 237: 1111-1113.

________. 1953b. Quelques applications de la coloration par la fuchsine-paraldehyde. Bull. Micro. Appl. 3: 153-162.

________. 1954. La neurosecretion chez les invertebres. Ann. Biol. 30: 5-62.

________. 1966. Neurosecretion. Pergammon Press, Oxford and NewYork. 872p.

Geldiay, S. 1966. Influence of photoperiod on imaginal diapause in *Anacridium aegyptium* L. Scientific reports of the Faculty of Science. Ege University. Izmur. Turkey 40.

Geldiay, S. 1967. Hormonal control of adult reproductive diapause in the Egyptian grasshopper *Anacridium aegyptium* L. J. Endocrinol. 37: 63-71.

Gerschenfeld, H.M., J.H. Tramezzani, and E. deRobertis. 1960. Ultrastructure and function in neurohypophysis of the toad. Endocrinol. 66: 741-762.

Girardie, J. 1973. Histological, histochemical and ultrastructural aspects of the lateral neurosecretory cells of the protocerebrum in *Locusta migratoria migratoria*, Insecta, Orthoptera. Z. Zellforsch. Mikr. Anat. 141(1): 75-91.

Gomez, R. 1965. Acceleration of development of gonads by implantation of the brain in the crab *Paratelphusa hydrodromous*. Naturwissenschaften 52(9): 216.

Gomori, G. 1941. Observations with differential stains on human islets of Langerhans. Amer. J. Path. Boston. 17: 395-406.

________. 1950. Aldehyde-fuchsin: a new stain for elastic tissue. Amer. J. Clin. Path. 20: 665-668.

Goslar, H.G., and B. Schultze. 1958. Autoradiographische Untersuchungen über den Einbau von S^{35}-Thioaminosauren im Zwuschenhirn von Kaninchen und Ratte. Z. Zellforsch. Mikr. Anat. 64: 556-574.

Graber, H. 1933. Uber die Gehirne der Amphipoden und Isopoden. Zeitschr. F. Morphologie 26: 332-371.

Green, J.D., and D.S. Maxwell. 1959. Comparative anatomy of the hypophysis and observations on the mechansim of neurosecretion, p. 368-386. *In* Comparative endocrinology (A. Gorbman ed.) Wiley, NewYork.

Grimley, P.M. 1964. A tribasic stain for thin sections of plastic-embedded, OsO_4-fixed tissues. Stain Technol. 39: 229-233.

Gundevia, H.S., and P.S. Ramamurty. 1972. On the intra-ganglionic neurohemal organs in the ventral nerve cord of *Hydrophilus olivaceus*, Hydrophilidae, Coleoptera. Experientia (Basel). 28(9): 1049-1050.

Halcrow, K. 1969. Sites of presumed neurosecretory activity in *Daphnia magna* Straus. Can. J. Zool. 47(4): 575-577.

Halmi, N.S. 1952. Differentiation of two types of basophils in the adenohypophysis of the rat and the mouse. Stain Technol. 27: 61-64.

Hanström, B. 1924. Untersuchungen über das Gehirn, insbesondere die Sehganglien der Crustaceen. Ark. Zool. 16: 10.

________. 1929. Das deutocerebrum der Crustaceen. Zool. Jb. Abt. Anat. 51:

________. 1931. Neue Untersuchungen über Sinnesorgane und nervensystem der Crustaceen I. Oecologia 23:

________. 1933. Neue Untersuchungen über Sinnesorgane und nervensystem der Crustaceen II. Zool. Jb. Abt. Anat. 56:

________. 1934. Neue Untersuchungen über Sinnesorgane und nerven system der Crustaceen III. Zool Jb. Anat. 58: 101-144.

________. 1935. Preliminary report on the probable connection between the blood gland and the chromatophore activator in decapod crustaceans. Proc. Nat. Acad. Sci., Wash. 21: 584-585.

________. 1937a. Die Sinusdruse und der hormomal bedingte Farbwechsel der Crustaceen. K. Svenska Vetensk., Acad. Handl. 16: 1-99.

________. 1937b. Vermischte Beobachtungen über die Chromatophoraktivierenden Substanzen der Augenstiele der Crustaceen und des Koptes der Insecten. Acta Univ. Lund. Avd. 2, 32: 1-11.

________. 1939. Hormones in invertebrates. Claredon Press, Oxford. 198p.

________. 1947. Three principle incretory organs in the animal kingdom. Einar Munksgaard, Copenhagen.

________. 1948. The brain, the sense organs, and the incretory organs of the head in the crustacean Malacostraca. Bull. Biol., Suppl. 33: 98-126.

________. 1953. Neurosecretory pathways in the head of crustaceans, insects, and vertebrates. Nature 171: 72-73.

________. 1957. Comparative aspect of neurosecretion with special reference to the hypothalamo-hypophyseal system. *In* The neurohypophysis. (H. Heller ed.). Butterworths, London.

Hentschel, E. 1963. Zum neurosekretorischen System der Anostraca, Crustacea (*Artemia salina* Leach and *Chirocephalus grubei*). Zool. Anz. 170: 187-190.

________. 1965. Neurosekretion und Neurohamalorgan liei *Chirocephalus guliei* Dykouisci und *Artemia salina* Leach (Anostraca, Crustacea). Z. Wiss. Zool. 171: 44-79.

Herman, W.S., and D.M. Preus. 1973. Ultrastructural evidence for the existence of two types of neurosecretory cells in the abdominal ganglia of the chelicerate arthropod *Limulus polyphenius*. J. Morphol. 140(1): 53-61.

Highnam, K.C. 1962. Neurosecretory control of ovarian development in the desert locust. Mem. Soc. Endocrinol. 12: 379-390.

________. 1965. Some aspects of neurosecretion in Arthropods. Zool. Jb. Physiol. 71: 558-582.

Hild, W. 1951. Experimentell-morpologische Untersuchungen uber das Verhalten der "neurosekretorischen Bahn" nach Hypophysenstieldurch-trennungen, Engriffen in den Wasserhaushalt und Belastung der Osmoregulation. Virchows Arch. 319: 526-546.

Hinsch, G.W. 1972. Some factors controlling reproduction in the spider crab *Libinia emarginata*. Biol. Bull. (Woods Hole). 143(2): 358-366.

________., and D. Bennett. 1973. Vitellogenesis in immature female spider crabs following implantation of thoracic ganglia from adults. J. Cell Biol. 59: 287.

Holms, R.L., and F.G.W. Knowles. 1960. 'Synaptic vesicles' in the neurohypophysis. Nature. London. 185: 710-711.

Hubschman, J.H. 1962. A simplified Azan process well studied for crustacean tissue. Stain Technol. 37: 379-380.

Huddart, H., and S.J. Bradbury. 1972. Fine structure of a neurosecretory axon in crustacean skeletal muscle. Experientia, (Basel). 28(8): 950-951.

Inoue, H. 1957. On the neurosecretory cells of *Pachigrapsus crassipes*. Mem. Gakugei Fac. Akita Univ. Nat. Sci. 70: 84-92.

Ittycheriah, P.I. 1967. Endocrine influence in reproduction in *Iphita limbata* Stal. J. Animal Morphol. Physiol. 141(1): 144-145.

________., and E.P. Marks. 1971. Performic acid-resorcin fuchsin technique for *in situ* demonstration of neurosecretory material in insects. Ann. Ent. S.A. 64: 762.

Johansson, A.S., and B. Schreiner. 1965. Neurosecretory cells in the ventral ganglion of the lobster, *Homarus vulgaris*. Gen. Comp. Endocrinol. 5: 558-567.

John, P.A. 1967. Observations on the role of moult hormone in Crustacea on its reproduction. J. Animal Morphol. Physiol. 14: 145-146.

Karlson, P., and D. Skinner. 1960. Attempted extraction of crustacean moulting hormone from isolated Y organs. Nature, (London). 185: 543-544.

Karnovsky, M.J. 1965. A formaldehyde-gluteraldehyde fixative of high osmolarity for use in elextron microscopy. J. Cell Biol. 27: 137 (Abstr.).

Kater, J. McA. 1928. Morphological aspects of protoplasmic synthesis in oogenesis of *Cambarus*. Z. Zellforsch. Mikr. Anat. 8: 186.

Kemp, N.E., and E. Hibbart. 1957. Protoplasmic bridges between follicle cells and developing oocytes of *Fundulus heteroclitus*. Biol. Bull. (Woods Hole). 113: 329.

Khatter, N. 1972. Neurohemal organs in the ventral nerve cord of *Schizodactylus monstrous*, Orthoptera. Bull. Soc. Zool. Fr. 97(1): 61-66.

Knowles, F.G.W. 1953. Neurosecretory pathways in the prawn *Leander serratus*. Nature, (London). 171: 131-132.

________. 1958. Electron microscopy of a crustacean neurosecretory organ. *In* II International symposium neurosekretion (W. Bargmann ed.). Springer, Berlin.

________. 1959. The control of pigmentary effectors, p. 115-168. *In* Comparative endocrinology (A. Gorbman ed.). Wiley, New York.

________. 1960. A highly organized structure within a neurosecretory vesicle. Nature (London), 185: 709-710.

________. 1963. The structure of neurosecretory systems in invertebrates, p. 47-62. *In* Comparative endocrinology vol. 2. (von Euler and Heller eds.). Academic Press, NewYork.

________., and D.B. Carlisle. 1956. Endocrine control in the Crustacea. Biol. Rev. 31: 396-473.

Koller, G. 1928. Versuche über die inkratorischen Vorange beim Garnellenfarbwechsel. Z. Vergl. Physiol. 8: 601-612.

________. 1930. Weitere Untersuchungen über Farwechsel und Farbwechselhormone bei *Crangon vulgaris*. Z. Vergl. Physiol. 12: 632-667.

Kono, Y. 1973. Ultrastructure of the brain corpus cardiacum system at the time of humoral determination of diapause in *Pieris rapae crucivora*. Part 4. Neurosecretory IV cell in the lateral part of the brain. Jap. J. Appl. Entomol. Zool. 17(2): 84-90.

________., and M. Kobayashi. 1972. Ultrastructure of the brain corpus cardiacum at time of humoral determination of the incidence of diapause in *Pieres rapae crucivora*. Part 2. Types of neurosecretory cells in the brain. Jap. J. Appl. Entomol. Zool. 16(19): 24-31.

Kratzsch, E. 1951. Experimentellmorphologische Untersuchungen am Zwischenhirn-Hypophysensystem der Ratte bei Palgerie infolge alloxanvergiftung (mit besonder Berücksechtegung der Pituizyten). Z. Zellforsch. Mikr. Anat. 36: 371-380.

Kulakovskii, E.E. 1970. Neurosecretory system of *Mysis oculata* (Fabricius), Crustacea, Malacostraca. Dokl. Akad. Nauk. SSSR. 192(1): 226-228.

Kupfermann, I. 1972. Studies on the neurosecretory control of egg laying in *Aplysia*. Am. Zool. 12(3): 513-519.

Lai-Fook, J. 1973. The fine structure of Verson's glands in moulting larvae of *Calpodes ethlius* (Hesperiidae, Lepidoptera). Can. J. Zool. 51: 1201-1210.

Lake, P.S. 1969a. Neurosecretion in *Chirocephalus diaphanus* Prevost (Anostraca). I. Anatomy and cytology of the nervous system. Crustaceana 16(3): 273-287.

________. 1969b. Changes in the histochemical nature of neurosecretory materials during axonal transport in the crab *Paragrapsus gaimardii*. Experientia (Basel) 25(12): 1314.

________. 1971. Histological and histochemical observations of the cephalic neurosecretory system of the crab, *Paragrapsus gaimardii.* Pap. Proc. R. Soc. Tasmania. 105: 87-96.

________., and J.E. Ong. 1972. Observations of the organ of Bellonci of the shrimp *Paratya tasmaniensis* Crustacea, Decapoda, atyidae with particular reference to the structure of the onion body cells. Aust. J. Zool. 20(3): 215-234.

Langenbuch, R. 1928. Über die Statocysten einiger Crustaceen. Zool. Jb. Allg. Zool. 44:

Laurence, B.R., and M.G. Simpson. 1974. Cell replication in the follicu;ar epithelium of the adult mosquito. J. Insect Physiol. 20(4): 703-715.

Lees, A.D. 1964. The location of the photoperiodic receptors in the aphid *Megoura viciae* Buckton. J. Exp. Biol. 41: 119-133.

Legrand, J.J., and G. Johnson. 1961. Contribution à l'étude du contrôle des changements de coloration chez *Ligia oceanica* L. C.R. Acad. Sci. Paris. 253: 1358-1360.

LeRoux, M.L. 1933. Recherches sur la sexualité des Gammariens. Croissance, reproduction. Déterminisme des caractères sexuels secondaires. Bull. Biol. Fr. Belg. Suppl. 16: 1-138.

Lowe, M.E. 1961. The female reproductive cycle of the crayfish *Cambarellus shufeldti*: the influence of environmental factors. Tulane Stud. Zool. 8: 157-176.

Madsen, N. 1960. The brain of the amphipod *Orchestia platensis* Krøyer. Crustaceana 1(3): 173-178.

Malhotra, S.K., and G.A. Meek. 1961. An electron microscope study of some cytoplasmic inclusions of the neurons of the prawn *Leander serratus*. J. Roy. Micro. Soc. 80(1): 1-8.

Marks. E.P., G.M. Holman, and T.K. Borg. 1973. Synthesis and storage of a neurosecretory hormone in insect brains *in vitro*. J. Insect Physiol. 19(2): 471-477.

Matsumoto, K. 1954. Neurosecretion in the thoracic ganglion of the crab *Eriocheir japonicus*. Biol. Bull. (Woods Hole). 106: 60-68.

________. 1956. Migration of the neurosecretory products in the thoracic ganglion of the crab *Chionectes opilio*. Biol. J. Okayama Univ. 2: 137-146.

________. 1958. Morphological studies on the neurosecretion in crabs. Biol. J. Okayama Univ. 4: 102-176.

________. 1959. Neurosecretory cells of an isopod *Armadillidium vulgare*. Biol. J. Okayama Univ. 5: 43-50.

________. 1962. Experimental studies of the neurosecretory activities of the thoracic ganglion of a crab *Hemigrapsus*. Gen. Comp. Endocrinol. 2: 4-11.

Maynard, D.M. 1961. Thoracic neurosecretory structures in Brachyura. I. Gross anatomy. Biol. Bull. (Woods Hole). 121: 316-329.

McLaren, D.J. Ultrastructural and cytochemical studies on the sensory organelles and nervous system of *Dipetalonema vitea* (Nematoda: Filaroidea). Parasitology 65: 507-524.

Menon, M. 1962. Neurosecretory system of *Streptocephalus* sp. (Anostraca, Branchiopoda). Proc. 3rd Intern. Symp. Neurosecretion, Bristol. 411-416.

Metalnikoff, S. 1900. *Sipunculus nudus*. Z. Wiss. Zool. 68: 261-322.

Meusy, J.J. 1963. The gametogenesis of *Orchestia gammarella* Pallas, Crustacea, Amphipoda. Bull. Soc. Zool. Fr. 88: 197-220.

Miyawaki, M. 1956. Histological observations on the incretory elements in the eyestalk of a brachyuran *Telmessus cheiragonus* (Tilesius). J. Fac. Sci. Hokkaido Univ. (VI) 12: 325-332.

________. 1960. On the neurosecretory cells of some decapod Crustacea. Kumamato J. Sci. 5: 1-20.

Mocquard, J.P., G. Besse, P. Juchault, J.J. Legrand, J. Maissiat, and G. Noulin. 1971. Contribution to the analysis of neurohemal control of growth; the moult and male and female sexual physiology in the oniscoid *Ligia oceanica* L. Ann. Embryol. Morphog. 4(1): 45-63.

Mouton, J. 1971. Influenece of neurosecretion on the reproduction of the stick insect *Caransius morosus* (Chelentoptera). Ann. Endocrinol. 32(5): 709.

Munger, B.L. 1961. Staining methods applicable to sections of osmium-fixed tissue for light microscopy. J. Biophys. Biochem. Cytol. 11: 502-507.

Murakami, M. 1961. Elekronenmikopische Untersuchungen über die neurosekretorischen Zellen im Hypothalamus von *Gecko japonicus*. Arch. Histol. Jap. 21: 323-337.

________. 1962. Elektronenmikroskopische Untersuchungen der neurosekretorischen Xellen im Hypothalamus der Mous. Z. Zellforsch. Mikr. Anat. 56: 277-299.

Nagabhushanam, R. 1962. The histology of the neurosecretory system of the clam, *Spisula solidissima*. Am. Zool. 2(4): 543.

________., and K. Rango Rao. 1966. Neurosecretory system of the portunid crab, *Scylla serrata*. J. Anat. Soc. India. 15(3): 138-144.

________., and R. Sarojini. 1969. Neurosecretion in the central nervous system of the hermit crab. Proc. India Acad. Sci. Sec. B. 69(1): 20-28.

Nansen, F. 1886. The structure and combination of the histological elements of the central nervous system. Bergens Mus. Arskr. (1886): 29-215.

Nath, V., B.L. Gupta, and B. Lal. 1958. Histochemical and morphological studies of the lipids in oogenesis. I. *Periplaneta americana*. Quart. J. Micr. Sci. 99: 315.

Nishiitsutsuji-Uwo, J. 1960. Fine structure of the neurosecretory system in Lepidoptera. Nature (London). 187: 953-954.

________. 1961. Electron microscopic studies on the neurosecretory system in Lepidoptera. Z. Zellforsch. Mikr. Anat. 54: 613-630.

Norman, T.C. 1965. The neurosecretory system of the adult *Calliphora erythocephala*. I. The fine structure of the corpus cardiacum with some observations on adjacent organs. Z. Zellforsch. Mikr. Anat. 67: 461-501.

Oguro, Ch. 1959a. Occurrence of an accessory sinus gland in the isopod *Idotea japonica*. Annot. Zool. Jap. 32: 71-73.

________. 1959b. On the sinus gland in four species belonging to Idoteidae (Crustacea, Isopoda). J. Fac. Sci. Hokkaido Univ. 14: 261-264.

________. 1960. On the neurosecretory system in the cephalic region of the isopod, *Tecticeps japonicus*. J. Endocrinol. 7: 137-145.

O'Leary, T.P., W.J. Bemrick, and K.H. Johnson. 1973. Serial section analysis of cells in the microfilariae of *Pirofilaria immitis* containing neurosecretory-like granules. J. Parasitol. 59(4): 701-705.

Ortmann, R. 1951. Über experimentelle Veranderungen de Morphologie des Hypophysenzwischenhirnsystems und die Beziehung der sag "Gomori-substanz" zum Adiuretin. Z. Zellforsch. Mikr. Anat. 36: 92-140.

________. 1958. Neurosekretion und Proteinsyntheses. Z. Mikro. Anat. Forsch. 64: 215-227.

Otsu. T. 1960. Precocious development of the ovaries in the crab *Potamon dehaani* following implantation of the thoracic ganglion. Annot. Zool. Jap. 33: 90-96.

________. 1963. Bihormonal control of sexual cycle in the fresh-water crab *Potamon dehaani*. Embryol. 8: 1-20.

________. 1965. Component amino acids of chromatophore concentrating hormones from Decapoda Crustacea. Naturwissenschaften. 52: 187-188.

________., and K.I. Hanaoka. 1951. Relation between the body weight and precocious differentiation of ova in eyestalkless crabs. Bull.. Yamogata Univ. Ser. Nat. Sci. 1: 269-274.

Palay, S.L. 1943. Neurosecretion. V. The origin of neurosecretory granules from the nuclei of nerve cells in fishes. J. Comp. Endocrinol. 79: 247-275.

________. 1960. The fine structure of secretory neurons in the preoptic nucleus. of the goldfish *Carassius auratus*. Anat. Rec. 138: 417-443.

________., and S.L. Wissig. 1953. Secretory granules and Nissl substance in fresh supraoptic neurons of the rabbit. Anat. Rec. 138: 417-459.

Panouse, J.B. 1943. Influence de l'ablation du pédoncle oculaire sur la croissance de l' ovaire chez la crevette *Leander serratus*. C.R. Acad. Sci. Paris. 217: 553-555.

________. 1944. L'action de la galnde du sinus sur l'ovaire chez la crevette *Leander*. C.R. Acad. Sci. Paris. 218: 293-294.

Pardoe, A.U., and M. Weatherall. 1955. The intracellular localization of oxytocic and vasopressor substances in the pituitary gland of rats. J. Physiol. 127: 201-212.

Parker, R.S. 1966. The influence of photoperiod on reproduction and moulting of *Daphnia schødleri* Sars. Physiol. Zool. 39: 266-279.

Passano, L.M. 1951. The X organ - sinus gland neurosecretory system in crabs. Anat. Rec. 111: 502.

________. 1952. Phase contrast observations on living neurosecretory cells of *Sesarma*. Anat. Rec. 112: 460.

________. 1954. Phase microscopic observations of the neurosecretory product of the crustacean X irgan. Pubbl. Staz. Zool. Napoli. 24(Suppl): 72-73.

Perkins, E.B. 1928. Colour change in crustaceans, especially in *Palaemonetes*. J. Exp. Zool. 50: 71-195.

Perryman, E.K. 1969. *Procambarus simulans:* light induced changes in neurosecretory cells and in ovarian cycle. Trans. Am. Micr. Soc. 88(4): 514-524.

Peute, J., and J.C. van de Kamer. 1967. On the histochemical difference of aldehyde-fuchsin positive material in the fibers of the hypothalamo-hypophyseal tract of *Rana tempararia*. Z. Zellforsch. Mikr. Anat. 83: 441-448.

Potter, D.D. 1954. Histology of the neurosecretory system of the blue crab *Callinectes sapidus*. Anat. Rec. 120: 716-720.

________. 1958. Observations on the neurosecretory system of portunid crabs, p. 113-118. *In* Neurosekretion, 2nd International symposium. (W. Bargmann *et al.*, eds.). Springer, Berlin.

Prunesco, C. The neurosecretory cells of the ventral nervous ganglions of epimorphous chilopods. Rev. Roum. Biol. Ser. Zool. 15(5): 323-327.

Pyle, R.W. 1943. The histogenesis and cyclic phenomena of the sinus gland and X organ in Crustacea. Biol. Bull. (Woods Hole). 85: 87-102.

Rangnecker, P.V., M.N. Madhyastaa, and A.N. Latey. 1971. Hormonal control of reproduction in the male crab *Scylla serrata*. J. Animal Morphol. Physiol. 18(1): 17-29.

Raven, Chr. P. 1961. Oogenesis: the storage of developmental information. Pergammon Press, MacMillan Co., NewYork. 274p.

Reupsch, E. 1912. Beiträge zur Anatomie und Histologie der Heteropoden. Z. wiss. Zool. 102: 249-376.

Roche, Par A. 1953. Contribution a l'étude histophysiologique de l'appareil digestif chez *Asellus aquaticus* L. Ann. Sci. Nat. Zool. Biol. Animal. Ser. II. 15: 347-358.

Rosenstadt, B. 1888. Beiträge zur Kenntrig der Organisation der *Asellus aquaticus* und verwondter Isopoden. Biol. Zbl. 8: 452-462.

Roubos, E.W. 1973. Regulation of neurosecretory activity in the freshwater pulmonate *Lymnaea stagnalis* (L.), a quantitative electron microscopical study. Z. Zellforsch. Mikr. Anat. 146: 177-205.

Ruby, J.R., R.F. Dyer, and R.G. Skalko. 1969. Continuities between mitochondria and endoplasmic reticulum in the mammalian ovary. Z. Zellforsch. Mikr. Anat. 97: 30-37.

Sahota, T.S. 1973. Yolk deposition in douglas fir beetle oocytes possible role od RNA synthesis in the follicular epithelium. J. Insect Physiol. 19(5): 1087-1095.

Sandifer, J.B., and A.S. Tombes. 1972. Ultrastructure of the lateral neurosecretory cells during reproductive development of *Sitophilus granarius* Insecta, Coleoptera. Tissue. Cell. 4(3): 437-446.

Sars, G.O. 1867. Histoire Naturelle des Crustaces d'Eau Douce de Norvege. I. Les Malacostraces. Johnsen Christiana.

Scharrer, B. 1935. Uber das Hanstromsche Organ X bei Opisthobranchiern. Pubbl. Staz. Zool. Napoli. 15: 132-142.

________. 1936. Uber Drusen-Nervenzellen im Gehirn von *Nereis virens* Sars. Zool. Anz. 113: 229-302.

________. 1937. Uber sekretorisch tatige Nervellen bei wirbellosen Tieren. Naturwissenschaften. 25: 131-138.

________. 1955. Hormones in invertebrates. p. 57-95, *In* The Hormones (G. Pincus and K.V. Thiman eds.). Academic Press, NewYork.

________. 1959. The role of neurosecretion in neuroendocrine integration. p. 113-168, *In* Comparative endocrinology (A. Gorbman ed.). Wiley, NewYork.

________. 1963. Neurosecretion XIII. The ultrastructure of the corpus cardiacum of the insect *Leucophaea moderae*. Z. Zellforsch. Mikr. Anat. 60: 761-796.

________. 1968. Neurosecretion XIV. The ultrastructural study of sites of release of neurosecretory material in blattarian insects. Z. Zellforsch. Mikr. Anat. 89: 1-16.

________. 1971. Histophysiological studies on the corpus allatum of *Leucophaea moderae*. V. Ultrastructure of sites of origin and release of a distinctive cellular product. Z. Zellforsch. Mikr. Anat. 120: 1-16.

Scharrer, E. 1928. Die Lichempfindlichkeit blinder Elirtzen (Untersuchungen über das Zwischenkirn der Fische). Z. Vergl. Physiol. 7: 1-38.

________. 1959. General and phylogenetic interpretations of neuroendocrine interrelations. p. 202-245, *In* Comparative endocrinology. (A. Gorbman ed.). Wiley, NewYork.

________., and S. Brown. 1961. Neurosecretion XII. The formation of neurosecretory granules in the earthworm, *Lumbricus terrestris* L. Z. Zellforsch. Mikr. Anat. 54: 530-540.

________., S.L. Palay, and R.G. Nilges. 1945. Neurosecretion VIII. The Nissl substance in secreting nerve cells. Anat. Rec. 92: 23-31.

Schmitt, F.O. 1959. Molecular organization of the nerve fiber. p. 57-68, *In* Biophysical Science. (J.L. Oncely ed.). Wiley, NewYork.

Schoumaker, H., and N. vanDamme. 1971. Maillet's OsO_4-ZnI_2 fixative and alcian blue staining in the study of neurosecretion: invertebrates. Stain Technol. 46(5): 233-237.

Schreiner, B., H. Staaland, and A. S. Johansson. 1969. Functional significance of neurosecretory cells in the last abdominal ganglion of the lobster *Homaris vulgaris* L. Gen. Comp. Endocrinol. 13(3): 399-402.

Segerstrale, S.G. 1937. Studien die Bodentierwelt etc. III. Zur Morphologie und Biologie des Amphipoden *Pontoporeia affinis* nebst, einer Revision der *Pontoporeia* - Systematik. Comentat. Biol. 7(1): 183p.

________. 1970. Light control of the reproduction cycle of *Pontoporeia affinis* Lindström (Crustacea, Amphipoda). J. Exp. Mar. Biol. Ecol. 5: 272-275.

________. 1971. Light and gonad development in *Pontoporeia affinis*. p. 573-581, *In* 4th European Mar. Biol. Symp. (D.J. Crisp ed.). Cambridge University Press.

Sexton, E.W. 1924. The moulting and growth stages of *Gammarus*, with descriptions of the normals and intersexes of *G. chevreux*. J. Mar. Biol. Ass. U.K. 13: 340-388.

Shyamasundari, K. 1973. A preliminary study of neurosecretory cells in *Talorchestia martensii* (Weber) and *Orchestia platensis* Krøyer (Amphipoda, Talitridae). Crustaceana 25(1): 1-4.

Smith, G., and E. Nayla. 1972. The neurosecretory system of the eyestalk of *Carcinus maenus*, Crustacea, Decapoda. J. Zool. Proc. Zool. Soc. Tand. 166(3): 313-321.

Smith, U., and D.S. Smith. 1966. Observations on the secretory processes in the corpus cardiacum of the stick insect, *Carausius morosus*. J. Cell. Sci. 1: 59-66.

Speidel, C.J. 1919. Gland cells of internal secretion in the spinal cord of the skates. Carnagie Inst. Was. 13(281): 1-31.

Stahl, F. 1938. Über das Vorkommen von inkretorischen organen und Farbwechselhormonen im Kopf einiger Crustaceen. Kungl. Fysiogr. Sällsk. Handl. N.F. Bd. 49(12): 4-20.

Steele, D.H., and V.J. Steele. 1969. The biology of *Gammarus* (Crustacea, Amphipoda) in the northwest Atlantic I. *Gammarus duebeni* Lillj. Can. J. Zool. 47(2): 235-244.

________., and ________. 1973. The biology of *Gammarus* (Crustacea, Amphipoda) in the northwest Atlantic VII. The duration of embryonic development in five species at various temperatures. Can. J. Zool. 51(9): 995-999.

Steele, V.J. 1964. Reproduction and metabolism in *Gammarus oceanicus* and *Gammarus setosus*. Unpublished Ph.D. Thesis, McGill University.

________. 1967. Resting stage in the reproductive cycles of *Gammarus*. Nature (London). 214: 1034.

________., and D.H. Steele. 1970. The biology of *Gammarus* (Crustacea, Amphipoda) in the northwest Atlantic II. *Gammarus setosus* Dementieva. Can. J. Zool. 48(4): 659-671.

Stephens, G.J. 1952. Mechanisms regulating the reproductive cycle in the crayfish *Cambarus* I, The female cycle. Physiol. Zool. 25: 70-83.

Stiennon, J.A., and P. Drochmans. 1961. Electron microscope study of neurosecretory cells in Phasmidae. Gen. Comp. Endocrinol. 1: 286-294.

Stoeckel, M.E., A. Porte, H.D. Delmann, and L. Gertner. 1972. Selective staining of neurosecretory material in semithin epoxy sections by Gomori's adledhyde-fuchsin. Stain Techn. 47(2): 81-85.

Suko, T. 1958. Studies on the development of the crayfish V. The histological changes of the developmental ovaries influenced by the condition of darkness. Sci. Rept. Saitama Univ. B. 3(1): 67-78.

Telfer, W.H. 1961. The route of entry and localization of blood proetins in the oocyte of saturniid moths. J. Biophys. Biochem. Cytol. 9: 2095-2103.

Teodorescu, M., F. Zaharia, and E. March. 1965. Investigations upon neurosecretion in nervous ganglions in some invertebrates. Rev. Rourn. Embryol. Cytol. Ser. Cytol. 1(2): 123-131.

Thore, S. 1932. Uber statocysten und frontalorgane bei *Gammarus pulex* und *Gammarus locusta*. Zool. Jb. Abt. Anat. 55: 489-504.

Tighe-Ford, D.J. 1967. Possible mechanism for the endocrine control of breeding in cirrepedes. Nature (London). 216: 920-921.

Tombes, A.S. 1970. An introduction to invertebrate endocrinology. Academic Press, NewYork and London. 217p.

Trump, B.F., F.A, Smuckler and E. Benditt. 1961. A method for staining epoxy sections for light microscopy. J. Ultrastr. Res. 5: 343-348.

van den Bosch Aguilar, P. 1971. The neurosecretory system of *Podon intermedius* Crustacea, Cladocera. Ann. Soc. R. Zool. Belg. 101(1-2): 57-63.

van Weel, P.B. 1955. Processes of secretion, restitution and resorption in midgut gland of *Atya spinips* Newport. Physiol. Zool. 28: 40-54.

Vevers, H.G. 1962. The influence of the ovaries on secondary sexual characteristics. p. 263-284, *In* The ovary, vol. II. (S. Zuckerman ed.). Academic Press, NewYork and London.

Vitez, I. Histophysiological studies on the effect of environmental conditions on terrestrial isopods. Ann. Univ, Sci. Budap. Rolando Eotvas. Nominatae Sec. Biol. 13: 329-338.

Vonk, H.J. 1960. Digestion and metabolism. p. 291-316, *In* The physiology of Crustacea (T.H. Waterman ed.). Academic Press, NewYork and London.

Walker, R. 1936. The central nervous system of *Oniscus* (Isopoda). J. Comp. Neurol. 62: 197-238.

Welsh, J.H. 1955. Neurohormones. p. 97-151, *In* The hormones. (G. Pincus and K.V. Thiman eds.). Academic Press, NewYork.

Wendelaar-Bonga, S.E.W. 1970. Ultrastructure and histochemistry of neurosecretory cells and neurohemal areas in the pond snail *Lymnaea stagnalis*. Z. Zellforsch. Mikr. Anat. 108: 190.

________. 1971. Formation, storage and release of neurosecretory material studied by quantitative electron microscopy in the freshwater snail *Lymnaea stagnalis*. Z. Zellforsch. Mikr. Anat. 113(4): 490-517.

Weyer, F. 1935. Über drusenartige Nervenzellen im Gehirn der Honigbiene. Apis. Mellifica L. Zool. Anz. 112: 137-141.

Williams, C.M., and P.L. Adkisson. 1969. Physiology of insect diapause XIV. An endocrine mechanism for the photoperiodic control of pupal diapause in the oak silkworm *Antheraea pernyi*. Biol. Bull. (Woods Hole). 127: 511-525.

Winklestein, J., and M.G. Menefee. 1963. Basic fuchsin as a stain for osmium-fixed, epon-embedded tissue. Stain Technol. 38: 202-204.

Yahata, T. 1972. Fine structure of ganglion cells in the central nervous system of the Neptune whelk, *Neptunea arthritica*. Bull. Fac. Fish. Hokkaido Univ. 23(3): 144-149.

Yamamoto, K. 1956. Studies on the formation of fish eggs III. Localization of polysaccharides in the oocytes of *Liopsetta obscura*. J. Fac. Sci. Hokkaido Univ. (VI) 12: 391.

Yonge, C.M. 1924. The mechanism of feeding, digestion, and assimilation in *Nephrops norvegicus*. Brit. J. Exptl. Biol. I: 343-389.

Závadský, Von K., and S.J. Prag. 1914. Die frontalorgane der Amphipoden. Zool. Anz. XLV: 65-73.